6-30-2005

Waldo Lake Research in 2004

Mark D. Sytsma
Portland State University, sytsmam@pdx.edu

John Rueter
Portland State University

Richard Petersen
Portland State University

Roy Koch
Portland State University

Scott A. Wells
Portland State University, wellss@pdx.edu

See next page for additional authors

Authors
Mark D. Sytsma, John Rueter, Richard Petersen, Roy Koch, Scott A. Wells, Michelle Wood, Yangdong Pan, Robert Leslie Annear, Aaron Hook, Laura Johnson, Rich Miller, Amanda Murphy, and Terry Stoltz

Waldo Lake Research in 2004

By

Dr. Mark Sytsma,

Dr. John Rueter,

Dr. Richard Petersen,

Dr. Roy Koch,

Dr. Scott Wells,

Dr. Michelle Wood

Dr. Yangdong Pan

Robert Annear, Aaron Hook, Laura Johnson, Rich Miller, Amanda Murphy and Terry Stoltz

Center for Lakes and Reservoirs

Department of Environmental Sciences and Resources
Department of Civil and Environmental Engineering
Portland State University
Portland, Oregon
&
Department of Biology
University of Oregon
Eugene, Oregon

June 30, 2005

Table of Contents

List of Tables

List of Figures

Executive Summary

Waldo Lake is one of the world's unique water bodies due to its exceptional water clarity, low productivity, low ionic strength, and rare benthic communities. The USDA Forest Service, Willamette National Forest has protected this resource over the past 30 years by promoting low-impact recreational development, ecological research, and long-term monitoring. Despite these efforts, there are indications of ecosystem changes. It is not known whether these changes are natural, human induced, artifacts of measurement errors, or a combination of these factors.

The Willamette National Forest has worked with Portland State University, Center for Lakes and Reservoirs (PSU) and the University of Oregon (UO) to investigate ecosystem changes, provide guidance on long-term monitoring methods, assess monitoring data, develop predictive water quality models, and conduct research that will lead to better protection and understanding of the Waldo Lake ecosystem. This report summarizes the second year of collaborative PSU-UO research at Waldo Lake. Research has focused on understanding physical, chemical and biological characteristics of Waldo Lake across a range of spatial and temporal scales. Research tasks that continued from 2003 into 2004 included temperature monitoring, hydrodynamic and water quality model development, climate and hydrological forcing scenario investigation, bathymetric map refinement, and analysis of phytoplankton and zooplankton community changes. Research tasks initiated in 2004 included evaluation of wavelength-specific light attenuation, diel phytoplankton and zooplankton vertical distribution patterns, phytoplankton photoinhibition and photoprotection, and the role of mixotrophy in the pelagic microbial food web. Preliminary efforts were made to characterize Waldo Lake benthos through assessment of algal species diversity and chemical composition of the benthic community, as very little is currently known about the Waldo Lake benthic ecosystem. In addition, an attempt was made to map benthic substrate types through reinterpretation of data collected during the 2003 bathymetric survey.

Major tasks initiated in 2004 included characterization of wavelength-specific light attenuation using an underwater scanning spectroradiometer; measurement of

photosynthetic efficiency of the phytoplankton using a Pulse Amplitude Modulated Fluorometer; assessment of the usefulness of underwater cellular fluorescence to determine the vertical distribution of phytoplankton; investigation of vertical migration of zooplankton using acoustical, depth-sounding equipment and grab samples; and evaluation of uncertainties in ^{14}C primary productivity methods with recommendations for future work to better understand variability in primary productivity estimates.

The utility of measurement of various chemical constituents was assessed based on the frequency of measurement that were above detection, seasonal and yearly variation, and the contribution of the constituent to the overall study of the lake. Suggestions for improved monitoring were provided to collect data in a manner meeting quality assurance standards. The recommended approach is for continued total phosphorus monitoring in conjunction with TKN analyses changing methods so that samples are filtered through a coarse mesh prior to analysis.

The quality assurance (QA) protocols followed during 2004 long-term monitoring activities did not meet goals outlined in the long-term monitoring quality assurance plan (Johnson 2003) therefore recommendations for improvements for long-term monitoring conducted during 2005 were suggested. Recommendations included the development of a datasheet to incorporate the QA plan during field work, and the completion of QA audits in the field by long-term monitoring staff (so corrective actions can be made when quality levels are not met). It is also recommended that adherence to the QA plan be a requirement of the contract signed by long-term monitoring staff and all participants in the long-term monitoring of the lake must read and sign the QA plan.

The initial phases of database development included the organization of historical data and checking the data for accuracy. In the chemistry dataset, changes to the method detection limit and precision estimate for each parameter were documented and updated in the database. Chlorophyll, light and secchi disk data have been organized and are incorporated into either a single MS ACCESS or MS EXCEL table. A database of phytoplankton data was designed for easy incorporation of datasheets provided by the taxonomist. The zooplankton database was designed in a similar format as the

phytoplankton database. Primary productivity data have not been made available by the investigator. No attempt has been made to date to incorporate available data into a cohesive database format. In the future, a plan for a relational database needs to be developed to incorporate all historic data and then implemented by a database specialist. Goals for database utility must be developed in collaboration with all potential users prior to database planning.

Preliminary estimates of wavelength specific light attenuation indicated optical properties of Waldo Lake are similar to pure water. Blue light penetrated to depths greater than 100 meters during July. Additionally, the attenuation of light changed throughout the summer; light penetrated more deeply in July than September. The depths of 1 % light estimated for monochromatic light in the blue light range were substantially deeper than those previously reported for Waldo Lake based on photometer data collected over a wide-bandwidth range. For example, on October 10, 2004 the 1 % depth estimated from the photometry data for blue light was 82 ± 8 m and on September 30, 2004 the spectroradiometer 1 % depth estimate for 440 nm was 101 m.

A multivariate review of long-term monitoring data indicated that bottom-up parameters, particularly changes in alkalinity, were more strongly correlated with changes in phytoplankton community structure than top-down changes in zooplankton species densities. The correlation between phytoplankton and alkalinity suggested that carbon availability may be of importance at Waldo Lake.

The prevalence of mixotrophic phytoplankton suggests the microbial loop is important in food chain dynamics at Waldo Lake. The ratio of mixotrophs to autotrophs has decreased since 1998. A seasonal change in the mixotroph to autotroph ratio was observed, the highest densities of mixotrophs occurred in August and September. Weak relationships were found between the distribution of mixotrophs and bacteria, possibly as a result of wind-driven mixing or phagotrophic feeding of mixotrophs on autotrophs. Future research of feeding activities of mixotrophs and modeling of wind-driven circulation patterns at Waldo Lake are needed in order to more thoroughly understand the role of mixotrophs in the lake ecosystem.

Flow cytometric analysis suggested that at least two major taxonomic groups, nearly always present in oligotrophic waters, were absent from the pelagic food web in Waldo Lake. Specifically, phycoerythrin-containing *Synechococcus*, a common component of the microbial loop in many high elevation lakes in Europe and Canada, and *Prochloroccous*, generally believed to be an obligately marine taxon, were not found in Waldo Lake.

The use of a Self-Contained Underwater Fluorescence Apparatus (SCUFA) allowed for the estimation of algal biomass for the entire water column very quickly, however, cellular fluorescence, measured using SCUFA, was affected by changes in ambient light. For example, during mid-day cellular fluorescence decreased, but the concentration of extracted chlorophyll did not. No localized peaks of SCUFA-inferred chlorophyll were found at any depth in the water column, therefore, samples collected for extracted chlorophyll at discrete depths accurately described the distribution of chlorophyll in the water column at the long-term monitoring station.

Results of experiments investigating the effects of UV radiation on phytoplankton photoinhibition, photoprotection and primary productivity were variable, either due to weather conditions or seasonal changes of incident UV. Non-photosynthetic quenching and electron transport rate increased with experimental increases in CO_2, suggesting that global carbon pollution may cause an increase in primary productivity even in this remote lake. Further research will include the affect of daily changes in UV on phytoplankton primary productivity as well as the affect of CO_2 limitation on phytoplankton primary productivity, which will be assessed by changing the dissolved inorganic CO_2 available to phytoplankton over time periods of minutes to hours.

Analysis of benthic communities previously described as 'living stromatolites' using a combination of biological and geological methods indicated that these unique formations are microbial mats dominated by a relatively few species of cyanobacteria with a mineral basis that is volcanic in origin. Additional analysis of data collected during 2003 for the purpose of benthic characterization was not possible because

Biosonics sonar data were not collected at a degree of sensitivity which enabled software inferences to be made regarding substrate types.

The use of hydroacoustic technology to monitor zooplankton distributions was not successful because of sparse populations, water depth, and equipment sensitivity. Schindler-trap zooplankton collections over two, 24-hour sampling events did not reveal diel vertical migration by the major zooplankton species; however, there was high variation between samples.

The development of the water quality model and the completion of the water balance and hydrodynamic models were hindered by the delay of survey work at Waldo Lake during 2003-2004. Initial steps of model development were made, including the calibration of temperature and hydrodynamics. Water temperature model-data error statistics ranged from 0.3 to 1.4 ^{o}C, indicating the model and observed data were in good agreement. Reliable outflow, water level and meteorological data, including precipitation data, are the cornerstone of accurate modeling. To hasten the availability of an adequate sequence of input data for the lake model, a methodology was developed for creating long time-sequences of climate data using a statistical approach. Data generated in this manner may be used in future investigations of climate change scenarios on the lake. Although the current climate record at the lake covers a very short period, the model was able to generate a reasonable sequence of weather data for a similar period. The continued monitoring of climate data in the vicinity of the lake will allow for further refinement of these "synthetic" sequences. With increased resolution into hourly time increments, stochastically generated data will be used in CE-QUAL-W2 and may better preserve the inter-annual and longer time scale behavior of the model. This, in turn, may help assess how local weather data are related to large scale patterns in the climate - in particular the El Niño/Southern Oscillation (ENSO) and the Pacific Decadal Oscillation (PDO).

In conclusion, continued research should focus on improving monitoring techniques and explaining variation in primary productivity estimates. Understanding variability of results in the context of short-term weather conditions was important in the interpretation

of data collected during 2004. The interpretation of short-term and long-term weather conditions may be important in understanding changes and variability observed in the long-term monitoring dataset. One overarching goal for future research at Waldo Lake should be synthesizing observed long and short-term responses. Future research should also include continued meteorological data collection and interpretation, expanding the CE-QUAL-W2 model to include simulating water quality and using the model to better understand longer term climate changes on the lake. Data collected and interpreted during 2004 also suggested carbon may be limiting at Waldo Lake. Short-term fluctuations in carbon availability due to mixing events and phytoplankton assimilation and long-term changes due to global carbon pollution may play a key role in ecological processes at Waldo Lake.

Acknowledgements

Funding for this work was provided by the USDA Forest Service, Willamette National Forest, through the guidance of Deigh Bates and Al Johnson. John Salinas conducted field sampling, Cam Jones, Jim Sweet and Allan Vogel analyzed chemical, phytoplankton and zooplankton samples respectively, for the long term monitoring program, and provided background information on Waldo Lake long-term monitoring data. In addition, Miguel Estrada provided assistance for the enumeration and taxonomic identification of phytoplankton samples. Dave Boone and Anna Louise Reysenbach provided assistance in the enumeration of bacteria. Adam Kennedy provided technical assistance in the development of climate and hydrology models. Al Johnson and Jim Pence both were instrumental in the maintenance, installation and collection of data associated with the meteorological station and outflow station. Sean Garretson, Erin Harwood, Steven Wells and Vern Huber aided in the downloading of temperature loggers.

1 Physical and Chemical Characteristics

1.1 Optical Characteristics: Wavelength Specific Light Attenuation

Introduction

The optical properties of Waldo Lake are extraordinary. Water clarity is among the best in the world; rivaling Crater Lake (Larson and Salinas 1995). There have been suggestions, however, of degradation in Waldo Lake's optical properties over the past 30 years (Larson and Salinas 1995). These suggestions are based on data collected with two light meters, a Lakelight, used prior to 2000, and a Kahl photometer, used 2001-2004. A photometer measures light over a range of wavelengths (~100 nm) with a peak response at a particular wavelength. The Center for Lakes and Reservoirs objectives for 2004 were to characterize the light field in Waldo Lake with more sensitive technology and to examine wavelength specific light attenuation (Sytsma et al. 2004). A LI-COR Biosciences LI-1800UW underwater spectroradiometer was used to obtain light attenuation estimates with depth at 2 nm resolution from 300 to 800 nm.

Methods and Analysis

Field Methods

Three profiles were obtained in the summer of 2004 (7/28, 9/24, and 9/30). Profiles were collected within ± 2 hours of solar noon to minimize effects of a changing solar angle. Triplicate air scans were followed by underwater scans at 5 m intervals to a depth of 60 m and scans at 10 m intervals to between 70 and 100-110 m.

Variable sky and wind conditions confound the quality of data obtained when collecting profiles of spectral irradiance. Therefore profiles were only collected on days with uniform sky conditions and calm winds. Notes were made on changes in sky and wind conditions during the profiles.

Data Analysis

Due to refraction of light by water, underwater irradiance values require different correction factors than values collected from air. Therefore all data were first transformed with the calibration file provided by LI-COR Biosciences (LI-COR Environmental Division, July 2003, filename-UCOS). Air scans were then back corrected with the air calibration file (filename COS).

Extinction coefficients describe the rate of light attenuation due to absorption and scattering in the water column and are expressed as a fraction per meter (i.e. a value of 0.1 per meter means that 10 % of the light is lost each meter). There are multiple methods for calculating light extinction coefficients (e.g., Kirk 1984; Morris et al. 1995; Wetzel and Likens 2000). The choice of calculation methods depends mainly upon the band-width of the light sensor and lake specific properties such as distinct turbidity layers of particulates or phytoplankton that affect light attenuation.

A profile of wide-band or multichromatic light attenuation through the water column (such as photometry data) does not conform to a linear model. Rather, it resembles an exponential function due to variable attenuation of individual wavelengths. Generally, an estimate of attenuation is derived by averaging extinction coefficients calculated for multiple depths relative to a fixed surface value (Wetzel and Likens 2000). This technique integrates the differential extinction of particular wavelengths and yields an estimate of attenuation at the wavelength of peak response for the instrument.

Monochromatic light adheres more closely to Beer's Law and a linear model of attenuation with depth. Therefore, an extinction coefficient is more accurately determined from the slope of a linear regression of the natural log of irradiance versus depth (Morris et al. 1995). The regression approach avoids placing undue reliance on the measured value of surface intensity and the ambiguity of treating a broad spectrum of light as a single physical entity.

The regression method was applied to the spectroradiometer dataset. Regressions were determined for each wavelength (every 2 nm). The quality of each estimate was assessed by goodness of fit and a minimum R^2 of 0.97 was set for reporting extinction

coefficients (e.g. Figure 1.1-1). Wavelength specific extinction coefficients were determined as the negative slope of the regression. The depths at which 1 % of irradiance remains (1 % depth) were estimated from the extinction coefficients (Wetzel and Likens 2000)

Three issues commonly associated with spectroradiometer measurements (LI-COR LI-1800UW instruction manual, 1984) were observed in the dataset and data were screened to remove affected values:

1) Data collected near the surface were often greater than air values. This was due to reflexing, a phenomenon in which light is reflected off the top of the spectroradiometer to the water surface, off the water surface, and then measured by the sensor. In shallow measurements, this process results in light measurements that are not only a function of incident light, but also reflexing. Regressions were determined only from data collected at 5 m or deeper to avoid values affected by reflexing.

2) Although care was taken to avoid this issue, variable sky conditions resulted in a few outlier values that were removed from the dataset prior to analysis.

3) At both the high (> 625 nm) and low (< 400 nm) ends of the wavelength spectrum, values had a low signal:noise ratio and data obtained were unreliable. For example, the intensity of very short wavelengths (UV) was low at the surface in September and data were too noisy to reasonably fit a regression line. At longer wavelengths when values had a low signal:noise ratio (i.e. at greater depths) a tailing affect was observed, and regressions were fit only to the data above the tail (Figure 1.1-1).

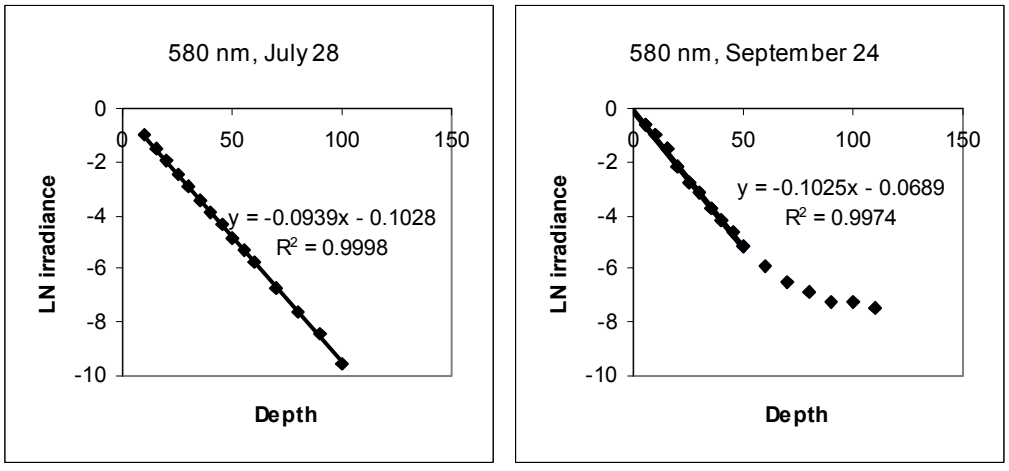

Figure 1.1-1. Example regressions for 580 nm wavelength calculated from data collected on July 28 and September 24.

Following data screening, the number of depths available for calculation of extinction coefficient varied with wavelength and incident light levels. During high incident light intensity in July, the number of depths included in calculations was greater than or equal to five for each wavelength up to 650 nm, n equaled four for each wavelength between 650 to 680 nm and n equaled three for each wavelength above 680 nm. During lower incident light levels in September, n was greater than five up to 600 nm, n equaled four from 600 to 624 nm, and n equaled three above 624 nm. No useable data were obtained for wavelengths above 721 nm on either date. All extinction coefficients calculated for wavelengths between 300 nm and 712 nm were reported regardless of the quality of the data available. However, due to low signal to noise ratios at short and long wavelengths, extinction coefficients of wavelengths below 400 nm on all dates, above 650 nm in July, and above 624 nm in September should be interpreted with caution.

Results and Discussion

Photons of light entering a lake are absorbed and scattered by water molecules, phytoplankton, and other particles. For pure water, absorption is highest in the longer infrared wavelengths, then decreases markedly in the shorter wavelengths to a minimum absorption in the blue range (at 480 nm). Absorption then increases again in the violet and ultraviolet wavelengths. The high absorption of longer wavelengths is so great that 53 % of total sunlight is transformed into heat in the first meter of water resulting in heating of surface water by incident light (Kirk 1984).

Wavelength specific light attenuation in Waldo Lake followed the pattern expected for pure water on all three days. Longer wavelengths were attenuated most quickly. Minimum attenuation occurred in the blue wavelengths, and attenuation increased in the shorter UV wavelengths (Figure 1.1-2). Due to limitations in the technology as discussed above, noise increased and signal decreased at both ends of the light spectrum resulting in suspect extinction coefficients for wavelengths shorter than 400 nm and longer than 624 nm.

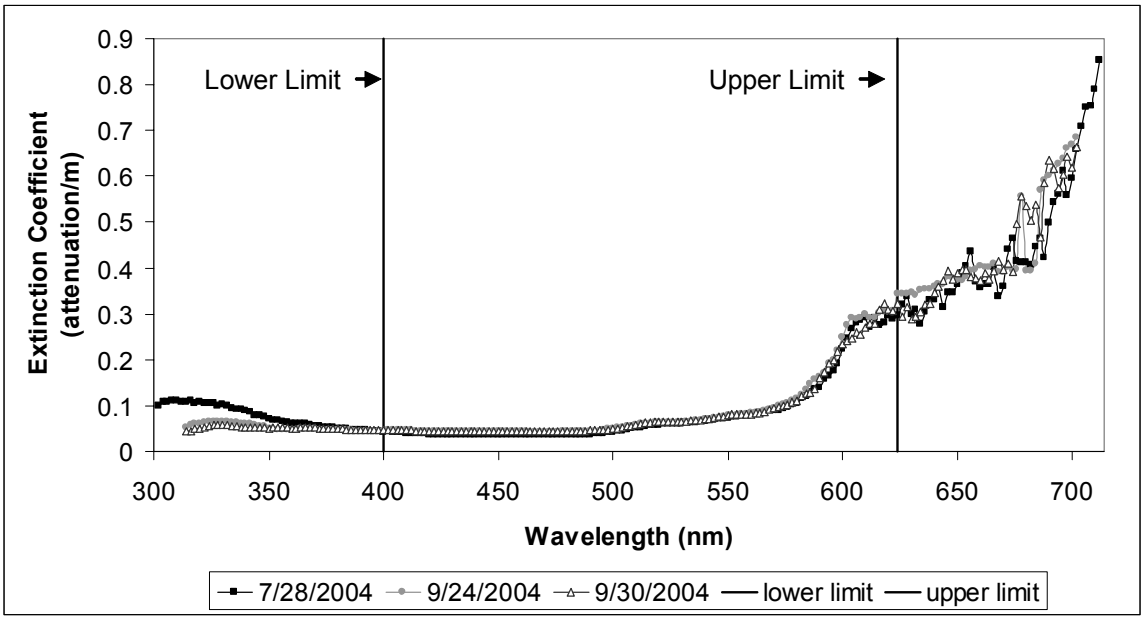

Figure 1.1-2. Wavelength-specific light extinction coefficients estimated from linear regressions of data collected on July 28, September 24, and September 30, 2004. Upper and lower limits represent that values were reliable between 400 and 624 nm.

For wavelengths in the blue light range an interesting seasonal pattern was evident in the three profiles. It appeared that from roughly 420 nm to 500 nm, light was more rapidly attenuated in September than in July (Figure 1.1-3). Those wavelengths correspond to an absorption peak for chlorophyll-a at 430 nm and could be related to increased phytoplankton biomass later in the growing season.

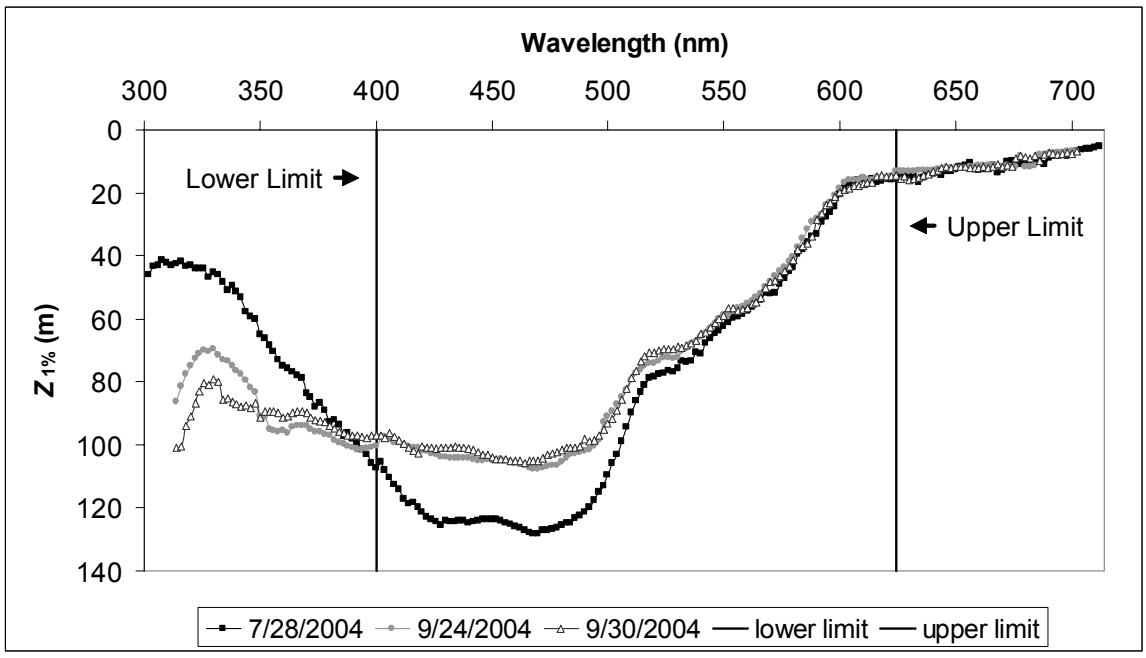

Figure 1.1-3. 1 % depths for each wavelength. Values were estimated from extinction coefficients and lower and upper limits depict reliable wavelengths between 400 and 624 nm.

The depths of 1 % light estimated for monochromatic light in the blue light range were substantially deeper than those previously reported for Waldo Lake (Larson and Salinas 2000). Previous estimates at Waldo Lake were made from photometry data. A photometer employs filters that measure over wide bandwidths with variable attenuation and sensitivity across bandwidths. For example, the blue filter for the Kahl photometer measures over a range of wavelengths from 400 to 475 nm with a peak response at 440 nm and the green filter measures from 475 to 600 nm with a peak response at 520 nm (Kahl manual).

Comparing the photometry estimates to those from the spectroradiometer, depths of 1 % light were similar in the green light range but differed in the blue light range. On October 10, 2004 the 1 % depth estimated from the photometry data for blue light was 82 ± 8 m and on September 30, 2004 the spectroradiometer 1 % depth estimate for 440 nm was 101 m. On October 10, 2004 the 1 % depth estimated from the photometry data for green light was 67 ± 6 m and on September 30, 2004 the spectroradiometer 1 % depth estimate for 520 nm was 71 m.

The discrepancies between instruments were likely due to the fact that the spectroradiometer measures equally well at all wavelengths while the two photometer filters have different transmission levels with greater transmission for the green filter (60 % at max wavelength) compared to that of the blue filter (50 % at max wavelength) (Kahl manual). As a result the photometry data collected since 1986 may have consistently underestimated the extent of transmission of blue light in Waldo Lake. Further, the photic zone likely extends to 120 m early in the season and moves up to 100 m as the phytoplankton abundance increases during the season, which helps explain the consistently higher chlorophyll-a concentration at depths below 80 m.

Recommendations

Accurate assessment of the optical characteristics of Waldo Lake requires an instrument that measures monochromatic light. Additionally, characterizing the ultra-violet portion of the light spectrum is critical to understanding the light climate experienced by the biological community in an ultra-oligotrophic system. While the spectroradiometer may have revealed limitations of the photometer, it was not successful in characterizing the ultra-violet wavelengths. It is therefore recommended that new technologies be examined for future use in the long-term monitoring program.

One example of a potential technology is Biospherical Instruments Inc.'s BIC (Biospherical Instruments Cosine) Radiometer which can measure four wavelengths at 10 nm FWHM (full-width at half-maximum- an expression of the spectral width of a detector or filter). The width is reported as the difference between the lower and upper wavelengths of the spectrum where the value of the response is equal to one-half the maximum value. Twenty-seven wavelengths are available. Stakeholders in the monitoring and research programs should discuss the wavelengths of interest (e.g., UV at 320 nm, blue at 443 nm, green at 555 nm, and red at 683 nm). Future light profile monitoring should incorporate incident light measurements during deployment to account for changes in sky or water surface conditions.

1.2 Temperature

Introduction

Thermal processes influence the physical properties, chemistry and biological community of lakes. Temporal and vertical changes in temperature can affect light attenuation, dissolved gas exchange, nutrient distributions, plankton energetics, and plankton distributions. Continuous temperature monitoring of Waldo Lake was initiated in July 2003 (Sytsma et al. 2004) and has continued to date. The data are critical to effective modeling of lake hydrodynamics and to plankton vertical distribution studies. Additionally, the timing of stratification and turnover are important considerations for planning long-term monitoring sampling trips.

Methods and Analysis

Temperature loggers were installed in Waldo Lake during July 2003 (Sytsma et al. 2004). Thermistor chains consist of two temperature logger models, Onset Waterproof Optic StowAway Temp 8K data loggers and Onset Waterproof Stowaway Tidbit 32K data loggers.

Temperature loggers were downloaded twice during 2004, on July 20-21 and September 21-23. During September 2004 additional temperature loggers were installed. One was placed at the outlet of the lake and three were placed at the 3-meter depth at three locations (Table 1.2-1). The 3-m depths were included to monitor affects of nighttime convection and short-term wind mixing events.

Table 1.2-1. Temperature logger station information.

Location		Station Depth	Approximate depth of Thermistors July 2004	Approximate depth of Thermistors Sept 2004
North Bay	New location September 2004	89 m		3,5,10,15,20,25,35,45,60 m
Mid Lake 2	New location September 2004	66 m		5,10,15,20,25,35,45,60 m
West Bay	No change	77 m	5,10,15,20,25,35,45,60 m	3,5,10,15,20,25,35,45,60 m
South Bay	No change	94 m	5,10,15,20,25,35,45,60 m	3,5,10,15,20,25,35,45,60 m
North Lake	Discontinued September 2004	65 m	5,10,15,20,25,35,45,60 m	
Mid Lake	Discontinued September 2004	74 m	5,10,15,20,25,35,45,60 m	
South Lake	No change	47 m	5,10,15,20,25,30,35,40 m	5,10,15,20,25,35,40 m

Temperature profiles downloaded in July 2004 indicated West Bay, Mid Lake and North Lake were very similar. Therefore, in September 2004, two temperature logger sites were discontinued and moved to new locations to improve understanding of spatial variation (Table 1.2-1, Table 1.2-2, and Figure 1.2-1).

Table 1.2-2. Coordinates of new temperature logger sites added to Waldo Lake, September 2004.

	UTM, NAD27		Geographic, NAD83	
Site Name	Easting-X, m	Northing-Y, m	Longitude, deg	Latitude, deg
North Bay	577136	4844807	122.043	43.7541
Mid Lake 2	577133	48409289	122.0436	43.7192

Spatial and temporal variation among thermistor chain locations was assessed by comparing average values for each location. The South Lake site was not included for comparisons between years of epilimnetic (5 m) temperatures due to data loss during summer of 2003. Detailed analysis of thermal profiles based on the exact depth of temperature loggers at each location was completed for modeling efforts (See Section 5).

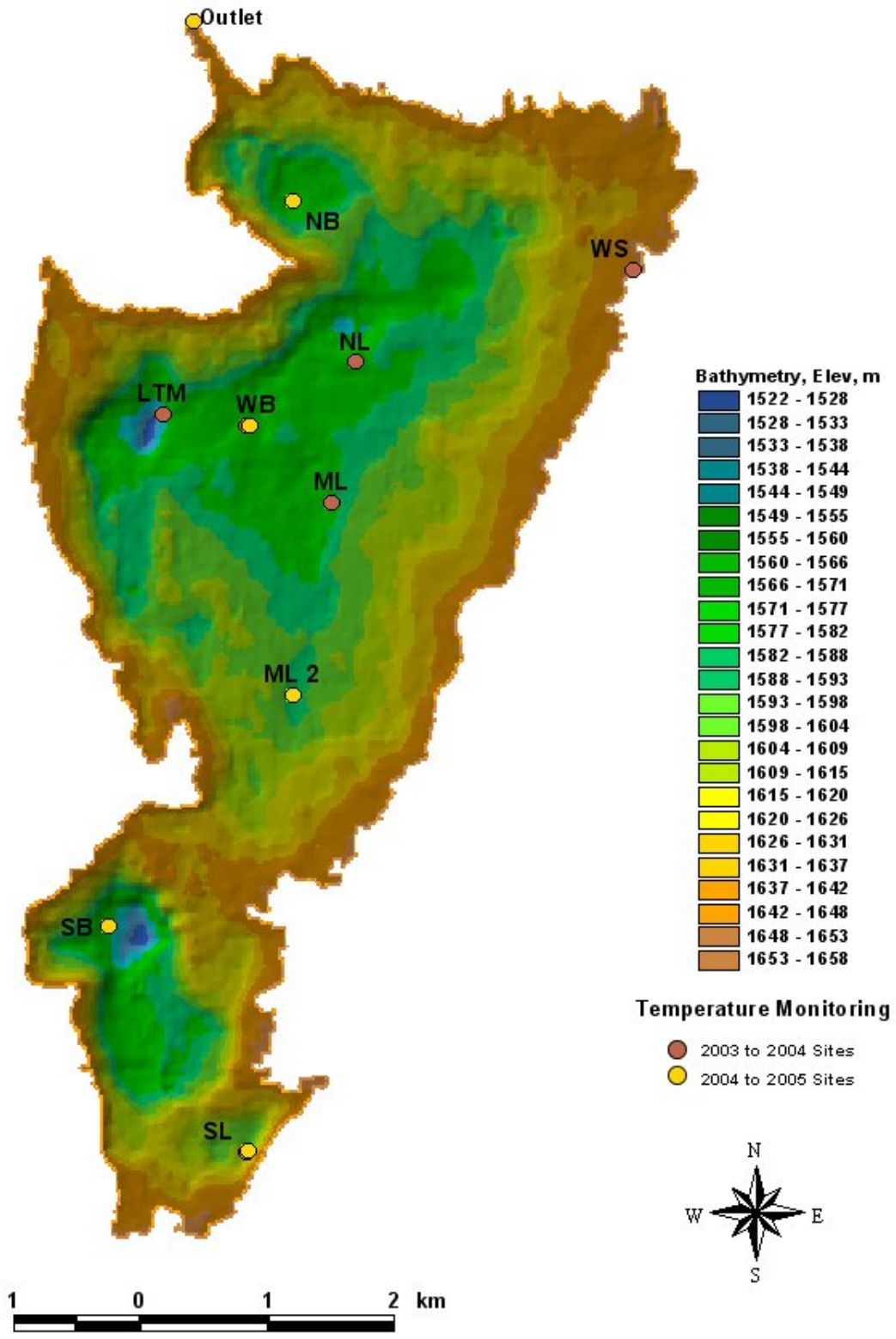

Figure 1.2-1. Map of temperature logger locations. Yellow dots indicate sites added in September 2004. Red dots indicate previous sites. The Mid Lake (ML) and North Lake (NL) sites were discontinued in September 2004.

Quality Assurance

Quality Assurance goals and protocol for temperature monitoring activities are available in Appendix A: Temperature Monitoring, Waldo Lake, Oregon Quality Assurance/Quality Control.

New temperature loggers were tested in the laboratory in an ice bath held at a constant temperature to ensure that loggers met manufacturer's standards prior to deployment in the field. The maximum difference between loggers and a NIST certified digital thermometer (VWR Scientific Inc., Traceable ™, accuracy of ± 0.2 °C) prior to deployment was less than 0.2 °C for all loggers deployed into the lake during 2004.

The overall completion rate for the project (July 2003 through September 2004) was 96 %, which met the quality assurance goal for data collection. Data gaps occurred due to loss of temperature loggers in the field and user error. In July 2004, at the West Bay site, temperature loggers at 5, 10, 20, and 25 meters were missing (they either fell off the thermistor array cable or were taken by SCUBA divers) and the 60-m logger was downloaded incorrectly; at these depths, data collected between October 2003 and July 2004 were lost. In July 2004, the South Lake 30-m logger was launched incorrectly, resulting in data loss between July and September 2004. The South Lake 5-m temperature logger was lost causing a data gap between July and October 2003.

Quality assurance goals for accuracy were also met. Logger-recorded temperatures were compared to thermal profile data collected by a multi-parameter probe at the time of downloading the temperature loggers. Four audits were completed. The temperature loggers received a grade of A on all occasions for all depths, indicating the difference between temperature logger and multi-parameter probe audit values was less than 1.5 °C.

Results

Waldo Lake was shown to be a dimictic lake – it is isothermal for two periods each year (spring and fall). Beginning in August 2003, periods of cool air temperatures appeared to influence epilimnetic temperatures (Figure 1.2-2). During that period surface waters cooled and became more dense, sinking to lower depths, deepening the

thermocline and beginning the erosion of stratification (Figure 1.2-3). Fall mixing was complete and the lake was isothermal by the beginning of December 2003. During January and February 2004 the lake was inversely stratified; 5-m waters were around 1.5 °C and 60-m waters were roughly 3 °C. Coldest surface temperatures observed were 1 °C in February. The individual thermistor locations exhibited variable episodes of inverse stratification, which were occasionally disrupted. Density gradients that exist during inverse stratification are generally weak and it is not uncommon for storms or winds to cause disruptions (Wetzel 2001). During spring 2004, the lake was again isothermal. Stratification began to develop in May 2004. The lake was stratified in July, with the thermocline again gradually deepening through September.

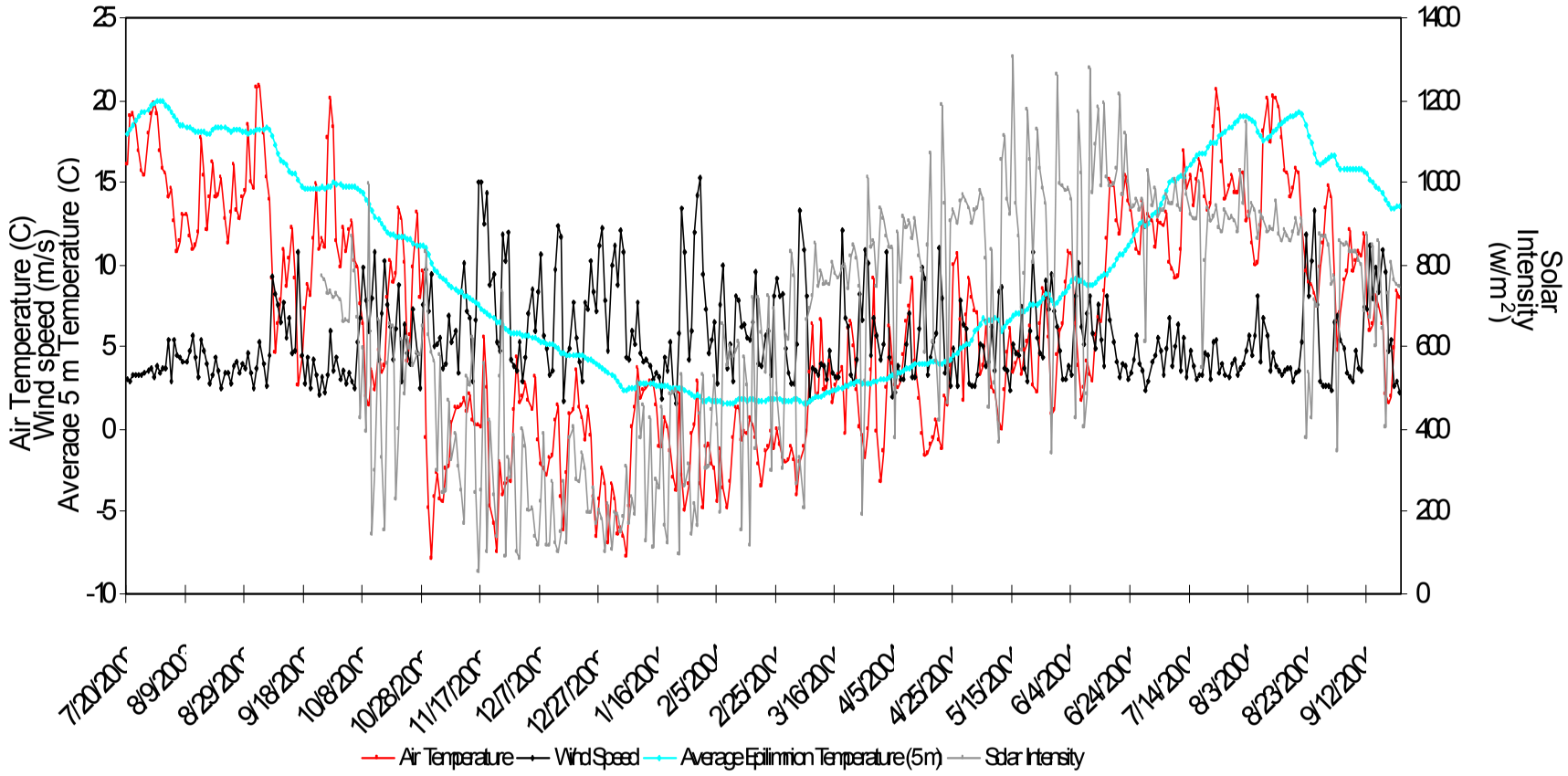

Figure 1.2-2. Daily average epilimnetic temperatures (5 m) from all locations, daily average air temperature, daily average maximum hourly wind speed and maximum daily solar intensity collected from hourly meteorological observations from the USFS weather station hourly meteorological observations from the USFS weather station hourly data located at the Islet Campground at Waldo Lake between 7/19/03 and 9/23/04.

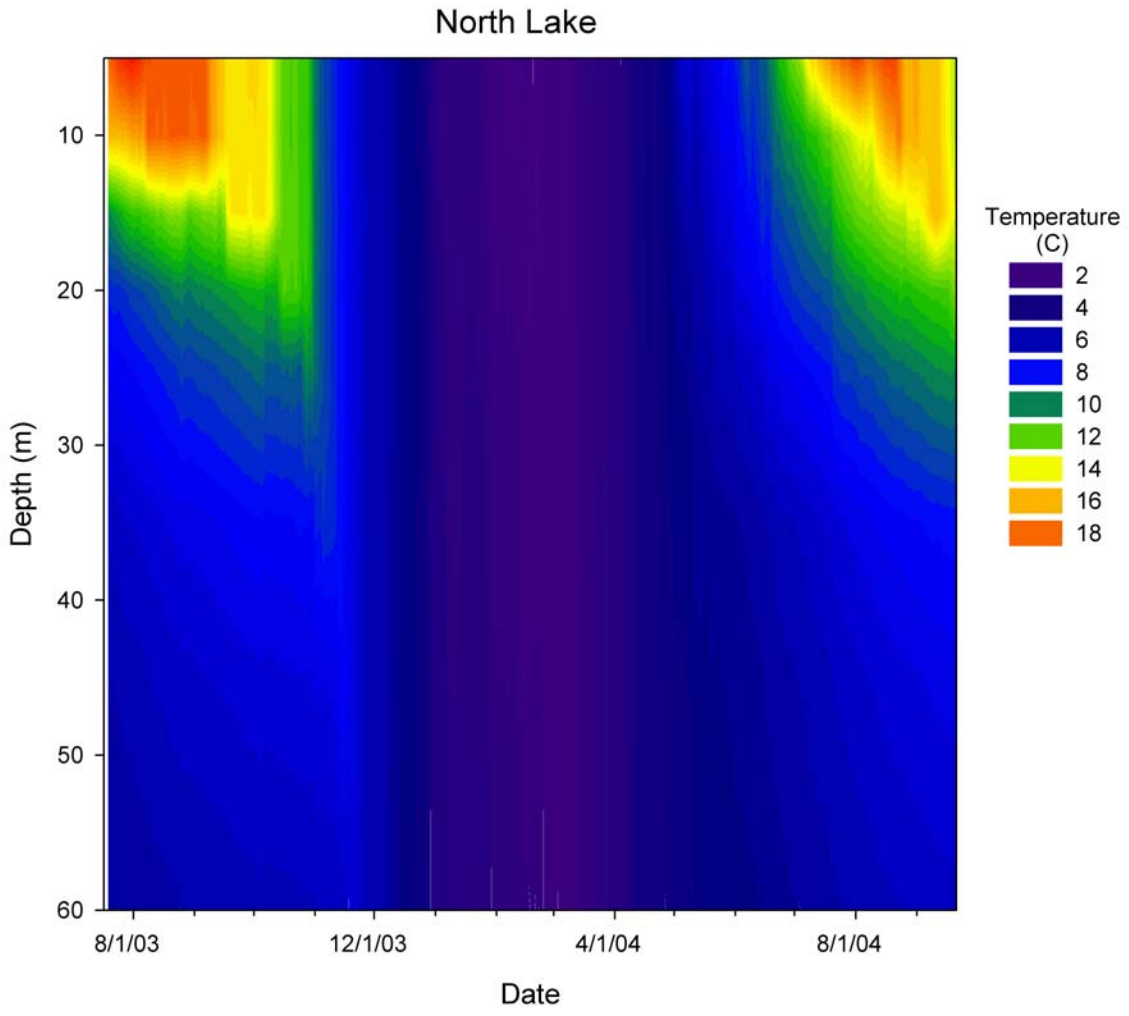

Figure 1.2-3. Representative thermal profiles between July 19, 2003 and September 24, 2004 collected at the North Lake location.

Maximum epilimnetic temperatures occurred on July 31 in both 2003 and 2004. The maximum temperature in 2003 was 20.1 °C, the maximum temperature in 2004 was 19.1 °C. During the period of maximum epilimnetic temperature, the median temperatures in 2003 were significantly higher than in 2004 (Mann-Whitney U-test, $p < 0.05$, $n = 1102$) (Table 1.2-3). July air temperatures, collected hourly at the USDA Forest Service meteorological station located at Islet Campground, were also significantly higher in 2003 than in 2004 (Mann-Whitney U-test, $p < 0.05$, $n = 1488$) (Table 1.2-3). Over the entire study period daily average air and epilimnetic temperatures were strongly correlated (Spearman Rank correlation statistic =0.82, 2-tailed $p < 0.0001$, $n = 433$).

Table 1.2-3. Comparison of 2003 and 2004 water and air temperatures (°C).

	2003	2004
Median 5-m water temperature July 20- July 31	19.3	18.1
Median July Air Temperature	15.0	14.3

Discussion

Epilimnion temperatures were correlated with air temperature during 2003 and 2004. Future modeling scenarios development will confirm or reject this correlation. The relationship between the ecology of Waldo Lake and climatic changes on various time scales will be examined from daily weather patterns (See Section 2.3) to decadal oscillations (see Section 4.1).

The epilimnion temperatures in Waldo Lake exhibited a seasonal warming of greater than 10 °C. Seasonal thermal changes at Waldo Lake may influence biological functions, productivity, and behavior. However, the one degree difference in epilimnetic temperatures between 2003 and 2004 was likely not large enough to affect the Waldo Lake biota. For example, a 10 °C increase in temperature resulted in a doubling of phytoplankton growth rates (Goldman and Carpenter 1974). While feeding rates of both *Daphnia pulicaria* and *Diaptomus oregonensis* were greater in warmer, epilimnetic waters (25 °C) than in cooler, metalimnetic waters (15 °C) (Williamson et al. 1996).

Epilimnetic temperatures during the growing season in Waldo Lake (12-20 °C) were not stressful for the biological community. For example, at temperatures above 15 °C bacterioplankton are commonly limited by factors other than temperature, including nutrient availability (Wetzel 2001). Zooplankton reproductive fitness and grazing rates are influenced by temperature. Maximum fecundity and survivorship of *Daphnia parvula* cohorts was reached at temperatures around 15 °C when food supplies were not limiting (Orcutt and Porter 1983).

Recommendations

Long-term monitoring activities should be completed following the onset of development of stratification (early June), during the period of strongest stratification

(early August) and after the thermocline begins to erode (in September). The early sampling event should be completed as soon as travel to the lake is feasible.

Temperature observation is relatively simple monitoring that is useful for both modeling purposes and monitoring the lake when it is not accessible to researchers. Temperature monitoring should be continued in 2005 with a single download and re-calibration event completed in early August. In 2005, the focus of temperature data collection will be to enhance our knowledge and understanding of epilimetic waters for the development of modeling scenarios to improve upon understanding particle mixing and short term changes in phytoplankton photosynthetic efficiency. Thermistor locations will be consolidated to record additional data from depths in the epilimnion at fewer locations.

1.3 Evaluation of Long-Term Water Chemistry Monitoring from 1986-2004

Introduction

Long-term monitoring of water quality at Waldo Lake is an important element of the management of this unique and pristine resource. One of the objectives of the Waldo Lake long-term monitoring program is early detection of changes in the lake's ecosystem, particularly an accelerated rate of eutrophication. Currently the program consists of three components: biological monitoring, in situ physical and chemical monitoring, and grab sample chemistry monitoring. In this report section we evaluated the effectiveness of analytical chemistry monitoring over the history of the program and recommended improvements for future sampling seasons. Effectiveness of monitoring each parameter was evaluated in terms of the proportion of samples collected that were measured above method detection limits and thereby provided useful information for management decisions and research purposes.

Water samples were collected by the Willamette National Forest since 1986 for analysis of total phosphorus (TP), ortho-phosphate (PO_4), total Kjeldahl nitrogen (TKN), nitrate plus nitrite-nitrogen (NO_x-N), ammonia (NH_3-N), dissolved silica (Si), total dissolved solids (TDS), pH, alkalinity (Alkal), and conductivity (Cond). All samples

were analyzed by the USFS Cooperative Chemical Analytical Laboratory (CCAL) in Corvallis, Oregon. Changes in analytical methods and an accurate record of detection limits were assembled for this evaluation of parameter effectiveness. Current detection limits and levels of precision for CCAL are provided in Table 1.3-1.

Table 1.3-1. Detection limits and levels of precision for CCAL analyses (Cam Jones, pers. comm.).

	TP	PO4	TKN	NH3-N	NO3-N	Si	TDS	pH	Alkal	Cond
Detection Limit	0.002	0.001	0.010	0.010	0.001	0.20	5.0	n/a	0.20	0.4
Precision	0.002	0.001	0.006	0.002	0.001	0.05	5.0	0.100	0.02	2%

Note: All values are mg/L except for conductivity (uS/cm) and pH (pH units). Detection limits are those currently effective for CCAL- some have changed over time.

Results

The percentage of samples with a concentration less than or equal to the analytical level of detection varied among parameters (Table 1.3-2). Dissolved inorganic nutrient concentrations were rarely detectable. Measured concentrations were less than or equal to the detection limit in 100 % of the nitrate plus nitrite-nitrogen samples (n = 351), in 98 % of the ammonia samples (n = 185), and 97 % of the ortho-phosphorus (n = 351) samples analyzed. The concentration of total dissolved solids was less than or equal to the detection limit in 71 % of the samples collected (n = 347). Alkalinity and conductivity were never below detection (n = 351 for each parameter). Total Kjeldahl nitrogen was also never below the method detection limit, however, samples were only collected and measured for this parameter on two occasions over the entire monitoring program (n = 13).

Table 1.3-2. Percent of samples collected from 1986-2004 at Waldo Lake measured at or below the method detection limit.

Sample Site	TP	PO4	TKN	NH3-N	NO3-N	Si	TDS	pH	Alkal	Cond
ALL	74%	97%	0%	98%	100%	40%	71%	0%	0%	0%
LTM	73%	96%	0%	98%	100%	53%	71%	0%	0%	0%
NS	75%	97%	0%	100%	100%	8%	70%	0%	0%	0%

Note- LTM refers to the West Bay long-term monitoring site and NS refers to the North Swim area.

The majority of the chemical parameters monitored in Waldo Lake are near the limits of analytical detection by currently available methods. To further examine the value of chemistry sampling, the data were screened by calculating the percentage of samples below the sum of the method detection limit plus the estimated precision of the CCAL

methods (i.e., the reported value was not necessarily different from the detection limit) (Table 1.3-3). Total phosphorus concentration was either below detection or could not be considered different from the method detection limit in 95 % of the samples collected (n = 345). Dissolved silica concentrations were either below detection or could not be considered different from the method detection limit in 91 % of samples collected at the long-term monitoring station (n = 255). Total dissolved solids concentrations were below detection or could not be considered different from the method detection limit in 95 % of samples collected at the long-term monitoring station (n = 237).

Table 1.3-3. Percent of samples collected from 1986-2004 at Waldo Lake measured at or below the method detection limit plus the precision estimates for each method provided by CCAL.

Sample Site	TP	PO4	NH3-N	Si	TDS
ALL	95%	99%	98%	82%	95%
LTM	95%	98%	99%	91%	94%
NS	94%	100%	100%	65%	95%

Note- LTM refers to the West Bay long-term monitoring site and NS refers to the North Swim area.

Conclusions and Recommendations

Dissolved Inorganic Nutrients

Dissolved inorganic nutrient concentrations were below method detection limits in more than 95 % of the samples. Therefore, we recommend that nitrate plus nitrite-nitrogen, ammonia, and ortho-phosphorus analyses be discontinued. The previous 18 years of monitoring dissolved inorganic nutrient at Waldo Lake were beneficial in that baseline concentrations have been established for nitrate plus nitrite-nitrogen (< 0.001 mg/L), ammonia (< 0.010 mg/L) and ortho-phosphate (< 0.002 mg/L).

Total Phosphorus and Total Nitrogen

Total nitrogen and total phosphorus are the nutrient parameters that define lake trophic status and are the core of long-term monitoring programs. Further, TN to TP ratios can be an important indicator of relative nutrient limitation and can influence interspecific competition. Although most of the total phosphorus sample concentrations over the past 18 years at Waldo Lake were at or below detection limits, the continued monitoring of total phosphorus and the addition of total nitrogen monitoring are

recommended. Measuring the total concentration of these nutrients integrates the dissolved inorganic fractions that are below detection and increases the likelihood of early detection of changes to the lake.

A change in methods from collecting unfiltered samples to coarse filtration of total nutrient samples may be warranted. Due to the low concentrations of nutrients in Waldo Lake, measurement of total phosphorus and total nitrogen in unfiltered water samples is beneficial because there is more material to measure than in a filtered sample. Unfiltered samples can be variable and hard to interpret, however, because large, mobile particles such as zooplankton are included in the sample but are not adequately or consistently sampled due to their avoidance of capture. Prepas and Rigler (1982) addressed these concerns by measuring phosphorus in two alternative size fractions, small and large, with two different sample collection techniques, sample bottles and net tows. The small fraction was collected with a sample bottle and was filtered through a 250 μm mesh. The large fraction was collected with a 250 μm zooplankton net. The mesh size used to separate the two fractions was based on the size of the smallest zooplankter that might be expected to escape from a sampling bottle. They found that by removing the larger fraction, the average variance associated with the mean phosphorus concentration was reduced from 1.0 to 0.02 μg/l. They concluded that the reduction of variance occurred because the larger fraction contained zooplankton with relatively high but variable amounts of phosphorus that occurred in densities too low to be adequately sampled with the smaller fraction.

The recommended approach is for continued total phosphorus monitoring in conjunction with TKN analyses with the following change in methods: samples should be filtered through a coarse mesh prior to analysis. The smallest dominant mobile zooplankton in Waldo Lake, *Bosmina longirostris*, ranges between 250-700 μm. Therefore filtering with a mesh size of 250 μm will eliminate problems associated with sampling large mobile zooplankton yet retain sufficient particulate material for measurable amounts of total phosphorus and nitrogen.

Carbonate System Parameters

A major goal of the summer 2005 sampling season will be to examine the uncertainties in measurements of the inorganic carbon complex in Waldo Lake. Although problems exist in the current methods used to measure pH and alkalinity (See Section 2.2), monitoring with current methods should continue until there is sufficient overlap for comparison with more accurate methods.

Dissolved Silica

Continued monitoring of dissolved silica is justified. Silica is an important parameter for interpreting changes in algal species composition. A considerable percentage of dissolved silica samples were measurable, relative to other parameters. Dissolved silica concentrations were above the method detection limit in 60 % of the samples, although when considering the method precision only 18 % were different than the detection limit.

Total Dissolved Solids

Total dissolved solids, a surrogate measure for the amount of salts plus carbonates in a sample, were above detection limits in 29 % of the samples and above the detection limit plus the precision in only 5 % of samples. Since there are more direct and accurate measures of salts and carbonates (conductivity and alkalinity) continued monitoring of total dissolved solids is not recommended.

Summary of Recommendations

The recommended plan for long-term monitoring of analytical chemistry in Waldo Lake is to analyze total phosphorus and total nitrogen (250 μm filtration); pH, alkalinity, and conductivity (unfiltered fraction); and dissolved silica (0.7 μm filtration). Four collections should be made each trip. One from the surface in the North Swim area, one from the surface at the LTM site, one from the hypolimnion at the LTM site (e.g., 100 m), and one randomized duplicate. If changes or trends in the lake are observed in total nutrients, pH, alkalinity, conductivity, biological monitoring, or in situ monitoring, the long-term monitoring plan can be expanded to include other variables that may help explain trends.

2 Biological Characteristics

2.1 Multivariate Analysis of Long-Term Monitoring Data

Introduction

An analysis of unpublished data collected by the USDA Forest Service at Waldo Lake between 1998 and 2003 (Sytsma et al. 2004) showed interesting changes in Waldo Lake biology compared to findings of previous publications (Sweet 2000; Vogel and Li 2000). The phytoplankton community, prior to 1998 was dominated by one species, *Woloszynskia neglecta*, (syn. *Glenodinium neglectum*). Beginning in 1998, *Oocystis pusilla* became a dominant member of the phytoplankton community (Sytsma et al. 2004). Vogel and Li (2000) discussed the changes in Waldo Lake zooplankton community following fish and predatory mysid shrimp stocking activities. Their findings highlighted the elimination of large bodied cladocerans as a result of predation, followed by an absence of zooplankton for a period of years and a more recent increase in smaller bodied zooplankton densities. Sytsma et al. (2004) discussed the vertical distribution of zooplankton in the water column. *Bosmina longirostris* was the dominant species of zooplankton in total density, occupying the hypolimnion. *Diaptomus kenai x shoshone* occupied the epilimnion in high densities.

Two mechanisms drive changes in phytoplankton assemblages and densities in a lake. The first, where phytoplankton respond to a bottom-up change in lake chemistry, light or other physical parameters and the second, a response to a top-down driver such as predation. The two theorized mechanisms are not necessarily independent, rather they may be closely coupled (Kalff 2002).

A multivariate statistical approach was used to investigate possible relationships among environmental factors and biological changes in Waldo Lake. Multivariate techniques are powerful tools for assessing seasonal, yearly and vertical variation within species assemblages. We had two objectives: (1) to assess the temporal and spatial variation in both environmental and biological data and examine possible correlations between patterns of change in biological and environmental factors and (2) use

correlations and patterns to develop future research questions and assess the current long-term monitoring protocol. The primary questions addressed were:

1) Are there seasonal, yearly and vertical differences in the phytoplankton and zooplankton communities?

2) Are there seasonal, yearly and vertical differences in physical and chemical variables?

3) Are there possible relationships between biological and physical variables?

Methods

Available data

Chemistry, light, phytoplankton and zooplankton data were collected by USDA Forest Service employees between 1993 and 2003 at Waldo Lake. A complete description of sampling methods and equipment used is described in the Waldo Lake Long-Term Monitoring Filed Sampling Quality Assurance and Quality Control Project Plan (Johnson 2003) and updated quality assurance protocols were implemented in 2004.

Consistent personnel made comparison between years feasible. All field samples were collected by John Salinas of Cascade Research Group. All chemistry samples were analyzed by Cooperative Chemical Analysis Laboratory (CCAL) at Oregon State University. All phytoplankton samples were identified and enumerated by Jim Sweet at Aquatic Analysts. All zooplankton samples were identified and enumerated by Allan Vogel of ZP's Taxonomic Services.

The availability of data in digitally archived form was a limiting factor for data included in this analysis. Data available included phytoplankton density and biovolume collected between 1993 and 2003, zooplankton density collected between 1996 and 2003, light (percent of surface light intensity with depth) collected between 1998 and 2003 and chemistry (pH, alkalinity, conductivity, total phosphorus (TP), soluble reactive phosphorus or orthophosphate (Ortho-P), nitrates (NO_2+NO_3-N), ammonia-nitrogen (NH_3-N), silica (Si) and total dissolved solids (TDS)) collected between 1993 and 2003; with two exceptions, in 1995 when phytoplankton samples were collected but were not available and 2000 when only chemistry samples were collected. Only samples collected

around or prior to mid day from the long-term monitoring station were included in this analysis.

Duplicate chemistry samples were not collected in the field during the 1993-2003 periods, but duplicate analyses of samples collected were completed in the laboratory. Relative percent differences between samples were analyzed previously (Sytsma et al. 2004). Duplicate laboratory analyses were not utilized in this analysis. Recording of light profiles were not repeated. No duplicate samples were collected or enumerated for phytoplankton or zooplankton.

Chemistry and phytoplankton were collected at discrete depths. Collection depths were inconsistent throughout the sample period. Common depths included 0, 4, 8, 12, 16, 24, 40, 60, 80, 100 and 120-meters. Zooplankton samples were collected with a series of 20 meter tows collected from 120 meters to the surface. "Ideal tows" were defined as 0-20, 20-40, 40-60, 60-80, 80-100 and 100-120 meters.

Light data included a percent of surface light at a given depth for Red, Green, Blue wavelengths and for photosynthetically active radiation (PAR) across the 400-700 nm range. Light data were only collected on sunny days with consistent cloud cover. Light data were only collected to 80-meters in depth.

Data Preparation

Samples collected at uncommon depths were removed from the dataset for assessing spatial and temporal variability among samples for a given variable. All phytoplankton, chemistry and light data collected at discrete depths were matched within ± 2.0 m for multivariate analyses comparing variation between physical and biological samples. Samples that did not coincide were removed from the dataset. All zooplankton tows collected were used when relating the phytoplankton dataset to the zooplankton dataset. When more than one phytoplankton sample coincided with a given zooplankton tow multiple phytoplankton samples were averaged.

Chemistry Data

For many of the constituents, nutrient concentrations were less than or equal to the method detection limit for most of the samples collected (See Section 1.3). The reliability of reported concentrations less than the method detection limit is unknown (Sytsma et al. 2004), but censored data, reported below the detection limit, carries a high degree of uncertainty (Helsel and Hirsch 1993). In this analysis, values reported below the detection limit, based on extrapolated values, were replaced with the detection limit (Table 2.1-1). Replacing values below the detection limit with the detection limit resulted in estimates above the true values for this analysis.

Table 2.1-1. Detection limit for chemical variables (CCAL laboratory reports)[1]

Chemical Parameter	Detection Limit
Total-P	0.002 mg/L
Dissolved PO_4-P	0.001 mg/L
NO_2+NO_3-N	0.001 mg/L
NH_3--N	0.002 mg/L
Dissolved Si	0.15 mg/L
Total Dissolved Solids	5.0 mg/L

Univariate analysis was used to determine the chemistry dataset used for multivariate analysis. Univariate analysis included the assessment of the variation between depths, months and years for all chemical constituents. Unchanging variables, (orthophosphate, pH, specific conductance, and nitrates) with high occurrences of the detection limit value, were not used for this analysis. Ammonia data were not included because samples were only collected for a limited period, between 2002 and 2003; and inadequate range of years for multivariate analysis. Therefore, the chemistry dataset was limited to total phosphorus, silica, alkalinity and total dissolved solids.

[1] Values in Table 2.1.1 were used for all analyses discussed in this section. Subsequent to completion of this work additional information regarding how detection limits and precision estimates have changed over time was obtained from CCAL (See Section 1.3).

Light Data

Light data were collected with two different instruments during the period of interest. In 1998-1999 a Lake Lite® photometer was used and profiles were very erratic (Sytsma et al. 2004). Poor data quality led to a change in instrumentation (Salinas pers. comm.). In 2001-2003 a Khal® photometer was used. There was no overlap of equipment. Therefore, the light dataset was treated in two ways for this analysis (1) a complete dataset of all data collected between 1998 and 2003 and (2) a subset of data collected between 2001 and 2003 with the new photometer.

Biological Data

Rare species were removed for portions of this analysis. Phytoplankton and zooplankton species were collated into a full dataset of all species present and a subset of "major species". A species was considered a "major species" when there were at least three occurrences where the percent density (relative abundance) was greater than one percent. The "major species" dataset included 43 species of phytoplankton and 13 species of zooplankton (Appendix B).

In addition to "all species" and "major species", phytoplankton species were grouped based on class. The class list included Bacillariophyceae, Dinophyceae, Chlorophyceae, Chryptophyceae, Chrysophyceae, Cyanophyceae and Unknown.

Zooplankton tow distances were not consistent throughout the sampling period. Only tows that were within ± 2.0 m of an "ideal tow" were utilized in comparing zooplankton samples for spatial and temporal variability.

The identification of the copepod species, *Diaptomus kenai x shoshone* was inconsistent throughout the sampling period. In 1996 this species was identified as *Diaptomus shoshone*, post-1996 it was identified with the hybrid nomenclature *Diaptomus kenai x shoshone* (Vogel and Li 2000). For this analysis all occurrences were changed to the hybrid nomenclature. Taxonomic identification remains unconfirmed.

Zooplankton species were grouped as Cladocerans, Copepods and Others (which include rotifers, protozoans, and other miscellaneous zooplankton). This classification

system removed inconsistencies in the dataset classification system between years made by the taxonomist, whereby, for example, rotifers and *Difflugia sp.*, were classified in different groups.

Transformations

Transformations were completed to normalize variables in the chemistry dataset. Transformations were used on the species datasets to put less weight on the dominant species and minimize the effect of to the high occurrence of rare species. All variables in the chemistry dataset, phytoplankton density and biovolume, and zooplankton density were log (x+1) transformed. Percentage data including light data, phytoplankton percent density and percent biovolume and zooplankton percent density were transformed using a square root + arcsine transformation (Zar 1996). Since the primary goal of this analysis was exploratory and not based on hypothesis testing, the assumptions of normal distribution were not met and non-parametric statistics were used.

Statistical Methods

Spatial and temporal trends among environmental and biological samples

Comparative univariate analyses of box plots representing mean and median values were completed to visually assess trends in chemical variables, phytoplankton density and biomass and zooplankton density. Spatial distribution was assessed with respect to thermocline depth and depth of sample collection. Temporal trends were also assessed based on monthly and yearly changes. Non-parametric Kruskal-Wallis ANOVA and Tukey-type multiple comparison test for unequal sample sizes within groups were used to test the significance of temporal and spatial variations (Zar 1996).

Relationships among environmental and biological samples

A number of exploratory multivariate techniques were used, the PRIMER program (Plymouth Routines in Multivariate Ecological Research) was used for these analyses. Principle component analyses (PCA) were carried out to determine the similarity of samples based on their chemical composition. PCA groups variables according to their co-occurrences in samples such that the underlying structure of the data can be viewed.

Log (x+1) transformed data for TP, SI, TDS and alkalinity were used for two PCA analyses: 1) the entire chemistry dataset available (1993-2003, n = 168), and 2) the chemistry samples which coincided with the phytoplankton dataset (1993-2003, n = 114). Non-metric multi-dimensional scaling (MDS) plots were created to depict the relative ecological distance among samples based on depth or strata (epi- meta-, and hypolimnion), month and year. Each MDS plot provided a measure of stress showing how well the 2- or 3-dimensional plot represented the multi-dimensional structure of the data. MDS plots were created for phytoplankton, based on 191 samples collected between 1993 and 2003 for "all species" and "major species" and for zooplankton data, based on 134 samples collected between 1996 and 2003 for "all species" and "major species". Finally, variation among groups of zooplankton and major groups of phytoplankton and zooplankton were assessed using non-parametric Spearman rank correlation.

Relationships between environmental and biological samples

The Biota and/or Environmental Matching (BIOENV) technique was used to calculate a rank correlation measure of agreement between the phytoplankton dataset and the sets of abiotic environmental data (Clarke and Gorley 2001). The phytoplankton dataset was compared with the chemistry dataset. The four chemistry variables (TP, SI, TDS and Alkalinity) were compared to the phytoplankton "all species" and "major species" datasets for data from 1993-2003. Additionally, the phytoplankton dataset was compared to the light dataset in two groups (1) the entire data set from 1998-2003, consisting of 86 samples and (2) 2001-2003 data, consisting of 52 samples.

The phytoplankton dataset was compared to the zooplankton dataset using the RELATE function in PRIMER, providing a measurement of how closely two sets of multivariate data were related (Clarke and Gorley 2001). The RELATE function developed a rank correlation between matching matrices and produced a measure of significance of the correlation. In these analyses, 119 samples with the distinctions of "all species" and the "major species" and species "groups" were examined for multivariate correlations based on percent density and density. To assess which groups

of phytoplankton were correlated with zooplankton groups, univariate non-parametric spearman rank correlations were completed.

It should be noted that the set of data used for multivariate analysis comparing environmental variables to the phytoplankton did not represent the data available to the fullest extent. Due to errors in the database, samples were not matched adequately. Specifically, for PCA and BIOENV analyses based on samples with both chemistry and phytoplankton data, two dates (September 6, 1996 and October 9, 1999) were inadvertently omitted. PCA for chemistry samples which match to phytoplankton samples was repeated including the two missing dates (Appendix A). This analysis was very similar to the PCA presented previously. The October 9, 1999 date was also omitted from BIOENV analyses between phytoplankton and light; this analysis was not repeated.

Results

Spatial and temporal trends among environmental and biological samples

Chemistry

Some chemical variables varied by depth and by year. Monthly variations were the least distinct. Total phosphorus, alkalinity, TDS and silica varied by year (Figure 2.1-1). Silica and TDS varied with depth (Figure 2.1-2). Specific conductivity, pH, orthophosphate and nitrates did not exhibit strong variation by year, month or by depth (Appendix B).

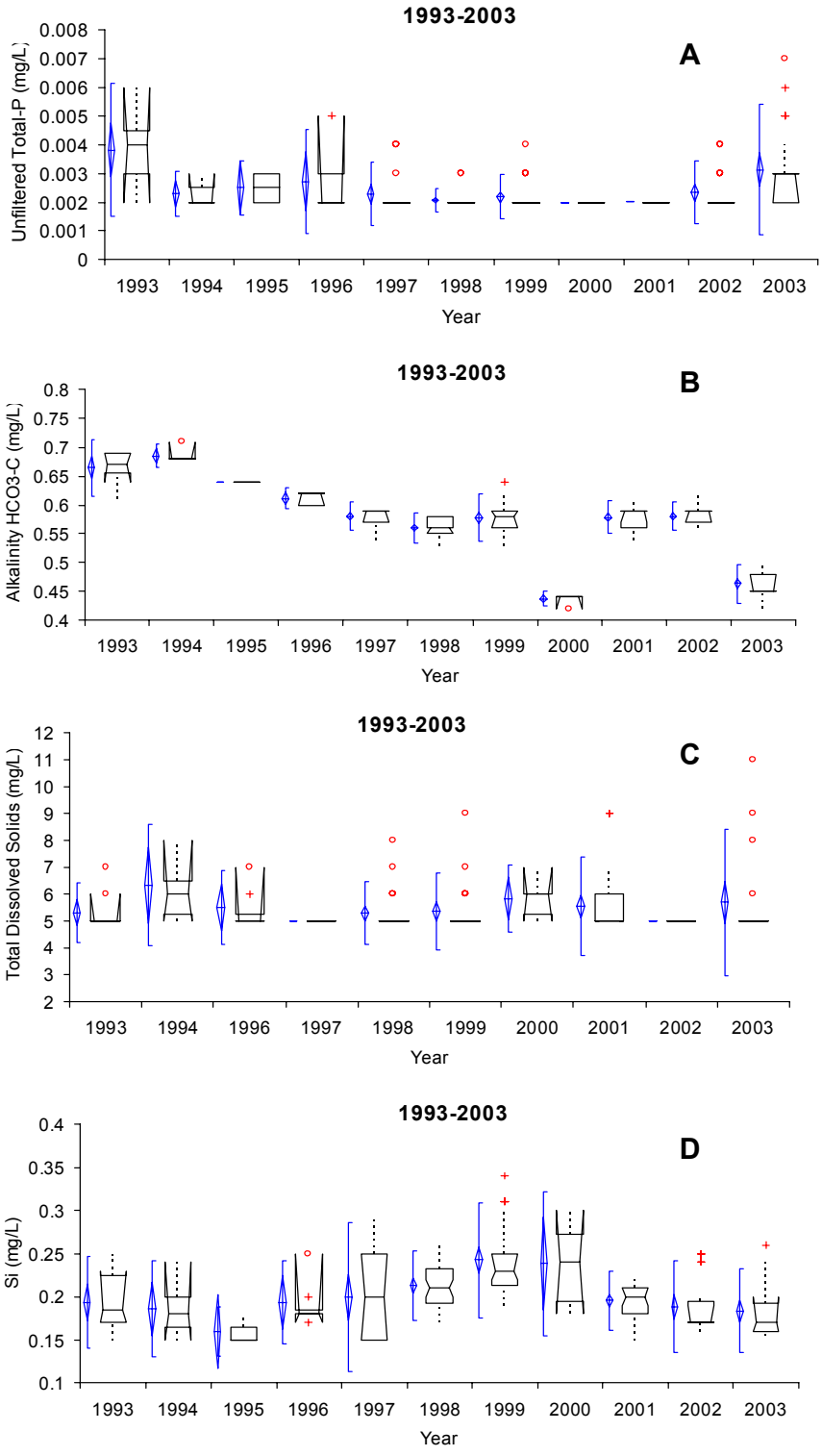

Figure 2.1-1. 1993-2003 annual variation in (A) total phosphorus (B) alkalinity (C) total dissolved solids and (D) silica. Diamonds represent the mean and error bars the 95 % confidence interval around the mean. The middle line of the boxes represents the median, and the top and bottom lines are the confidence interval around the median. Circles and plus signs are outliers.

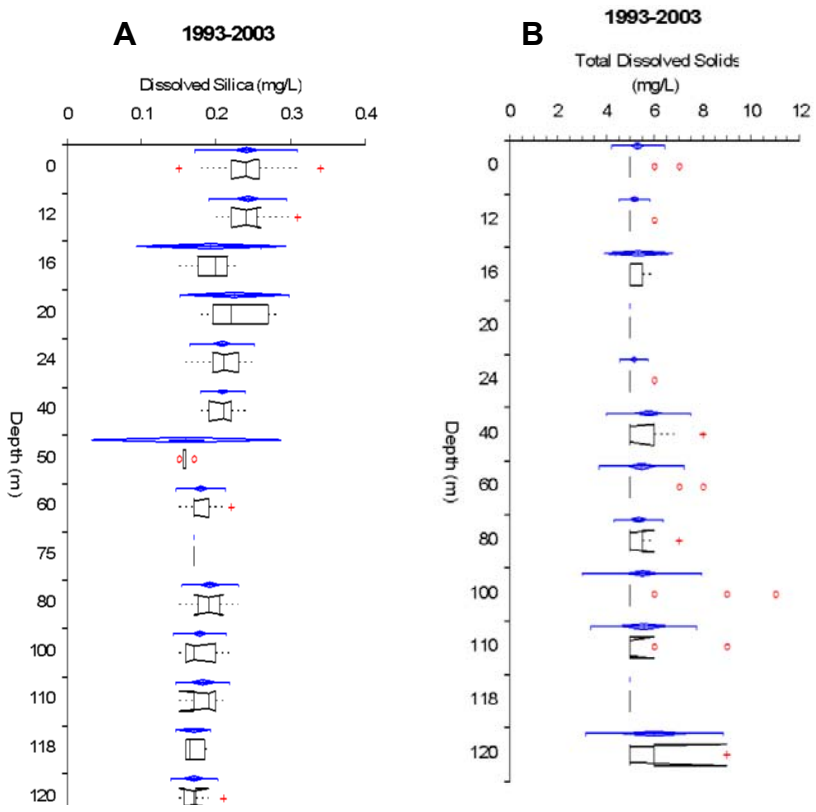

Figure 2.1-2. 1993-2003 variation with depth in (A) dissolved silica and (B) total dissolved solids. Diamonds represent the mean and error bars the 95 % confidence interval of the mean. The middle line of the boxes represents the median, and the top and bottom lines are the confidence interval around the median. Circles and plus signs are outliers.

Total phosphorus varied significantly by year (Kruskal-Wallis non-parametric ANOVA $p < 0.0001$). TP was highest in 1993 and 2003; 1993 concentrations were statistically different from 1998 through 2002 concentrations but were not different from other years; 2003 was statistically different from 2001, but not other years (non-parametric Tukey-type multiple comparison test for unequal sample sizes within groups (Table 2.1-2; Zar 1996).

Table 2.1-2. The significance of yearly differences in total phosphorus between 1993 and 2003: Calculated Q values (shown) indicate the difference between years was significant. (Q critical = 3.317 (α = 0.05, n = 11 years) an X indicates the difference between years was not significant, Q calculated < Q critical).

	1993	1994	1995	1996	1997	1998	1999	2000	2001	2002	2003
1993											
1994	X										
1995	X	X									
1996	X	X	X								
1997	X	X	X	X							
1998	4.13	X	X	X	X						
1999	3.87	X	X	X	X	X					
2000	3.2	X	X	X	X	X	X				
2001	4.51	X	X	X	X	X	X	X			
2002	X	X	X	X	X	X	X	X	X		
2003	X	X	X	X	X	X	X	X	3.62	X	

Alkalinity varied significantly by year (Kruskal-Wallis non-parametric ANOVA $p < 0.0001$). Alkalinity was highest in 1993 and 1994 and lowest in 2000 and 2003. Alkalinity was not significantly different between 1993 and 1997. In 2000 alkalinity was significantly different from all years with the exception of 1998 and 2003; in 2003 alkalinity was significantly different from all years except 1998 and 2000 (non-parametric Tukey-type multiple comparison test for unequal sample sizes within groups, (Table 2.1-3; Zar 1996).

Table 2.1-3. The significance of yearly differences in alkalinity between 1993 and 2003: Calculated Q values (shown) indicate the difference between years was significant. (Q critical = 3.317 (α = 0.05, n = 11 years) an X indicates the difference between years was not significant, Q calculated < Q critical.)

	1993	1994	1995	1996	1997	1998	1999	2000	2001	2002	2003
1993											
1994	X										
1995	X	X									
1996	X	X	X								
1997	X	X	X	X							
1998	5.46	4.72	3.19	3.92	X						
1999	3.86	3.4	X	X	X	X					
2000	6.08	5.62	4.32	4.99	4.08	X	3.81				
2001	3.63	X	X	X	X	X	X	4.03			
2002	3.26	X	X	X	X	X	X	4.03	X		
2003	7.47	6.45	4.54	5.67	5.01	X	5.03	X	5.38	5.16	

TDS varied significantly by year (Kruskal-Wallis non-parametric ANOVA $p = 0.0012$). TDS were highest in 1994 (mean = 6.3 ± 1.3 s.d., n = 6) and lowest in 1997(mean = 5.0 ± 0.0 s.d., n = 14). No specific years were significantly different from one another (non-parametric Tukey-type multiple comparison test for unequal sample sizes within groups) (Zar 1996).

Silica varied significantly by year (Kruskal-Wallis non-parametric ANOVA $p < 0.0001$). Silica concentrations were highest in 1999 and lowest in 1995. In 1999, silica concentrations were significantly different from 1994-1995 and 2001-2003 concentrations (non-parametric Tukey-type multiple comparison test for unequal sample sizes within groups) (Table 2.1-4; Zar 1996).

Table 2.1-4. The significance of yearly differences in silica between 1993 and 2003: Calculated Q values (shown) indicate the difference between years was significant. (Q critical = 3.317 (α = 0.05, n = 11 years) an X indicates the difference between years was not significant, Q calculated < Q critical.)

	1993	1994	1995	1996	1997	1998	1999	2000	2001	2002	2003
1993											
1994	X										
1995	X	X									
1996	X	X	X								
1997	X	X	X	X							
1998	X	X	X	X	X						
1999	X	3.56	3.53	X	X	X					
2000	X	X	X	X	X	X	X				
2001	X	X	X	X	X	X	4.02	X			
2002	X	X	X	X	X	X	4.26	X	X		
2003	X	X	X	X	X	X	4.79	X	X	X	

TDS were highest in the hypolimnion, but differences between limnetic layers of the lake (Epi-, Meta-, Hypolimnion, based on thermal profiles) were not significant (Kruskal-Wallis non-parametric ANOVA $p=0.1385$). Silica concentrations varied significantly between limnetic layers (Kruskal-Wallis non-parametric ANOVA $p<0.0001$). Silica was lowest in the hypolimnion. Concentrations were significantly different between the hypolimnion and the epilimnion and metalimnion, but not between the epilimnion and the metalimnion (non-parametric Tukey-type multiple comparison test) (Table 2.1-5).

Table 2.1-5. The significance of differences in silica from 1993-2003 between limnetic layers. Calculated Q values indicate the difference between years was significant (Q critical = 2.394(α = 0.05, n = 3 layers) X indicates the difference between years was not significant Q calculated < Q critical).

	Epilimnion	Metalimnion	Hypolimnion
Epilimnion			
Metalimnion	X		
Hypolimnion	7.6	3.56	

Principle Component Analysis

For the PCA of all samples in the chemistry dataset (n = 168, Figure 2.1-3 A and Table 2.1-6 A), PC1 explained 31 % of the variation in the dataset, PC2 explained an

additional 25.3 %, and the cumulative variation of the first two principle components was 56.3 %. Eigen vectors for the first principle component were highest for total phosphorus, with a gradient of phosphorus concentrations along the PC1 axis, eigen vectors for silica and total dissolved solids were equally as high, indicating that the first principle component did not have a strong underlying structure. The structure of the second principle component was based on alkalinity, with a gradient of alkalinity in the PC2 axis, the eigen vector for alkalinity equaled 0.908. There was a general yearly trend along the PC2, based on alkalinity. Alkalinity was higher in 1993 than in 2003.

For the PCA based only on the chemistry samples corresponding with phytoplankton samples collected (n = 114, Figure 2.1-3 B and Table 2.1-6 B), PC1 explained 34.6 % of the variation in the chemistry dataset, PC2 explained an additional 25.5 % of the variation; cumulatively the first two principle components explained 60.1 % of the total variation of the chemistry dataset. The structure of the first principle component was not solely based on any individual component; eigen vectors for all four variables were similar. The structure of the second principle component was based most strongly on total dissolved solids; the eigen vector for TDS equaled 0.832.

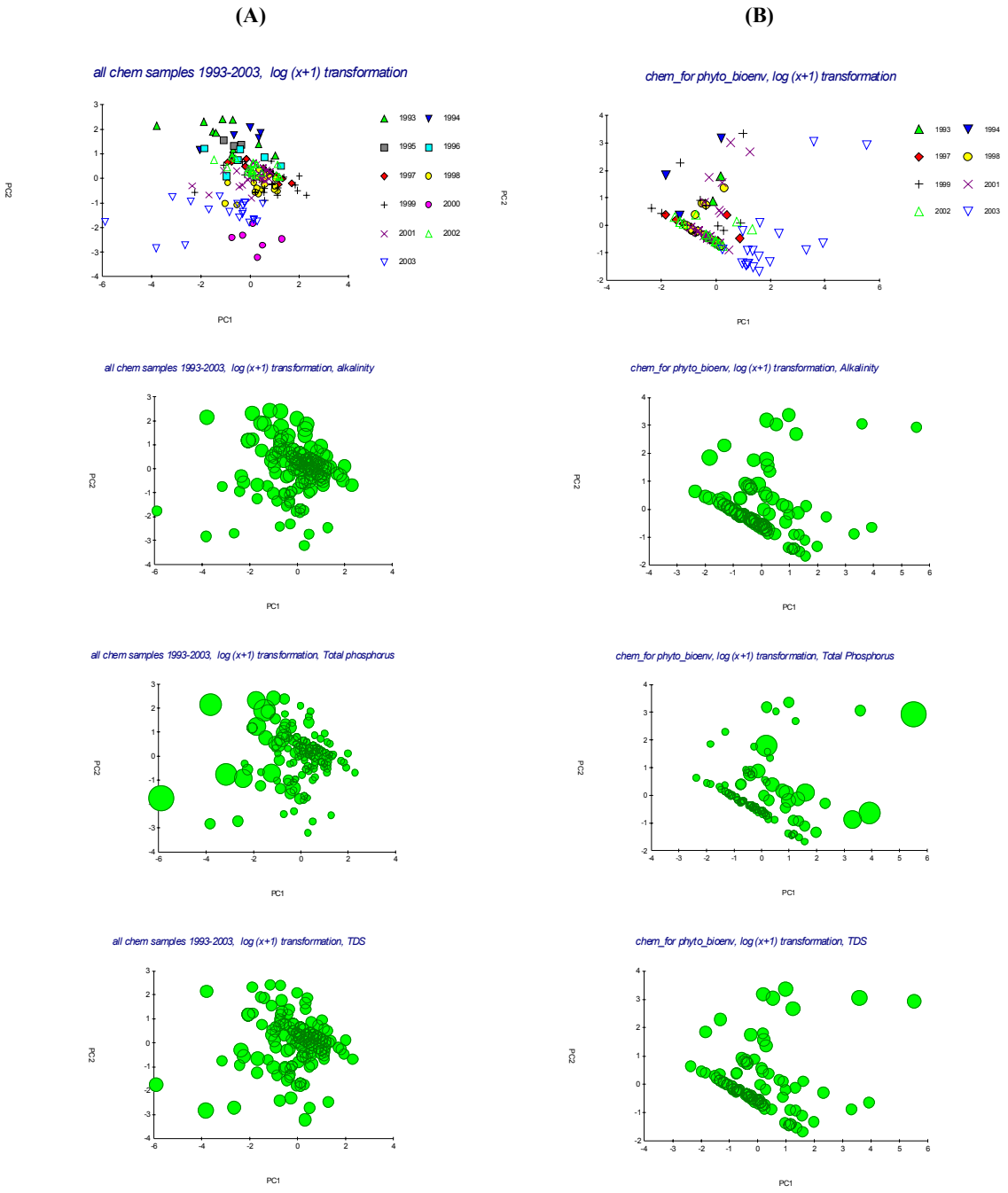

Figure 2.1-3. Principle component analysis of 1993-2003 Waldo Lake chemistry data for all samples (Column A) and for only corresponding chemistry and phytoplankton samples (Column B). Parameters included: total phosphorus, alkalinity (measured in mg/l HCO3-C), dissolved silica and total dissolved solids.

Table 2.1-6. Principle component analysis scores for all samples (Column A) and for only corresponding chemistry and phytoplankton samples (Column B). Parameters included: total phosphorus (TP), alkalinity (measured in mg/l HCO3-C), dissolved silica and total dissolved solids (TDS).

(A)

Eigen values

PC	Eigen values	% Variation	Cumulative % Variation
1	1.24	31	31
2	1.01	25.3	56.3
3	0.93	23.3	79.6
4	0.82	20.4	100

Eigen vectors

Variable	PC1	PC2	PC3	PC4
TP (mg/l)	-0.649	0.156	0.096	-0.738
Alkalinity	0.108	0.908	0.378	0.146
Si (mg/l)	0.519	-0.278	0.686	-0.427
TDS (mg/l)	-0.545	-0.271	0.614	0.502

(B)

Eigen values

PC	Eigen values	% Variation	Cumulative % Variation
1	1.39	34.6	34.6
2	1.02	25.5	60.1
3	0.92	22.9	83
4	0.68	17	100

Eigen vectors

Variable	PC1	PC2	PC3	PC4
TP (mg/l)	0.548	0.239	0.613	-0.516
Alkalinity	-0.594	0.432	-0.187	-0.653
Si (mg/l)	-0.504	0.253	0.709	0.423
TDS (mg/l)	0.304	0.832	-0.294	0.358

Light

Analysis of light data was completed previously (Sytsma et al. 2004). In summary, light penetrated deep in to the water column. One percent of surface PAR commonly reached depths below 70 m. Seasonally, light attenuation increased as the summer progressed and resulted in changes in the depth of the photic zone.

Phytoplankton

The Waldo Lake community currently consists primarily of three major species of phytoplankton: two species of dinoflagellates, *Woloszynskia neglecta* and *Hemidinium sp.* and a chlorophyte, *Oocystis pusilla*. *W. neglecta* was the dominant species of phytoplankton until 1998-1999 when the density of *O. pusilla*, increased and it became a key species in the phytoplankton community at Waldo Lake (Figure 2.1-4).

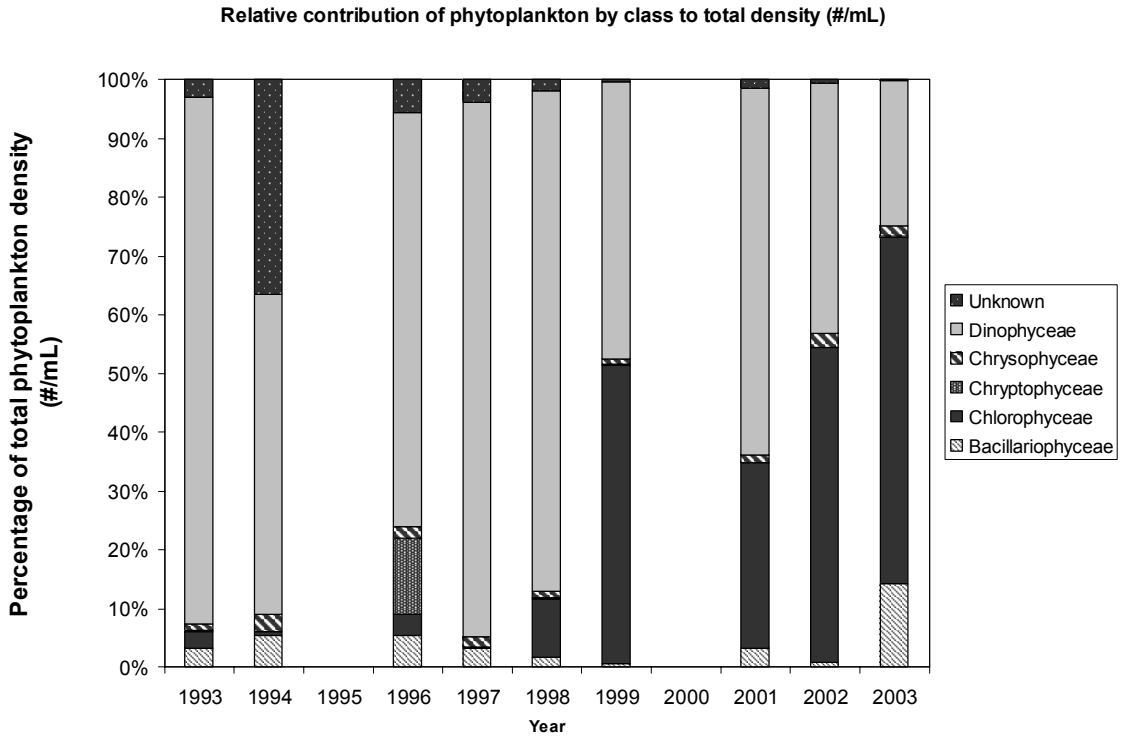

Figure 2.1-4. Total average density for all depths and all dates sampled from 1993-2003, shown as percentage of total phytoplankton density for each class.

No consistent monthly patterns (May-October) were found for the three major species of algae in the lake, *W. neglecta*, *Hemidinium sp*. and *O. pusilla* (Figure 2.1-5).

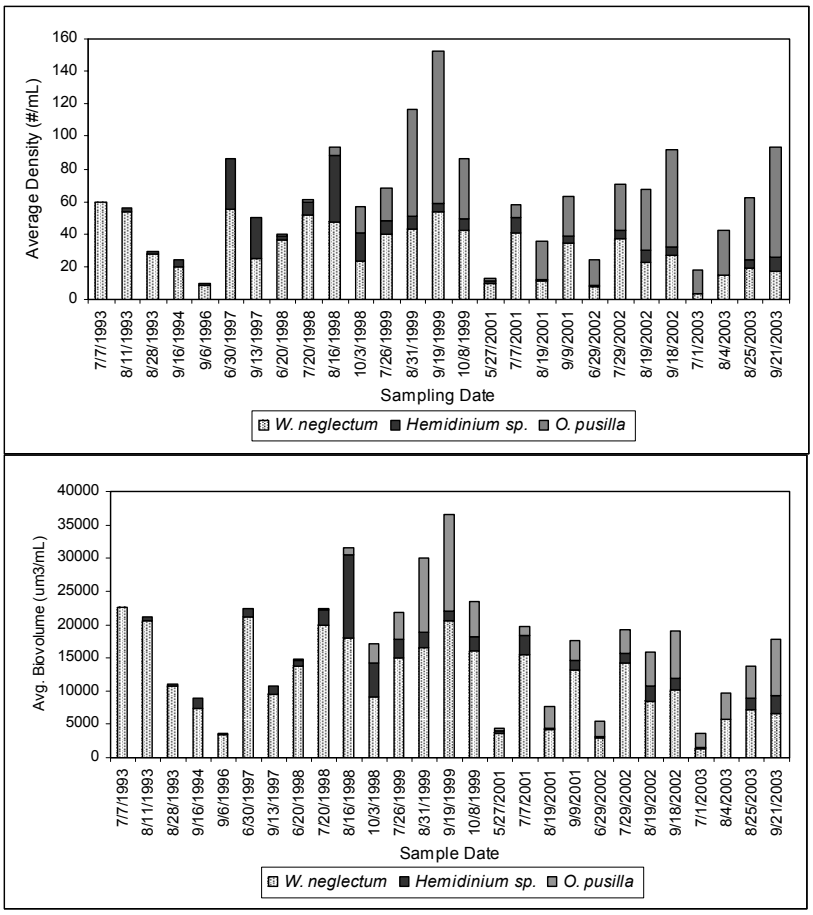

Figure 2.1-5. Average density and biovolume for all depths collected on each sampling date, for *W. neglectum*, *Hemidinium sp*. and *O. pusilla*, the three most prominent species at Waldo Lake, 1993-2003.

Yearly trends varied among species. Density and biovolume are shown for comparaison of overall abundance and biomass contribution (Figure 2.1-6 and Figure 2.1-7). All phytoplankton decreased in 1996. *W. neglecta* decreased in relative abundance in 2001-2003. *Hemidinium sp*. was variable between 1993 and 2003, peaking in 1997 and 1998. *O. pusilla* was practically non-existent until 1998; their abundance increased since.

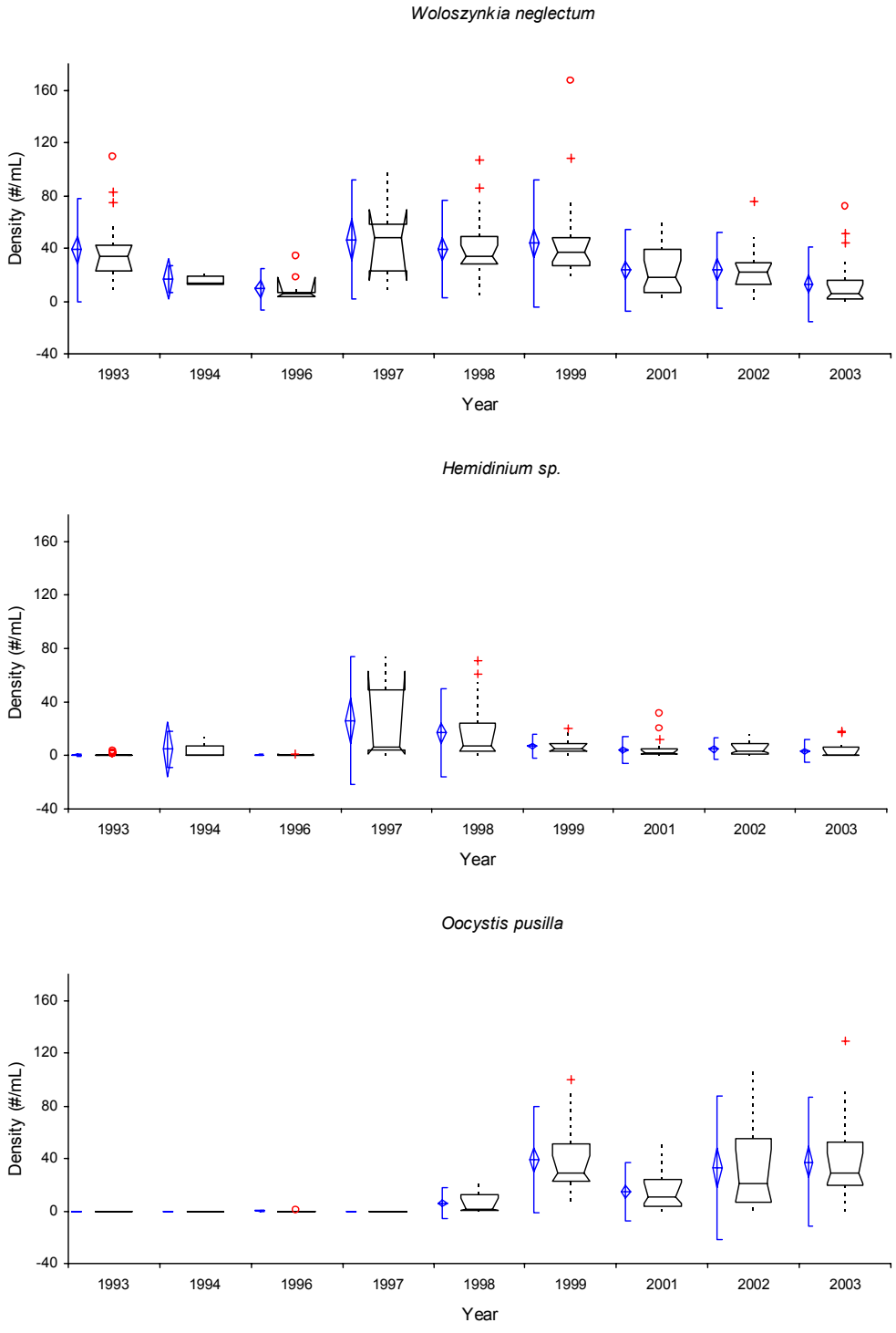

Figure 2.1-6. Semi-quantitative comparisons of yearly variations in density of three prominent species of phytoplankton at Waldo Lake, *W. neglectum*, *Hemidinium sp.*, and *O. pusilla*, 1993-2003. Diamonds represent the mean and the lines are 95 % confidence intervals around the mean. The middle line of the box represents median, and the top and bottom lines are the 95 % confidence intervals around the median. Circles and plus signs are outliers.

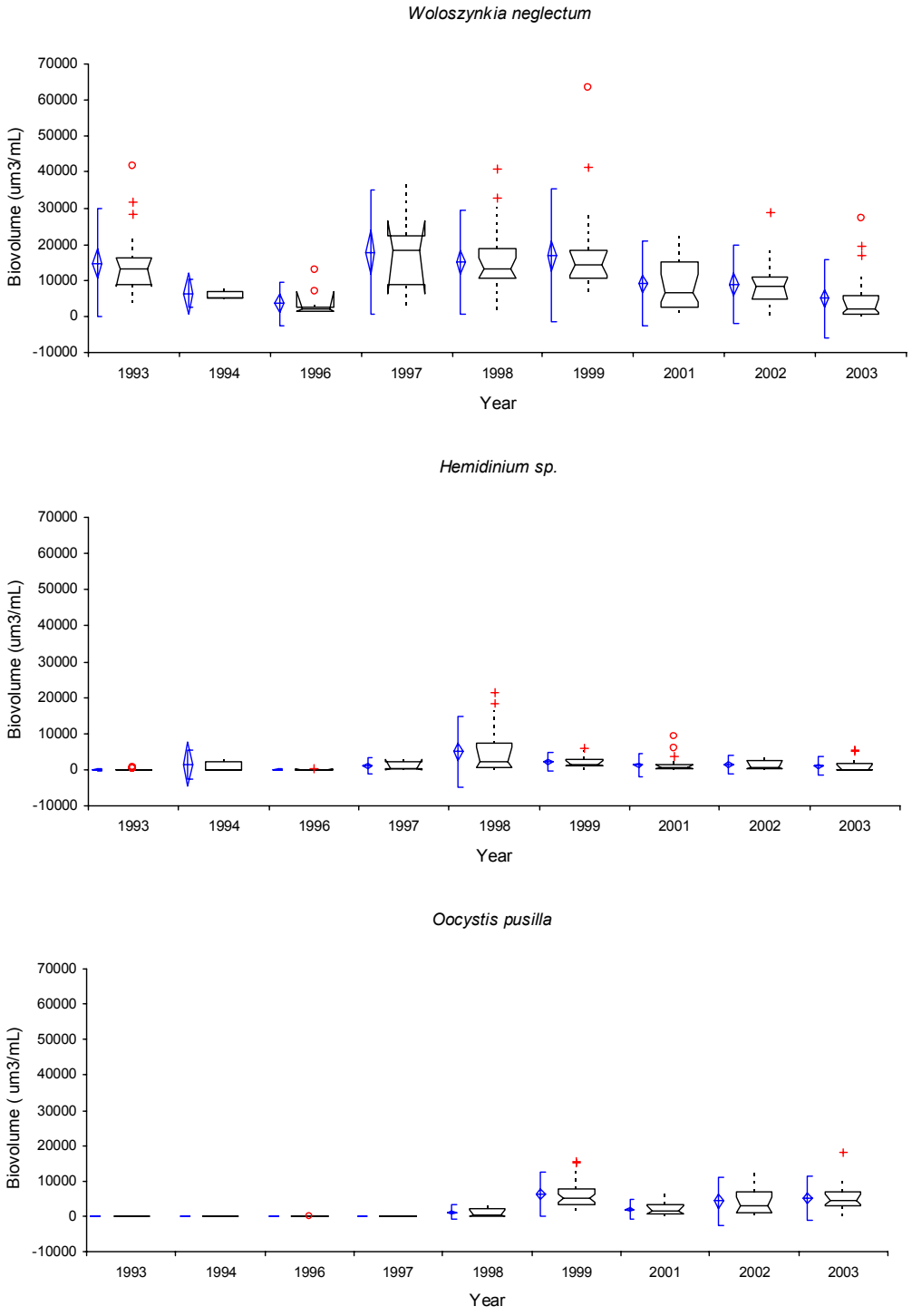

Figure 2.1-7. Semi-quantitative comparisons of yearly variation in biovolume of three prominent species of phytoplankton at Waldo Lake, *W. neglectum*, *Hemidinium sp.*, and *O. pusilla*, 1993-2003. Diamonds represent the mean and the lines are 95 % confidence intervals around the mean. The middle line of the box represents median, and the top and bottom lines are 95 %confidence interval around the median. Circles and plus signs are outliers.

Vertical partitioning of species in the water column is evident on some sampling dates. However, the vertical distributions for an individual species, were inconsistent during the analysis period. Prior to 1998, the vertical distribution of *W. neglecta* was variable; between 1993 and 1998 mean abundance was highest in depths between 60 and 90 m (Sweet 2000). Between 1998 and 2003, the vertical distribution of phytoplankton also was highly variable among sampling dates. On average, *W. neglecta* had a higher relative abundance in the upper depths of the water column and *O. pusilla* was higher in the lower depths. The vertical distribution of *Hemidinium sp.* was variable, with high relative abundance in the upper 40 m for many sampling dates (Sytsma et al. 2004).

Non-metric multi-dimensional scaling

The stress produced with three-dimensional plots of the ecological distance between phytoplankton samples represented the data to a higher degree of certainty than the two-dimensional plots (Table 2.1-7) (Clarke and Gorley 2001).

Table 2.1-7. Stress levels of non-metric multi-dimensional scaling plots of Waldo Lake phytoplankton data collected 1993-2003.

		3-Dimensional stress	2-Dimensional stress
Percent Density	All species	0.1	0.14
	Major species only	0.1	0.13
Percent Biovolume	All species	0.1	0.14
	Major species only	0.1	0.13

The ecological distance among samples shown in the MDS plots was based on the species composition of each sample. Samples with high percent density of the three major species *W. neglecta*, *Hemidinium sp*. and *O. pusilla* were clustered in the MDS plots (two-dimensional plots shown; Figure 2.1-8), the same patterns were true for percent biovolume (not shown).

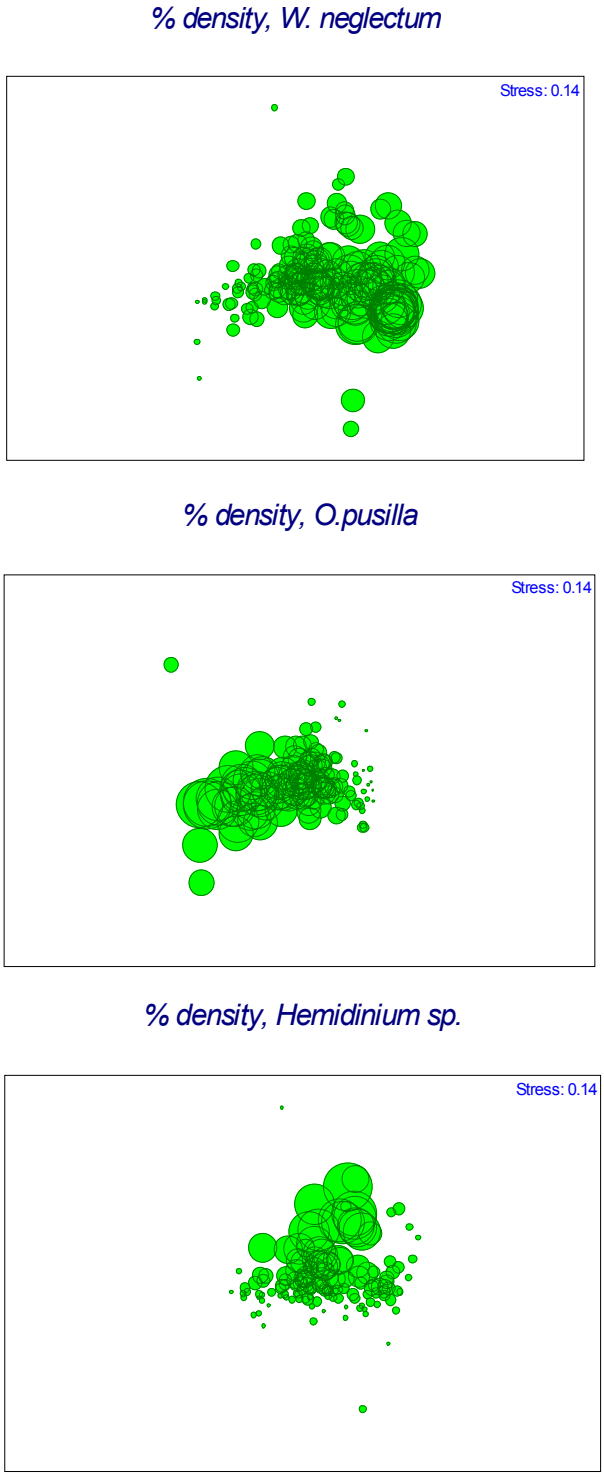

Figure 2.1-8. Waldo Lake phytoplankton species percent density from 1993-2003, non-metric multi-dimensional scaling (MDS) plots for *W. neglecta*, *Hemidinium sp*. and *O. pusilla*.

Vertical distribution patterns based on ecological distance between sample groups were not apparent. MDS plots did not display distinguishable patterns in phytoplankton percent density or percent biovolume based on depth (Figure 2.1-9 and Figure 2.1-10). All of the samples were in a single clustered group. The representation only plotting the major species of phytoplankton did not aid in distinguishing any patterns with depth compared to the representation based on all species.

Temporal patterns were apparent in MDS plots. Clustering of phytoplankton percent density and percent biovolume samples based on month of sampling showed that August and September were grouped and June and July were grouped, with May and October mixed between them. Additionally, yearly trends existed; 1993-1996 samples were grouped, and 2001-2003 samples were grouped with 1997-1999 in the intermediate. Density and biovolume (figures not shown) did not show distinctions between months and years as clearly as percent density and percent biovolume.

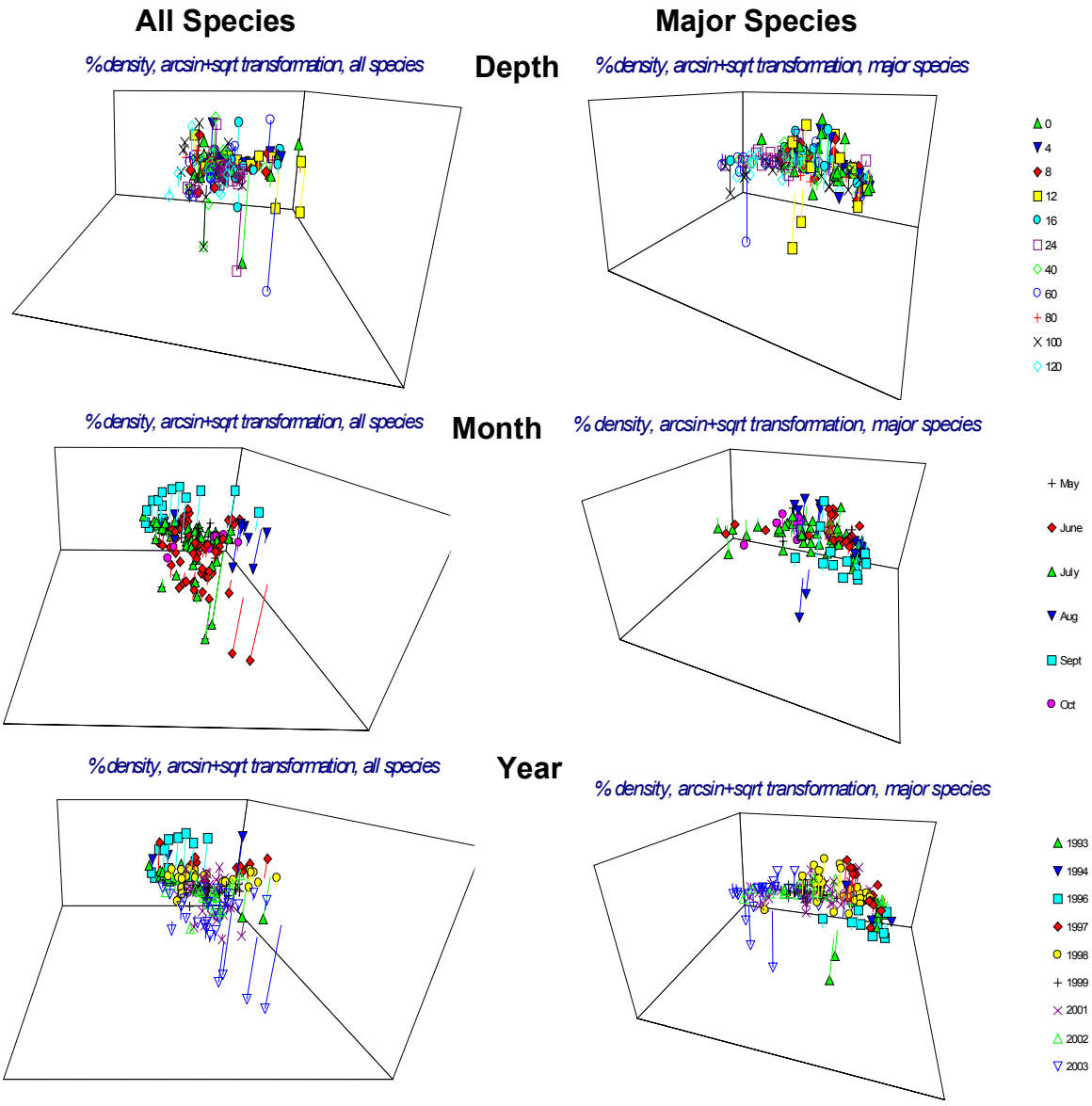

Figure 2.1-9. Waldo Lake phytoplankton percent density for samples collected 1993-2003, non-metric multi-dimensional scaling (MDS) plots based on depth, month, and year. No discernable patterns or clustering were evident due to depth.

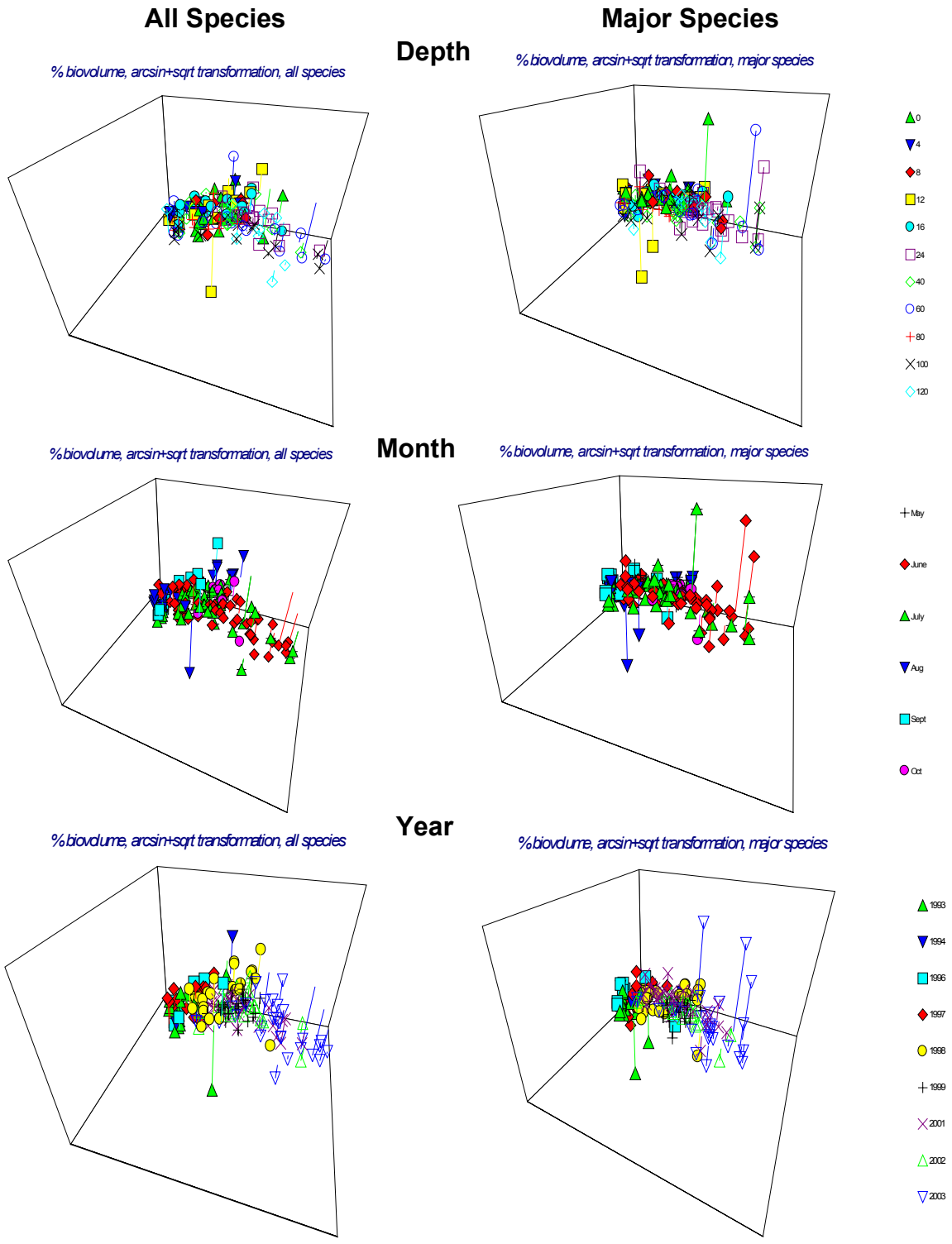

Figure 2.1-10. Waldo Lake phytoplankton percent biovolume for samples collected 1993-2003, non-metric multi-dimensional scaling (MDS) plots based on depth, month, and year. No discernable patterns or clustering were evident due to depth.

Correlation between groups of phytoplankton

Correlations between most of the groups of phytoplankton based on group percent density, were not significant ($p > 0.05$). Significant negative correlations existed between the group of plankton termed unknown (unidentified flagellate cells) and chlorophytes (Figure 2.1-11). The group of plankton termed unknown and cryptophytes were positively correlated, although, the correlation is based only on a few data points and $p = 0.05$ (Figure 2.1-11).

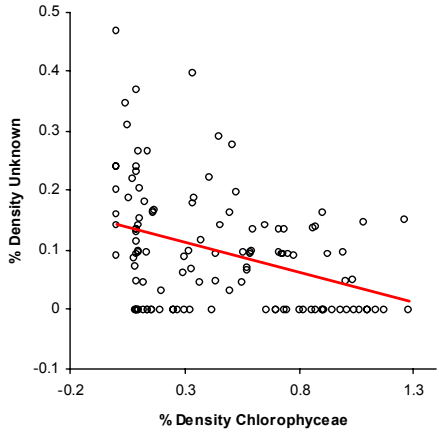

n	119
Spearman correlation coefficient	-0.38
95% CI	-0.52 to -0.21
2-tailed p	<0.0001

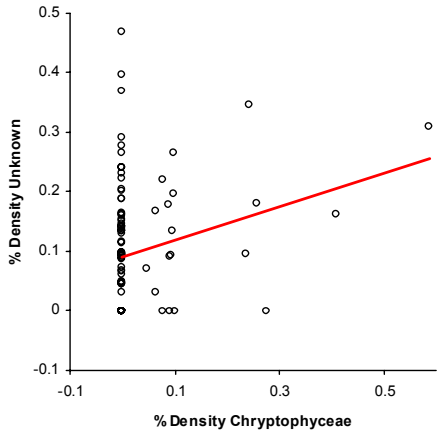

n	119
Spearman correlation coefficient	0.18
95% CI	0.00 to 0.35
2-tailed p	0.0517

Figure 2.1-11. Spearman-rank correlation between groups of phytoplankton based on percent density at Waldo Lake between 1993 and 2003.

Zooplankton

Zooplankton densities were highest in 1998 (2784 ± 1854 organisms/m^3, mean ± 95 % confidence interval), lowest in 1999 (228 ± 85 organisms/m^3, mean ± 95 % confidence interval), then slowly increased from 2001 to 2003 (Figure 2.1-12). *Bosmina*

longirostris, a cladoceran was the dominant zooplankton species at Waldo Lake and occupied the hypolimnion during daytime sampling events. *Diaptomus kenai x shoshone*, a copepod, was second highest in total density, it occupied the epilimnion (Figure 2.1-13). "Others" occured in the highest densities in the hypolimnion.

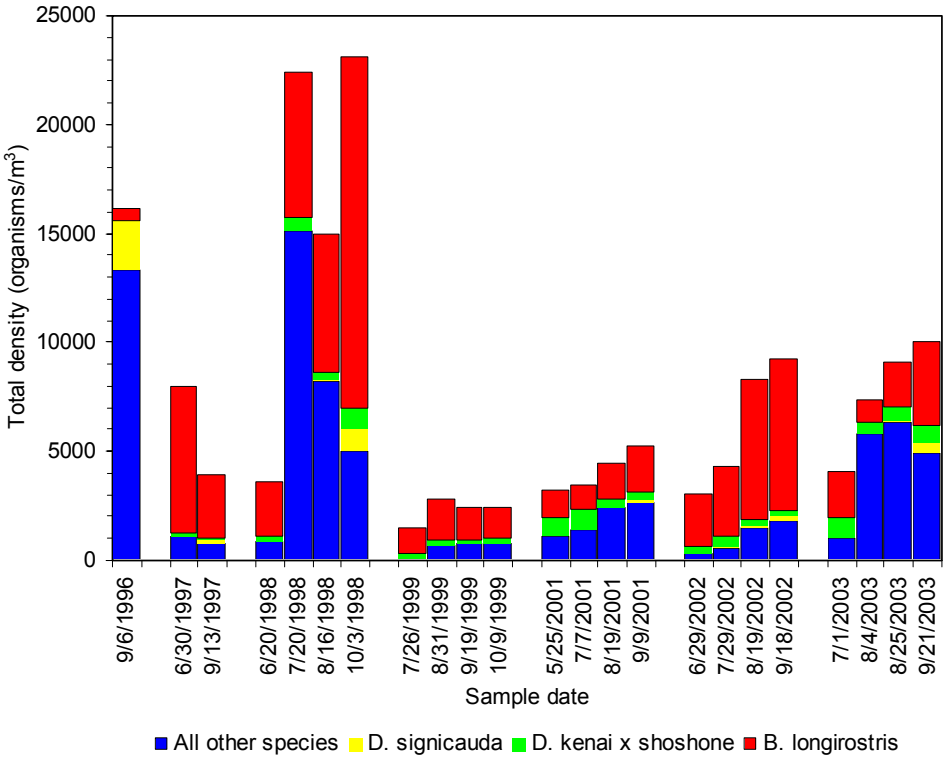

Date	No. of Tows
9/6/1996	7
6/30/1997	5
9/13/1997	6
6/20/1998	6
7/20/1998	5
8/16/1998	6
10/3/1998	6
7/26/1999	6
8/31/1999	6
9/19/1999	5
10/9/1999	5
5/25/2001	5
7/7/2001	6
8/19/2001	6
9/9/2001	6
6/29/2002	6
7/29/2002	6
8/19/2002	6
9/18/2002	6
7/1/2003	6
8/4/2003	6
8/25/2003	6
9/21/2003	6

Figure 2.1-12. Total zooplankton density for all 20 m tows collected on each sampling date. The numbers of tows for each sample date are shown on the right.

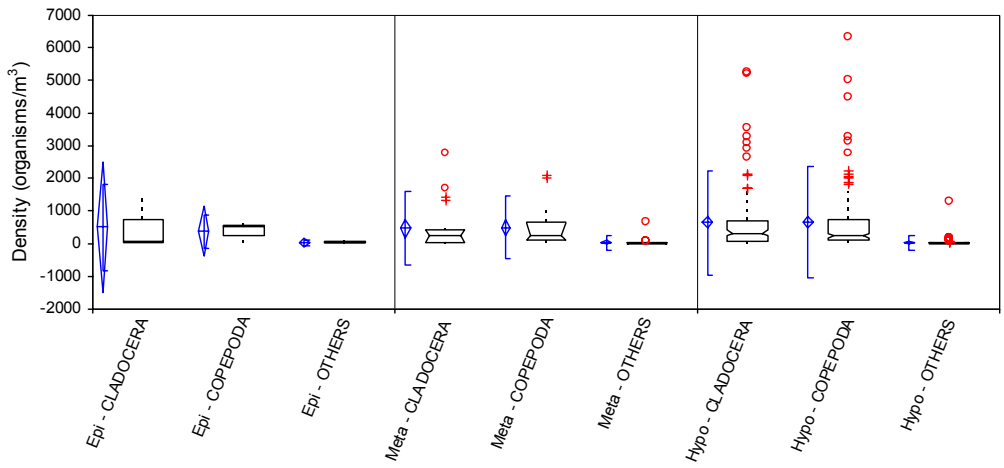

Figure 2.1-13. Vertical distribution of zooplankton groups at Waldo Lake, 1996-2003. Lines represent parametric statistics; the diamond shows the mean and the lines are 95% confidence intervals around the parametric mean. The middle line of the box represents the non-parametric median, and the top and bottom lines are the confidence interval around the median. Circles and plus signs are outliers.

Months and years with higher cladocera density were accompanied by lower copepod densities and vice-versa and suggesting the temporal distribution of groups of copepods and cladoceran were inversely related (Figure 2.1-14 and Figure 2.1-15).

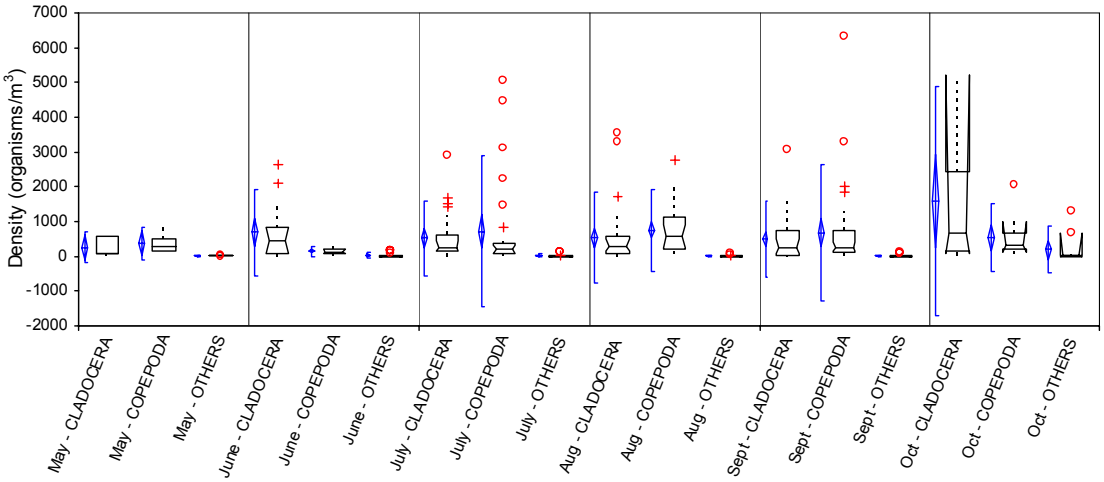

Figure 2.1-14. Zooplankton density for cladocera, copepods and "others", showing mean and median values for each month sampled. Lines represent parametric statistics; the diamond shows the mean and the lines are 95 % confidence intervals around the parametric mean. The middle line of the box represents the non-parametric median, and the top and bottom lines are 95 % confidence interval around the median. Circles and plus signs are outliers.

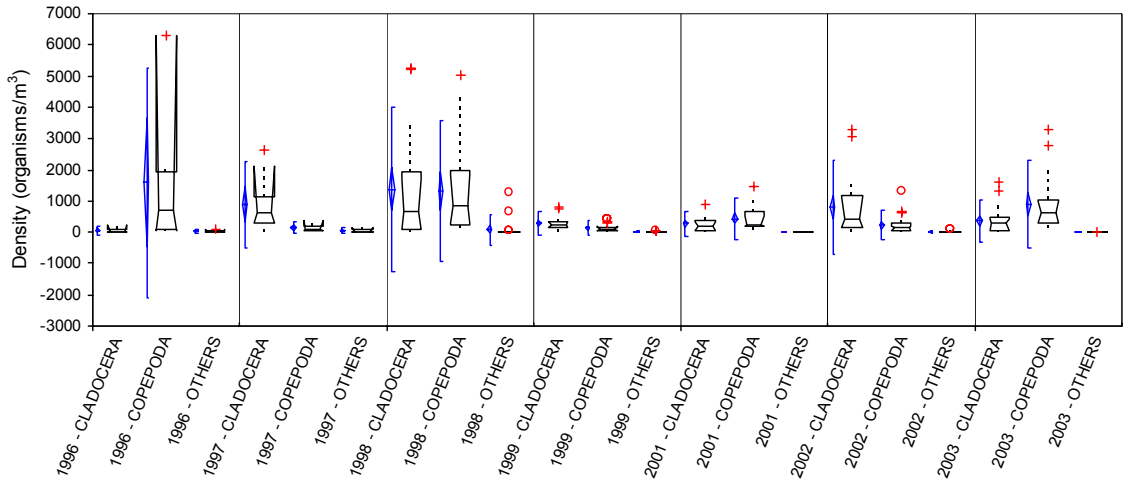

Figure 2.1-15. Zooplankton percent density for cladocera, copepods, and "others", showing mean and median values for each year sampled. Lines represent parametric statistics; the diamond shows the mean and the lines are 95 % confidence intervals around the parametric mean. The middle line of the box represents the non-parametric median, and the top and bottom lines are the 95 % confidence interval around the median. Circles and plus signs are outliers.

Non-metric multi-dimensional scaling

MDS plots shown in a three-dimensional space represented the dataset with a higher degree of certainty than two-dimensional plots (Table 2.1-8).

Table 2.1-8. Stress levels of non-metric multi-dimensional scaling plots of Waldo Lake zooplankton data collected 1996-2003.

		3-Dimensional stress	2-Dimensional stress
Percent Density	All species	0.08	0.14
	Major species only	0.08	0.13
Density	All species	0.13	0.17
	Major species only	0.12	0.16

Species composition of each sample determined the ecological distance among samples shown in the MDS plots. The densities of the major species in each sample explained some degree of the clustering of the MDS plots (two-dimensional plots shown, Figure 2.1-16). *B. longirostris* and *D. kenai x shoshone* occurred in higher densities in

opposite ends of the large cluster. *D. signicauda* and copepod nauplii occurred in higher densities in the samples which were distinct from the large cluster.

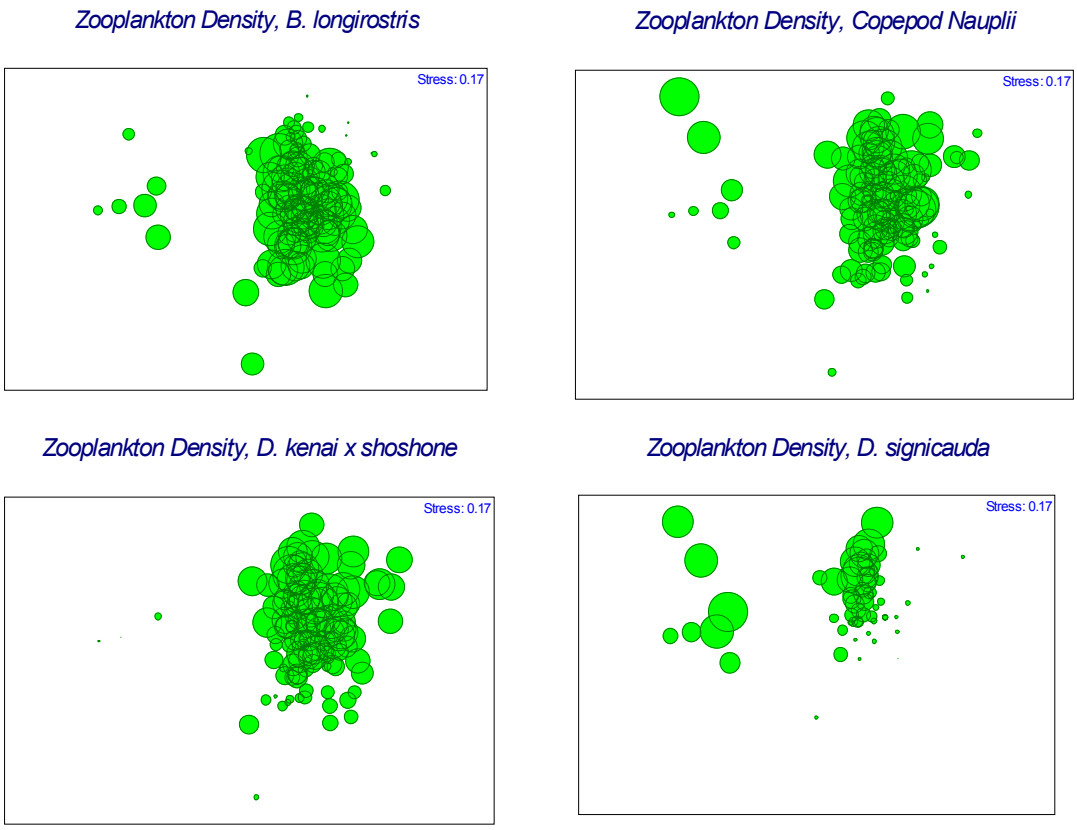

Figure 2.1-16. Waldo Lake zooplankton species density from 1996-2003, MDS bubble plots for *B. longirostris*, *D. kenai x shoshone*, *D. signicauda* and copepod nauplii.

Vertical distribution patterns based on ecological distance between sample groups were shown by MDS plots based on zooplankton density (Figure 2.1-17). There was some distinction between samples collected in the various limnetic layers of the lake (circled). Temporal patterns based on clustering in MDS plots were apparent (Figure 2.1-17). Samples collected on September 6, 1996 (circled) were distinctly different from other samples collected between 1996 and 2003. Zooplankton percent density plots did not add any degree of clarity to the visualization of vertical or temporal patterns in the dataset (not shown).

All Species	Major Species

Layer of Thermocline

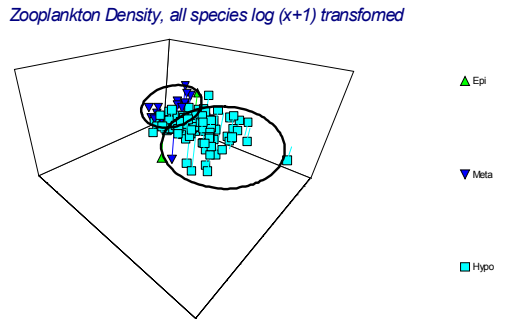

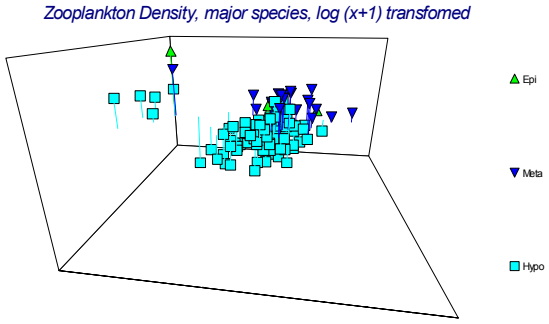

Month

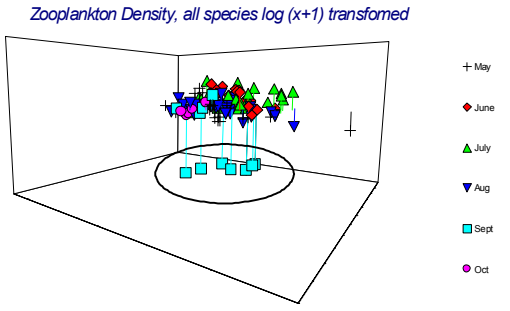

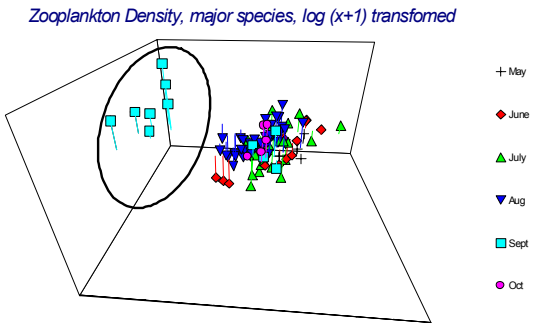

Year

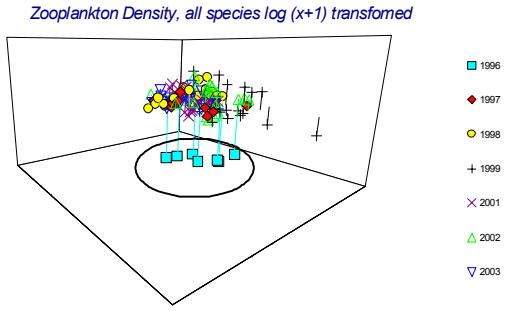

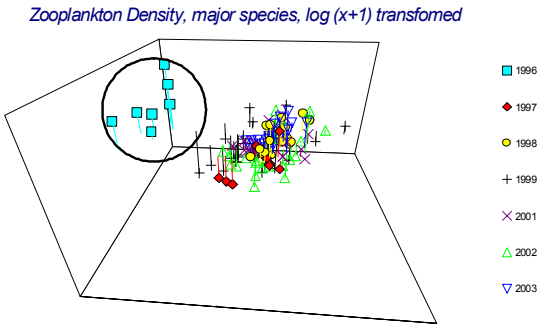

Figure 2.1-17. Waldo Lake zooplankton density (organisms/m^3) for samples collected 1996-2003, non-metric multi-dimensional scaling (MDS) plots based on thermocline layer, month and year.

Correlation between groups of zooplankton

The significance of correlations between groups of zooplankton, based on density, were questionable due to the fact that they were based on relationships where most of samples had high densities of only one group and correlations were based on few data points which strayed from this general pattern (Appendix B).

Relationships between environmental factors and phytoplankton samples

Chemistry

The highest correlation between phytoplankton and chemistry variables was between alkalinity and phytoplankton biovolume represented by the set of 43 "major" phytoplankton species (Table 2.1-9). Total phosphorus and dissolved silica were less important variables. Total dissolved solids were not correlated with the phytoplankton dataset.

Table 2.1-9. Rank correlation of agreement between Waldo Lake phytoplankton and chemistry data, 1993-2003, calculated in PRIMER using BIOENV analysis. Parameters are abbreviated: Total Phosphorus (TP), Alkalinity (Alk), Silica (Si) and Total Dissolved Solids (TDS).

		Highest	Key
Percent Density	All species	0.308	TP, Alk, Si
		0.307	Alk
	Major species	0.31	TP, Alk, Si
		0.308	Alk, Si
		0.306	Alk
		0.304	TP, Alk
Density	All species	0.313	Alk
		0.312	TP, Alk
	Major species	0.314	Alk
		0.312	TP, Alk
Percent Biovolume	All species	0.322	Alk
		0.314	TP, Alk
	Major species	0.325	Alk
		0.318	TP, Alk
Biovolume	All species	0.36	Alk
		0.356	TP, Alk
	Major species	0.372	Alk
		0.37	TP, Alk

Alkalinity was significantly correlated with 10 out of the 43 "major" species of phytoplankton (Univariate non-parametric Spearman rank correlation, $p < 0.05$, $n = 114$

(Table 2.1-10). Alkalinity was negatively correlated with key species of chlorophytes, but positively correlated with key species of flagellates. Two species of diatoms were also correlated with alkalinity, but their response varied. Correlations with other species, including chrysophytes and cryptophytes were not significant ($p > 0.05$).

Table 2.1-10. Spearman rank correlation coefficients between alkalinity and species percent density. Only significant correlations are shown.

Species Name	Species Code	Class	Spearman correlation coefficient	2-tailed p
Gomphonema tenellum	GFTN	Bacillariophyceae	-0.28	0.0025
Eunotia elegans	EUEL	Bacillariophyceae	0.31	0.009
Crucigenia sp.	CGXX	Chlorophyceae	-0.56	<0.0001
Selenastrum minutum	SLMN	Chlorophyceae	-0.35	<0.0001
Oocystis pusilla	OCPU	Chlorophyceae	-0.39	<0.0001
Sphaerocystis schroeteri	SCSC	Chlorophyceae	-0.32	0.0006
Tetraedron minimum	TEMN	Chlorophyceae	-0.21	0.0222
Woloszynskia neglecta	GDNG	Dinophyceae	0.32	0.0005
Hemidinium sp.	HDXX	Dinophyceae	0.23	0.0138
Unidentified flagellate	MXFG	Unknown	0.34	0.0002

Total phosphorus was significantly correlated with 3 out of the 43 "major" species of phytoplankton (Univariate non-parametric Spearman rank correlation, $p < 0.05$, $n = 114$ (Table 2.1-11). Total phosphorus was positively correlated with select species of diatoms and with *Selenastrum minutum*, a chlorophyte. Correlations with other species were not significant ($p > 0.05$).

Table 2.1-11. Spearman rank correlation coefficients between unfiltered total phosphorus and species percent density. Only significant correlations are shown.

Species Name	Species Code	Class	Spearman correlation coefficient	2-tailed p
Achnanthes minutissima	ACMN	Bacillariophyceae	0.34	0.0002
Gomphonema subclavatum	GFSB	Bacillariophyceae	0.29	0.0018
Selenastrum minutum	SLMN	Chlorophyceae	0.27	0.0037

Light

Light data collected between 1998 and 2003 and phytoplankton were not correlated (73 species, 86 samples, Table 2.1-12) based on BIOENV rank correlation analyses. The correlations were slightly higher between light data collected between 2001 and 2003 and

phytoplankton (62 species, 52 samples, Table 2.1-3). The highest correlations were obtained between phytoplankton percent density and red light data. Blue light and phytoplankton were not correlated.

Table 2.1-12. Rank correlation of agreement between Waldo Lake phytoplankton and light data, 1998-2003.

		Highest Correlation Coefficient(s)	Key factor(s)
Percent Density	All species	0.070 0.057	RED RED, PAR
Density	All species	0.053 0.044	RED RED, PAR
Percent Biovolume	All species	0.030	RED
Biovolume	All species	-0.005 -0.008	RED GREEN

Table 2.1-13. Rank correlation of agreement between Waldo Lake phytoplankton and light data, 2001-2003.

		Highest Correlation Coefficient(s)	Key factor(s)
Percent Density	All species	0.164 0.163	PAR RED, PAR
Density	All species	0.127 0.122	PAR RED, PAR
Percent Biovolume	All species	0.125	RED
Biovolume	All species	0.096	PAR

Phytoplankton and zooplankton exhibited a low, but significant correlation based on multivariate analyses. "All species" and "major species" had higher correlation coefficients (Rho (ρ)) than species "groups". Plankton density had higher correlations overall than percent density (Table 2.1-14 and Table 2.1-15), although the species "groups" were not significantly correlated.

Table 2.1-14. Rank correlation between phytoplankton and zooplankton percent density of all species, major species and groups of plankton collected at Waldo Lake, 1996-2003. Significance expressed as a percent which can be likened to alpha (α = 0.05 is the same as 5.0%).

	# of samples	# of species/groups	Rho (ρ)	Significance level
All Species	119	Zooplankton: 41 Phytoplankton: 107	0.081	1.0 %
Major Species	119	Zooplankton: 13 Phytoplankton: 42	0.081	0.3 %
Groups	119	Zooplankton: 3 Phytoplankton: 6	0.04	4.2 %

Table 2.1-15. Rank correlation between phytoplankton and zooplankton density of all species, major species and groups of plankton collected at Waldo Lake, 1996-2003. Significance expressed as a percent which can be likened to alpha (α = 0.05 is the same as 5.0%). Correlation coefficients with a significance level greater than 5 % are not significant.

	# of samples	# of species/groups	Rho (ρ)	Significance level
All Species	119	Zooplankton: 41 Phytoplankton: 107	0.159	0.2 %
Major Species	119	Zooplankton: 13 Phytoplankton: 42	0.155	0.3 %
Groups	119	Zooplankton: 3 Phytoplankton: 6	0.06	10.7 % not significant

Cladocerans were positively correlated with chrysophytes (Spearman correlation coefficient = 0.30, 2-tailed p = 0.001, n = 119; Figure 2.1-18). Copepods were negatively correlated with chlorophytes (Spearman correlation coefficient = -0.19, 2-tailed p = 0.04, n = 119; Figure 2.1-18). "Others" were positively correlated with diatoms (Spearman correlation coefficient = 0.23, 2-tailed p = 0.0114, n = 119) and with chrysophytes (Spearman correlation coefficient = 0.29, 2-tailed p = 0.0014, n = 119; Figure 2.1-18). Densities for "others" were very low. These correlations, based on only a few data points when the density of "others" is high, were not considered reliable (Figure 2.1-18). No other correlations between groups were significant (p > 0.05).

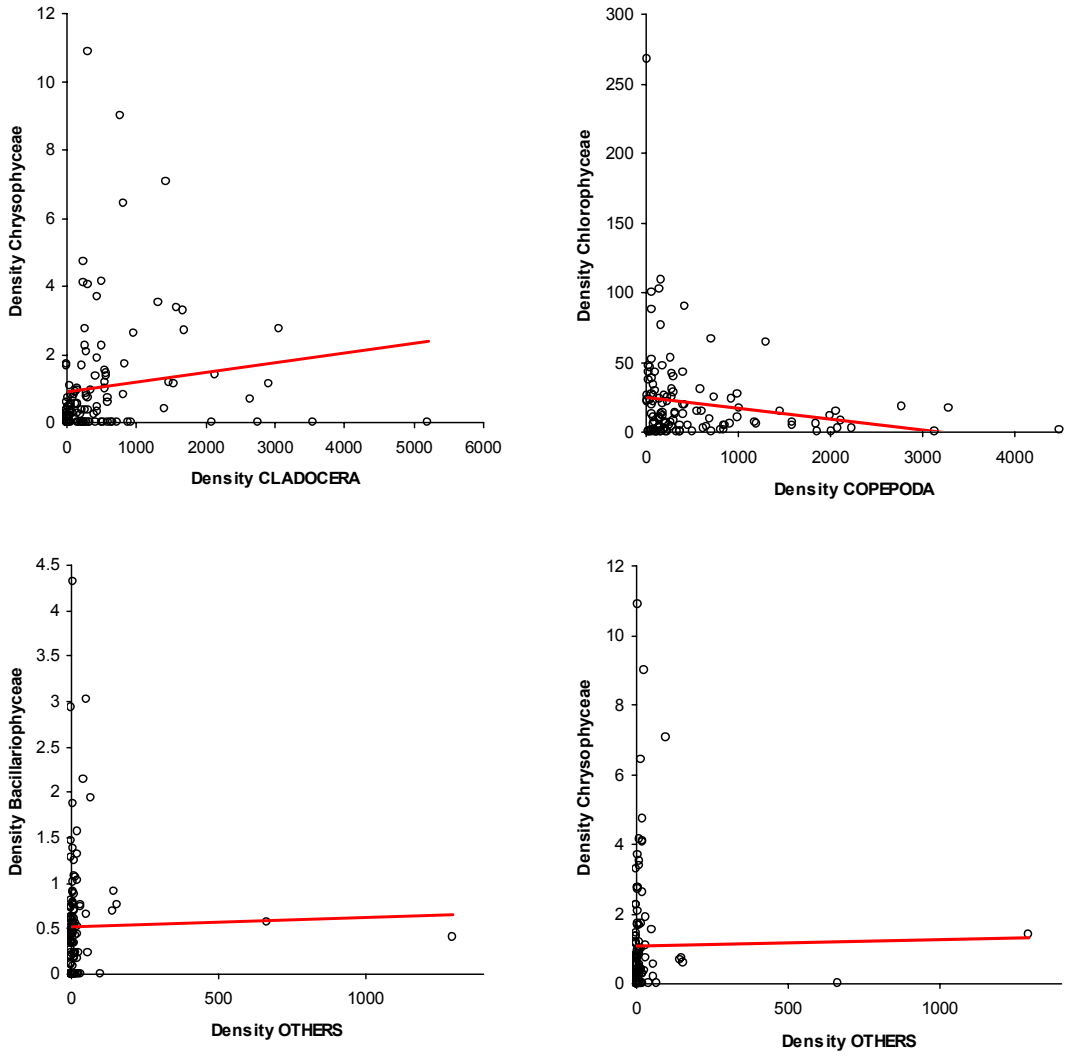

Figure 2.1-18. Relationships between total density of zooplankton groups and total density of phytoplankton groups for samples collected at Waldo Lake from 1996-2003.

Discussion

Indications of bottom-up regulation of the phytoplankton community were stronger than evidence of top-down regulation by zooplankton predation. The chemistry dataset obtained the strongest correlation with phytoplankton while the correlation between phytoplankton and zooplankton were low. Alkalinity was the constituent most strongly correlated with the dominant species of phytoplankton (*O. pusilla, W. neglecta, Hemidinium sp.*). Vertical distribution of zooplankton may vary throughout the day, which may explain the low correlation between phytoplankton and zooplankton (See Section 2.6 for additional zooplankton discussion).

The correlation between alkalinity and phytoplankton suggests the possibility of carbon limitation of Waldo Lake phytoplankton. Chlorophytes were at the highest percent densities in conjunction with samples with the lowest alkalinity. Chlorophytes may be more efficient competitors for carbon because they can utilize bicarbonate. In addition, their small cell size and high surface area to volume ratio reduces boundary layer resistance to nutrient (carbon) uptake (Hein 1997). Conversely, dinoflagellates were found in highest densities from depths with relatively higher alkalinity.

There were no strong environmental gradients in the Waldo Lake dataset, as are generally observed in multivariate analyses. For example, there were no distinct seasonal changes in chemistry. Further, the effects of watershed disturbances such as the 1996 fire did not produce measurable changes in the dataset. The variation in chemical constituents may be slight compared to sampling noise. Strict adherence to sampling protocol will improve confidence in data quality and allow for assessment of those measurement uncertainties.

Light in the visible spectrum was not correlated with phytoplankton. In an ultra-oligotrophic lake such as Waldo Lake, light is most likely not a limiting factor for phytoplankton. Light penetrates very deeply into Waldo Lake, plankton able to adapt to very low light conditions may be able to photosynthesize at depths below 100 m.

The five year light dataset was too short to capture any optical changes occurring in the lake. Changes in plankton density between 1998 and 2003 were less distinct than changes occurring between 1993 and 2003. Changes in phytoplankton between 1998 and 2003 did not appear to have influenced the optical properties of Waldo Lake.

Light intensity instead of percent of surface intensity, may provide additional insight to the seasonal changes in phytoplankton. Light intensity varies seasonally (See Section 1.1) and phytoplankton respond to varying levels in light intensity (Raven and Richardson 1984). Additionally, the erratic nature of 1998 and 1999, data resulting in the change in equipment for light data collection seems to be a logical explanation for poor correlations with the phytoplankton dataset.

No consistent patterns in the vertical distribution of phytoplankton were found. One potential explanation for this is the variability of the time of sample collection. Although efforts were made to limit this analysis to samples collected in the morning, the exact time of sampling was often not recorded. Daily vertical migration may bias the depth distribution of flagellates (Johnson in prep).

Recommendations

There are numerous factors acting on multiple scales in Waldo Lake that could influence phytoplankton community structure and vertical distribution. Some of these factors were considered in this report, including temperature (See Section 1.2) and relationships between mixotrophs and bacteria (See Section 2.4). Other factors have not been examined, including: UV intensity, functional feeding groups or size-class of plankton, fish stocking history and the timing of the emergence of insects. Fish captures were completed by the Department of Fish and Wildlife in 1991, 1992, 1993 and 1998 (Swanson et al. 2000) has continued in other years (A. Johnson pers. comm.).

The prevalence of chironomid larvae to the Waldo Lake ecosystem may be of importance. The predatory feeding of first larval instar on phytoplankton (Merrit and Cummins 1978) as well as the release of nutrients from the decomposition of exoskeletons deserves further investigation in the current body of literature.

Varying spring and winter assemblages may exist. Sampling four times a year, during the summer months may not accurately represent species present in the lake. The seasonal succession of phytoplankton pre- and post-ice coverage before the development of the thermocline is unknown.

2.2 Phytoplankton Productivity: Uncertainty Analysis of ^{14}C Method

Introduction

^{14}C uptake by phytoplankton, a surrogate for primary productivity, has been monitored consistently in Waldo Lake for almost 20 years (Larson and Salinas 1995; Salinas and Larson 2000). Original productivity experiments indicated that Waldo Lake

was among the least productive lakes in the world (Larson 1970; Malueg et al. 1972). More recent productivity estimates were on the order of 20-fold higher, suggesting that the unique ecosystem of Waldo Lake may be rapidly becoming more eutrophic (Salinas and Larson 2000). Results from the most recent experiments have not been made available due to a lack of confidence in their reliability (Salinas pers. comm.; Sytsma et al. 2004).

An analysis of the variation inherent to productivity methods employed at Waldo Lake is required to establish a consistent and quantitative approach for calculating the overall uncertainty in productivity estimates for the lake. A quantitative assessment of the uncertainty in the productivity estimates will provide a proper context for discussing the suggested changes in the lake ecosystem.

The objective of this section was to develop a framework for an uncertainty analysis. The major uncertainties are described along with proposed analysis methods to accurately estimate their magnitude. Preliminary experiments from 2004 designed to understand uncertainty related to ultra-violet light inhibition and filter size are reported. Finally, an approach for the propagation of uncertainty estimates through the primary productivity calculations is described.

The ^{14}C Method at Waldo Lake

The radiocarbon ^{14}C-CO_2 tracer method for estimating dissolved inorganic carbon uptake by phytoplankton has changed little since it was first used by Steeman and Nielsen in 1952 (Peterson 1980). According to Peterson (1980) "The purpose of the method is to estimate the uptake of dissolved inorganic carbon (DIC) from the water by planktonic algae as they photosynthesize in the light. The carbon taken up either remains in the algae as particulate organic carbon (POC) or is excreted into the water as dissolved organic carbon (DOC)". It is important to note that excreted DOC is readily incorporated into bacteria, another pool of POC (Flynn 1988).

In practice, a known amount of ^{14}C is added to both clear and dark bottles containing water samples of interest. After incubation under appropriate conditions of light and temperature, organic carbon is separated from inorganic carbon by filtration. Carbon

uptake can be calculated from radioactive carbon counts as:

$$carbon\ uptake = \frac{counts\ in\ particulate\ organic\ fraction}{total\ counts\ added} \times available\ inorganic\ carbon \times 1.05$$

The isotope discrimination factor 1.05 accounts for the fact that the heavier ^{14}C is taken up more slowly than the lighter ^{12}C.

Field methods used by previous investigators to estimate ^{14}C uptake at Waldo Lake were generally consistent from 1969-1998 (Salinas and Larson 2000). Specifically: multiple depths were sampled (although there were differences in total depths sampled: surface to 40 m depth in 1969, surface to 60 m depth in 1973, and surface to 110 m depth in 1989-1998); water samples were collected with a Scott-modified Van Dorn bottle made of PVC; similar 125 ml glass bottles were used for incubations; dark bottles were taped with black tape and covered in foil; bottles were inoculated with 1 ml of $NaH^{14}C0_3$ (activity 5.0 μCi/ml) and incubated at depth for four hours after which samples were filtered with 0.45 μm membrane filters; and filter radioactivity was determined by liquid scintillation counting.

Uncertainties: ^{12}C Available

A major uncertainty in the primary productivity calculation is the amount of ^{12}C, or dissolved inorganic carbon (DIC), available (Equation 1). DIC in Waldo Lake has been calculated from alkalinity and pH measurements according to Wetzel and Likens (2000). There are significant issues with this approach in low ionic strength waters such as Waldo Lake. In fact, Wetzel and Likens (2000) specifically recommend that: "Particularly in nutrient-poor, soft waters, direct analysis of DIC will be necessary" (pg. 225). Uncertainty about the accuracy of pH measurement in Waldo Lake was noted by Salinas (2000) and Larson (1972). In addition, methods that have been used to measure alkalinity are not tailored for low ionic strength conditions and may not be accurate or precise.

The main problem with calculating DIC from alkalinity and pH measurements is the difficulty of obtaining accurate pH measurements in low ionic strength waters, such as Waldo Lake. Pure water is poor conductor and potentiometric measurement of pH relies

on an electrical signal. When a pH electrode is placed in the water a potential develops across the membrane surface. The strength of the potential varies with pH and is compared to a reference potential (Orion manual). When the conductivity of a solution is low the potential is hard to measure and noisy values or drift are generally experienced. Values of pH from 5.5 to 6.7 have been measured in Waldo Lake over time. Assuming the same alkalinity value (2.45 mg/L $CaC0_3$; Salinas and Larson 2000) and a temperature of 5 °C, the variation in pH results in a range of 1 to 7 mg/L ^{12}C available.

A review of the Waldo Lake literature was unsuccessful in determining exactly how the pH values used in the calculations were measured. It appears that *in situ* pH values obtained with a multi-parameter probe (a Hydrolab™) were used in the 1989-1998 estimates, yet the quality assurance procedures described were not the same as those recommended by the manufacturer (Hach Environmental). At Waldo, occasional calibrations of the *in situ* pH probe were made to minimize sources of analytical error (Salinas 2000), however, calibrations were made with standard buffered solutions rather than the recommended low ionic strength buffers. The resulting pH probe accuracy may have been compromised because pH electrodes that are moved from high ionic-strength solutions to low ionic-strength solutions require a long time for stabilization (Orion manual 1991).

To address the uncertainty associated with ^{12}C available a comparison of calculated DIC concentrations with directly measured DIC concentrations will be made during the summer of 2005. DIC will be measured in the laboratory at Portland State University (PSU) with a Shimadzu® model TOCVCSH Carbon Analyzer. Field measurements of pH will be made with an Orion 290A meter equipped with a Series A Triode (recommended for low ionic strength waters). Alkalinity will be measured by Gran titration in the laboratory at PSU (Wetzel and Likens 2000).

A paired t-test will be completed to compare means of calculated and measured DIC values. Pairs will be based on measurements within five replicate Niskin bottle grab samples. Additionally, a two-way ANOVA will be used to evaluate DIC sample bottle type, holding time, and sample bottle by holding time interactions (Table 1.2-1). Since

the influx of air into Niskin bottles may affect DIC and pH measurements, the order in which the different types of samples are decanted from the Niskin bottles will be randomized and recorded. Measured and calculated DIC values will also be compared with DIC calculated from measurements by the Cascade Research Group according to current Waldo Lake standard operating procedures.

Table 2.2-1. Two-way ANOVA design to test the effect of sample container and sample holding time on directly measured DIC.

	Holding time	
Sample container	One day	Four days
300 ml BOD bottle	N=5	N=5
40 ml TOC vial	N=5	N=5

In addition to the problems with determining the DIC concentration in the lake, other complications may arise when determining the amount of ^{12}C in incubation bottles. Since bulk ^{14}C ampules are acidic, ^{12}C is added to the inoculums in the form of sodium bicarbonate for neutralization of the inoculums prior to incubations. This may add a significant and variable amount of ^{12}C to the incubation bottles.

Uncertainties: ^{14}C Available and Assimilated

The variability associated with ^{14}C available in the inoculant is another uncertainty that needs to be quantified. Bulk ^{14}C ampules were purchased and then diluted to the proper concentration for past productivity experiments (Salinas pers comm.). This approach introduces a measurable uncertainty. Replicate scintillation counts of the final product prior for inoculation would provide an estimate of the uncertainty of ^{14}C added. There are data available to use in this type of analysis (Salinas pers comm.) and more replicates will be completed during 2005 for consideration of this type of uncertainty.

The ^{14}C assimilated depends on many factors. The standard operating procedures for the primary productivity experiments includes replicating final scintillation counts to assess variation. Examining all replicate scintillation counts available in the dataset will allow for assessment of the uncertainty associated with ^{14}C assimilated.

Uncertainties: Van Dorn Bottle

A Scott-modified Van Dorn with latex rubber bands was used for collection of all samples for primary productivity measurement at Waldo Lake (Salinas and Larson 2000; and Salinas pers. comm.). Latex rubber bands inside of Van Dorn bottles have been shown to be toxic to phytoplankton (Fahnenstiel et al. 2002). For this reason, the Center for Lakes and Reservoirs uses a modified Niskin 1010X sampler that does not contain latex (O-rings are made from silicon).

To test for latex toxicity in Waldo Lake primary productivity incubations, five tandem collections will be made from the same depth. The samples will be incubated as duplicates (bottles incubated in tandem at the same depth). The means of the two populations will be compared with a Student's t-test. The null hypothesis will be that the Niskin collections are not different than the Van Dorn collections. This experiment will be performed in August 2005 during long-term monitoring.

Uncertainties: UV Inhibition

Ultra-violet light (UV) is known to inhibit phytoplankton productivity (Williamson 1995). UV has been shown to penetrate deeper into the water column in oligotrophic lakes than in other types of lakes (Morris et al. 1995). There are two hypotheses regarding the affects of UV inhibition on primary productivity measurements in Waldo Lake. First, certain types of glass block UV wavelengths. If the type of glass used was changed to a UV-blocking type between 1973 and 1986 then the observed increase in productivity could be partly a result of less UV inhibition in surface incubations. Second, UV inhibition may occur when samples are brought to the surface. Therefore variable handling times and sky conditions during the filling of incubation bottles and variable cellular recovery rates based on the light history of the cell could introduce uncertainty into the calculations.

During July and September, 2004, two preliminary experiments were conducted to enhance understanding of UV inhibition in primary productivity measurements at Waldo Lake. The experiments were conducted using a single, 1-liter sample collection from 24 m. The sample was inoculated with 50 μCi of ^{14}C, mixed thoroughly, and partitioned into

aliquots of 30 ml in Whirlpaks™. The Whirlpaks™ were incubated for 4 hours in two sets of enclosures constructed of layers of plastic window screening to obtain a range of six different light intensities (Figure 2.2-1). One complete set of bags was incubated below a sheet of acrylic plastic to remove UV radiation (Without UV, Figure 2.2-1), while the other was exposed to ambient solar radiation (With UV, Figure 2.2-1).

The experiment in July suggested that UV may inhibit primary productivity in the surface water of Waldo Lake. Figure 2.2-1 depicts the results from the whole water fraction (i.e., all fixed carbon, particulate or dissolved).

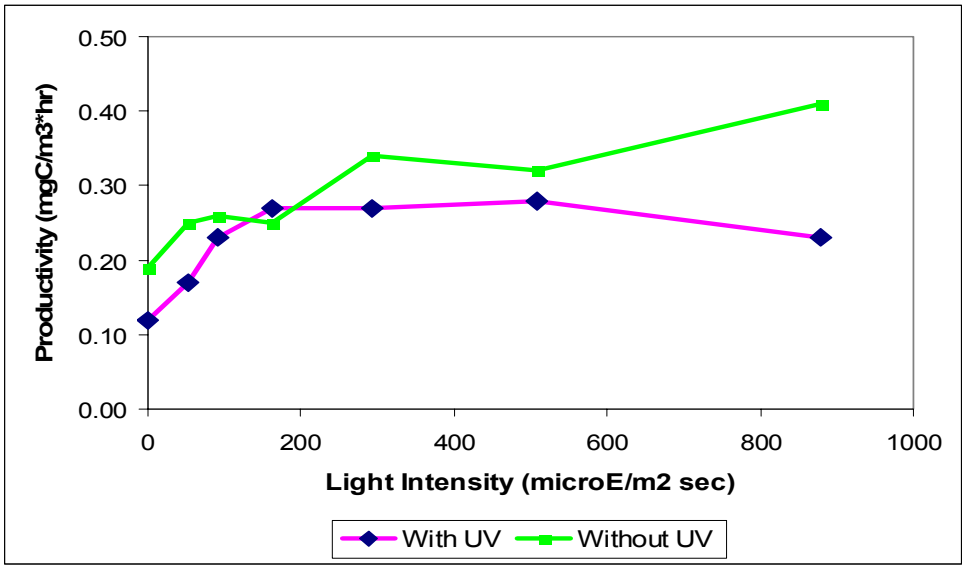

Figure 2.2-1 . Photosynthesis vs. light intensity (P vs. I) curves for July 19 UV inhibition of primary productivity experiments.

The experiments conducted in September did not indicate any inhibition by UV (Figure 2.2-2). However, less UV reached the lake surface in September than July because of low sun angle (See Section 1.1). Accordingly, the September results do not necessarily contradict the July results. Definite conclusions are not warranted, however, because too few experiments were conducted. These results can serve as a guide to designing further experiments. For additional discussion of photoinhibition see Section 2.3 which describes daily patterns of productivity, UV inhibition, and UV recovery.

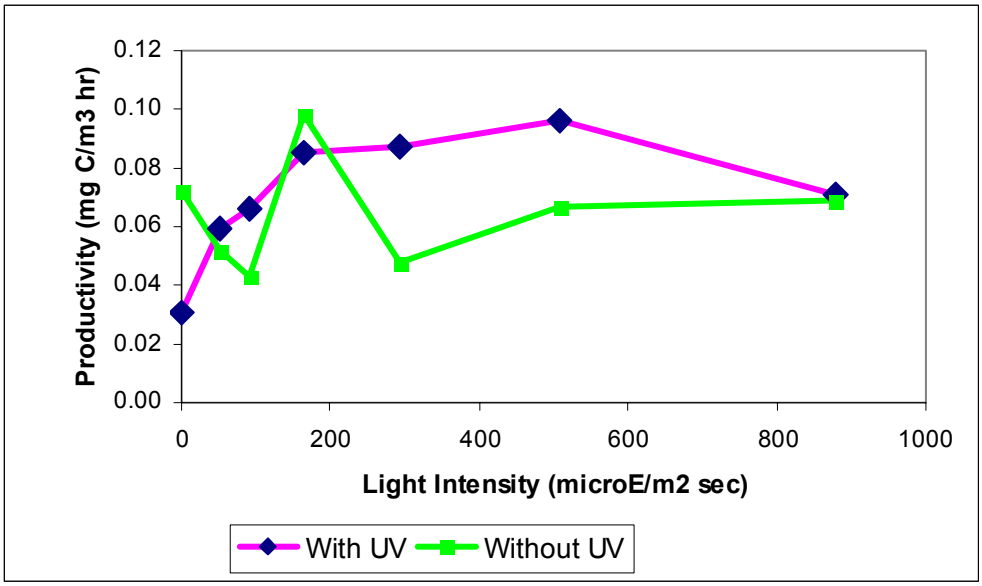

Figure 2.2-2. P vs. I curves for September UV inhibition of primary productivity experiments.

Uncertainties: Filter pore size

After incubation for the UV experiments described above, the contents of each Whirlpak™ were partitioned into 7 fractions: whole water, 2-micron filters, 2-micron filtrate, 0.45-micron filters, 0.45-micron filtrate, 0.22-micron filters and 0.22-micron filtrate. Each fraction was acidified to remove any remaining inorganic ^{14}C, and counted in a scintillation counter. Results of the fractionation experiment can be used to identify possible differences in primary productivity estimates based on the pore size of the filter. Results for the 2-micron filter differ noticeably from the other two filters: less of the total productivity is retained on the 2-micron filters, and more passes through into the filtrate (Figure 2.2-3). There appears to be little difference between the results from the 0.45-micron filters and the 0.22-micron filters. It appears unlikely that using 0.22-micron filters instead of 0.45-micron filters would make a difference in the results of productivity experiments at 24 m.

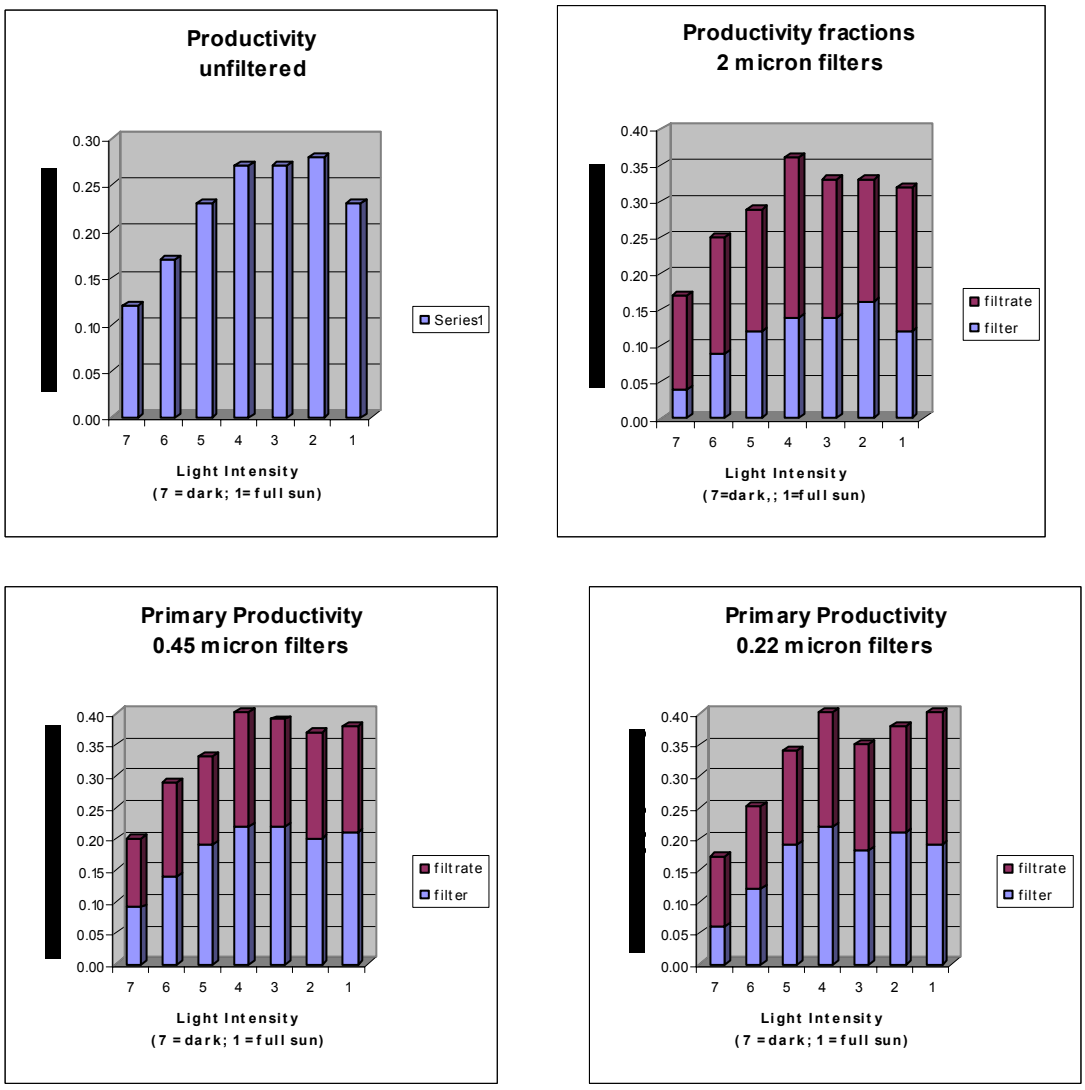

Figure 2.2-3. Fractionation (0.45 vs 0.22 µm filters) of UV inhibition of primary productivity experiment results.

Analysis of Uncertainties

The general rule for error propagation is that if x and y are assumed to have independent and random errors then the quadratic sum of the uncertainties in x and y equals the uncertainty in z (Taylor 1982). If those assumptions cannot be met then the errors associated with x and y are simply summed to estimate the error in z. The specific computational forms pertaining to quadratic sums are described as:

Sums and differences: i.e., when z = x + y, $\sigma_z = \sqrt{\sigma_x^2 + \sigma_y^2}$ (2.2-1)

Products and quotients: i.e., when z = x × y, $\sigma_z / z = \sqrt{\left(\sigma_x / x\right)^2 + \left(\sigma_y / y\right)^2}$ (2.2-2)

Functions: i.e., when z = f(x), $\sigma_z = |f'(x)| \times \left(\sigma_x / x\right)$ (2.2-3)

Constants: i.e., when z = B(x), $\sigma_z = |B| \times \sigma_x$ (2.2-4)

where:
σ is the uncertainty for the measurement (Taylor 1982).

Subsequent to identification and estimation of the major uncertainties in the primary productivity method at Waldo Lake an uncertainty analysis will be performed. This analysis will allow for an accurate assessment of the range of variation in the primary productivity estimates over time. Uncertainties calculated for each measured term in the primary productivity calculations will be propagated through the equations to estimate the uncertainty associated with the final productivity estimate.

2.3 Photoinhibition and Photoprotective Mechanisms in Natural Phytoplankton Samples from Waldo Lake

Introduction

The combination of exceptional clarity and altitude leads to high ultraviolet radiation (UVR) potential in Waldo Lake. On a clear summer day, the incident UVR (UVA+UVB) can exceed 100 µmol photons m^{-2} sec^{-1}. To put this in perspective, in many lakes the phytoplankton would be physiologically acclimated to shift from light limitation to light saturation (the Ik point) at a similar level (100 µmol photons m^{-2} sec^{-1}) of total photosynthetically active radiation (PAR). UVR inhibition could be a major factor in the net productivity of the phytoplankton population and variations in UVR (either natural or related to sampling methods) could have a large effect on the measurements of productivity. Sampling completed during summer 2003 indicated a depression of the photosynthetic yield (measured as the Fv/Fm') during the middle of the day for cells incubated in the presence of UVR (Sytsma et al. 2004). The primary objective for summer 2004 was to determine if phytoplankton in Waldo Lake have photoprotective

mechanisms and how these mechanisms may affect our estimates of productivity patterns in the lake. A secondary goal was to document potential diel variation in photosynthesis.

Phytoplankton have three types of photoprotective mechanisms; protective pigments, water column movement or biochemical quenching. Johnson and Castenholtz (2000) described the photoprotective "sunscreen" pigments in benthic cyanobacteria from Waldo Lake. These pigments in the exocellular sheath are very efficient in screening out harmful UVR. Zooplankton in Waldo Lake have been observed to be rich in carotenoid pigments, but there have been no studies on protective pigments in the phytoplankton. Some algae are motile and are therefore able to avoid high light encountered in the upper water column. Whether this movement is to avoid predation, find better food (bacteria), optimize PAR or avoid UVR has not been determined. Finally, algae and plants have biochemical mechanisms to reduce light damage through increased heat dissipation. This report section describes and measures the third mechanism, known as non-photochemical quenching.

The total light energy absorbed by any cell has three fates; 1) the energy can be used in photochemical reactions leading to photosynthesis, 2) the light energy can be re-emitted at a longer wavelength (fluorescence), or 3) the light energy can be processed through a series of chemical reactions that dissipate the energy as heat (Figure 2.3-1).

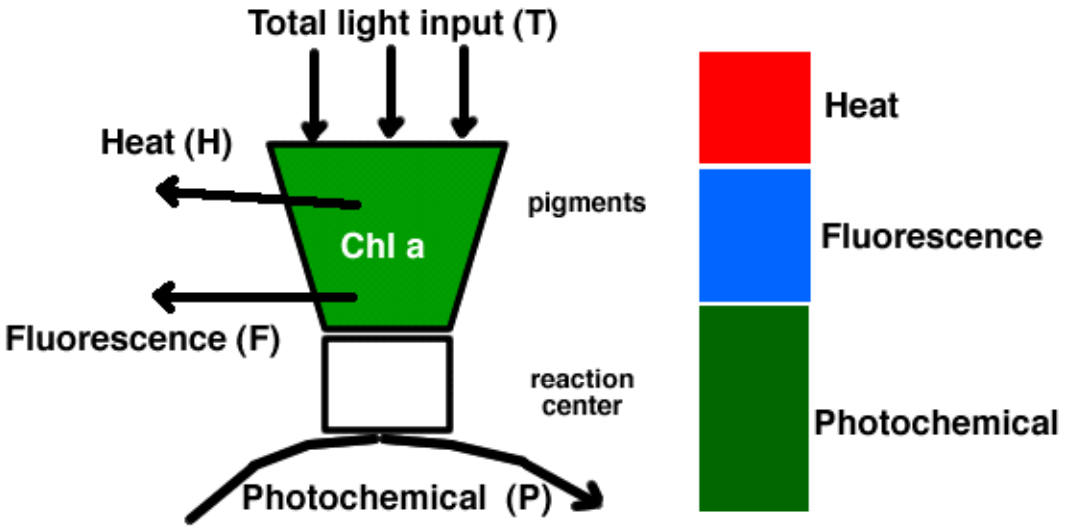

Figure 2.3-1. A model of the absorption of light energy by photosynthetic membrane in algae and the fate of that energy. Adapted from Schreiber (1997). The total input of light energy must be accounted for as heat, fluorescence and photochemical use.

Pulse Amplitude Modulated Fluorometery (PAM-F) directly measures fluorescence, by manipulating the conditions and scale of measurements, the energy that goes into photochemical reactions or is dissipated as heat can also be estimated. The energy that is used in photochemical pathways, recorded by PAM-F is reported in this text as Yield (Fv/Fm') and electron transport rate (ETR). These two parameters should be directly related to the potential rate of photosynthesis and the actual rate at a specific light intensity, respectively. The energy dissipated through heat is particularly interesting to this study because there are biochemical mechanisms that stimulate heat dissipation. The heat dissipation mechanism is called "down-regulation" but is also referred to as "xanthophyll-cycle" or "membrane energized stimulated heat loss" in other studies.

PAM-F can be used to measure three different levels of fluorescence in both dark-adapted cells and light-adapted cells. Dark-adapted cells have been in the dark or very low light intensities long enough that all of the electron acceptors downstream of Photosystem II (PSII) have been oxidized and are available to be reduced. In this state, any photons that reach PSII are readily passed on to the cytochrome b6/f complex and fluorescence is minimal. In cells that are operating in a growth light level, some of those electron acceptors are already reduced, and additional light will result in a larger increase

in fluorescence because there are few open sites to accept the light energy. PAM-F machines can be programmed to provide a series of light levels. The three levels are; 1) the background in the dark, 2) a measuring level that is in the environmental range 0-2500 μmol photons m^{-2} s^{-1}, and 3) a very strong pulse of saturating light. The saturating light level is sufficient to saturate all the electron acceptors from PSII and results in maximum fluorescence.

Parameters that describe the photosynthetic competence of the cell can be calculated from these light conditions and resulting fluorescences. The relative amount of light energy used for photosynthesis is described by the "Yield" parameter. The maximum Yield is determined in dark-adapted cells and it equals the variable fluorescence (after the pulse) compared to the total fluorescence, i.e. Fv/Fm. Another useful version of the yield parameter is to look at that in the cells operating at a particular light level. In this case the yield is the (Fm' – F)/Fm'. This is the value that is used in generating light response curves.

For this work, several other parameters, including the level of non-photochemical quenching and estimates of photoinhibition, were of interest. Non-photochemical quenching is the amount of energy that the cell dumps to heat (Figure 2.3-2). This can only be measured by comparing dark-adapted to light-adapted cells. In a light curve, zero light values at the beginning of the sequence are used to determine the Fv and Fo. There are two different parameters that can be calculated to estimate non-photochemical quenching. These are called "qN" and "NPQ". The difference between these parameters is beyond the scope of this report, but we are using the NPQ.

$$qN = (Fm – Fm')/(Fm – Fo)$$

$$NPQ = (Fm – Fm')/Fm'$$

The shift from Fm to a lower Fm' (measured in light-adapted cells) indicates the enhancement of heat dissipation by the energized thylakoid membrane.

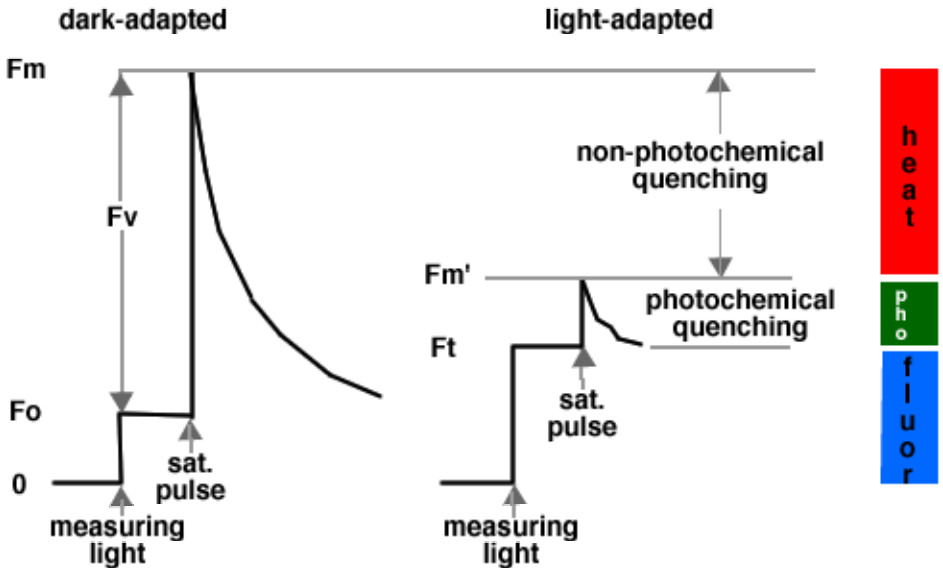

Figure 2.3-2. Saturation pulse technique for non-photochemical quenching analysis. From PAM-F handbook of operation (1999 pg 55). Details are described in the text.

There are two indicators of photoinhibition. The first is the increase in Fo, an increase in fluorescence at the same level of measuring light due to damage of the photocenters. (This potential for an increase in Fo complicates the interpretation of qN and makes NPQ the preferred parameter for non-photosynthetic quenching under conditions that might include photoinhibitory effects.) The second indicator of photoinhibition is to follow recovery of the yield in the dark. For example, after a 10 to 20 minute exposure to high light algae will have a multiphasic recovery. In the first few minutes PSII recovers, followed by relaxation of down-regulation. The level of recovery after 30 or 40 minutes compared to the maximum yield before exposure to inhibitory light is taken as the degree of photoinhibition (Figure 2.3-3). Thus, there are two decreases in Yield occurring on distinct time scales. After several minutes of exposure to high light, there is an enhanced non-photochemical quenching due to the energizing of the thylakoid membrane. This mechanisms decreases potential photosynthesis but recovers very quickly. After more prolonged exposure or exposure to higher light, there is a photoinhibitory loss of photosynthesis that doesn't recover even after 30 minutes. These two time scales are crucial for the studies on phytoplankton in mixed waters.

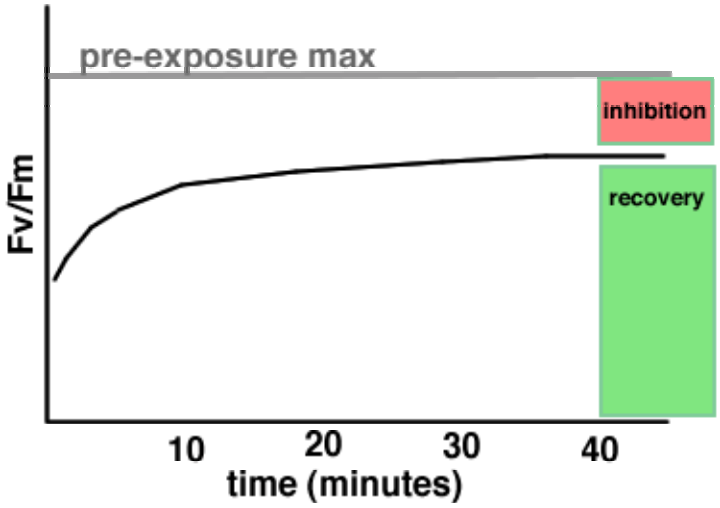

Figure 2.3-3. Theoretical recovery of the Yield parameter in the dark following a photoinhibitory exposure to high light.

Methods

Waldo Lake was sampled on nine different days during the summer and fall of 2004 (Table 2.3-1). Samples were collected every several hours from a site about 200 meters west of the meteorological station at N43.74918 W122.01252. Surface water samples, with a volume of 250 to 300 mL were collected from 0.5 meters. Sample bottles were rinsed prior to filling with water sample. .

Table 2.3-1. Sampling dates for 2004.

July 10
July 17
July 18
July 19
August 21
August 22
September 9
September 22
October 10

Light data were collected in parallel to water sample collection. Light data were logged at a location near the meteorological station located at the Islet Campground boat launch using a HOBO micro station. PAR (400 to 700 nm) was measured with a HOBO PAR sensor and total solar radiation was measured with a HOBO silicon pyranometer.

Ultraviolet radiation was measured using spot measurements with a Spectrum Technologies UVR meter that measures between 250 and 400 nm in µmol photons m^{-2} sec^{-1}. Wind, temperature and solar radiation (wavelengths 305-2800 nm) data were also obtained from the meteorological station.

Photosynthetic parameters were determined using a Walz Water Pulse Amplitude Modulated Fluorometer. A typical protocol was to collect surface water samples from the nearshore station (200 meters out in the lake) and then keep this sample in the dark for at least 10 minutes before measuring the photosynthetic parameters. This protocol allowed for the measurement of Fv/Fm and the calculation of non-photochemical quenching parameters by running a light curve.

Results

UVR could be an important factor in the photoinhibition of photosynthesis. On clear days and overcast days there was a reliable relationship between UVR and PAR (Table 2.3-2). On cloudy days, however, the PAR and UVR both varied so rapidly that it was impossible with our instrumentation to make a valid comparison over the entire day.

Table 2.3-2. Correlation between PAR (400 – 700 nm) and UVR (250 – 400 nm) on different days. Both PAR and UVR were measured with quantum sensors, giving values in umol photons m^{-2} sec^{-1}. * The weather on July 18 was so variable that the 12 readings 5 seconds apart were made on the UVR meter and compared to the PAR reading.

Date	Equation	n	R2	Weather
18-Jul-04	UVR = 0.1097*PAR			cloudy *
9-Sep-04	UVR = 0.0758*PAR	37	0.9279	overcast
22-Sep-04	UVR = 0.0622*PAR	33	0.9438	clear
10-Oct-04	UVR = 0.0606*PAR	24	0.9225	clear

During the course of a day, multiple samples were collected from the surface water to assess diurnal variations in photosynthesis. On a clear day, with exposure to full sun and with little mixing, the surface water samples show a progressive decrease in photosynthetic rate over the day (Figure 2.3-4). Another indicator of variation in the *in*

situ photosynthetic rate is the mid-day depression in the maximum Yield (Figure 2.3-5). Both of these related indicators demonstrated that the photosynthetic rate of the cells may change dramatically from 8:50 and 14:30, the time bracketing the traditional ^{14}C method. The highest light rate decreased by 73 to 80 % from the first reading (Figure 2.3-4) and the Fv/Fm decreased to 66 % of the initial morning maximum by 10:05 am and to 35 % by 11:40 am. Thus this time series of surface productivity demonstrates a potential 2 or 3 fold variation in the maximum rates over the morning hours.

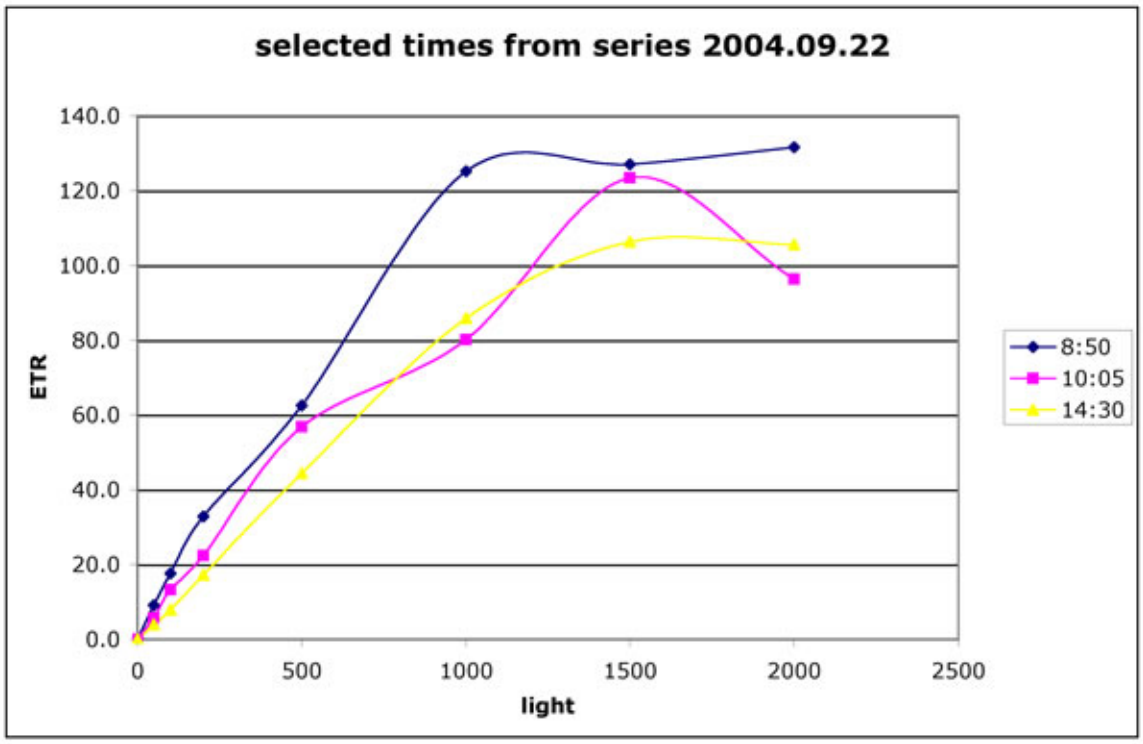

Figure 2.3-4. Representative light curves selected from the set of 7 curves taken over the day on September 22, 2004. ETR is the electron transport rate, which is calculated from the measured Yield and the light. The light is in µmol photons m^{-2} s^{-1}. Each point is the average of four separate measurements of the light curve.

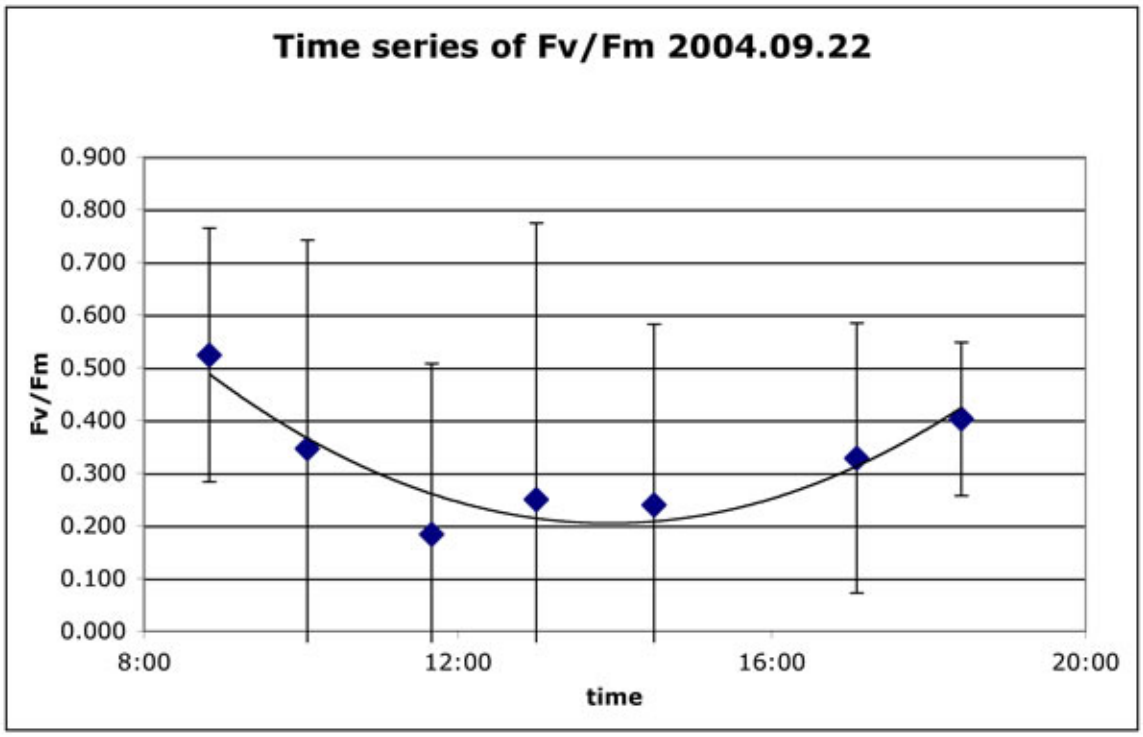

Figure 2.3-5. Maximum photosynthetic Yield of surface samples collected over the day on September 22, 2004. Each sample has been dark-adapted for about 10 minutes to give the maximum Yield. Each point is the average of 5 readings on 2 subsamples of 2 lake samples, about 20 readings per point. The error bars show 2 standard deviations.

The decrease over the day could be the result of inhibition of the entire surface population by small doses of high light. Even though these cells are being mixed, it only takes several minutes of exposure to full light to decrease the photosynthetic rate (Figure 2.3-6). A large portion of this decrease can be attributed to an increase in non-photosynthetic quenching (i.e., the enhanced heat dissipation that results from the active energization of the thylakoid membranes, Figure 2.3-7). This is a photo-protective mechanism that will relax after several minutes after the cells are out of damaging light. This set of measurements shows how the PAM-F provides information at the time scale of cellular response and surface mixing that is important for understanding the coupling between the physical and biological processes. In fact, in the time span of a PAM-F measurement run a decrease in photosynthesis yield can occur. The PAM-F is usually programmed to proceed from low to high light and by the end of a measurement sequence, the cells have started to down-regulate (Figure 2.3-8) but recover almost completely within about 6 minutes in the dark.

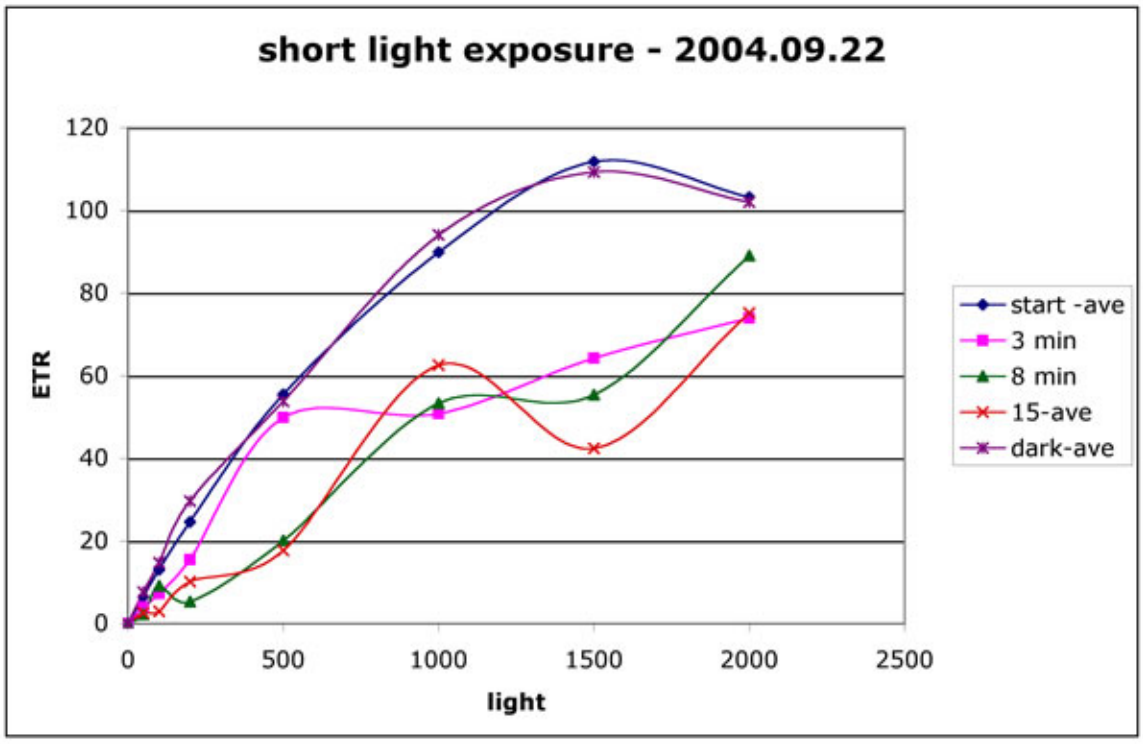

Figure 2.3-6. Light curves run on samples that had been exposed to full light for 3, 8 or 15 minutes. The original sample was kept in the dark and assayed again after the other runs were complete.

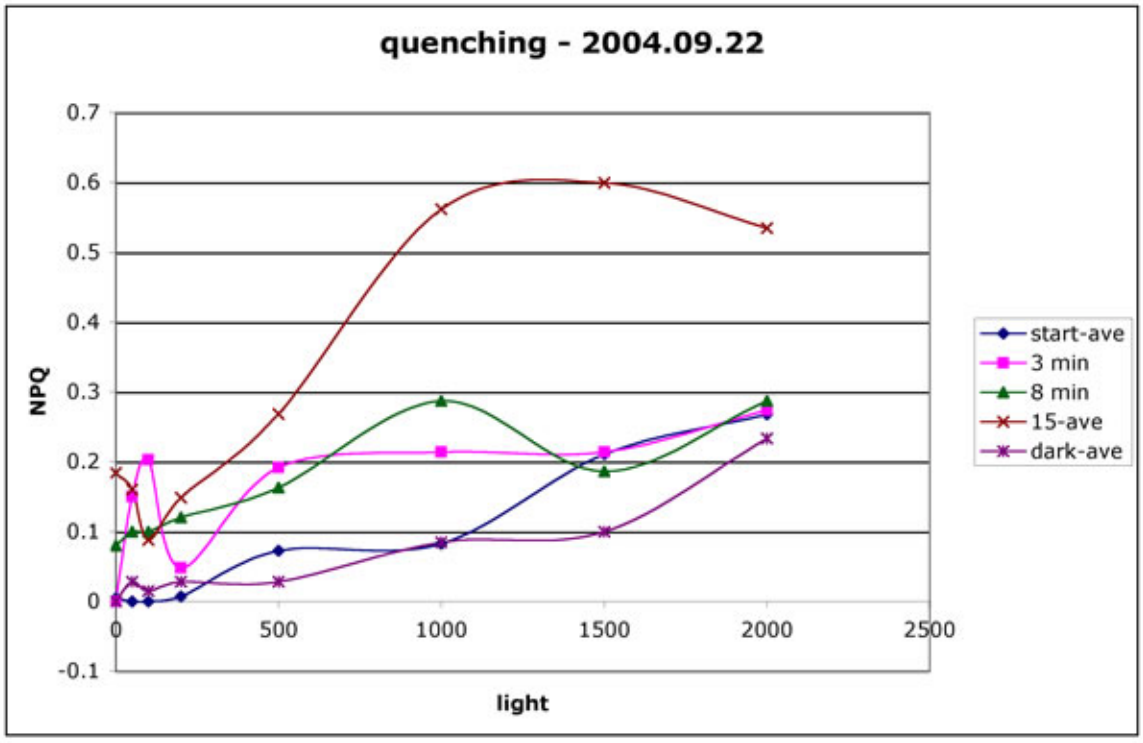

Figure 2.3-7. Non-photosynthetic quenching of the same samples as shown in Figure 2.3-6.

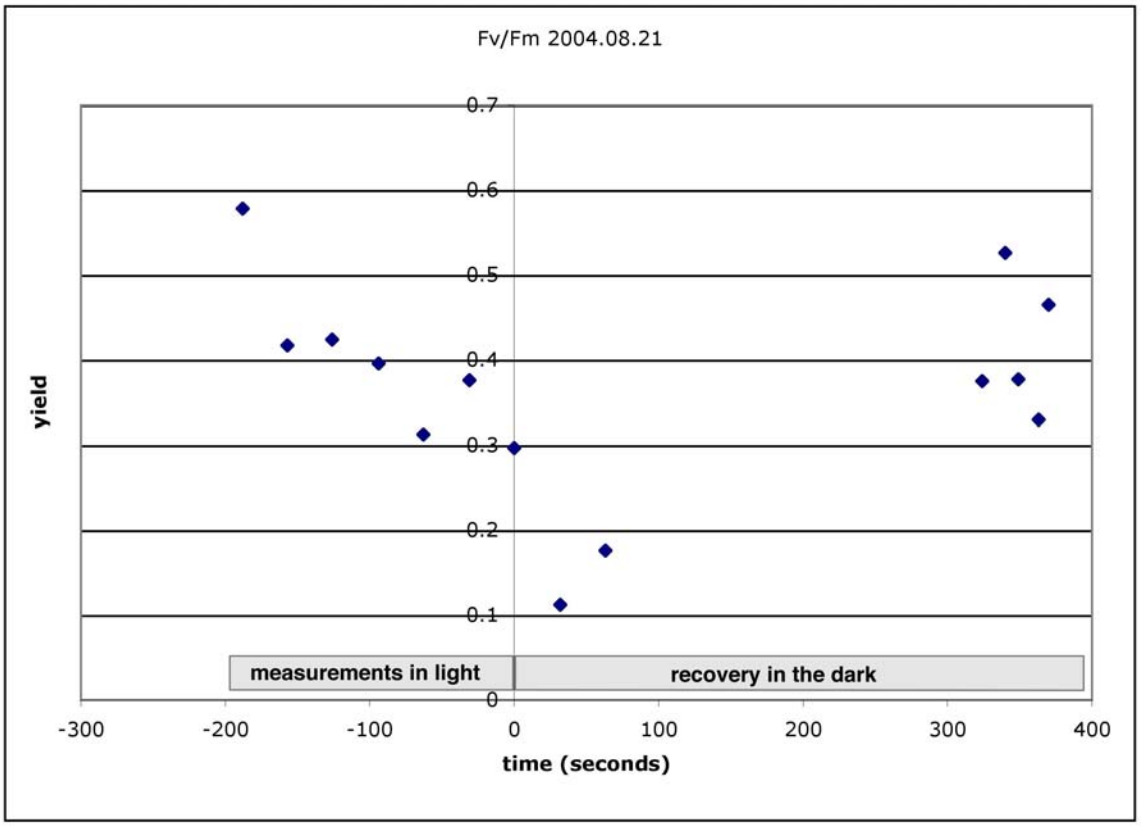

Figure 2.3-8. Decease in Fv/Fm during the measurement of a light curve (before time = 0) and the recovery in the dark for the next 400 seconds.

The rapid changes in photochemistry versus quenching processes in these cells could indicate that it will be necessary to be aware of the order of light exposures. For example, a simple light curve in which the cells are exposed to measuring light levels that increase from 0 to 2000 µmol photons m^{-2} sec^{-1} results in a lower response (ETR) at high light than is observed if the light levels are set to jump around between high and low values during the run (Figure 2.3-9). This presents a challenge for measurement because it may be that when cells are mixed through the surface water light field they experience a particular rate of increase or decrease in light, not a simple jump to a high light. So, whereas a single measurement at 2000 µmol photons m^{-2} sec^{-1} bracketed by dark periods might give a higher (and potentially more reproducible) measurement, that may not be a hydrodynamically or physiologically realistic value for productivity.

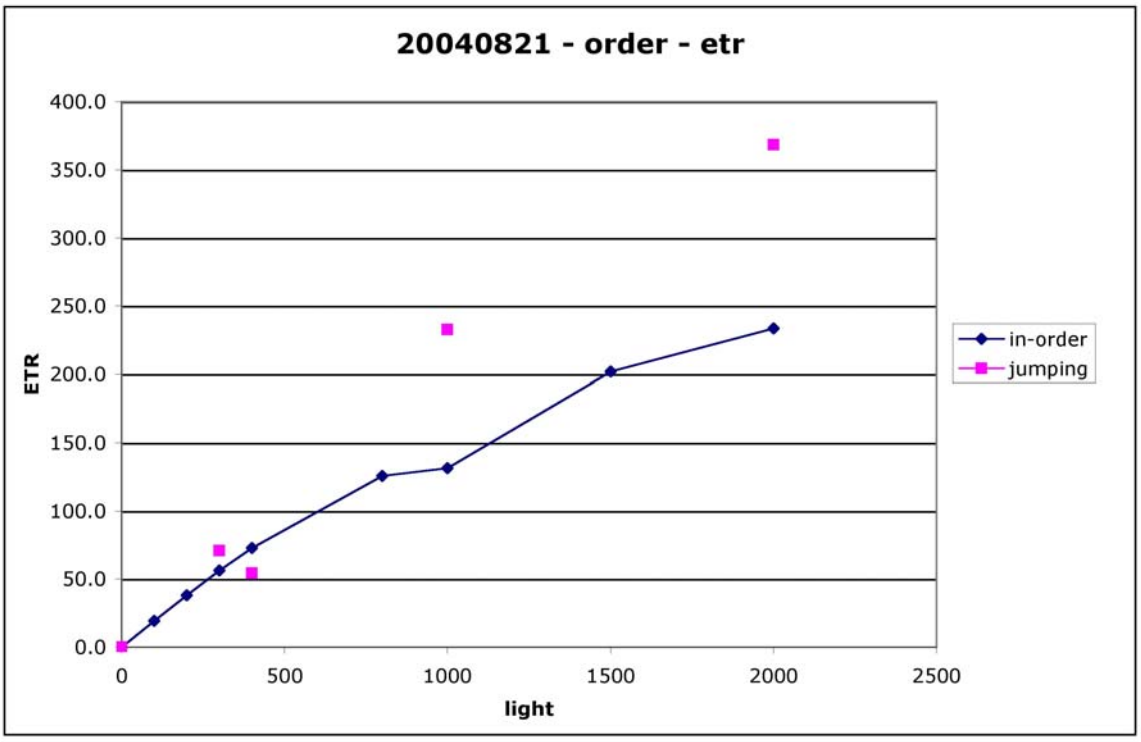

Figure 2.3-9. Comparison of two light curves, on in which the light levels ramp up from 0 to 2000 and the other in which the measuring light levels were set to jump around in the sequence 0, 1000, 300, 0, 2000, 0, 400.

Even though there are rapid photoprotective responses, it is also possible to demonstrate photoinhibition. The working definition of photoinhibition is the decrease in photosynthesis that doesn't recover after 40 minutes in the dark or low light (Figure 2.3-3).

Of particular interest in this study was whether there was increased photoinhibition due to the high UV radiation at Waldo Lake. Other studies have used simple comparison of incubations with total light to those in which the UV was screened out using a plexiglass filter (See Section 2.2). Using PAM-F to study photoinhibition due to UV radiation at Waldo Lake did not demonstrate any clear effect of PAR + UV vs. PAR. The general pattern of photoinhibition and recovery is a decrease in Fv/Fm after about a 20 minute exposure to ambient light and then a slow recovery over the next 40 to 100 minutes (Figure 2.3-10). The recovery rate in this run was linear at a rate of 0.0015 Fv/Fm units per minute, which means that it would take over 2 hours to recover to the original Fv/Fm of the starting culture. In one run of this experiment, the UV screened condition showed more severe inhibition than the full light (PAR+UVR) (data not

shown). On another sampling day (September 9, 2004) the exposure to PAR or PAR+UVR resulted in the same level of inhibition and none of the samples recovered (Figure 2.3-11). In the natural system, such inhibition would have a major impact on estimates of daily integrated productivity.

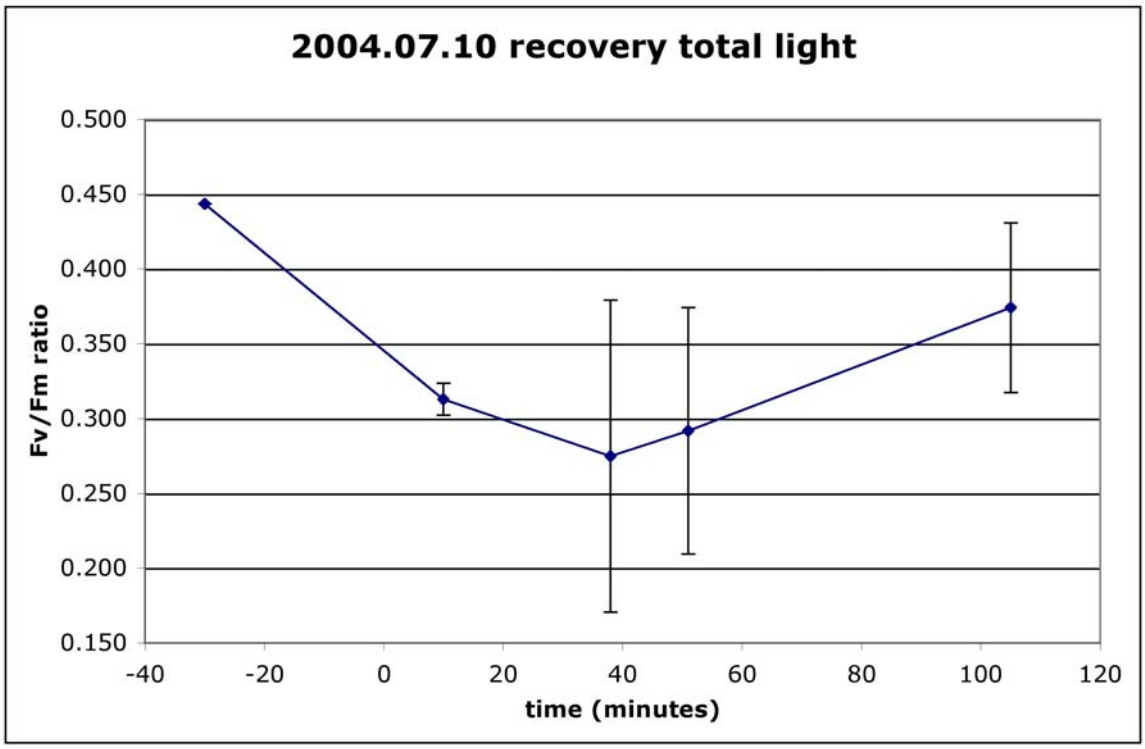

Figure 2.3-10. A surface water sample was incubated on-shore with exposure to full light and then put in the dark for the recovery phase. Samples were incubated in Whirl-Pak bags that have a high transmittance of UVR.

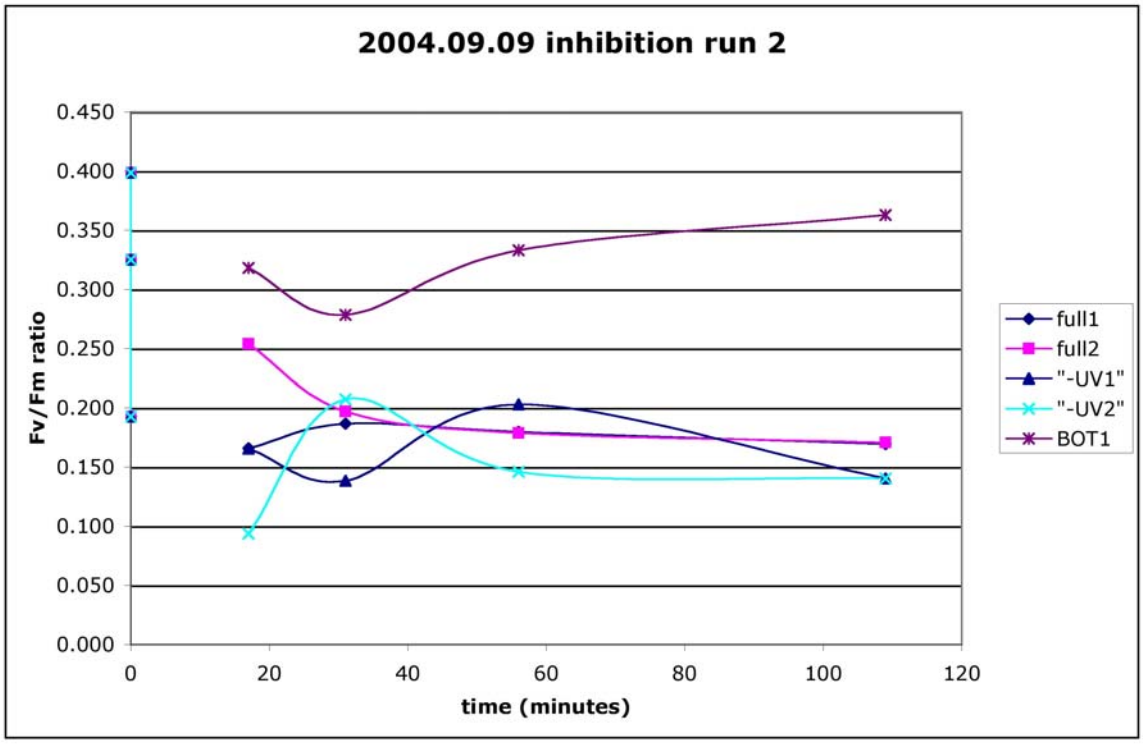

Figure 2.3-11. Samples were exposed to 20 minutes of full light (full) or without UV ("-UV"). The original sample was kept in the dark and measured during the time course (BOT1).

Different weather conditions of sampling dates complicated the analysis of data collected (Table 2.3-3). The weather changes the incident light level, and potentially the ratio of UVA, UVB and PAR as well as the surface water mixing rate. A typical pattern in Waldo Lake is to have a calm morning and a windier afternoon. The maximum wind speed for the hour from 9 am to 10 am was lower than the maximum wind speed from 1 to 2 pm on all sampling days but one (October 10). Previous studies (Sytsma et al. 2004) implicated this afternoon medium wind (around 5 m sec^{-1}) in the recovery of the surface population Fv/Fm. One of the goals for the ongoing analysis is to relate photoinhibition and photorecovery parameters to the weather on the date of sampling (and maybe the days preceding the sampling) and the mixing rates expected in the surface water.

Table 2.3-3. Comparison of weather conditions from the meteorological database. The wind speeds are the maximum wind speed during the hour up to that time.

DATE	noon temp deg C	sky condition	10 am wind max m sec^-1	2 pm wind max m sec^-1	noon solar W m^-2
10-Jul	9.9	overcast	5.1	8.59	917
17-Jul	20.5		1.83	4.61	982
18-Jul	18.4	overcast	1.83	4.38	510
19-Jul	15.6		2.97	6.27	257
21-Aug	17.6		3.01	9.18	911
22-Aug	8.1	heavy overcast	13.62	14.44	239
9-Sep	13.5	partly overcast	1.7	5.75	807
22-Sep	14.8	clear	0.85	5.16	727
10-Oct	5.3	clear	6.4	5.82	659

Discussion

The response of phytoplankton to light on three different time scales of observation has been described in this section and Section 2.2 of this report. The methods chosen were matched to the expected response. Each method has its strengths and weaknesses. The net-daily productivity is measured by 4-hour incubations with ^{14}C (see Section 2.2). This method provides good estimates over a 4-hour time period, but misses short-term variations in light and regulatory response. Photoinhibition is examined on scales of 30 minutes to 1 hour, enhanced heat quenching takes about five minutes and the relaxation of the redox state of PSII takes about 30 to 60 seconds. In this work, at the response of phytoplankton to light was measured on the shortest time scale in order to potentially capture all of these phenomena.

Unfortunately, it is not as simple as just summing up the results from the measurement of short time periods to understand the slower processes. There are two crucial considerations in working across these scales. First, there is an expected relationship between time scale of response and the time scale of light changes in the environment. For example, if cells are well mixed at the surface, they may only be exposed to high light for minutes rather then hours. Second, we should also expect relationships between faster and slower processes that lead to resilient regulation. For

example, the processes that lead to enhanced heat quenching should overlap with the processes that regulate photosynthesis and photoinhibition. The challenge of studying these processes at multiple scales is to understand how the different scales of regulation work together, and how the fast rates are moderated by slower processes and how slower processes lead to metabolic resilience.

This study examined physiological, physical and hydrodynamic processes that ranged over two orders of magnitude of characteristic time scales (from 1.2×10^2 sec to 1.4×10^4 sec) (Table 2.3-4). The rate of mixing in surface waters and the attenuation coefficient of light will lead to changes in the light level for cells as they are mixed around. The surface water mixing velocity (u*) can be estimated using the formula surface_wind_velocity/800. Reynolds (1997) describes this as a simple yet robust estimation from wind speeds between 5 and 20 m sec^{-1}. For example, if u* = 0.003 m sec^{-1} and attenuation of PAR = 0.1 m^{-1}, a 5 meter change in depth will halve the light and (at this mixing rate) it would take about 1.6×10^3 seconds (about 26 minutes) for cells to be mixed that far. I would expect that the resident population of algae would be adapted or acclimated to have efficient regulation of photosynthesis for changes of light over this time scale. This time scale for mixing can also be used to estimate the amount of time that any cell would be exposed to full surface light intensity. Exposures to full light of several minutes resulted in cellular photoprotective responses that should rapidly recover (Figure 2.3-6; Figure 2.3-7; Figure 2.3-8), whereas longer 20 minute exposures to full light were essentially irreversible in some cases (Figure 2.3-11). The standard methods for using PAM-F to explore photoinhibition need to be refined to differentiate the time scale of exposure that leads to photoprotection compared to photoinhibition.

Table 2.3-4. Characteristic time scales for photosynthetic measurements and physical factors that change light.

Measurement or Process	Time Scale	Seconds
net photosynthesis	4 hours	1.4×10^4 seconds
photoinhibition – dose	10 minutes	6.0×10^2 seconds
photoinhibition - recovery	1/2 hour	1.8×10^3 seconds
relaxation of membrane energization	5 minutes	3.0×10^2 seconds
daily change in light (half change from noon on a 12 hour solar day)	240 minutes	1.4×10^4 seconds
2 fold light change on a cloudy day (such as July 17-19, 2004)	2 to 20 minutes	1.2×10^2 seconds to 1.2×10^3 seconds
mixing velocity x extinction for halving of light	26 minutes	1.6×10^3 seconds

Non-photochemical quenching has been shown to be enhanced in cells under carbon limitation (Reddy and Gnanam 2000). To explore this possibility, samples of cells were gently bubbled with higher CO_2 air by exhaling through a straw. This method of raising the CO_2 can be reversed by gently bubbling again with ambient air from a syringe.

The productivity response to increased CO_2 varied among samples. For example, in a sample that increased, the productivity was higher at all light levels and the maximum rate was almost two times higher than ambient CO_2 samples (Figure 2.3-12). Other samples that didn't respond to bubbling may have already been photoinhibited, but further verification is required.

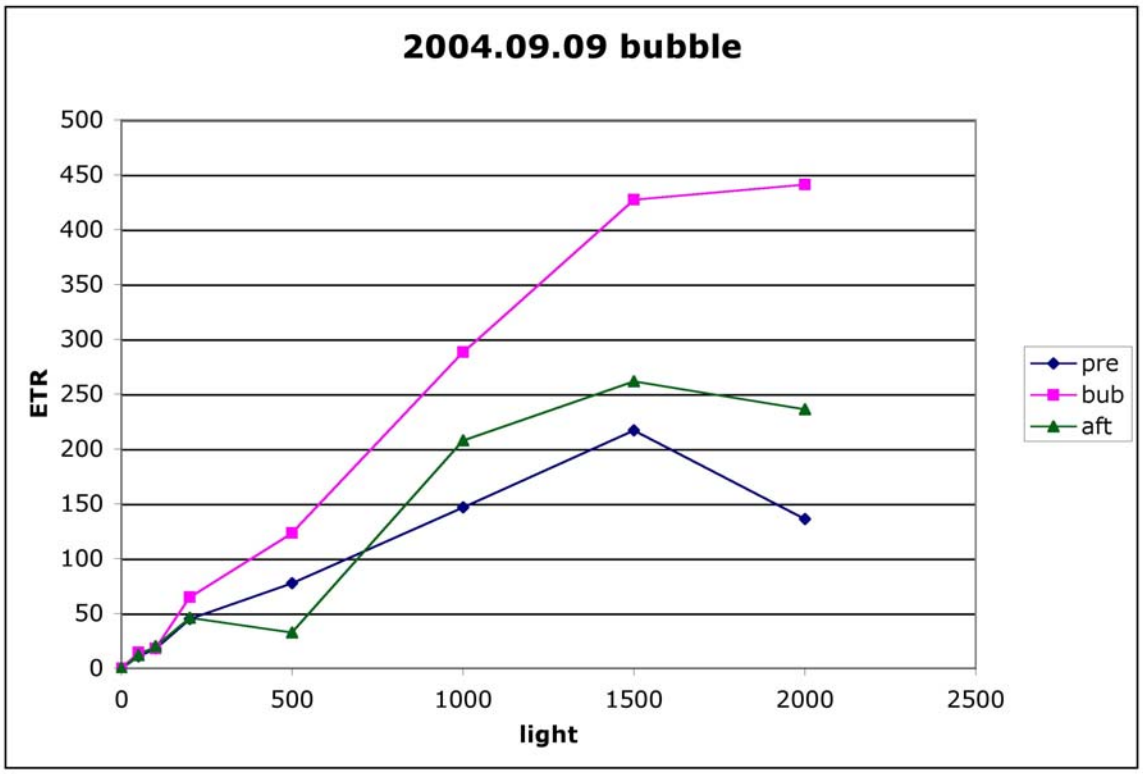

Figure 2.3-12. Samples were measured for the light curve response then gently bubbled by breathing out through a straw for 2 minutes. The sample was then bubbled gently with air from a syringe to re-equilibrate with ambient air CO_2 levels.

Non-photosynthetic quenching was expected to decrease with higher CO_2. Instead, the NPQ was higher after the samples were bubbled with CO_2 and stayed high after the samples were bubbled with ambient air (Figure 2.3-12). In other bubbling experiments there was a wide range of responses, indicating that more systematic study is required.

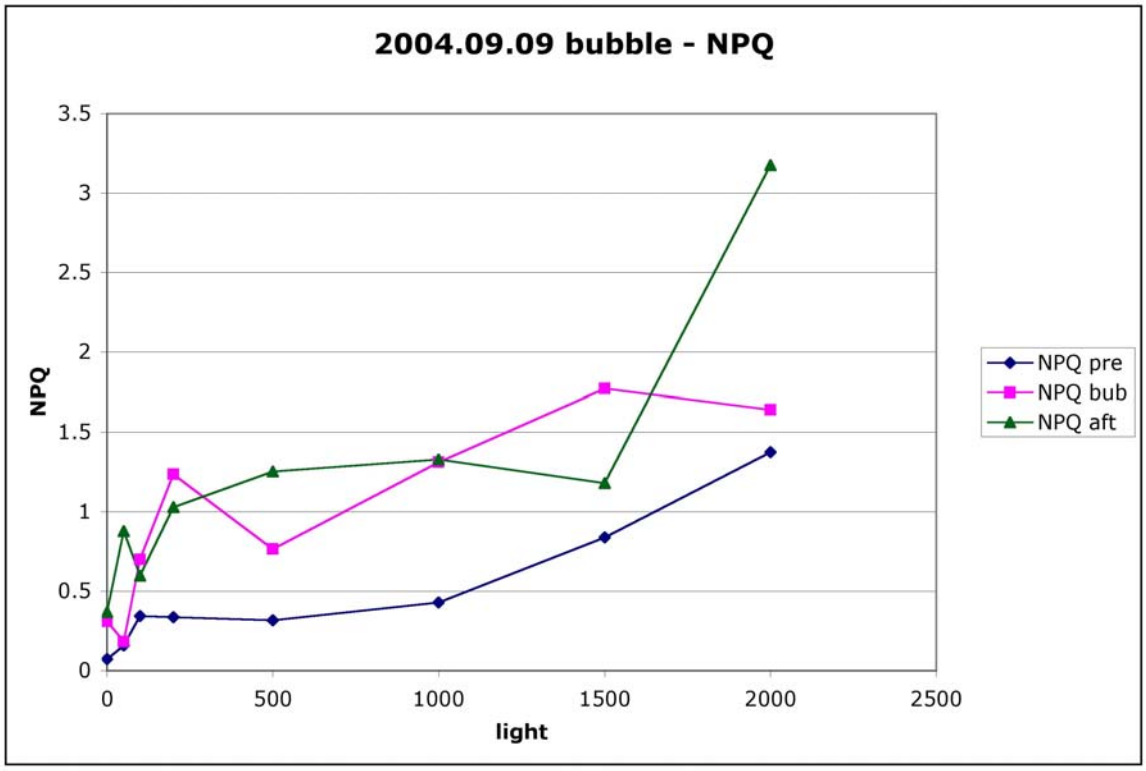

Figure 2.3-13. NPQ data for the same samples as in Figure 2.3-12.

There was a general trend that the ETR was higher and the NPQ was also increased. For example, on September 9, 2004, the first set of bubbling experiments showed an increase of ETR only at the highest lights (1500 and 2000). The maximum rate in the bubbled sample was 2.4 times higher than before bubbling. The NPQ was higher at all lights, averaging 5 times higher for the entire light curve and 3.9 times higher at the maximum rate.

These studies indicate that CO_2 conditions affect both the net productivity estimates and the rapid quenching mechanisms. Even in remote, wilderness lakes it may be possible that increasing atmospheric CO_2 concentrations due to global carbon pollution could easily lead to enhanced productivity and it could help cells protect themselves from short term exposures to high light.

Recommendations for future work

Use of the WATER PAM-F in Waldo Lake has been very successful because of the high sensitivity of this instrument. This is the only instrument capable of detecting

changes in productivity and photoprotection over the time scales of several minutes. This sensitivity can be used to examine processes over a wider range of time scales.

The results and analysis from this portion of the work also indicate that there is still substantial room for improving techniques that are designed to examine patterns of productivity, photoprotection and photoinhibition. Two specific improvements are needed. First, a reliable method is needed to screen UVA and UVB to determine the relative effects of these wavelengths on photoinhibition and photoprotection mechanisms. This task will probably require the ability to measure UVA and UVB in the water and in incubation chambers. Second, the use of a pump to sample small volumes from a range of depths in the surface mixed layer. Other investigators have used a peristaltic pump to obtain samples from between 5 and 20 meters depth. Using such a pump would allow for almost real time monitoring of the Fv/Fm at depth and how it changes with wind and light.

In this work, a very simple relationship between wind speed and surface water mixing rate was used. In future work, we plan to compare the mixing rate (as estimated here) to the mixing rate estimated by the CE-QUAL-W2 model. The approach used in modeling the photosynthetic competency of the algae is a rudimentary version of modeling the behavior of individual particles. The Lagrangian frame used here could be greatly improved by using a more sophisticated mixing model. The predictions that photosynthesis should vary due of weather, being higher during mixing and lower during times of low wind and high sun could be tested with this more sophisticated model. If global climate change scenarios are to be explored (See Section 5.1), changes in the climate may have a big effect on the productivity of this lake. The preliminary observations that CO_2 increases enhanced the yield and quenching are also significant in this age of atmospheric carbon dioxide increase and should be investigated further.

There will be two foci for summer 2005 research; 1) comparison of the pattern of inhibition and recovery from UVR vs. PAR and 2) investigation of the possibility that the phytoplankton populations are limited by dissolved inorganic carbon. The first project will examine the time scale of photosynthesis, photoregulation (i.e. down-regulation) and

irreversible photoinhibition on cells that have been exposed to total surface irradiance compared to total minus UVR. Overlapping time scales of these three processes are expected. Setting up the incubation and measurement times to look for this overlap will be a major improvement over last summer's work. The second project, looking for CO_2 limitation, will use a combination of bubbling and weak $NaHCO_3$ buffers to change the dissolved inorganic CO_2 available to the phytoplankton over minutes to hours. Their immediate response to CO_2 availability can be monitored by examining shifts in the ETR/light curves and by looking at the suppression of down regulation. It is expected that cells with more carbon available will be able to push more energy through photochemical quenching paths (i.e. CO_2 fixation) and less through heat dissipation and fluorescence. The combination of these two projects should provide a better description of the patterns of photosynthesis in the surface waters of Waldo Lake.

2.4 Mixotrophs in Waldo Lake

Introduction

Mixotrophs are phytoplankton capable of both photosynthesis and phagotrophy. There are several genera of mixotrophs that have been identified in Waldo Lake including: *Chromulina, Dinobryon, Rhodomonas, Cryptomonas, Chroomonas, Woloszynskia, Hemidinium,* and *Peridinium*. The dinoflagellate *Woloszynskia neglecta* (syn. *Glenodinium neglectum*) is the predominant mixotroph.

The ability to obtain nutrients from autotrophs and bacteria provides mixotrophs with a competitive advantage, possibly explaining the dominance of mixotrophs in many oligotrophic conditions (Isaksson 1998). Stressful conditions, such as nutrient or light limitation, may produce a shift to phagotrophy to allow mixotrophs to acquire energy. For example feeding by mixotrophs increased with nitrogen and phosphorus deficiency, and phagotrophy was useful for acquiring carbon (Bergstrom et al 2003; Li et al. 2000; Medina-Sanchez and Villar-Argaiz 2004; Raven 1997).

Bacteria populations in a lake may be related to cell density of mixotrophs and autotrophs. Several studies have shown that mixotrophs dominated over autotrophic phytoplankton when bacterial production was high (Bergstrom et al. 2003; Jansson et al.

1996). Mixotroph dominance was explained by their use of bacteria as a nutrient source. This process could be particularly important in high altitude lakes, in which UV-stressed algae releases organic carbon which could stimulate bacterial growth (Medina-Sanchez and Villar-Argaiz 2002).

Due to interactions between mixotrophs, autotrophs, and bacteria, a potential link between mixotrophy and trophic status has been suggested (Isaksson 1998). It is possible that mixotrophs may help to maintain clearer bodies of water, by consuming phytoplankton, which may result in a reduced biomass of algae in lakes. In addition, mixotrophs may out-compete autotrophs, thereby reducing the numbers of autotrophs, particularly in oligotrophic waters. During their growth, mixotrophs give off organic carbon, which bacteria take up. Bacteria are able to take up inorganic P and N from the water, making these nutrients less available for autotrophs. Bacteria are then consumed by mixotrophs, which allows mixotrophs to dominate in a nutrient depleted system (Stockner and Porter 1988). Therefore, it is possible that the presence of mixotrophs acts to maintain a more oligotrophic state in lakes (Figure 2.4-1).

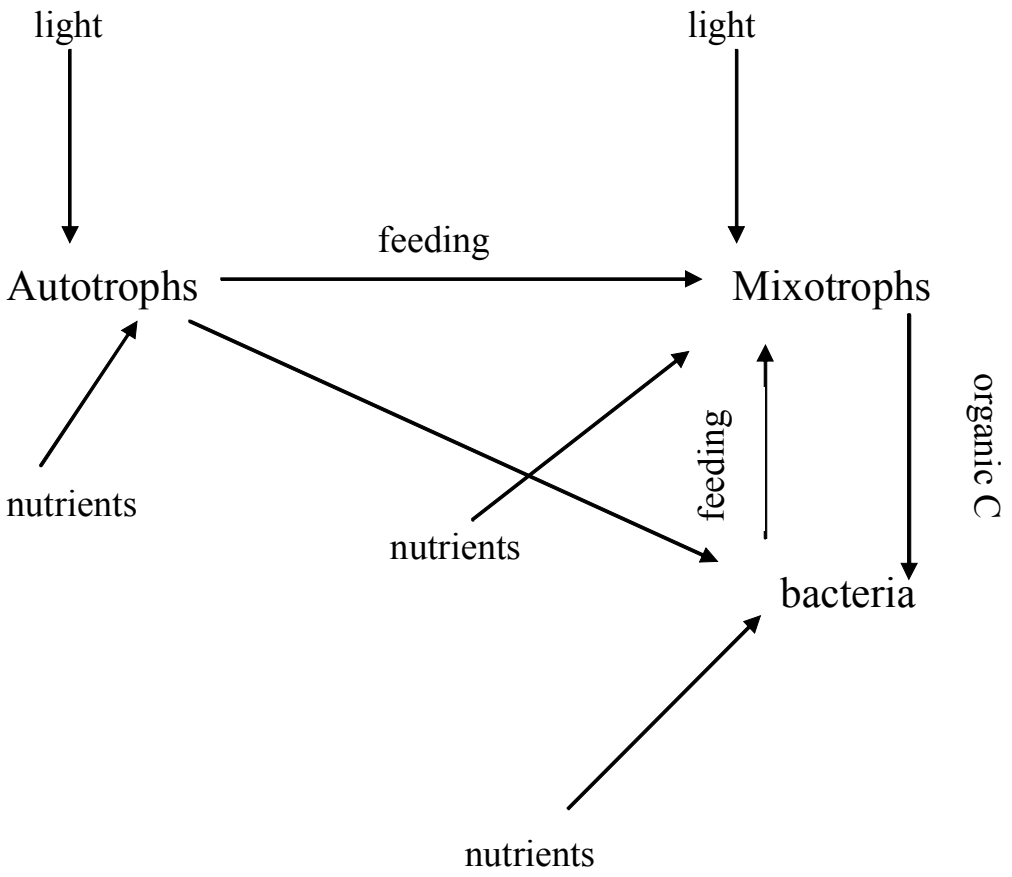

Figure 2.4-1. The microbial loop depicting interactions among mixotrophs, autotrophs, and bacteria.

The purpose of this report section was to investigate mixotrophy in Waldo Lake. This section examines cell densities of and relationships among mixotrophs, autotrophs and bacteria over the course of the sampling season and at varying depths in the water column. A review of data from past Forest Service reports was completed to explore variation in the M/A ratio over the past twelve years.

Methods and Analysis

Fieldwork and laboratory methods

Water samples were collected from 1, 12, 24, 40, 60, 80, and 100 meters using a 2.5-L Model 1010X Niskin bottle. All samples were collected at the long-term monitoring site. Samples were collected on four 24-hour periods throughout the sampling season (Table 2.4-1).

Table 2.4-1. Sampling schedule for 2004.

Sampling Date	Sampling Time	Depths
7/27/04	1900	1,12,24,40,60,80,100
7/28/04	730	1,12,24,40,60,80,100
8/20/04	2000	1,12,24,40,60,80,100
8/20/04	2300	1,12,24,40,60,80,100
8/21/04	600	1,12,24,40,60,80,100
8/21/04	1100	1,12,24,40,60,80,100
8/21/04	1500	1,40,100
9/13/04	900	1,12,24,40,60,100
9/13/04	1500	1,12,24,40,60,80,100
10/6/04	730	1,12,24,40,60,80,100
10/6/04	1500	1,12,24,40,60,80,100

Samples were divided into 2 parts: 5-ml bacteria samples and 200-ml phytoplankton samples. Ten percent of all samples were randomly chosen as duplicate and duplicate slides were prepared and analyzed. Bacteria samples were preserved with a 2 % formaldehyde solution and kept below 4º C in the dark. Bacteria samples were stained with DAPI at a concentration of 0.1 ∝g/ml. Samples were filtered within two weeks of collection onto black 0.2 micrometer membrane filters. Filters were mounted onto slides, and bacteria were enumerated using epifluorescence microscopy. A standard Zeiss microscope was used at 1000x to count random fields of view until 20 fields or 200 cells was reached (Clesceri et al. 1998).

Phytoplankton samples were preserved with a 1 % Lugol's solution. Phytoplankton samples were filtered onto 0.45 micrometer membrane filters and mounted onto slides. Slides were prepared with immersion oil and painted with nail polish in order to archive the samples. Algal units were counted either along a measured transect of the microscope slide or with random field of view using a Zeiss standard microscope at 1000x (Alverson et al. 2003). A minimum of one hundred algal units were counted; only algae with intact chloroplasts were counted (APHA 1992). Phytoplankton were identified to genus.

Results

Mixotrophs were a prevalent part of the phytoplankton community throughout the sampling season, although greater cell densities of autotrophs early in the season resulted in a larger number of autotrophs in 2004 overall (Figure 2.4-2). A sample taken on 7/28

(80 m, 1500), showed an unusually large number of autotrophs (1978.24 cells/ml). This sample had a large effect on the average cell density of autotrophs for the 7/28 sampling date and the overall autotroph density.

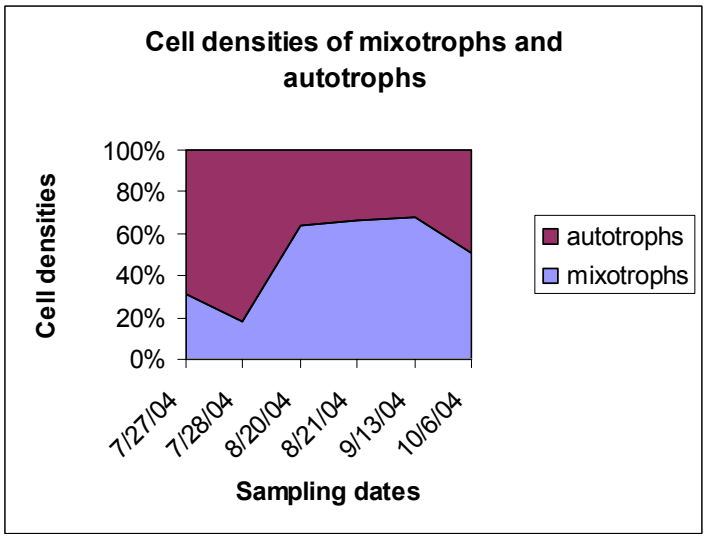

Figure 2.4-2. Percent of total average cell densities (number of cells per ml) of mixotrophs and autotrophs throughout the sampling season. Average densities were calculated on each sampling day.

The mixotroph/autotroph (M/A) ratio was lowest on 7/28, when the cell density of autotrophs was unusually high. The M/A ratio was highest on 8/20-8/21 and 9/13 and decreased on 10/6 (Figure 2.4-3).

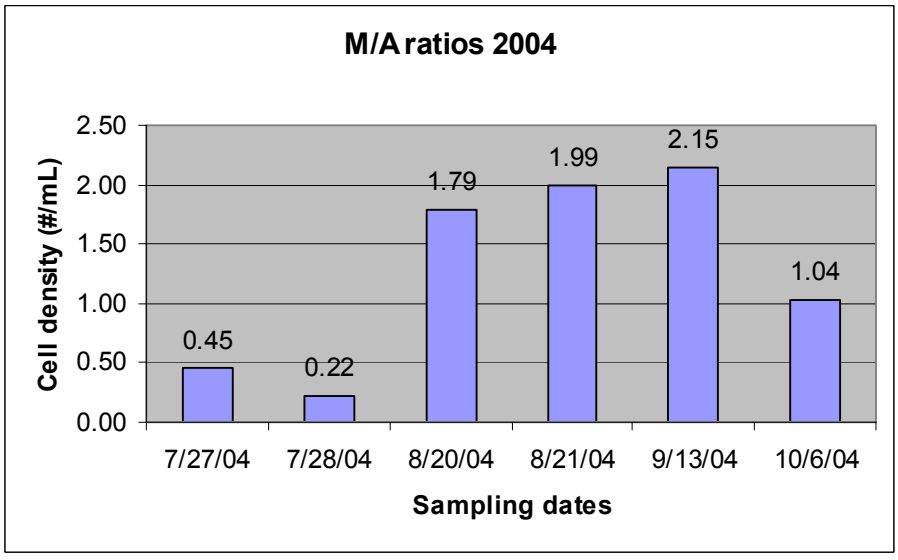

Figure 2.4-3. Total mixotroph and autotroph densities were calculated for each sampling date. The M/A ratio was calculated by dividing total densities on each date.

Changes in mixotroph/autotroph ratio from 1993-2004

The M/A ratio varied over the past twelve years (Figure 2.4-4). The M/A ratio ranged from 0.4 to 15.0. Highest values were found in 1993 with an M/A ratio of 15.0. The ratio decreased in 1994 and 1996 when samples were taken only in the month of September. The ratio from 1998-2004 is much lower than the M/A ratio found in 1993-1997. The ratio in 2003 was the lowest at 0.4, with only a slight increase in 2004 to 0.8.

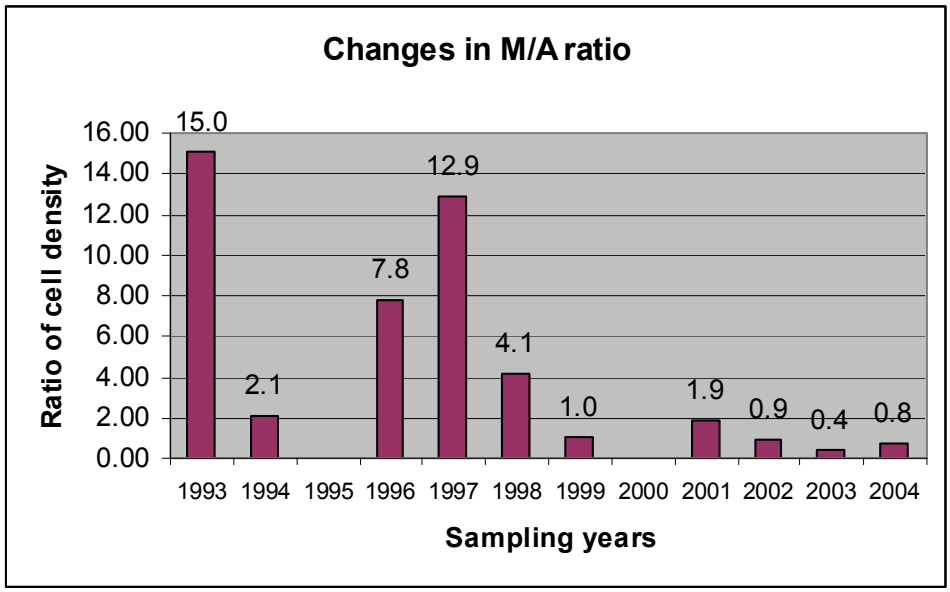

Figure 2.4-4. The M/A ratio of cell density (# cells/ml) dropped over the past 12 years sampled. No sampling occurred in 1995 or 2000.

Mixotrophs and bacteria

Bacteria density in Waldo Lake was relatively low. Density of bacteria at all depths was approximately 10^4 (cells/ml) (Table 2.4-2).

Table 2.4-2. Bacteria density at seven depths throughout the 2004 season (#cells/ml *10^4)

Depth	Jul-04	Aug-04	Sep-04	Oct-04
1	1.8	3.9	6.2	4.1
12	1.6	4.9	7.1	6.2
24	1.4	5.2	6.1	4.8
40	1.3	5.0	10.1	4.7
60	2.4	5.4	2.0	4.1
80	1.1	7.6	no data	4.9
100	4.8	4.0	7.5	6.4

The relationship between mixotrophs and bacteria showed a slight increase in bacterial density as mixotroph density increased (Figure 2.4-5). However, this relationship was not statistically significant (Pearson's $r^2 = 0.03$, d.f. = 57, p = 0.83).

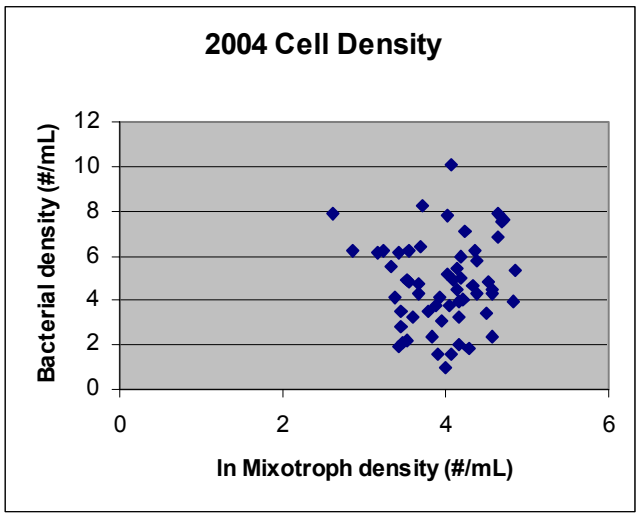

Figure 2.4-5. Only a weak relationship between cell density of mixotrophs and density of bacteria was found.

As the density of bacteria increased, density of autotrophs decreased slightly (Figure 2.4-6). Again, this relationship was not statistically significant (Pearson's $r^2 = -0.10$, d.f. = 57, p = 0.44). No seasonal patterns or patterns of varying depth were found.

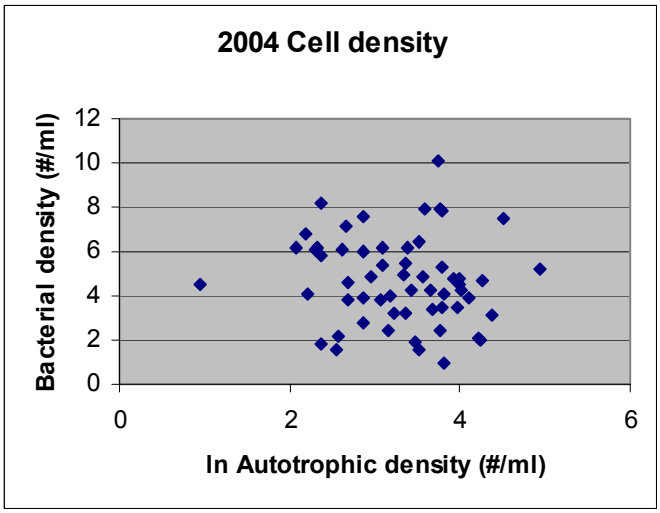

Figure 2.4-6. Only a weak relationship between bacteria density and density of autotrophs was found.

Discussion

The presence of mixotrophs in Waldo Lake may be related to the trophic status. Phosphorus limitation has produced mixotrophic behavior (Li et al. 2000). It is possible that the low nutrient environment in Waldo Lake allows mixotrophs to effectively compete with autotrophs. The ratio of mixotrophs to autotrophs was greater in samples collected during August and September than in samples collected during July and October. The ratio of mixotrophs to autotrophs dropped slightly in October. This decrease in cell density of mixotrophs in the fall could be due to the naturally expected decline of dinoflagellates in October-November (Carty 2003).

Data from the last twelve years showed that the M/A ratio much lower in the 1998-2004 period than the 1993-1997 period. If this trend continues, the M/A ratio could lower significantly. Changes in species composition, particularly a decrease in numbers of mixotrophs could result in an increase in autotrophs (Isaakson 1998). Additionally, there was a dip in the M/A ratio in 1994 and 1996. In these years seasonal mixotroph abundance may not be accurately represented, as samples were only collected in September. Comparatively, other sampling years included samples taken earlier in the season as well as fall sampling times.

In addition, weather was possibly a factor in the vertical distribution of dinoflagellates during the 2004 sampling season. Weather conditions varied from clear, sunny days to stormy days with high winds. For example, on 8/20-8/21, the average wind speed was greater than 4 m/s for three out of five sampling events. According to Reynolds (1984), flagellated phytoplankton were unable to overcome currents generated by wind speeds greater than 2-3 m/s. Thus, the distribution and vertical movement of mixotrophs may have been affected by wind-driven mixing.

The numbers of bacteria in Waldo Lake were relatively low. Bacterial abundance in lakes normally ranges from 10^5 to 10^6 (Kalff 2002). Bacterial density is approximately 10^5 in Crater Lake, Oregon (Page et al. 2004). All values in Waldo Lake were within the range of 10^4, suggesting ultra-oligotrophic conditions. Stressful environmental

conditions, such as high levels of UV could also be inhibiting bacterial growth (Medina-Sanchez and Villar-Argaiz 2002).

It would be interesting to examine the food chain, particularly the microbial loop in detail at Waldo Lake. The microbial loop plays a particularly important role in oligotrophic waters (Stockner and Porter 1988). The microbial loop is the food chain into which heterotrophic bacterial production flows to phagotrophic algae (Kalff 2002). Carbon and nutrient flow within the microbial loop is the result of three processes: the production of DOM by phytoplankton (which is subsequently used by bacteria), competition for nutrients between phytoplankton and bacteria and predation by flagellates (Stockner and Porter 1988). The interaction between bacteria and mixotrophs results in reduced growth of autotrophs. Bacteria growth is enhanced by the increased release of carbon from UV-stressed algae, which is common in high-altitude lakes (Medina-Sanchez and Villar-Argaiz 2002). Nitrogen and phosphorus are removed from the water column by bacteria, leaving few nutrients available for autotrophs. Bacteria have been shown to be superior competitors for both phosphorus and nitrogen when compared to autotrophs (Currie and Kalff 1984; Caron et al. 1988). Mixotrophs then consume bacteria, meeting their need for nitrogen and phosphorus through bacterivory. This process may reduce the growth of autotrophs, resulting in a lower biomass of non-phagotrophic phytoplankton and maintaining oligotrophic conditions.

Results from this study indicated a lack of statistical evidence for a strong microbial loop in Waldo Lake. Numbers of bacteria only decreased very slightly when mixotroph cell density increased and similarly the relationship between bacterial density and the density of autotrophs was very weak. However, it is possible that the mixotrophs present in Waldo Lake are feeding primarily on autotrophs, rather than bacteria. Studies have shown that some species of mixotrophs are efficient consumers of autotrophs rather than bacteria (Tittel et al. 2003). Dinoflagellates in particular have been found to feed on other phytoplankton (Boraas et al. 1988; Isaksson 1998).

Recommendations

The most important area of continued study is the monitoring of species composition in Waldo Lake. A continued trend of decreasing mixotroph to autotroph ratio could be indicative of a shift in the overall trophic status of the lake. In addition, a change in species composition of phytoplankton may indicate larger changes in the food web. Early warning signals that precede an ecosystem shift can be subtle (Scheffer 2001). It is important to continue to collect data and monitor any changes in the phytoplankton community structure in Waldo Lake.

Further investigation of the food web is an important next step in Waldo Lake. The weak statistical relationships in this report demonstrate that understanding trophic relationships will probably entail more than simply collecting and counting more phytoplankton and bacteria samples. Phytoplankton response to the environment is both species and habitat specific (Vinebrook and Leavitt 1999). Species of mixotrophs exhibit a wide range of feeding behaviors (Jones 2000). It is important to study the feeding behavior of the species of mixotrophs found in Waldo Lake (primarily *Woloszynskia* and *Hemidinium*). It is unknown whether these species are primarily consuming bacteria or other autotrophs. Feeding behavior of the main species of mixotrophs found in Waldo Lake could be assessed with fluorescently labeled bacteria. Bacterial production can be assayed using radio-labeled thymidine (Medina-Sanchez and Villar-Argaiz 2002). A combination of intense sampling with depth and short-term feeding incubation experiments would probably provide the most information.

2.5 Assessment of SCUFA Techniques for Determination of Chlorophyll-a Distribution

Introduction

In 2003, a preliminary assessment of *in vivo* fluorescence profiles collected with a Self-Contained Underwater Fluorescence Apparatus (SCUFA, Turner Designs™) in Waldo Lake was completed for the USDA Forest Service (Sytsma et al. 2004). The results indicated that the discrete sampling employed by the long-term monitoring program may not accurately represent the vertical distribution of chlorophyll-a.

No data are currently available regarding the complete distribution of phytoplankton in the water column. Samples collected for chlorophyll extraction at discrete depths can hit or miss a chlorophyll peak in the water column. Fee (1976) reported that chlorophyll estimates from discrete samples (which may miss a localized chlorophyll peak) have an estimated error of 40 %, whereas estimates from a single integrated fluorometer had a probable error of 25 %. The use of a SCUFA provides rapid water column profiles of in vivo fluorescence, and provides a more complete representation of the distribution of chlorophyll and, thus, phytoplankton in the water column than samples collected at discrete depths.

In vitro chlorophyll-a extraction is a common method for estimating algal biomass. The use of fluorescence to assess algal biomass has also been a long-recognized tool in limnology (Fee 1976; Abbott et al. 1982; Harris 1986). SCUFA fluorescence readings are expected to be positively correlated with in vitro chlorophyll-a concentrations: as chlorophyll-a increases the fluorescence signal increases. SCUFA transmits an excitation beam of saturating light at 440 nm (blue) into the water and detects the energy re-emitted (fluorescence) at 680 nm (red) by algal chlorophyll molecules. By analyzing chlorophyll-a samples using traditional extraction methods in tandem with SCUFA profiles, fluorescence values can be calibrated to provide an estimate of chlorophyll-a for depths that were not measured directly.

In vitro extracted chlorophyll and cellular fluorescence methods to estimate algal biomass both carry a degree of variability and uncertainty. The chlorophyll concentration and light harvesting processes of an individual cell may vary among species. Extracted chlorophyll methods involve laboratory procedures which can easily be contaminated. The fluorescence signal is influenced by biological and physical factors. Ambient light levels and history of light exposure affect the fluorescence response of a chlorophyll molecule. A cell experiencing a light environment representative of its maximum photosynthetic efficiency will fluoresce more than a cell from a damaging or limiting light environment (Turner Designs 2002). High turbidity may interfere with the excitation beam before it reaches the chlorophyll molecules of the cell. Dead or unhealthy algae containing viable chlorophyll molecules may also interfere with the

fluorescence signal (Turner Designs 2002). Pheophytin (chlorophyll degradation products) fluoresces less than chlorophyll. As temperature decreases the fluorescence signal increases independently of chlorophyll concentration.

The objectives for the summer of 2004 were to further evaluate the effectiveness of SCUFA technology in Waldo Lake, based on its accuracy, precision and ease of use and to develop a protocol for its use in the future. These objectives were accomplished during a study to assess diurnal variation in the vertical distribution of phytoplankton (Johnson *in prep*.) Goals for this research included: (1) characterize the distribution of chlorophyll-a for the entire water column and (2) assess diurnal changes in the vertical distribution of phytoplankton/ chlorophyll.

Materials and Methods

Vertical profiles of fluorescence were collected from the long-term monitoring station located at the deepest spot in the lake (120 m) over four 24-hour periods: July 27-28, August 20-21, September 13 and October 6, 2004. Grab samples were collected for in vitro chlorophyll extraction in conjunction with fluorescence measurements for the development of a calibration equation to predict chlorophyll-a from fluorescence.

Data were divided post hoc into five time periods: morning, mid day, afternoon, twilight, and midnight (Table 2.5-1). Additional sampling occurred in late morning on September 13, and October 6 and before sunrise on October 6 (The late morning sampling events were grouped in the morning time period and the before sunrise sampling event was grouped in the midnight time period, based on time period definitions).

Table 2.5-1. Sampling events and post hoc time periods. Sunrise, solar noon and sunset times were provided by NOAA Surface Radiation Research Branch, Sunrise/Sunset Calculator.

Time Period	Definition	Sampled
Morning	Sunrise until 2 hours prior to solar noon	July 28, August 21, Sept 13, Oct 6
Mid day	2 hours prior to solar noon until 2 hours after solar noon	July 28, August 21, Sept 13, Oct 6
Afternoon	2 hours after solar noon until 2 hours prior to sunset	July 28, August 21, Sept 13, Oct 6
Twilight	2 hours prior to sunset until 2 hours after sunset	July 27, August 20, Sept 13, Oct 6
Midnight	2 hours after sunset until sunrise	August 20, Oct 6

A 2.5-L Model 1010X Niskin bottle was used for sample collection at discrete depths (1, 12, 24, 40, 60, 80 and 100 m), although weather and time constraints limited collections during some sampling events. The Niskin bottle was immediately decanted into a 2.5-L amber-colored plastic container. The volume filtered was measured with a graduated cylinder. On July 27-28, 500-ml were filtered. The volume was increased to 750-ml for subsequent sampling events. Samples were filtered immediately with the exception of September 13, when inclement weather postponed filtration for approximately 2 hours.

Chlorophyll-a samples were vacuum filtered under low light onto Whatman GF/F glass fiber filters (0.7 μm pore size) aboard ship. Samples were gently agitated prior to filtration, protected from sunlight exposure, and pressure was kept below 15 cm Hg to avoid cell damage. All filtering equipment were rinsed with deionized water prior to use. Duplicate chlorophyll-a samples were filtered for 45 out of 63 samples, and triplicate samples were filtered for 17 out of 63 total samples collected (one sample was collected without replication). Immediately following filtration, filters were labeled and placed in a light proof container and kept on dry ice until returning to the laboratory where they were kept frozen for up to 45 days. In vitro pheophytin-corrected chlorophyll-a concentrations were determined following EPA method 445.0 (Arar and Collins 1997) using a Turner Designs Model 10-005 R fluorometer.

The SCUFA was programmed to record fluorescence and turbidity. An automatic temperature correction factor was utilized. Fluorescence data were recorded every three seconds. In vivo fluorescence was measured each meter from 0-20 meters and every five meters from 20 meters to the maximum depth. Multiple readings were collected at each depth. Upcast readings were collected at 10 % of the depths sampled, for quality assurance purposes.

Multiple readings for in vitro chlorophyll as well as fluorescence and turbidity were averaged. The coefficient of variation of fluorescence and turbidity readings was calculated for each depth when $n > 2$. Relative percent difference (RPD) was calculated for the rare case where $n = 2$ for readings at a particular depth. Additionally, RPD between the mean fluorescence value for a given depth and its mean upcast value were calculated to assess precision.

Quality Assurance

Quality assurance analyses were completed for in vitro chlorophyll measurements. One duplicate sample was removed from the dataset due to acid contamination and was not included in these mean values. Quality assurance could not be evaluated for samples not collected in replicate ($n = 2$). The mean coefficient of variation for triplicate samples ($n = 17$) was 10.12 ± 3.7 % (mean ± 95 % C.I.). The mean relative percent difference for duplicate samples ($n = 44$) was 5.93 ± 1.5 % (mean ± 95 % C.I.).

Upcast fluorescence readings were collected for all sampling events with the exception of August 21, 2004 at 16:00, due to high winds and time constraints. RPD between readings varied (range 0.05 to 184 % RPD ($n = 114$)). The surface (0 and 1 m) upcasts, exhibited very high RPD (range 0.27 to 184 %, mean 30 % ($n = 25$) compared to upcasts from other depths (range 0.04 to 22 %, mean 5.5 % ($n = 89$).

The surface (0 and 1 m) depths had higher coefficients of variation for fluorescence than other depths (Table 2.5-2). High variation at 0 and 1 meters occurred in July and October; all readings collected during August and September had a coefficient of variation less than 10 %. On August 21, 2004 at 6:00, the 40 m sample had a high coefficient of variation (35.78 %); all other measurements from 40 m were less than 5 %.

High irradiance (particularly in the red wavelengths) and changes in light intensity due to wave action and surface reflection may contribute to the high variability of fluorescence at the near-surface depths. Further, variability at near-surface depths may be due to mixing of algae caused by turbulence, resulting in algal cells with variable light adaptation (See Section 2.3).

Table 2.5-2. Range of variation in fluorescence readings collected with SCUFA at individual depths.

Depth	Minimum Coefficient of Variation (%)	Maximum Coefficient of Variation (%)
0	0.82	76.03
1	0.52	38.93
2	0.68	6.46
3	0.23	4.9
4	0.56	4.43
5	0.8	4.57
12	0.55	4.68
25	0.82	7.66
40	0.32	35.78
60	0.53	4.65
80	0.95	5.64
100	1.35	8.52

Results and Discussion

Turbidity at Waldo Lake is very low. Turbidity readings collected at Waldo Lake during the summer of 2004 using a multi-parameter probe indicated turbidity was commonly less than 1.0 NTU. One Hydrolab® Datasonde 4a profile collected in tandem with SCUFA on July 27, 2004. A turbidity of 0.4 NTU's registered as 0.2 volts by the turbidity channel of SCUFA.

Turbidity did not significantly influence cellular fluorescence at Waldo Lake. Turbidity over 60 NTU is expected to produce a 1 % change in fluorescence signal and over 120 NTU a 2 % change (Turner Designs, E-support, website). The turbidity channel utilized in SCUFA profile data collection confirmed the low turbidity findings for Waldo Lake. Turbidity (volts) was very low for the entire water column, with highest readings at the surface (Figure 2.5-1).

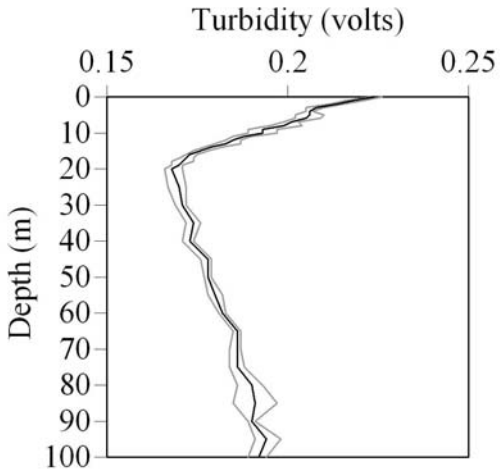

Figure 2.5-1. SCUFA turbidity readings for all 2004 sampling events, mean (black line) and 95 % CI (gray lines). Turbidity is very low in all depths.

In vivo fluorescence readings were expected to be linearly related to in vitro chlorophyll-a concentrations from samples collected in tandem with SCUFA profiles. Cellular fluorescence and chlorophyll were linearly related (Figure 2.5-2) at all depths except the surface (1 m), where cellular fluorescence was variable.

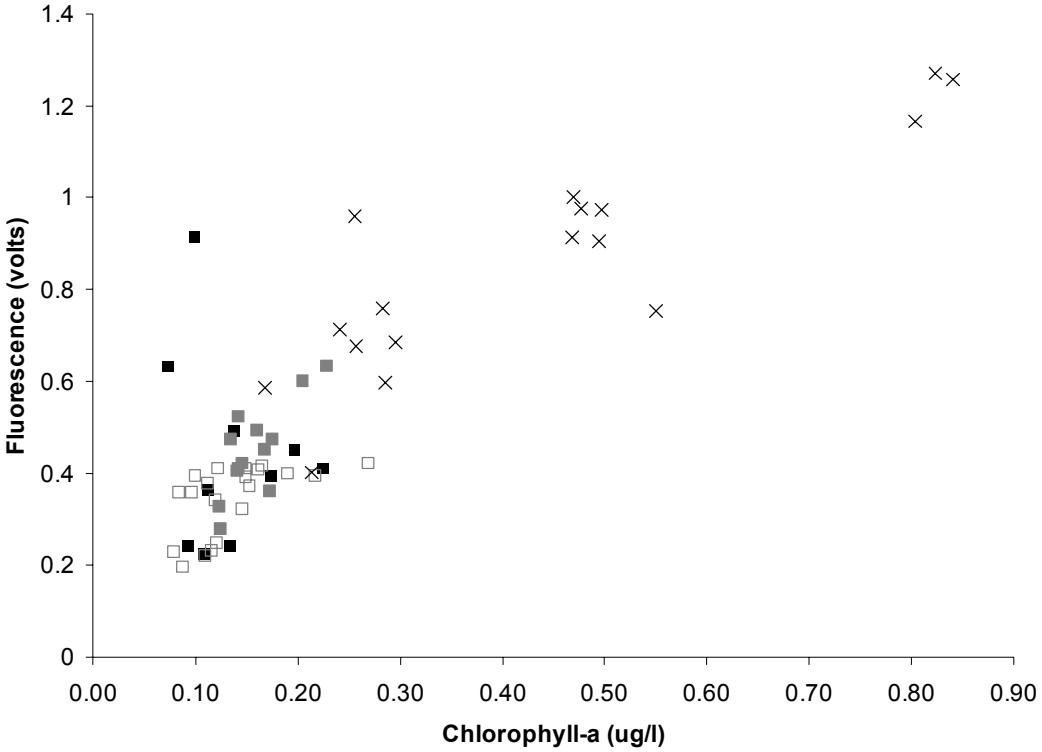

Figure 2.5-2. The fluorescence response to chlorophyll-a in the water column at varying depths. The 1 m depth exhibits a variable fluorescence response to chlorophyll-a. (■) 1 m, (□) 12 and 24 m, (■) 40 and 60 m, (x) 80 and 100 m.

Light history of algal cells affected fluorescence readings. During the five time periods, the relationship between chlorophyll and fluorescence was variable (Figure 2.5-3). Cells from a high light environment (during mid day) fluoresced less than cells adapted to a low light environment.

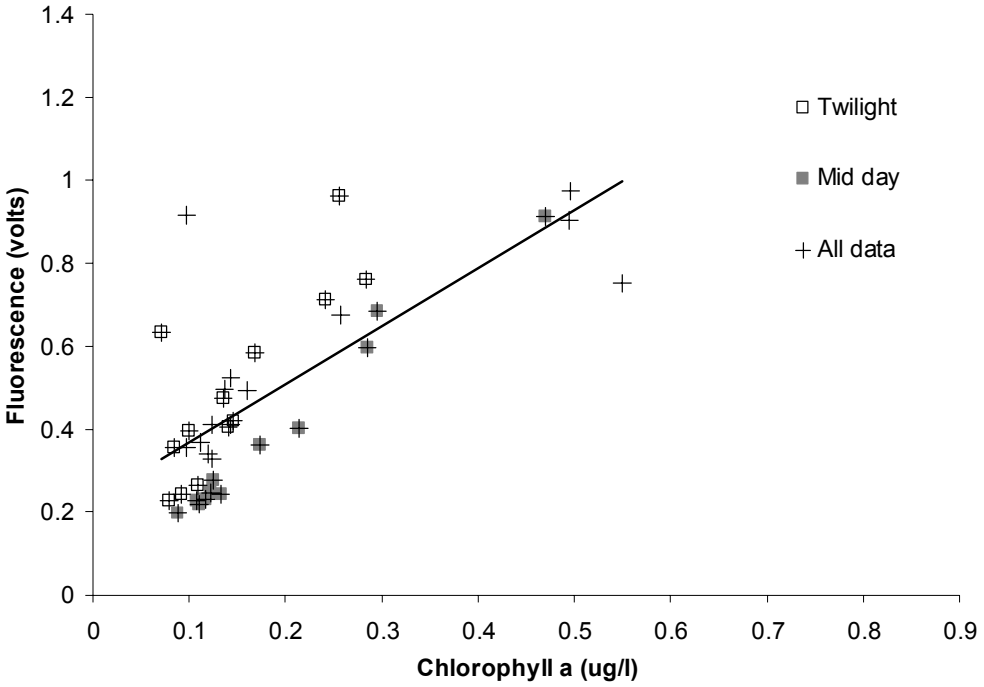

Figure 2.5-3. The measured fluorescence response to varying chlorophyll varies with light history, data collected at all depths in July and August (sunny conditions) are shown.

The relationship between fluorescence and chlorophyll-a was used to develop a calibration equation to estimate chlorophyll-a from SCUFA fluorescence (Equation 2.5-1, Table 2.5-3, Figure 2.5-4). Turbidity did not significantly contribute to the regression and was not included. Due to high variability of surface fluorescence readings and variability of the fluorescence response to chlorophyll at 1 m depth, 0 and 1 m depths were not included in the regression.

$$[Chlorophyll-a] = -0.10 + (0.62 \times Fluorescence) \qquad (2.5\text{-}1)$$

Table 2.5-3. Regression statistics for the inference of chlorophyll from fluorescence.

r^2	**0.84**
Standard Error	0.08
Observations	51
Significance F	3.54E-21

	Coefficients	Standard Error	p-value	Lower 95%	Upper 95%
Intercept	-0.1	0.02	0.000174	-0.14	-0.05
Fluorescence	0.62	0.04	3.54E-21	0.55	0.7

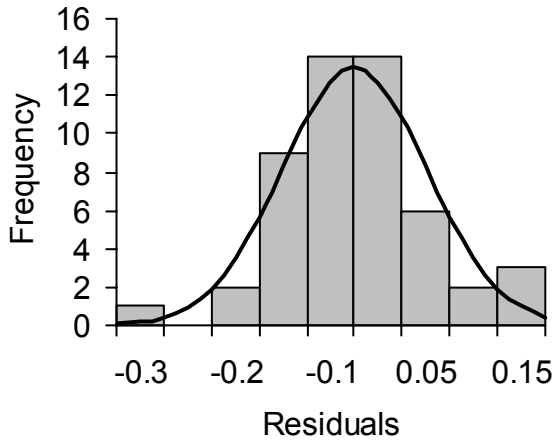

Figure 2.5-4. Residuals from prediction model estimating chlorophyll from fluorescence. Residuals were normally distributed (Kolmogorov-Smirnov test for normality, p > 0.15).

The SCUFA-inferred chlorophyll concentrations did not reveal localized, high concentrations of chlorophyll. Samples collected for chlorophyll analysis using traditional methods accurately described the distribution of chlorophyll in the water column.

The effects of light history on fluorescence caused diurnal changes in SCUFA-inferred chlorophyll concentrations in the upper water column (Figure 2.5-5). SCUFA-inferred chlorophyll-a concentrations were lower than measured chlorophyll during mid day for all sample dates, during afternoon in August, September and October and late morning in October.

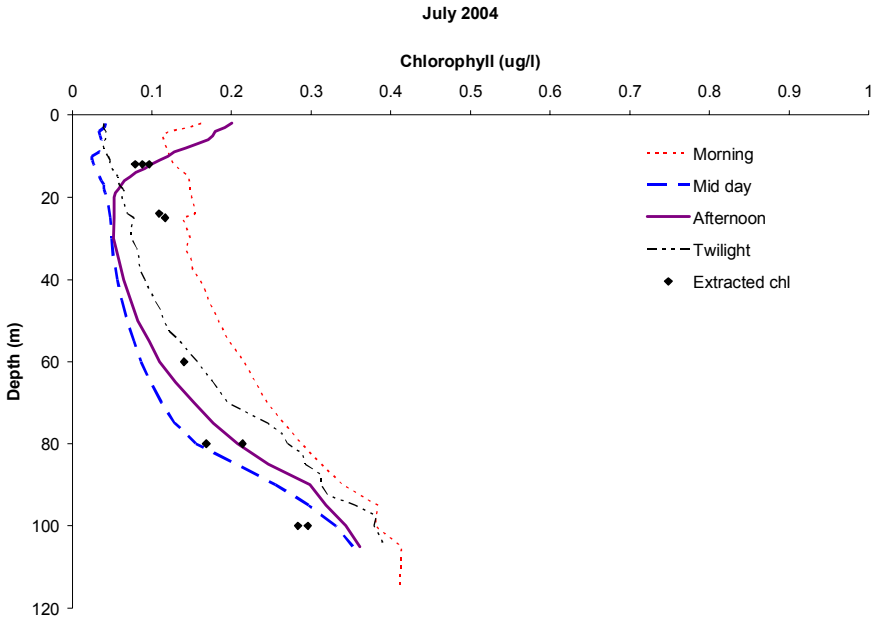
July 2004
Chlorophyll (ug/l)
0
0.1
0.2
0.3
0.4
0.5
0.6
0.7
0.8
0.9
1
Depth (m)
0
20
40
60
80
100
120
Morning
Mid day
Afternoon
Twilight
Extracted chl

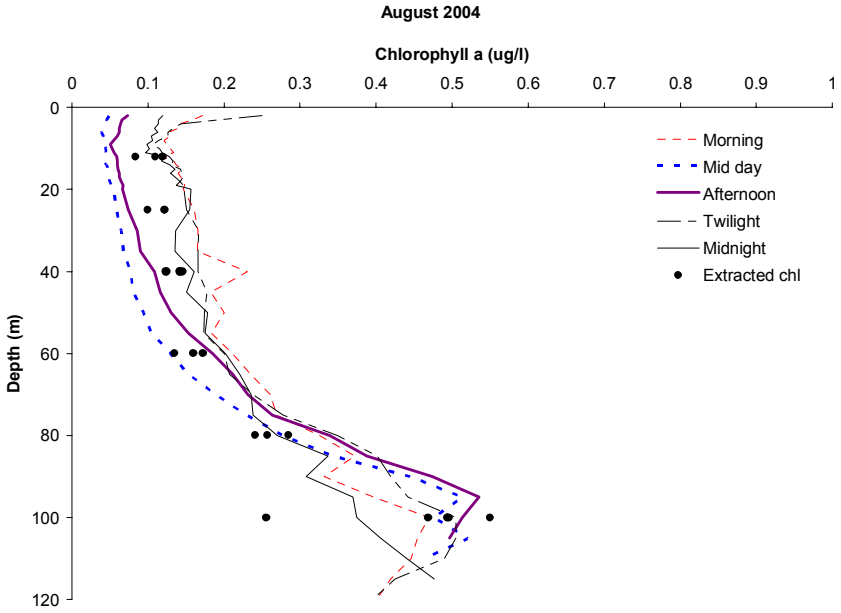
August 2004
Chlorophyll a (ug/l)
0
0.1
0.2
0.3
0.4
0.5
0.6
0.7
0.8
0.9
1
Depth (m)
0
20
40
60
80
100
120
Morning
Mid day
Afternoon
Twilight
Midnight
Extracted chl

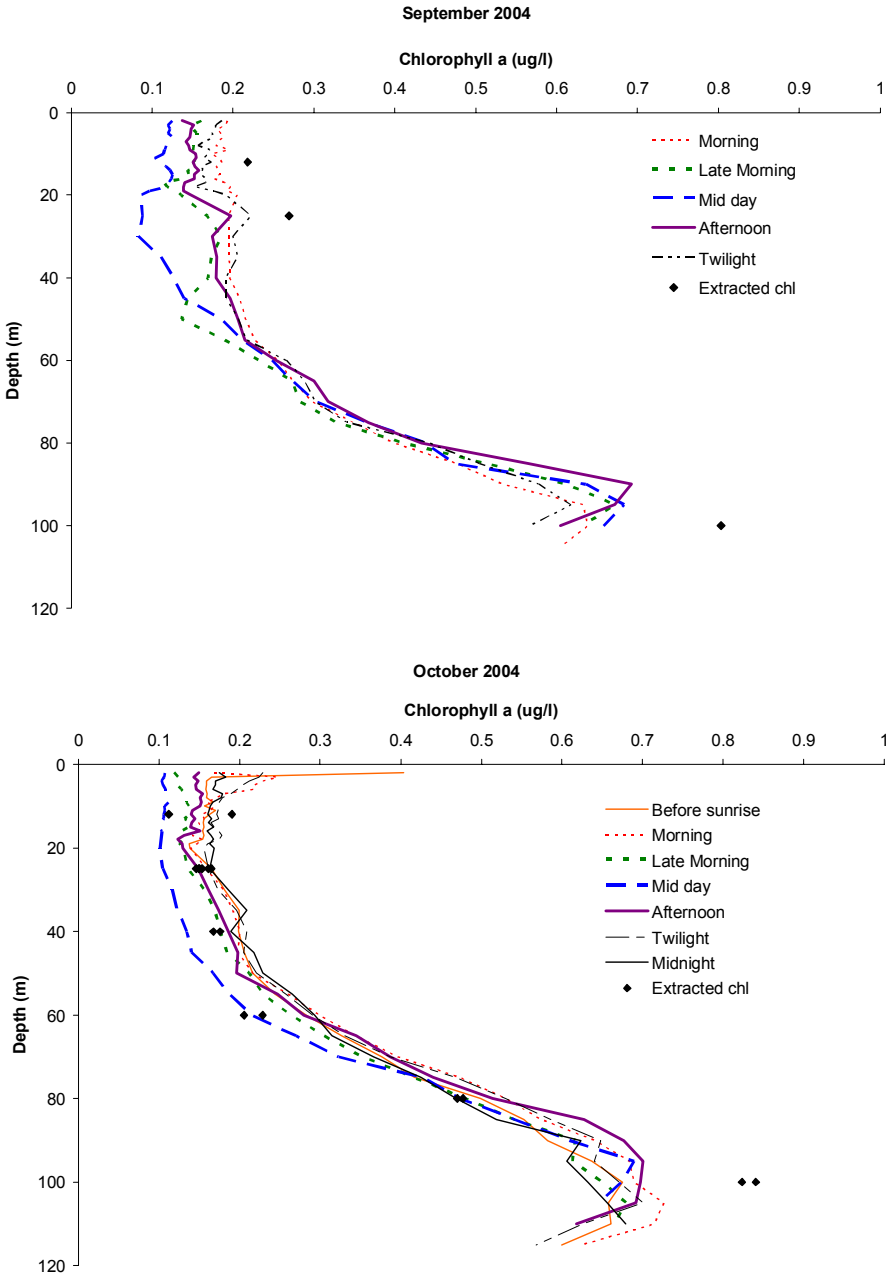

Figure 2.5-5. Vertical profiles of SCUFA-inferred chlorophyll during the summer of 2004 at Waldo Lake.

Conclusions and Recommendations

The SCUFA was a good tool in assessing the vertical distribution of chlorophyll in the water column. It was easy to use in the field, and provided an assessment of the distribution of chlorophyll in the entire water column with minimal additional analysis required. With the exception of near-surface depths the precision of SCUFA was very high.

The strong affects of light history in this ultra-clear, high light environment hindered the analysis of fluorescence data in the context of diurnal changes in the distribution of phytoplankton. However, including ambient light in the calibration equation corrected for these affects (Johnson, *in prep*.) and increased the accuracy of predicted chlorophyll.

The development of protocols for future use of the SCUFA at Waldo Lake must take into consideration the affects of light history. It is recommended profiling be completed during the morning or twilight periods when the affects of light on fluorescence are minimal. If this is not possible, the SCUFA profiles should be collected in tandem with PAR measurements. All SCUFA profiles should be collected in tandem with samples collected at discrete depths for in vitro chlorophyll-a extraction. In addition, multiple samples and upcast audits should be collected to assess precision. The turbidity function was not shown useful in the prediction of chlorophyll from fluorescence, but was useful in determining when the SCUFA hit the bottom of the lake; its use is recommended. The use of a deck cell, measuring ambient light, in conjunction with the SCUFA profile may prove useful in assessing the short-term fluorescence response of algal cells in relation to changes in cloud cover during data collection.

To compare data collected in 2003 and 2004 more information is required about chlorophyll extraction techniques and the fluorometer used in order to determine if settings used in 2003 were consistent with those used in 2004. It needs to be determined if the temperature correction setting was used and if in vitro chlorophyll concentrations were pheophytin corrected in 2003.

It is unlikely that the extremely high fluorescence values recorded in the upper 5 m on August 25, 2003 (which were outliers in the correlation between chlorophyll-a concentration and SCUFA fluorescence (Sytsma et al. 2004)) were due to changes in the vertical distribution of algal cells. Alternatively, high irradiance in the red wavelengths, the movement of cells in upper depths due to turbulence or allochthonous particulates are likely causes of variability in upper water column. Metadata of original datasheets indicate “small rafts of insect and algae were seen on the lake's surface”.

Little is known about spatial variability in the vertical distribution of chlorophyll, specifically in shallow locations. A preliminary assessment of the spatial variations around the lake (Figure 1.2-1) will be completed in August 2005. SCUFA profiles will be collected in conjunction with standard Hydrolab® audits during the downloading of temperature loggers. PAR measurements will be collected at depth using a LI-COR spherical radiation sensor to correct for the affects of light on cellular fluorescence. A deck cell will also be used.

2.6 Picophytoplankton

Picophytoplankton are oxygenic photoautotrophs in the size range 0.2 – 2.0 micrometers in diameter. While only recognized as an important group of phytoplankton in the last 25 years, they are clearly abundant in all aquatic habitats. There are three major groups of picophytoplankton, defined primarily by their size and the pigments they contain: phycoerytrhin (PE)-containing *Synechococcus*, *Prochloroccous*, and picoeucaryotes. *Synechoccocus* and *Prochlorcoccus* are prokaryotes and both are very small, generally about 0.8 microns for *Prochlorococcu*s and 1-1.5 microns for *Synechococcus*. The picoeucaryotes are a taxonomically diverse group of phytoplankton and are generally about close to two microns in diameter.

Differences in their pigment composition lead to detectable differences in the color of light they fluoresce when excited with blue light. Thus, the primary means for counting them is based on either epi-fluorescence microscopy or flow cytometry. With flow cytometry, the three groups are distinguished by size, as reflected in the side scatter, and whether or not they show red or orange fluorescence when excited with light at 488 nm. *Synechococus*, the most abundant form of picoplankton in most lakes, show orange fluorescence and are intermediate in size between *Prochlorococcus* and the picoeucaryotes, which both show red fluorescence.

Flow cytometric analysis of Waldo Lake samples collected in September showed that picoeucaryotes were abundant in the lake, as were slightly larger eukaryotes. *Prochloroccus*, generally believed to be an obligately marine taxon, was not detected in the samples and this was not a surprise. However, since phycoerythrin containing *Synechococus* have been widely reported from the phytoplankton of high elevation lakes in Europe and Canada, we were surprised by the fact that they were not detected in any of our samples. The samples were collected during a single vertical profile, but at a range of depths, including the fluorescence maximum, as defined by the SCUFA (See Section 2.5).

One goal for the upcoming summer season is to look more carefully for the presence of phycoerythrin-containing planktonic forms of *Synechococcus* and to test the idea that, if they are absent, it is correlated with the low nutrient content of the lake. PE-containing picocyanobacteria have a high cell quota for nitrogen because of the size of the protein component of the light harvesting system; we predict that, if they are excluded from Waldo because of a low nitrogen concentration, then we will find them in Odell and some other less oligotrophic local lakes.

Extending this idea to its management implications, then, it may be worth monitoring Waldo Lake for the presence of PE-containing picoplankton. Their appearance in the water column may turn out to be an indicator that the lake has passed a certain threshold of eutrophication.

2.7 Benthic Substrate Mapping

Introduction

The benthic substrates of Waldo Lake are diverse consisting of sand, rock, and mud. These substrates are covered with a wide array of phytobenthos including diatoms, filamentous blue-green algae, rare deep water bryophytes, and unique microbial mat formations referred to as "living stromatolites" (Johnson and Castenholz 2000; Jones 2000; Geiger 2000; Wagner et al. 2000; also see section 2.8). There are currently no detailed maps of Waldo Lake's benthic substrates and biota although trends of biota with depth have been noted. For example, bryophyte communities occur at depths greater than 40 m and living "stromatolites" are scattered at depths between 1 and 5 m (Jones 2000; Johnson and Castenholz 2000).

Two of the characteristics that can distinguish these substrate types are their hardness and their roughness. For instance, mud is smooth and soft while boulders are hard and rough. Sound waves that hit each of the bottom types are affected in distinct manners. Much of the sound wave energy is reflected off hard bottoms into the water, while less energy is reflected off soft bottoms as more energy is absorbed. Waves are reflected off smooth bottoms in a focused manner, while waves are reflected off rough bottoms in a scattered manner. We attempted to map Waldo Lake's substrate types based on distinct acoustic reflectance signatures of each substrate type.

Methods

A Biosonics DE-4000 digital echosounder equipped with a 420 kHz, 6º analog transducer was used to measure acoustic reflections off the substrate types at 22 sites in the lake while simultaneously recording location with differentially corrected global positioning unit. Substrate types and benthic

phytobenthos were assessed at each of the sites via grab sample collection and visual inspection. Ekman dredge grab samples were collected at six of the sites and gravity core samples were collected at 12 of the sites (Figure 2.7-1). Sediment types in shallow water were visually identified using an Aquascope viewing tube. Grab samples and visual identifications were categorized as sand, boulders, mud with bryophytes, or "stromatolites". An attempt was made to relate acoustic reflectance signatures from each of the sites to substrate categories using data analysis techniques developed by Biosonics Inc. These methods analysis method included the First Echo Normalization, First Echo Division, First to Second Bottom Echo Ratio, and the Fractal Dimension methods (Biosonics Inc. 2002).

The intent was to then classify acoustic data collected for bathymetric mapping in 2003 (Sytsma et al. 2004) into the four substrate categories using the relationships developed between acoustic signatures and substrate categories at the 22 sites.

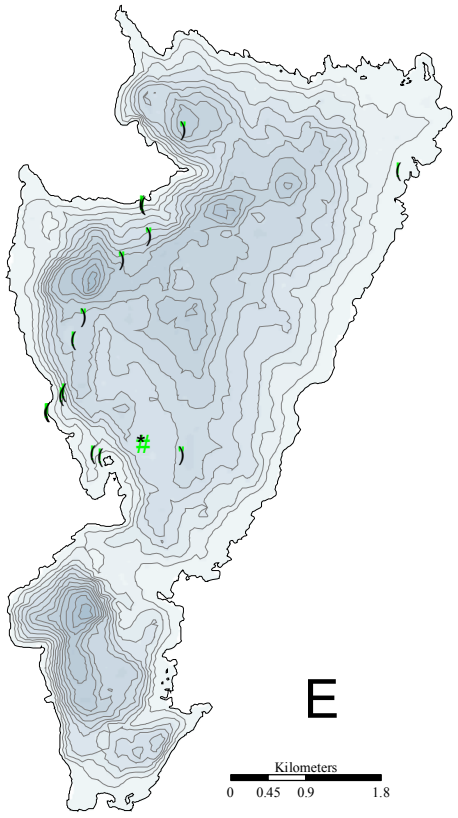

Figure 2.7-1. Ekman dredge (squares), gravity core (circles), and Ekman dredge plus gravity core (triangle) sample collection points

Results and Discussion

Acoustic reflection signatures were not successfully related to substrate types and therefore maps could not be generated from the acoustic data collected in 2003. There are at least two reasons for this

problem. 1) While the 420 kHz transducer is effective at detecting the sediment water interface, the energy sent out at such high frequencies is reflected quickly by the surface of substrates and does not penetrate far into the sediment. A lower frequency transducer can penetrate further into the sediment and reflect back more information that just the surface of the sediment. 2) The analog signal received by the transducer from the sediment reflection is transmitted back to the computer via a 3 m long analog cable. Unfortunately, this cable serves as an antenna and picks up electrical noise created by the gas generator used to power the echosounder system. This electrical noise can mask small differences in acoustical signal that may be important for distinguishing between sediment types.

The general observations of benthic community distributions noted by Jones (2000) and Johnson and Castenholz (2000) were not refuted by our study. Our grab samples revealed that bryophytes are common on muddy sediments deeper that 40 m while shallow areas are comprised of a mixture of sand beds, boulders, filamentous algae, and "stromatolites".

Conclusions and Recommendations

Although our hydroacoustic system was not successful at distinguishing between substrate types in Waldo Lake, other systems would be effective. Systems that convert analog signals to digital at the transducer itself rather than at the shipboard computer would minimize noise. These systems are available from several manufacturers including Biosonics Inc. In addition, lower frequency transducers would be more effective at characterizing substrates. Transducers with frequencies of 120 kHz or lower are commonly used to map sediments (Biosonics Inc. 2002). New multiple frequency systems are available (e.g. 420 kHz and 120 kHz) that could potentially distinguish between similar substrate types, such as sand and stromatolites.

2.8 Benthic Phytobenthos

Samples for benthic phytobenthos were collected from Waldo Lake in July, August, and October. For the most part, we concentrated on describing the microbial mat formations that have been referred to as 'living stromatolites'. We also visited the lake with Greg Retallack, Professor of Geology at the University of Oregon, and expert on paleosols, at the beginning of the field season. Professor Retallack worked with us on characterizing the mineral content of the 'stromatolites' using petrographic thin sectioning techniques and also provided a new interpretation of the mechanism of formation of these interesting and unique microbial communities.

Analysis of the 'stromatolite' samples by petrographic thin sectioning showed that the material under the microbial surface layer was volcanic ash, dominantly pumice fragments of sand to granule size, with lesser phenocyrsts of feldspar, biotite, and amphibole. The ash shows signs of weathering and redeposition as opposed to simple airfall. It appears that the 'stromatolites' may be formed as a result of binding of the sediments by the microbial mat, producing localized differences in erosion rates on the paleosedimentary surface. Preliminary chemical analysis shows that the lower layers of the 'stromatolites' are as much as 40 % organic matter by dry weight, consistent with binding by extracellular polysaccharides.

We have not analyzed the bacterial composition of the subsurface layer of the 'stromatolites' or even estimated the abundance of heterotrophic bacteria in these layers. It is possible that the photosynthetic mat at the surface produces either the energetic substrate for heterotrophic bacteria that create a binding polysaccharide, or that there is diffusion of organic binding material from the photosynthetic layer into the underlying pumice. In any case, we now favor the hypothesis that the 'stromatolites' are not accreting as a result of microbial activity, as would be the case of a true living stromatolite. Rather, we think that the microbial mat has the effect of slowing and shaping the erosional process.

The microbial composition of the 'stromatolites' has been examined by microscopy by Professor Richard Castenholtz, one of the main collaborators on this project. We collected six different stromatolite cores during an exercise intended to help calibrate the acoustic detection of different benthic environments (See Section 2.7). A total of two diatom species and twelve cyanobacterial morphospecies were observed in the mats and surface crust of the six cores.

Interestingly, the dominant taxa differed between cores. For example, two cores collected relatively close together differed dramatically; one was dominated by a single morphospecies of *Leptolyngbya* and the other was co-dominated by a species of *Calothrix* and *Stigonema*, suggesting significant potential for nitrogen fixation in the second mat. There was also a small amount of *Leptolyngbya* detected in the second mat sample, but it was not the same morphospecies as that which dominated the first sample. These differences indicate that there is no single microbial community responsible for the 'stromatolite' formations, and confirms the potential of the mats to contribute to the lake's nitrogen budget.

We are using molecular methods to further identify the diversity of cyanobacteria associated with the microbial mats and also trying to establish clonal cultures of some of the dominant taxa.

2.9 Vertical Distribution Patterns of Macro-Zooplankton Communities

Introduction

Vertical distribution patterns of zooplankton communities are influenced by many factors including gradients in temperature (Marcogliese and Esch 1992; Orcutt and Porter 1983), predation risk (Stich and Lampert 1981)), food quantity and quality (Cole et al. 2002; Williamson et al. 1996), interspecific competition (DeMott and Kerfoot 1982), and light (Boeing et al. 2004; Rhode et al. 2001). The relative importance of these factors varies by lake, year, season, and time of day resulting in diverse and complex vertical distribution patterns.

Significant changes in the Waldo Lake zooplankton community have been well documented (Larson and Salinas 1995; Sytsma et al. 2004; Vogel and Li 2000). Since 1997, the macro-zooplankton community has been predominantly comprised of three species: a cladoceran, *Bosmina longirostris*, and two calanoid copepods, *Diaptomus shoshone x kenai* and *Diaptomus signicauda*. These species have consistently exhibited different daytime vertical distribution patterns with the majority of the *Bosmina longirostris* populations in waters deeper than 40 meters and the majority of copepod populations in waters shallower than 40 meters (Figure 2.9-1). The difference between the weighted mean depths of the two populations has been significant over the time period of 1997 to 2003 (t-test, $p < 0.000$).

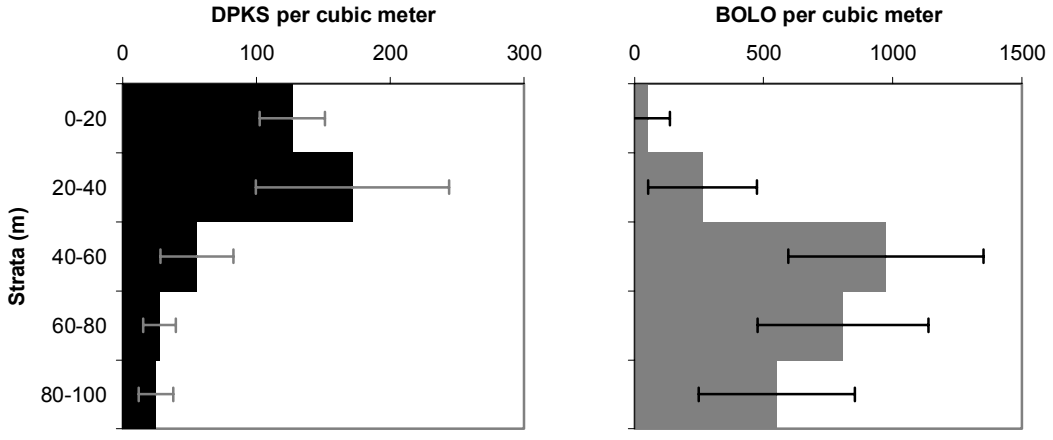

Figure 2.9-1. 1997-2003 mean daytime density of *Diaptomus shoshone x kenai* (DPKS) and *Bosmina longirostris* (BOLO) by depth in Waldo Lake. Bars represent means of zooplankton tows from 19 sample dates and whiskers represent 95 % confidence intervals.

Limited data from two series of nighttime zooplankton tows collected during the summers of 1991 and 1992 suggested that *Bosmina longirostris* populations may migrate towards the surface at night (Vogel and Li 2000). Vogel and Li (2000) hypothesized that *Bosmina longirostris* migrate to deeper waters before daylight to avoid harmful ultraviolet light. They also suggested that the two copepod

species do not exhibit diel vertical migration because their pigmentation protects them from the harmful effects of ultraviolet radiation.

During the summer of 2004, the diel vertical migration activities of zooplankton at Waldo Lake were studied to test Vogel and Li's (2000) hypothesis; specifically, that *Bosmina longirostris* populations exhibit diel vertical migration while *Diaptomus shoshone x kenai* populations do not. In this section results of the diel vertical migration study are presented. In addition, directions for future zooplankton research in Waldo Lake are recommended.

Methods

Vertical distribution patterns of zooplankton were monitored over the course of two 24-hour sampling events during the summer of 2004. Data were collected four times on August 20-21 and three times on October 6 (Table 2.9-1). All data were collected at the-long term monitoring station located near the deepest part of the lake.

Hydroacoustic backscatter from organisms in the water column was used to track vertical distribution patterns. The method works by emitting a sound pressure pulse or ping into the water. As the sound pressure waves impact an object with different density than the surrounding water, a fraction of the energy is reflected back (backscatter) and is detected by the transducer. The timing and intensity of the returning energy provides information on the density and location of organisms such as fish or zooplankton in the water column (Biosonics Inc. 2002; Stanton et al. 1998). To validate hydroacoustic backscatter inferences, zooplankton grab samples were collected from discrete depths with a 10-L Schindler-Patalas trap and were enumerated using a compound microscope.

Table 2.9-1. Zooplankton data collection times.

Sampling event	Sample collection times	Time periods
August 20 - 21, 2004	9:00 - 9:30 pm	Evening
	11:30 pm - 12:30 am	Night
	7:00 - 8:00 am	Morning
	11:30am - 12:30 pm	Midday
October 6, 2004	8:30 - 9:30 am	Morning
	3:00 - 4:00 pm	Afternoon
	10:30 - 11:30 pm	Night

Hydroacoustic backscatter data were collected with a Biosonics DE-4000 digital echosounder equipped with a 420 kHz, 6º analog transducer (Biosonics Inc. 2002). The data collection threshold was set to -140 kHz to maximize detection sensitivity and the echo pulse width was set to 0.1, 0.4, 0.7 and 1 milliseconds. The shorter pulse widths were used to maximize spatial resolution and the longer pulse

widths to maximize detection range. The pulse ping rate was set at one ping per second to minimize file size and maximize data collection range. Data were collected from 1 to 100 meters over ten minute increments at each echo pulse setting. Two analytical techniques were used to determine zooplankton distributions from the backscatter data: individual target identification and echo integration (Visual Analyzer, Biosonics Inc. 2002). Individual target identification is appropriate for scattered individuals while echo integration is appropriate for dense layers of zooplankton.

Zooplankton grab samples were collected with a 10-L Schindler-Patalas trap equipped with a 50-µm mesh net (Method 10200 G, APHA et al. 1998). Samples were collected from 1, 12, 24, 40, 60, 80, and 100 meters. Replicates were not collected. Zooplankton were rinsed into 125 ml sample bottles and preserved using ethanol and Lugol's solution to final concentrations of approximately 1 %. Formalin was added in the lab to a final concentration of 5 %. Zooplankton samples were later concentrated to approximately 5 ml by the pipet method (Dodson and Thomas 1964). Briefly, a tube fitted with a 53-µm mesh screen at the bottom was lowered into the sample bottles. Sample water that filtered into the tube was removed with a pipet leaving concentrated zooplankton samples in the sample bottles. All macro-zooplankton in the concentrated samples were transferred in 1-ml increments to a Sedgwick-Rafter counting cell and were enumerated with a Zeiss compound microscope under 16X magnification. Identification was limited to *Bosmina longirostris*, adult calanoid copepods, and copepod nauplii. *Diaptomus shoshone x kenai* and *Diaptomus signicauda* were not differentiated from each other because of the difficulty of distinguishing larger immature *Diaptomus shoshone x kenai* individuals from the adults of the smaller copepod *Diaptomus signicauda* (Williamson and Reid, 2001). Densities were reported as numbers per cubic meter.

Results

Hydroacoustic Backscatter

Zooplankton were not detectable in the water column using hydroacoustic backscatter methods. There are two interrelated reasons why the method failed: 1) the small size of individual zooplankton and the low density of the populations resulted in weak backscatter signals; and 2) inherent electrical noise within the echosounder system was large enough to obscure small backscatter signals created by zooplankton in the water column. Unfortunately, much of the noise in the system was a result of the cable that transmitted analog signals from the transducer to the computer. The cable served as an antenna and picked up a small amount of electrical noise created by the generator that was used to power the hydroacoustic system. Although this background noise was small, it was large enough to mask weak

signals from zooplankton found in Waldo Lake. *Bosmina longirostris* in Waldo Lake are less than 1 mm in length adult *Diaptomus signicauda* are less than 2 mm in length, and adult *Diaptomus shoshone x kenai* can be larger than 2 mm in length (Vogel and Li 2000). Individual target recognition decreases markedly for targets smaller than 3 mm for the 420 kHz transducer (Biosonics Inc. 2002; Stanton et al.1998). This problem is even more significant for zooplankton in deep water because a transmitted sound wave is attenuated before it reaches the deep zooplankton and the reflected signal is attenuated even more before it reached the transducer resulting in a very weak signal. Despite these problems with methods, dense aggregations of zooplankton would have been detectable through echo integration techniques (Biosonics Inc. 2002). Echo integration techniques did not reveal any dense aggregations of zooplankton during any of the sampling events.

Grab samples

Bosmina longirostris densities ranged from 0 to 300 individuals per cubic meter in August (Figure 2.9-2) and from 100 to 9100 in October (Figure 2.9-3). Adult calanoid copepod densities ranged from 600 to 3200 individuals per cubic meter in August (Figure 2.9-2) and from 600 to 3600 in October (Figure 2.9-3). *Bosmina longirostris* densities appeared to be lower near the surface during midday than at night during the August event; however, lack of replication did not allow the statistical significance of this interaction between time of day and depth to be assessed. Statistical significance of an interaction between time of day and depth would indicate diel vertical migration. In order to overcome this replication problem, data were pooled into two stratum, shallow (1, 12, and 24 m) and deep (40 meters or greater). Two-way ANOVA analyses were conducted on the pooled datasets to test the significance of time of day by strata interactions as well as the influence of the time of day alone and strata alone.

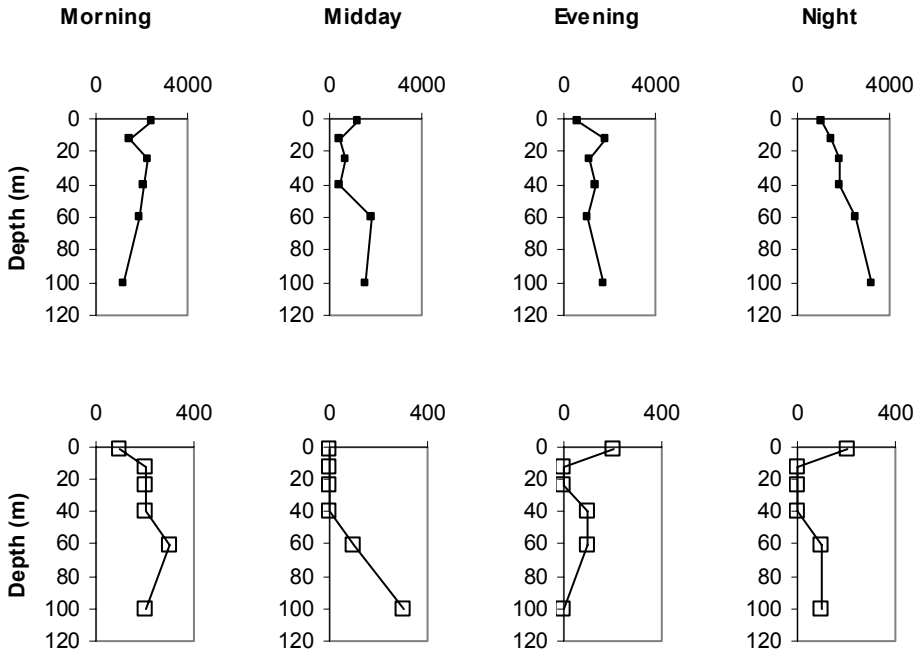

Figure 2.9-2. August 20-21 2004 calanoid copepod (■) and *Bosmina longirostris* (□) density (numbers per cubic meter) by depth and time of day. Note the copepod density scale is ten fold higher than the *Bosmina longirostris* scale.

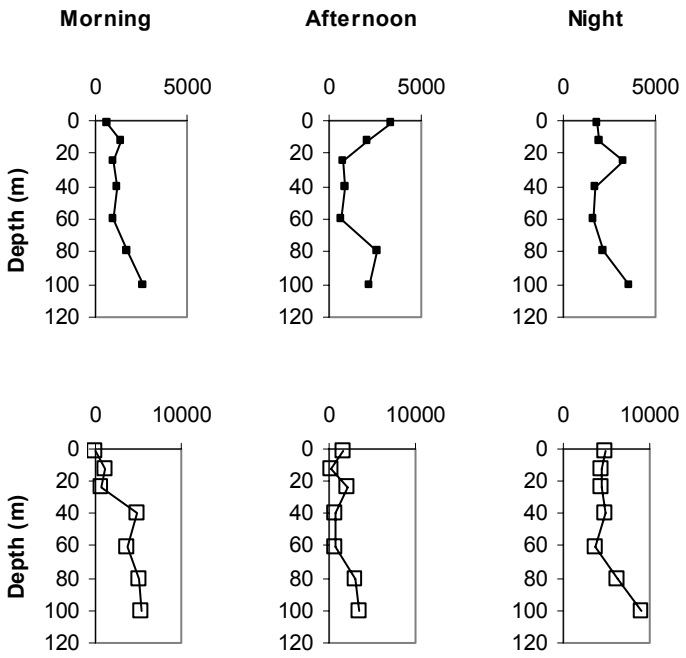

Figure 2.9-3. October 6 2004 calanoid copepod (■) and *Bosmina longirostris* (□) density (number per cubic meter) by depth and time of day. Note the *Bosmina longirostris* scale is twice the copepod scale.

Based on the pooled depth datasets, no significant interactions ($p < 0.05$) were observed between stratum and time of day indicating diel vertical migration by *Bosmina longirostris* and calanoid copepods (Table 2.9-2) did not occur. However, there were significant differences in distribution

patterns of *Bosmina longirostris* when considering pooled strata or time of day separately. In August, *Bosmina longirostris* density was significantly higher during the morning sampling period. In October density was higher at night than daytime sampling periods. In August, *Bosmina longirostris* density was not significantly different between pooled strata. In October, density was higher in the lower pooled strata than in the upper pooled strata.

No diel changes in the distribution of calanoid copepods were detected by the pooled strata by time ANOVA's (Table 2.9-2). Neither time nor strata were significant factors for calanoid copepods distributions during August or October.

Table 2.9-2. Significance of time of day, upper v. lower strata, and the interaction of time and strata on *Bosmina longirostris* and calanoid copepod density based on two-way ANOVA tests.

		Significance	
Species	Factor	August	October
Bosmina longirostris	time	0.045	0.000
	strata	0.188	0.004
	time x strata	0.526	0.076
Calanoid copepods	time	0.096	0.142
	strata	0.481	0.978
	time x strata	0.094	0.508

Discussion

Results from this study did not support the hypothesis that *Bosmina longirostris* exhibit diel vertical migration. Although results suggested that diel vertical migration may not be occurring, methods may not have been sensitive or accurate enough to detect migration patterns.

The echosounder methods currently utilized by the Center for Lakes and Reservoirs are not effective in monitoring zooplankton distributions in Waldo Lake due to small organism size, low density, the depth of the lake, and electrical noise within the system. Several alterations of our acoustical equipment would be necessary for effective monitoring of zooplankton distributions. Background noise could be reduced through the use of a digital transducer as well as a higher frequency transducer. A digital transducer would eliminate the electrical interference problems that were encountered. Higher frequency transducers (i.e. 1000 kHz) can effectively distinguish smaller individual targets. However, higher frequencies signals are attenuated quicker in the water column resulting in a shallower effective range. Collecting vertical profiles using a submersible transducer with an internal data logger would eliminate this problem.

Although Schindler trap grab samples can provide accurate estimates of zooplankton densities at discrete depths, the method may not be appropriate for Waldo Lake. High variation between samples collected using the Schindler trap occurs due to the small sample volume and low zooplankton densities in Waldo Lake. Trap avoidance is a potential problem in Waldo Lake due to the extreme clarity of the water.

Avoidance of a zooplankton net can also be a problem; however, there are advantages of net tows over traps in Waldo Lake. Net tows provide larger sample volumes and thus less variable samples. In addition, the use of net tows also allows for direct comparison with zooplankton data collected during long-term monitoring efforts.

A larger volume Schindler trap is recommended if grab sample techniques are used in the future. Replication of grab samples would allow for error estimates and calculation of time by depth interactions in two-way ANOVA's.

3 Quality Assurance Plan and Database Development

3.1 Quality Assurance Assessment of Long-Term Monitoring in 2004

A Quality Assurance/Quality Control (QA/QC) plan was developed for the long-term monitoring program at Waldo Lake (Johnson 2003). The plan was reviewed by all participants in the program. The original purpose for this section was to document the effectiveness of the QA/QC plan and provide estimates of sampling variation via an analysis of duplicate samples. The analysis was uninformative, however, because the QA/QC plan was not implemented in a coordinated manner. Therefore, this section will describe what portions of the QA/QC plan were completed this year and provide recommendations for successful QA/QC implementation from this point forward.

The QA/QC plan established guidelines for both completion and compliance rates (Johnson 2003). Completion and compliance percentages were calculated to assess the level of implementation of the QA/QC plan and develop useful recommendations for effectively addressing the shortcomings of execution during the 2004 season's sampling. Percent completion represents the amount of data collected relative to the stated goal in the QA/QC plan (reported for both trips and sample depths). Percent compliance represents the rate of adherence to the QA/QC plan requirements for calibration methods, replication, and field audits (i.e., if there were four calibration steps required per trip and three of those steps were completed each trip then the compliance rate was 75%).

Table 3.1-1. Implementation rates for the QA/QC plan during the 2004 field season.

Component of Program	% Completion: Trips	% Completion: Sample Depths	% Compliance: Calibration	% Compliance: Replication	% Compliance: Other
Analytical Chemistry	100%	75%	n/a	50%	50% Blanks
Multi-Parameter Probe	100%	100%	18%	50%	Inconsistent Audit Grades
Light Transmission	100%	100%	100%	50%	
Photometer	50%	100%	75%	0%	
Secchi Disk	100%	n/a	n/a	100%	
Chlorophyll	100%	90%	n/a	25%	33% Size Classes, 0% Blanks
Phytoplankton	100%	95%	n/a	25%	0% Split Samples
Zooplankton	100%	92%	n/a	50%	0% Split Samples

Generally, recommended levels of completion were attained and the long-term monitoring program accomplished the goal of data collection. All components were sampled completely except for the photometer, which was only used on 50% of the trips instead of 75% as indicated in the QA/QC plan (Table 3.1-1). Collection depths were also completely sampled with one exception. Only 75% of the recommended depths for chemistry collections were sampled (Table 3.1-1). In sum, a sufficient number of chemistry samples were collected yet the depths sampled were inconsistent, hence the lower completion rate. Consistent collection depths are critical for detection of trends, analysis of seasonal and yearly variation and for replicate comparisons.

Compliance with replication and calibration requirements was unsatisfactory. Unreliable calibration and replication compliance renders quality assurance and grading of data impossible and calls into question the quality of data collected. Recommended multi-parameter probe calibration procedures were not implemented; only 18% of the steps were successfully completed (Table 3.1-1). Replication rates were also very low. Only Secchi disk measurements were replicated according to recommendations in the plan. For all other parameters, half or less than half of the recommended replicates were collected (Table 3.1-1). Blank and split sample recommendations were not fully addressed.

General Recommendations

- Develop new field datasheets that incorporate the QA/QC plan.
- Develop data quality assessment and audit worksheets that incorporate QA/QC plan.
- Data quality should be assessed in the field with audit worksheets when possible so that corrective actions can be made when quality levels are not met.
- Data quality assessments should be made by the investigator who was responsible for data collection.
- Data quality assessments should be copied to all members of the team along with the data and uploaded into the database.

- All participants in the long-term monitoring program must read and sign off on the QA/QC plan. It is recommended that adherence to the QA/QC plan be made a requirement of the long-term monitoring contract.

3.2 Long-Term Monitoring 2005 Sampling Plan

Timing and Coordination

- Three long-term monitoring trips will be completed in 2005.
- Recommended sample dates: early-June, early-August, and mid-September.
- All 3 trips will be coordinated with Center for Lakes and Reservoirs staff to facilitate QA/QC plan implementation and coordination.

Analytical Chemistry

- 2 locations will be sampled each trip: the LTM station (West Bay), and the North Swim site.
- 2 depths will be sampled at the LTM station (surface and 100 m), 1 depth will be sampled at the North Swim site (surface), and 1 depth will be re-sampled (randomly selected) to obtain a field duplicate. Total = 4 depths sampled per trip.
- The following constituents will be analyzed by the USDA Forest Service Cooperative Chemical Analytical Laboratory (CCAL) for each depth collected: total phosphorus (TP), total nitrogen (TN- TKN analysis until persulfate TN method is available), alkalinity, pH, conductivity, and dissolved silica.
- TP and TN samples will be filtered thru a 200-250 micron mesh in the field.
- Alkalinity, pH and conductivity will be measured in an unfiltered sample.
- Dissolved silica samples will be filtered in the field with filters provided by CCAL.

In situ Monitoring

- No changes to sampling and completion goals from the 2004 QA/QC plan (Johnson 2003) are recommended for 2005 sampling.

Biological Monitoring

Phytoplankton

- 7 phytoplankton samples will be collected each trip. 1 each from 0, 12, 25, 60, 100, 120 m and a randomized duplicate.
- Samples will be sent to Jim Sweet for analysis, the randomized duplicate will be sent to Jim Sweet for analysis (not a blind sample, e.g., 60 m B).
- 2 of the samples will be split with a sample splitter for QA/QC analyses.
- Twice the normal volume will be collected for the split samples and samples will be split with a Folsom plankton splitter in the field.
- 1 of the split samples will be sent to Jim Sweet as a blind sample.
- 1 of the split samples will be archived until October 2005 when it will be sent to an alternative taxonomist yet to be determined.

Zooplankton

- 7 zooplankton tows will be collected each trip. 1 each from 0-20, 20-40, 40-60, 60-80, 80-100, and 100-120 m and a randomized duplicate tow.

- Samples will be sent to Alan Vogel for analysis, the randomized duplicate tow will be sent to Alan Vogel for analysis (not a blind sample, e.g., 40-60 m B).
- 2 of the samples will be split with a sample splitter for QA/QC analysis.
- Twice the normal volume will be collected for the split samples and samples will be split with a Folsom plankton splitter in the field.
- 1 of the split samples will be sent to Alan Vogel as a blind sample.
- 1 of the split samples will be archived until October 2005 when it will be sent to an alternative taxonomist yet to be determined.

Chlorophyll and Primary Productivity

- No changes to sampling completion and compliance goals from the 2004 QA/QC plan (Johnson 2003) are recommended for 2005.

3.3 Database Development

Long-term monitoring at Waldo Lake has been ongoing since 1986. The valuable information about the lake that this program produces needs to be maintained in a manner that allows access for research and sound management of this unique resource. An objective for this report period was to begin development of a comprehensive database for Waldo Lake. For most parameters data have been collected and checked for consistency. The following steps have been completed:

Chemistry

Chemistry data have been collated and are stored in a single MS EXCEL™ spreadsheet file. The data were double checked against all available hardcopy and digital files. Questionable data were omitted from the database. In coordination with CCAL, changes to the method detection limit and precision estimate for each parameter were documented and updated in the database. Sample site location codes and geographic coordinates, and sample depths were entered for each sample. The chemistry data are ready to be uploaded to a relational database.

Fields in the spreadsheet include: Delivery Date, Sample Date, Location Code, Depth (m), lab number, a notes column for information such as field duplicates and a value, below detection, and detection limit field for each parameter. Parameters include: total phosphorus, orthophosphorus, pH, alkalinity, conductivity, nitrate-N, total Kjeldahl nitrogen, ammonia-N, dissolved silica, dissolved solids, and chlorophyll-a.

Light and Secchi Disk

Photometer data have been collated and are stored in single MS EXCEL™ spreadsheet file. The data were double checked against all available hardcopy and digital files. For many of the profiles the only

data available were percent of surface values therefore all photometry data were reduced to this level. A secondary data file is also available with raw data. Light data are ready to be uploaded to a relational database. Fields in the spreadsheet include: Date, Location Code, Starting Time, Depth, and percent of surface values for red, green, blue and PAR bandwidths.

Currently, Secchi disk data collected between 1996 and 2003 are digitally preserved in a MS ACCESS™ table. Fields include; date, time, location wave and sky conditions, use of aquascope, initials of viewer, and Secchi disk depth. All repeat readings are included and an average could be linked to the table. All Secchi disk data are ready to be uploaded into a relational database.

Transmissometer data have not been QA checked and are not in electronic format. Hence, data are not ready to be uploaded to a relational database.

Multi-Parameter Probe

Hydrolab data from the years 2003 and 2004 have been processed and are ready to uploaded to a database. Fields in the spreadsheet include: site code, date, time, depth, temperature, dissolved oxygen, pH, conductivity, redox potential, turbidity, battery, dissolved oxygen percent saturation and notes. All other years are not ready. Quality assurance audit grades will be included with data collected beginning in 2005.

Biology

All phytoplankton and zooplankton data currently available in electronic format have been collated in a two table MS ACCESS™ database. The phytoplankton database was designed for easy incorporation of datasheets provided by the taxonomist and includes data collected between 1993 and 2004. The zooplankton database was designed in a similar format as the phytoplankton database. Zooplankton data includes samples collected between 1996 and 2003. Further coordination is required to ensure that zooplankton data provided by the taxonomist can be easily incorporated into this database. Phytoplankton, zooplankton and chlorophyll data are ready to be uploaded to a relational database.

The first table of data provides general information for samples collected on a given date and depth. Phytoplankton fields included are slide code, lake name, station of collection, depth, date, time, total cell density and total cell biovolume, TSI, diversity index and number of species per sample. Zooplankton fields included are date, time, location, depth of tow, volume of tow, total zooplankton density and standard error, density of edible zooplankton and standard error and percent edible zooplankton. The

taxonomist responsible for identification should be added to this table. The second table is linked to the first table and gives a more complete description of the sample. Phytoplankton fields included are date, depth, species name, four-letter species code, species class, cells per colony, and species density, percent density, species biovolume and percent biovolume. Zooplankton fields included are date, depth of tow, group name, group total density and standard error and species name, four-letter species code, and species density and standard error for zooplankton. There are some inconsistencies in the nomenclature and species groupings in the zooplankton database that need to be resolved (See Section 2.1).

Chlorophyll data collected between 1995 and 2003 have been collated and are incorporated into a single MS ACCESS table. Fields include; date, location, depth, concentration of chl-a with a 0.45 um pore size filter, and concentration of chl-a with a 0.2-um pore size filter. Additional fields to add could include method used and initials person who completed the analysis and time of collection from original datasheets or phytoplankton dataset (if indicated).

Primary productivity data have not been made available by the investigator. No attempt has been made to date to incorporate available into a cohesive database format. Hence, data are not ready to be uploaded into a relational database.

Recommendations

Long-term monitoring at Waldo Lake has been ongoing since 1986. This program produces valuable information about the lake that needs to be maintained in a manner that allows access for research and sound management of this unique resource. A Waldo Lake database would provide a model that could be adapted to benefit USDA Forest Service management activities at other lakes. Many models exist for multiple user databases including STORET, and LASAR.

A plan for a relational database needs to be developed and then implemented by a database specialist. Goals for database utility must be developed in collaboration with all potential users prior to database planning. A coherent strategy that incorporates multiple users' requirements will ensure the usefulness of the database for future research and management activities. Sample site location codes, sample dates, sample depths, and sample times are potential unique identifiers among data categories. All data need to be checked for consistency between dates and times to ensure accuracy of reporting based on original field data sheets prior to uploading into a relational database. Data management and database accessibility need to be improved to allow direct uploading of quality assurance checked data by the investigator. Continued preservation and distribution of hardcopies of field datasheets to other

members of the research and management team by the investigator responsible for the data collection is required.

4 Climate and Hydrology

4.1 Background

The physical and chemical characteristics of the waters in Waldo Lake are closely connected to the local climate and the hydrology of the watershed. The climate, as reflected in the air temperature, solar radiation, humidity, wind speed and direction and precipitation, dictates the temporal and spatial distribution of temperature and the hydrodynamics of the lake and the input of water to the lake from the watershed. These climatic characteristics are also primary inputs to the lake model, CE-QUAL-W2, being developed to simulate the hydrodynamics, temperature and chemical quality.

The model will be used to assist in understanding observed variations in the physical characteristics and the ecosystem of the lake and to investigate various scenarios of land management and potential climate variation on the behavior of the lake. In doing so, it will be useful to have long, continuous sequences (at least several years) of climate data to drive the model simulations. The extensive climatological data required for this purpose have not been collected in the vicinity of the lake and a meteorological station has only recently been installed. As such, a statistical approach to simulating climate data for the lake will allow these longer sequences of data to be generated based on comparatively short periods of observation.

4.2 Simulation model for climate characteristics at Waldo Lake

The objective of stochastic simulation is to generate a "synthetic" sequence of values that have the same statistical characteristics (e.g. mean, standard deviation, time dependence) as an observed sequence. Due to the statistical nature of this process, the actual values of a modeled variable differ from any specific historic data, but over the long run, exhibit the same variation. The process of statistical simulation has been a part of climatology and hydrology for many years. A well developed approach for the simulation of daily precipitation occurrence and amount, maximum and minimum temperature and solar radiation was presented by Richardson (1981) and has been used extensively over time (e.g. Koch 1992). This and similar approaches have been expanded to form the basis for several generations of climate simulation models (WGEN, CLIGEN, USCLIMATE, and GEM) used by the U.S. Department of Agriculture (USDA) for various purposes including providing climatic input to hydrologic models where no long term data were available. A description of two of these models

(CLIGEN and USCLIMATE) and comparison of their simulation results is presented by Johnson et al. (1996). The basic elements of these models include:

- Simulation of the occurrence of precipitation (wet or dry day) using a first order Markov occurrence model so that precipitation occurrences depend on the whether it rained the previous day or not,
- Simulation of the amount (depth) of precipitation on rainy days assuming precipitation based on an appropriate probability distribution,
- Joint simulation of maximum and minimum daily temperature, dew point temperature, relative humidity, solar radiation and wind speed as a first order multivariate autoregressive process thus preserving the temporal and cross correlations among these variables. The values each of these variables are determined assuming different means and standard deviation depending on whether a wet or dry day is simulated.

The model accommodates the seasonal behavior of each of the climatological variables by using parameters that vary throughout the year. In particular, each variable is defined in terms of its mean and standard deviation and these characteristics vary in a seasonal pattern. Fourier series are fit to sample estimates of the parameters to provide a smooth variation of parameters throughout the year.

Precipitation occurrence is defined in terms of the Markov chain transition probabilities, p_{ij} where j is the current state (rainy = 1 or dry = 0) given i, the state the previous day (rainy or dry). Each of these probabilities varies with the day of the year. The precipitation depth is simulated as:

$$X(\nu,\tau) = \hat{\mu}(\tau) + \hat{\sigma}(\tau)K \qquad (4.2\text{-}1)$$

where $X(\nu,\tau)$ is the precipitation depth in year ν and period (in this case day) τ of the simulation, $\hat{\mu}(\tau)$ is the estimate of the mean daily precipitation depth, $\hat{\sigma}(\tau)$ is the estimate of the standard deviation for period τ and K is a standard deviate for the appropriate distribution. Commonly, either the gamma distribution or the mixed exponential distribution is fit to the precipitation data. The mean and standard deviation vary with the day of the year.

The other variables are modeled in a similar manner, such that each can be represented as:

$$X(\nu,\tau) = \hat{\mu}_i(\tau) + \hat{\sigma}_i(\tau)\chi(\nu,\tau) \qquad (4.2\text{-}2)$$

where $X(\nu,\tau)$ is the value of the variable in year ν and period (in this case day) τ of the simulation, $\hat{\mu}_i(\tau)$ is the estimate of the mean daily value of the variable depending on the precipitation state, i (rainy = 1 or dry = 0), $\hat{\sigma}_i(\tau)$ is the estimate of the standard deviation for period τ and χ is a standard normal deviate. For each of these variables, the mean and standard deviation vary depending on whether it is a rainy day

or not. The random deviate, χ, is related to the random deviate for each of the other variables through a multivariate autoregressive (MAR) model:

$$\boldsymbol{\chi}(v,\tau) = \boldsymbol{A}\boldsymbol{\chi}(v,\tau\text{-}1) + \boldsymbol{B}\boldsymbol{\varepsilon}(v,\tau) \qquad (4.2\text{-}3)$$

In this equation, χ is the vector of values for all of the variables, $\boldsymbol{A}$ and $\boldsymbol{B}$ are matrices of parameters and $\boldsymbol{\varepsilon}$ is vector of standard normal random deviates. Note that neither the parameter matrices ($\boldsymbol{A}$ and $\boldsymbol{B}$) nor the vector of random components ($\boldsymbol{\varepsilon}$) vary with day of the year or with the precipitation state.

The result of this process is a stochastic simulation of six climatological variables representing daily conditions of the climate. By virtue of the model structure, many of the statistical characteristics of the observed climate variables are explicitly preserved including the inter-relationships between the five non-precipitation variables. The relationship of these five variables to precipitation is accounted for by maintaining two distinct distributions for each, corresponding to wet and dry days.

4.3 Historic data

A simulation model is dependent on the availability of data from which the parameters of the model can be estimated. Meteorological data have been collected at Waldo Lake beginning in 2003 as described in Section 5.1. There are two primary issues associated with the currently available data set. First, there period of record is less than two years. Since the analysis is based on the identification of periods within the year, (described in the subsequent section) and only the data within that period is used in the estimation, the result is a very small sample for estimating some of the parameters of the stochastic model, e.g. mean and standard deviation of temperature or rainfall depth on rainy days during the dry summer period. Second, there are no precipitation data at the Waldo Lake site. As described in Section 5.1, it is necessary to look to a surrounding location for data. We have chosen to use the data collected at the Oakridge Ranger station and subsequently the Oakridge Hatchery. Data for daily precipitation are available at this site for over 50 years. Thus, the data set is not only suitable for assessing the parameters of the precipitation models but can be used in future analyses to determine whether the characteristics of daily data vary with large scale climate features. So, data on precipitation for Oakridge will be used and other variables at Waldo Lake will be related to these data.

4.4 Implementation of the stochastic simulation model

The implementation of the stochastic simulation model is based on a two step process: data analysis and simulation. Historical data were collected and analyzed to develop the various parameters for the models, e.g. Markov chain transition probabilities, mean and standard deviations of daily rainfall depth,

daily maximum and minimum temperature, relative humidity, solar radiation and wind speed, and the correlation and cross correlation characteristics of the non-precipitation variables. Then the parameters are used with a random number generation scheme to simulate sequences of the various characteristics. The data were analyzed using Excel, an add-in, Analyse-it and FORTRAN programs developed to estimate the parameters of the MAR model.

Data analysis and parameter estimation approach

The climate variables that drive the energy and water balance of the lake all vary both seasonally and from year to year. The seasonal variation follows a reasonably regular pattern for most of the variables and is the basis for the parameter estimation. To capture the seasonal variation, the year is divided into 26 periods each containing 14 or 15 consecutive days. This is a common practice for this type of simulation model. Statistical parameters are then estimated for each of these periods based on the assumption that the data fit a certain distribution within the period. For precipitation, the gamma distribution was selected (e.g. Johnson et al. 1996). This three-parameter distribution has been shown to fit daily rainfall in a large number of cases, and fit the existing precipitation data reasonably well for most periods. The exceptions were a few periods during the summer months with very few rainy days. The normal distribution is used for the remainder of the variables, again following Johnson et al. (1996). Insufficient data was generated by this study to judge the correctness of this assumption.

Therefore, to build the model, the following parameters had to be calculated for the existing weather data: the transition probabilities for precipitation, the mean, variance and skew of the daily rainfall depth on days when rain occurs, and the mean and standard deviation of minimum and maximum temperature, solar radiation, relative humidity and wind speed for either rainy or dry days. Precipitation transition probabilities were tracked according to dry days, or more specifically, P_{00} and P_{10}, the chance of a dry day given the previous day was dry and the chance of a dry day given the previous day was wet. These parameters are calculated by simply tallying the number of dry days following dry days as a fraction of all days following dry days, and so forth. A distinct gamma distribution was fit to the precipitation data for each period, as determined by mean, variance and skew. The means and standard deviations of the other parameters were computed separately for wet and dry days for each 14-day period.

To provide a smooth transition between the discrete values calculated for each period, each parameter was then fit with a Fourier series following the procedure described by Salas et al. (1980). The number of significant harmonics was selected based on the cumulative variance explained and by visual inspection of the fit. In the end, the use of eight harmonics was deemed to be sufficient for the

variables of concern. Using the Fourier series representation of the parameters allows for the ability to estimate the parameter values in a continuous manner for each day of the year.

Data analysis and parameter estimates

Following the procedures described in the previous section, parameters were estimated and Fourier series were fit to those parameters. Eight harmonics were used to fit the Fourier series to the periodic parameters. A graphical presentation showing the parameter values computed from the data for each 14 day period and the Fourier fits to these values are shown in Figure 4.4-1 through Figure 4.4-15. Finally, the parameter matrices for the MAR model were estimated using the residuals, $\chi(v,\tau)$, for the temperature, solar radiation, relative humidity and wind speed data. These matrices are presented in Table 4.4-1 and Table 4.4-2.

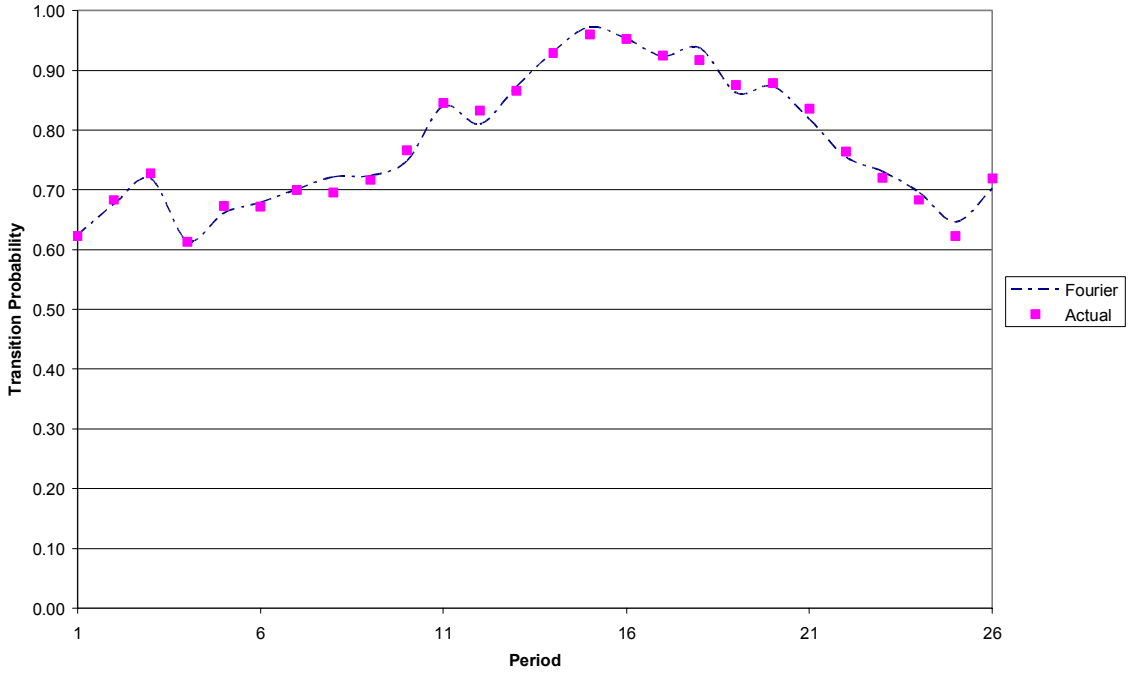

Figure 4.4-1. Fourier series approximation of P00 (Dry-Dry) transition probabilities (8 Harmonics).

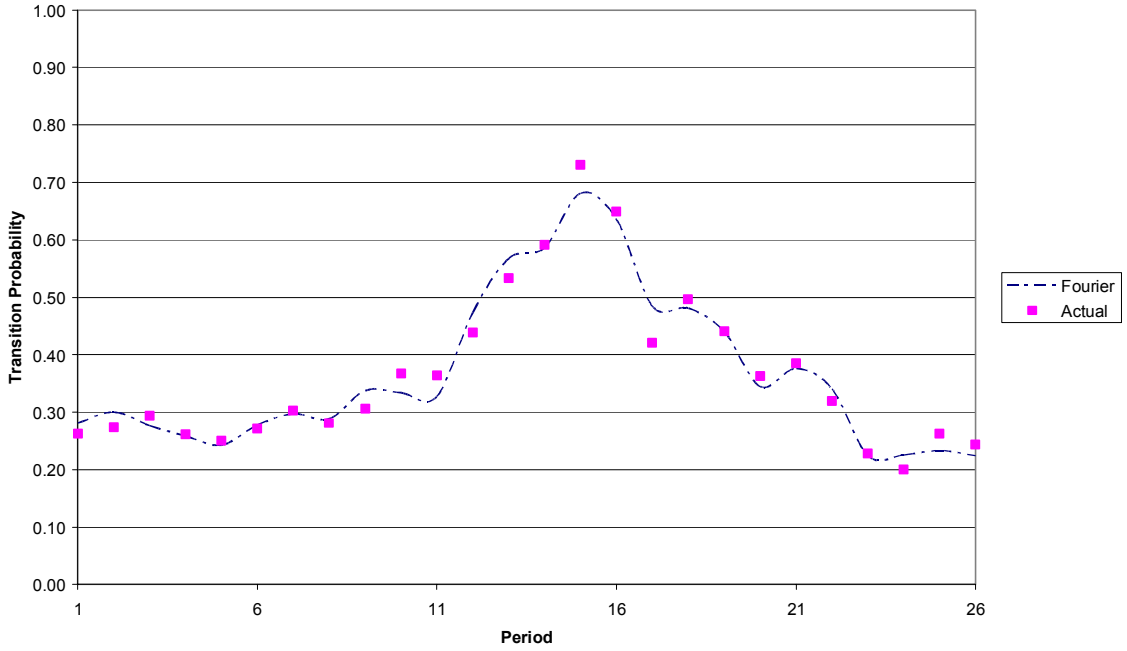

Figure 4.4-2. Fourier series approximation of P10 (Wet-Dry) transition probabilities (8 Harmonics).

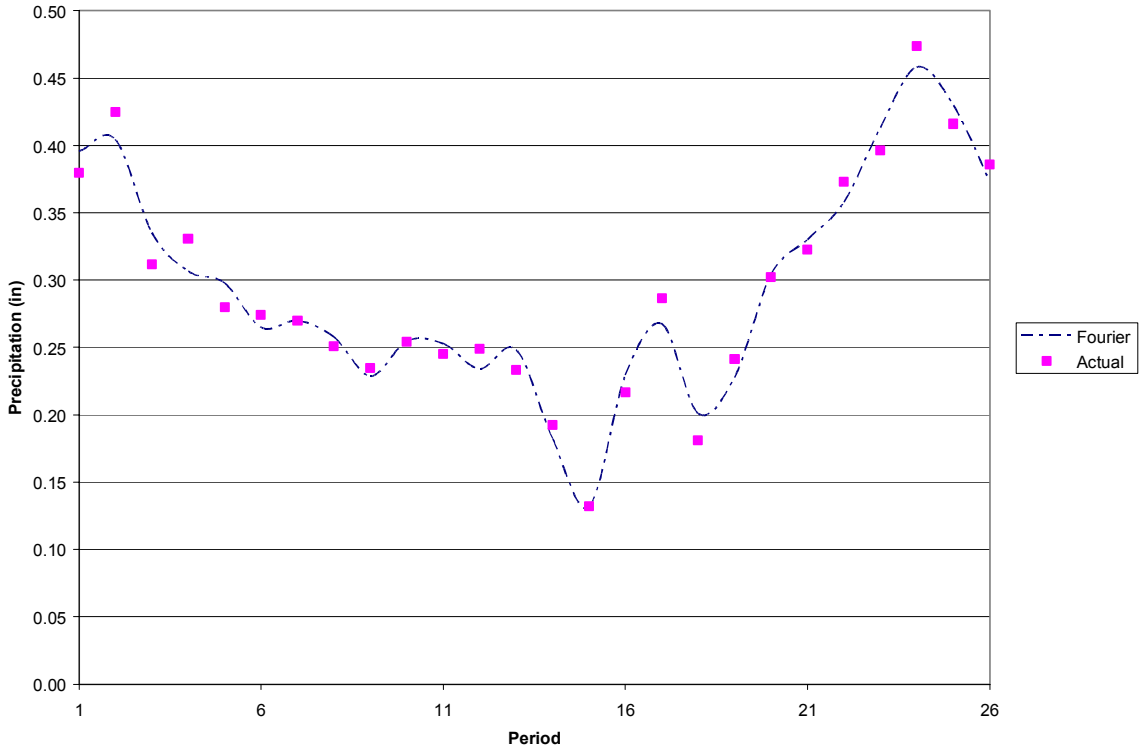

Figure 4.4-3. Fourier series approximation of mean precipitation on wet days (8 Harmonics).

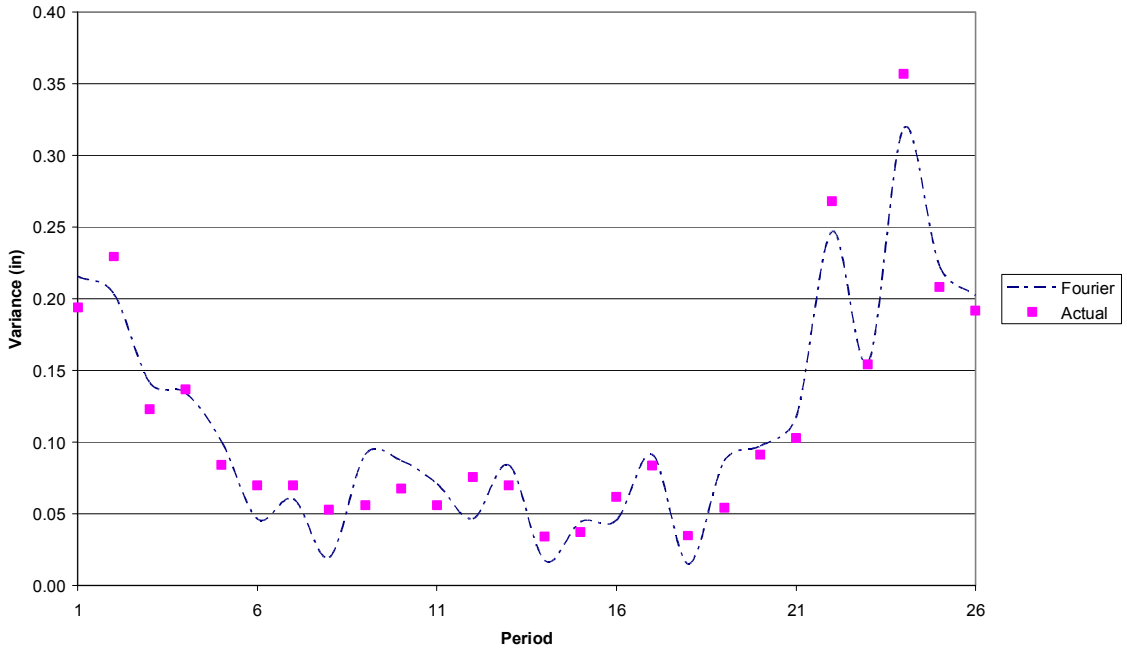

Figure 4.4-4. Fourier series approximation of variance of precipitation on wet days (8 Harmonics).

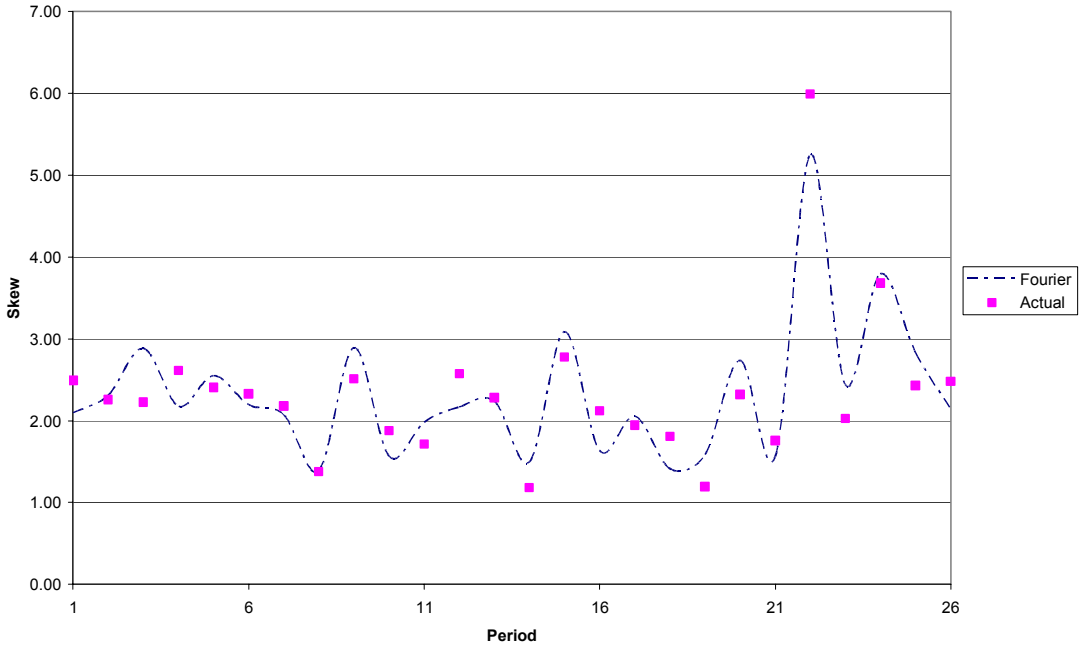

Figure 4.4-5. Fourier series approximation of skew of precipitation distribution on wet days (8 Harmonics).

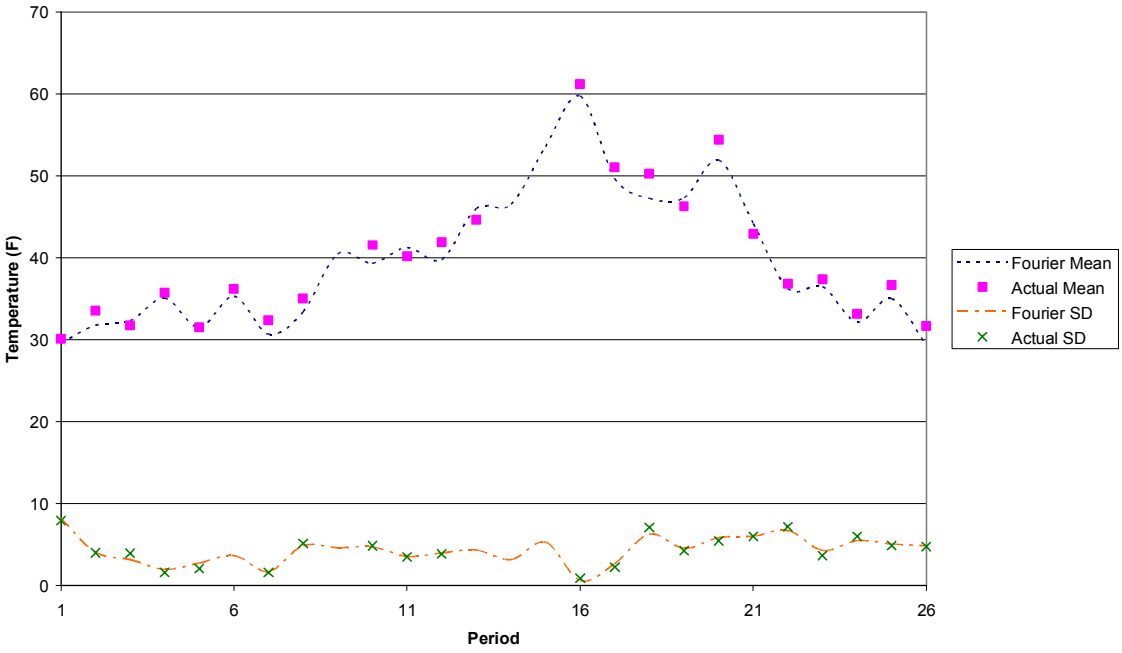

Figure 4.4-6. Fourier series approximation of maximum temperature mean and standard deviation on wet days (8 Harmonics).

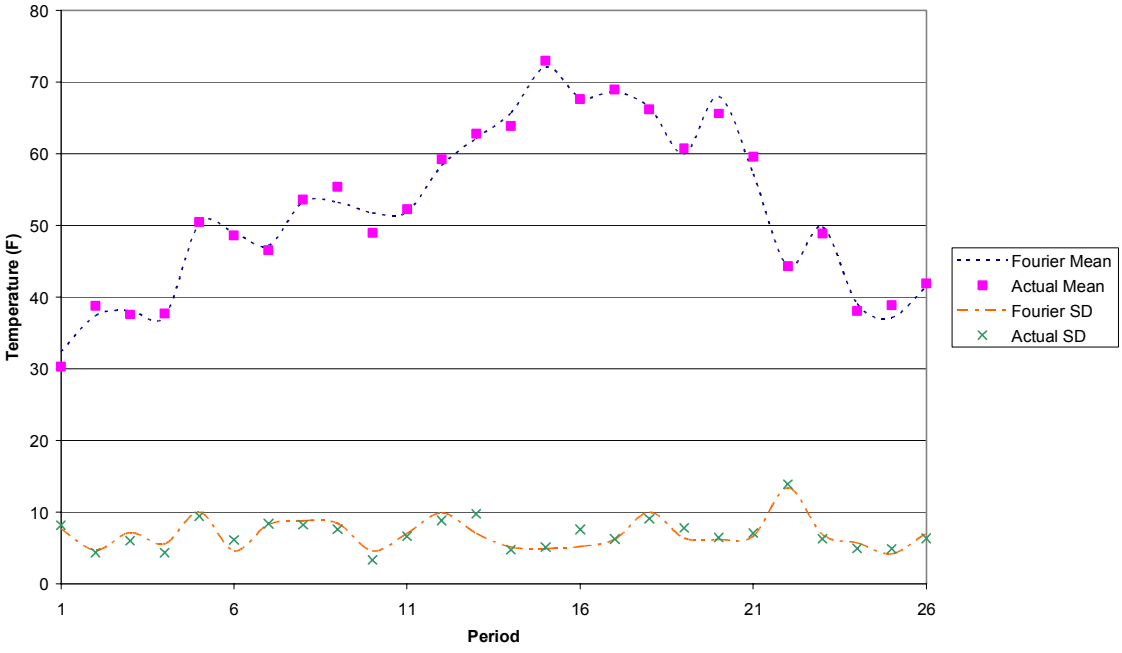

Figure 4.4-7. Fourier series approximation of maximum temperature mean and standard deviation on wet days (8 Harmonics).

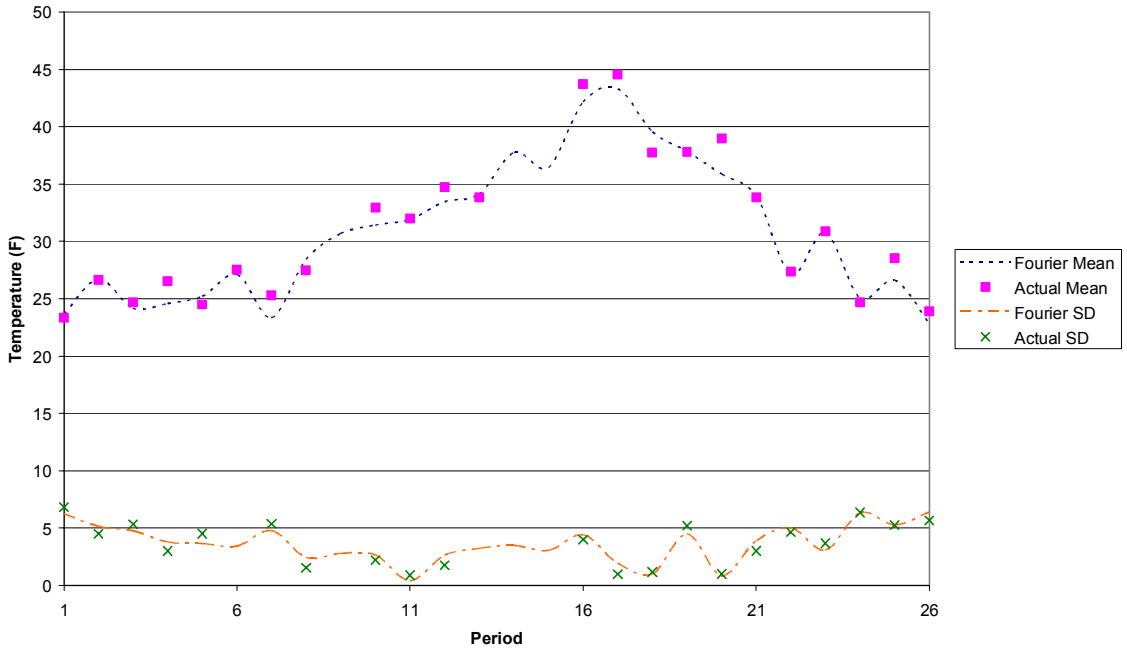

Figure 4.4-8. Fourier series approximation of minimum temperature mean and standard deviation on wet days (8 Harmonics).

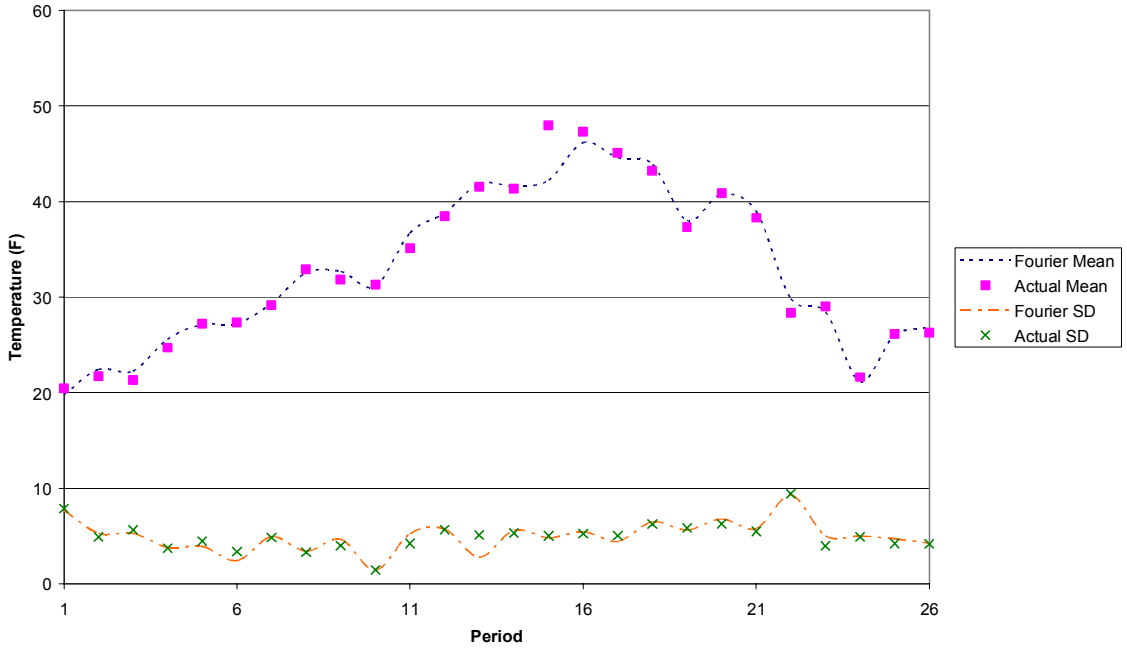

Figure 4.4-9. Fourier series approximation of minimum temperature mean and standard deviation on dry days (8 Harmonics).

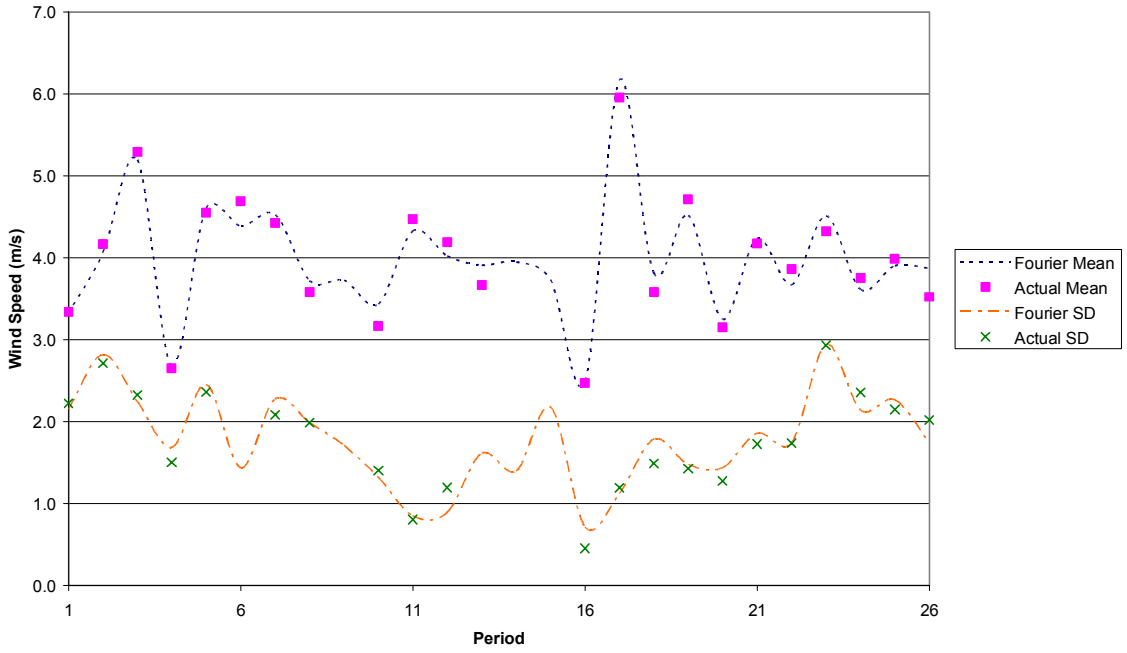

Figure 4.4-10. Fourier approximation of average wind speed mean and standard deviation of wet days (8 Harmonics).

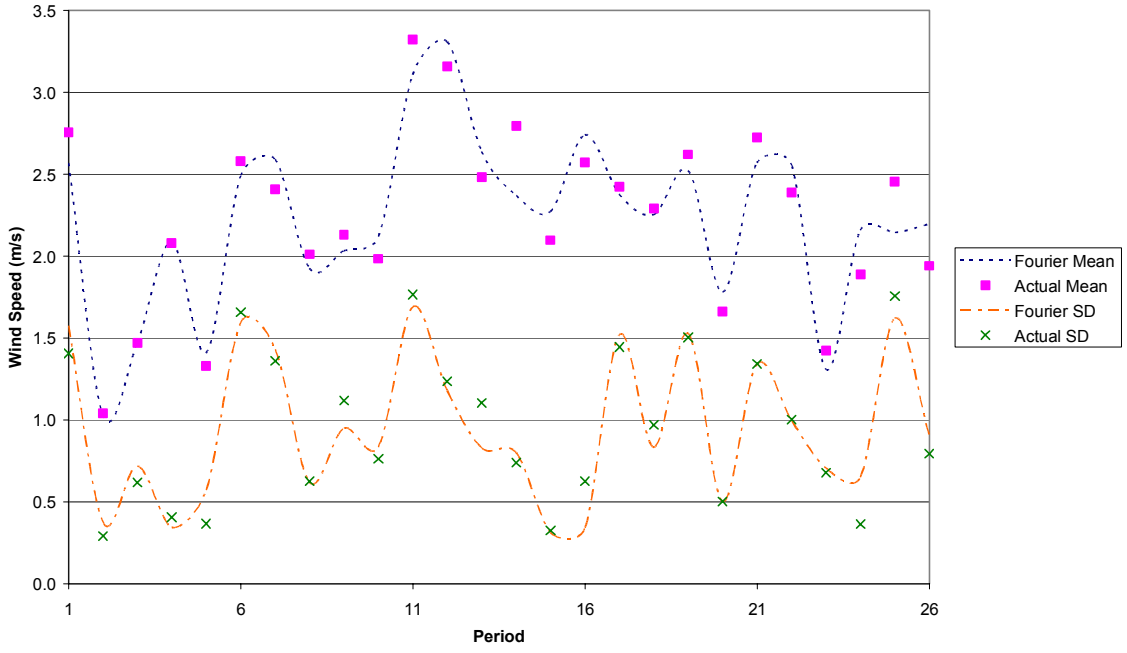

Figure 4.4-11. Fourier series approximation of average wind speed mean and standard deviation on dry days (8 Harmonics).

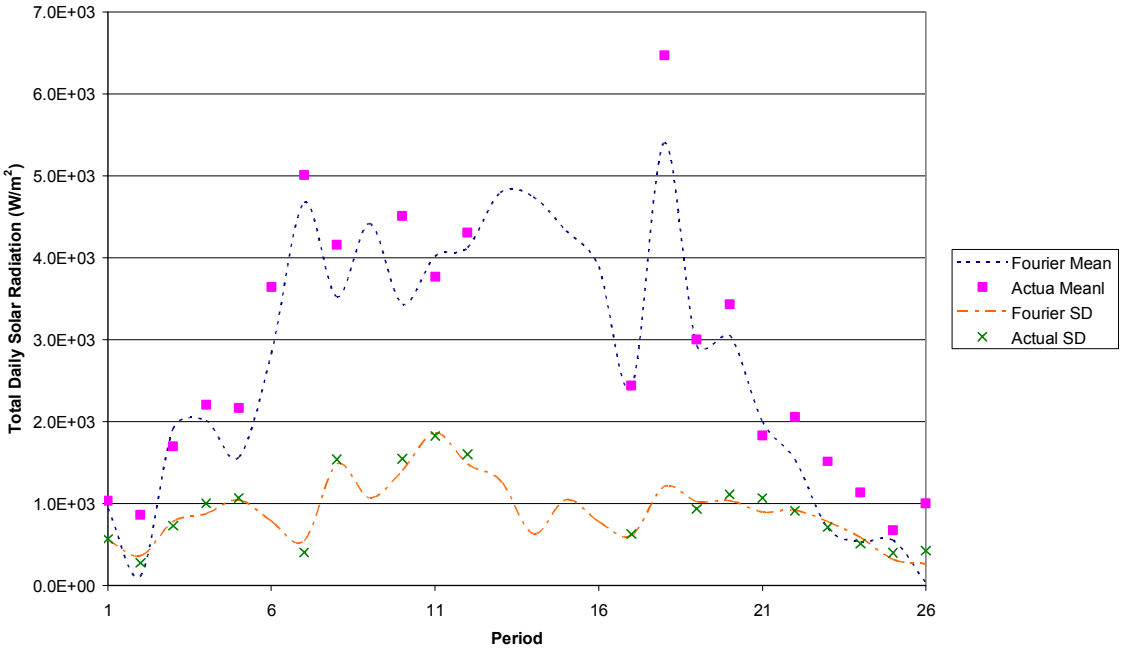

Figure 4.4-12. Fourier series approximation of solar radiation mean and standard deviation on wet days (8 Harmonics).

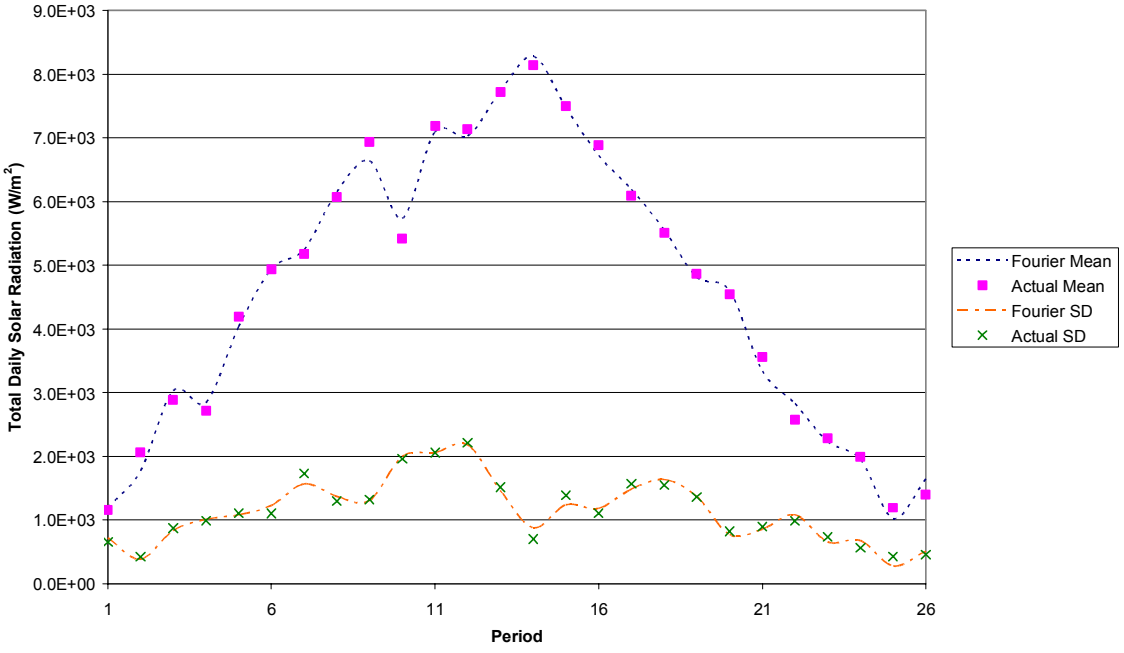

Figure 4.4-13. Fourier series approximation of solar radiation mean and standard deviation on dry days (8 Harmonics).

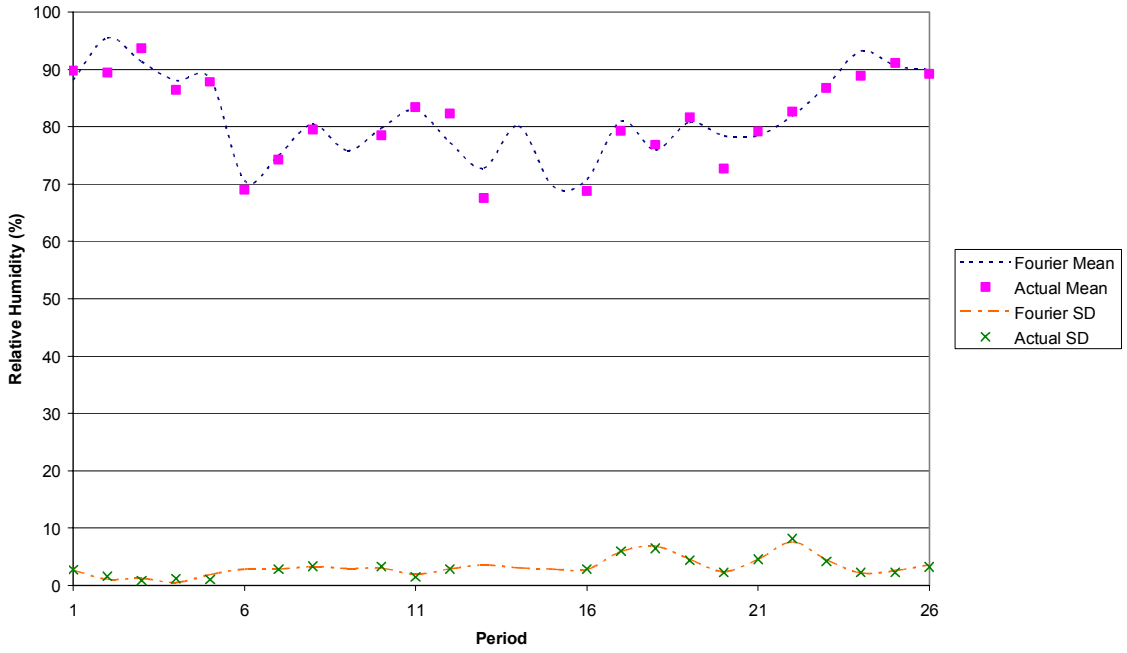

Figure 4.4-14. Fourier series approximation of relative humidity mean and standard deviation on wet days (8 Harmonics).

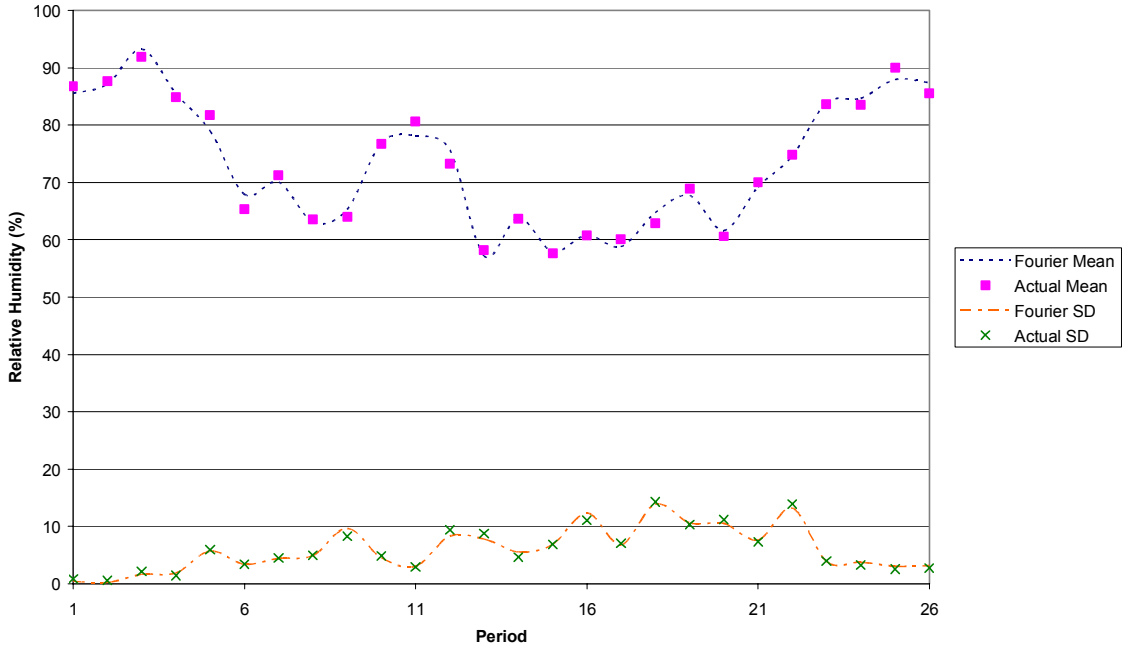

Figure 4.4-15. Fourier series approximation of relative humidity mean and standard deviation on dry days (8 Harmonics).

Table 4.4-1. Coefficients for the A matrix in the MAR model.

	Maximum temperature	Minimum temperature	Wind Speed	Relative humidity	Solar Radiation
Maximum temperature	0.316	0.131	0.007	0.094	0.057
Minimum temperature	0.303	0.234	-0.214	0.050	-0.150
Wind Speed	0.103	-0.078	0.164	-0.014	-0.128
Relative humidity	-0.069	0.094	-0.057	0.692	0.005
Solar Radiation	0.037	-0.029	0.086	0.049	0.087

Table 4.4-2. Coefficients for the B matrix in the MAR model.

	Maximum temperature	Minimum temperature	Wind Speed	Relative humidity	Solar Radiation
Maximum temperature	0.925	0.000	0.000	0.000	0.000
Minimum temperature	0.264	0.824	0.000	0.000	0.000
Wind Speed	-0.416	0.282	0.842	0.000	0.000
Relative humidity	-0.352	-0.069	0.048	0.626	0.000
Solar Radiation	0.415	-0.338	-0.132	-0.067	0.824

Evaluation of the simulations

Given the parameter estimates, the simulation process proceeds as follows for each day:

1. Generate a uniform random number and, based on the precipitation state of the previous day, determine whether the current day is wet or dry based on its magnitude in comparison with the transition probability.
2. If the day is wet, generate a rainfall depth by first generating a standard normal random number, transforming it to a standardized gamma random variable and computing the depth of rainfall using equation 4.2-1. If the day is dry, precipitation depth is set to zero.
3. Generate five standard normal random variables and simulate the standardized random variables using equation 4.2-3.
4. Compute the values of the simulated temperature, solar radiation, relative humidity and wind speed using equation 4.2-2 with the appropriate mean and standard deviation depending on whether the day is wet or dry.

Using the estimated parameters based on the Fourier series approximations, values were simulated for each of the variables using the simulation scheme described above. Values were simulated for a time period consistent with the time period used to estimate the parameters. For precipitation, 50 years of

data were generated (consistent with the period of record at Oakridge) while for the remaining parameters, only two years of data were generated (consistent with the data for Waldo Lake). During the simulation process, accommodation was required due to the rare simulation of negative rainfall depth. Although this cannot occur in nature and it should not occur in theory, because the simulation of the gamma distributed random variables is based on a mathematical approximation, a negative value does occasionally occur. These values were simply discarded from the simulated sample. Similar accommodation had to be made for impossible values of other parameters, as they arise from the use of a normal distribution, which has infinite tails in both positive and negative directions.

The simulated data were evaluated by comparing statistics of the monthly and annual values – time periods that were not used in estimating the parameters – for the observed and simulated samples. Comparisons of monthly values of observed and generated means and standard deviations of maximum and minimum temperature, average wind speed, total daily solar radiation, and relative humidity are shown in Figure 4.4-16Figure 4.4-20. Comparisons of annual values are shown in Figure 4.4-21, and Figure 4.4-22Figure 4.4-23 show comparative statistics for precipitation. A nonparametric statistical test - the Mann-Whitney test - was used to provide a quantitative comparison between observed and simulated values to avoid the issue of the underlying distribution. These tests demonstrated that the simulations reproduced the aggregate monthly and annual statistical characteristics.

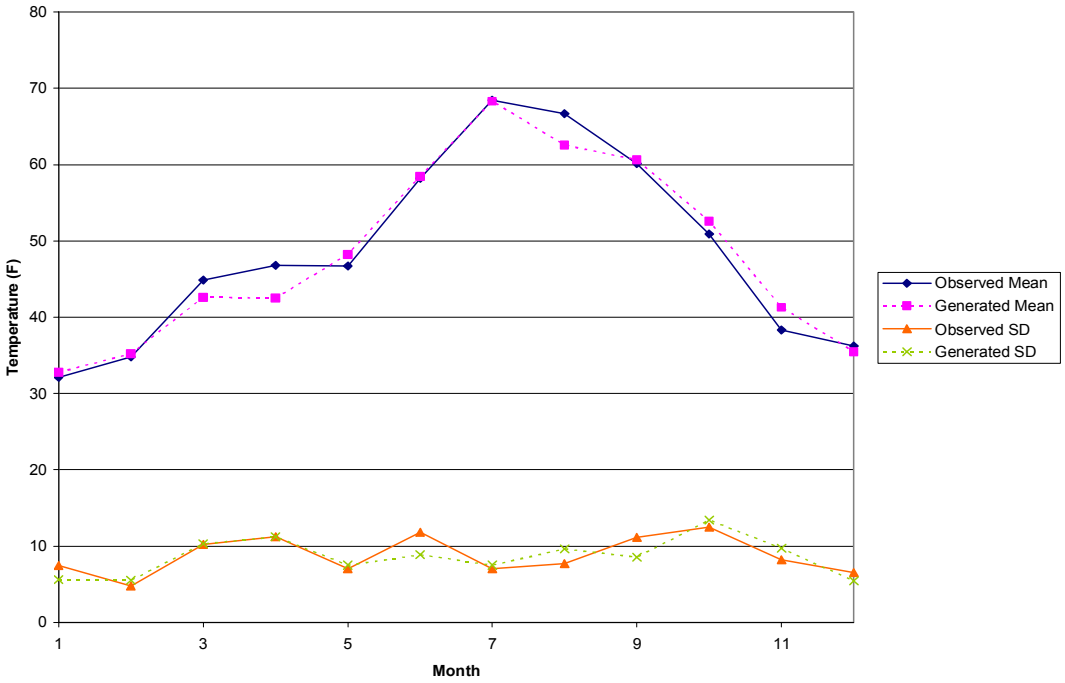

Figure 4.4-16. Monthly variation of maximum temperature, mean and standard deviation.

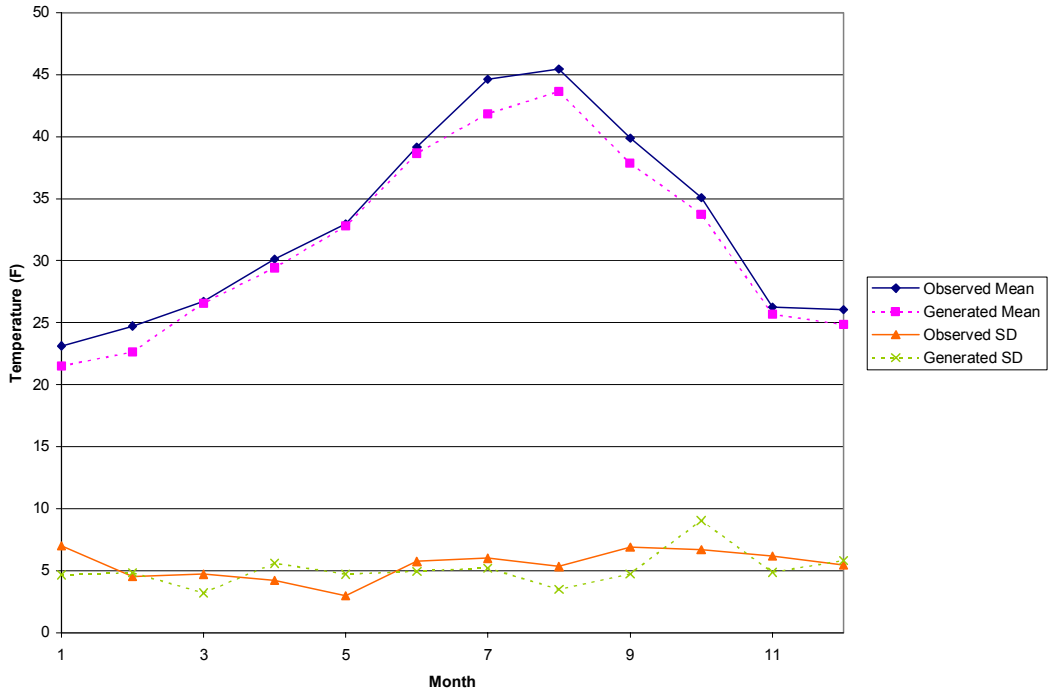

Figure 4.4-17. Monthly variation of minimum temperature, mean and standard deviation.

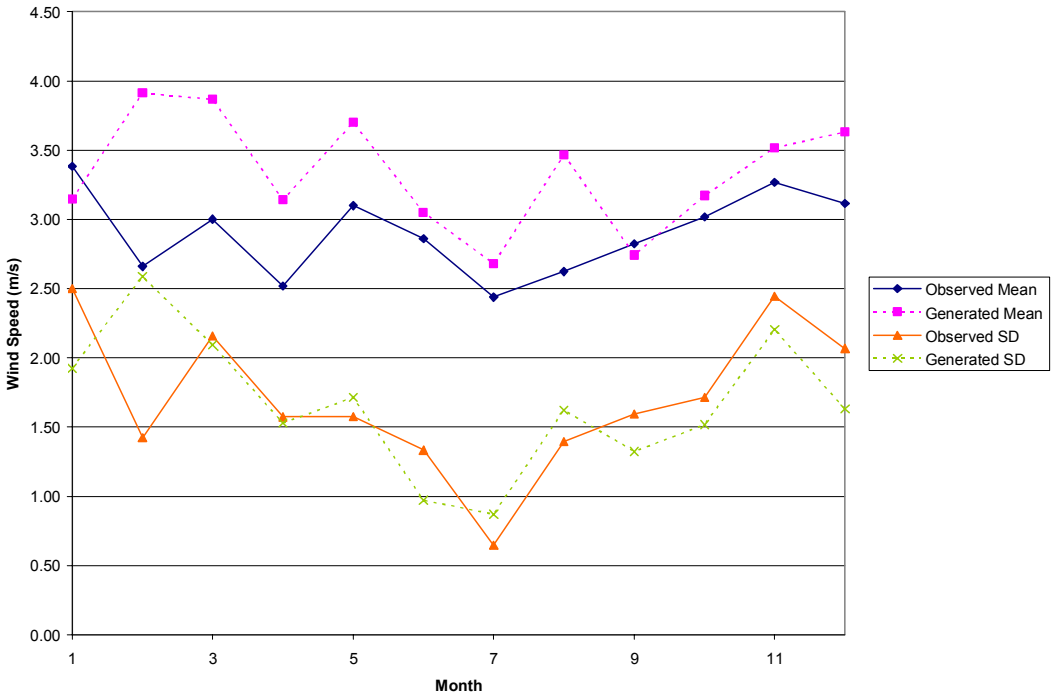

Figure 4.4-18. Monthly variation of average wind speed, mean and standard deviation.

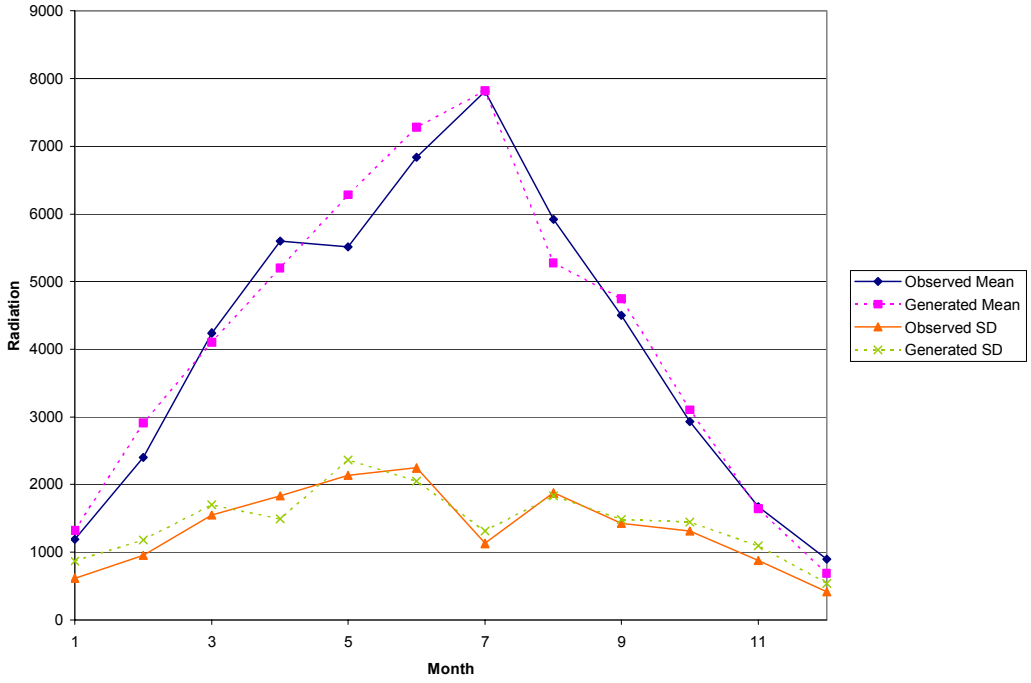

Figure 4.4-19. Monthly variation of solar radiation, mean and standard deviation.

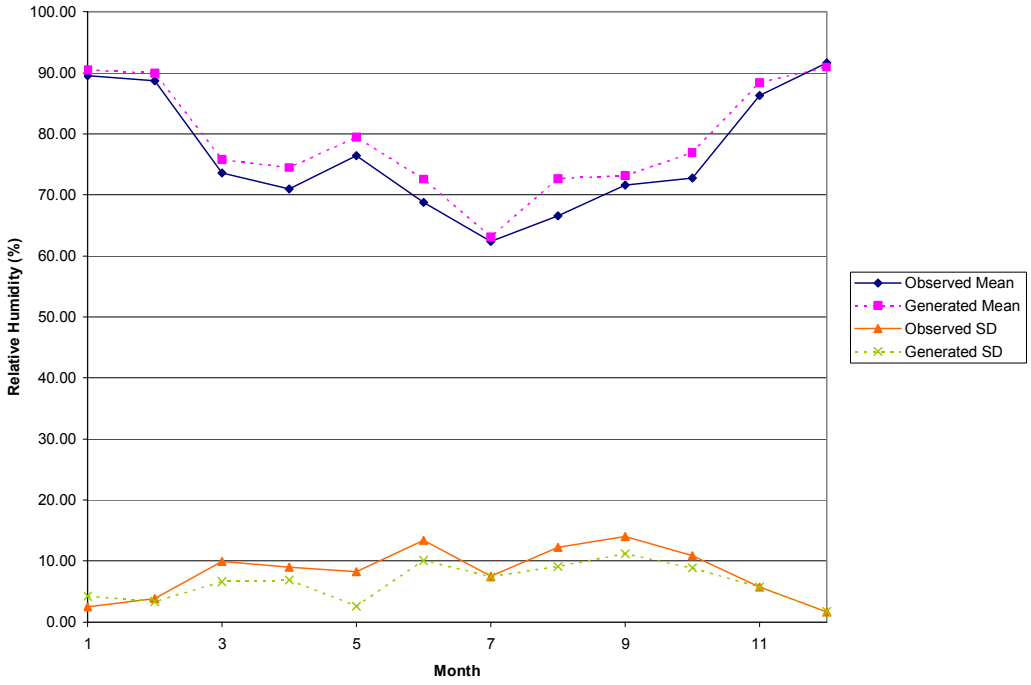

Figure 4.4-20. Monthly variation of relative humidity, mean and standard deviation.

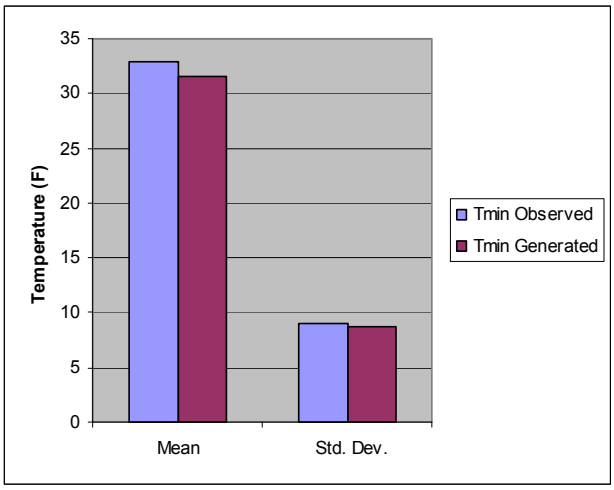

(a) Maximum Temperature

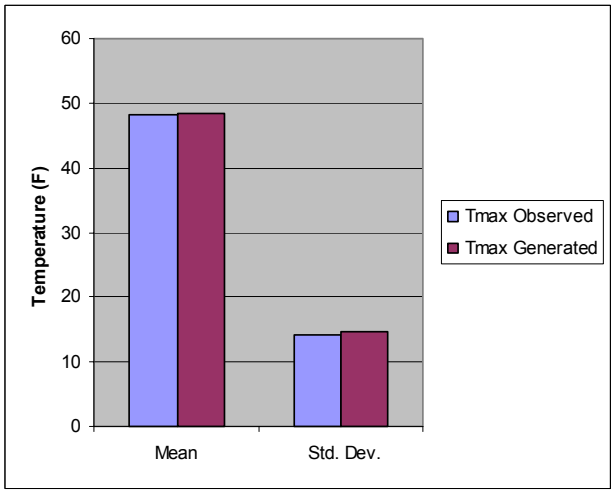

(b) Minimum Temperature

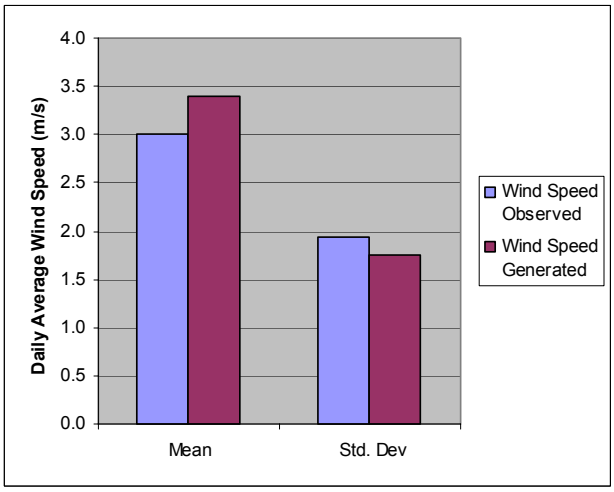

(c) Average Wind Speed

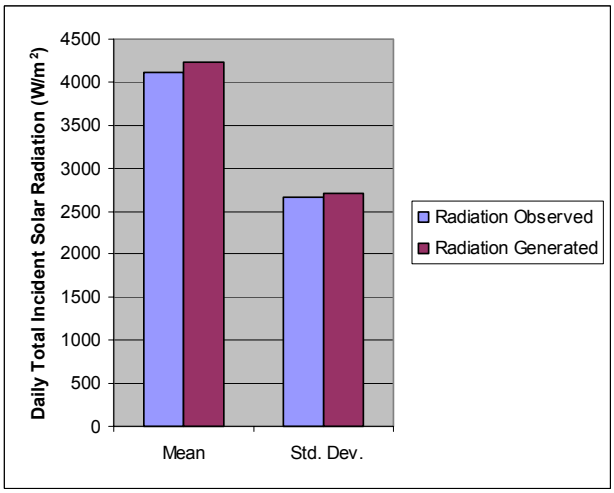

(d) Solar Radiation

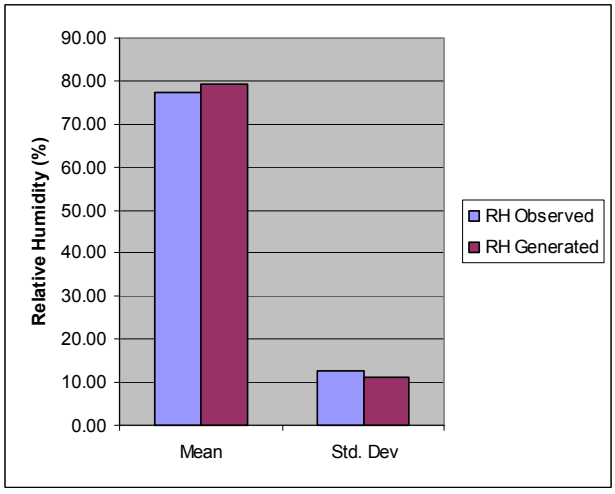

(e) Relative Humidity

Figure 4.4-21. Comparison of observed and generated annual mean and standard deviation of climate variables.

Figure 4.4-22. Comparison of observed and generated mean monthly precipitation.

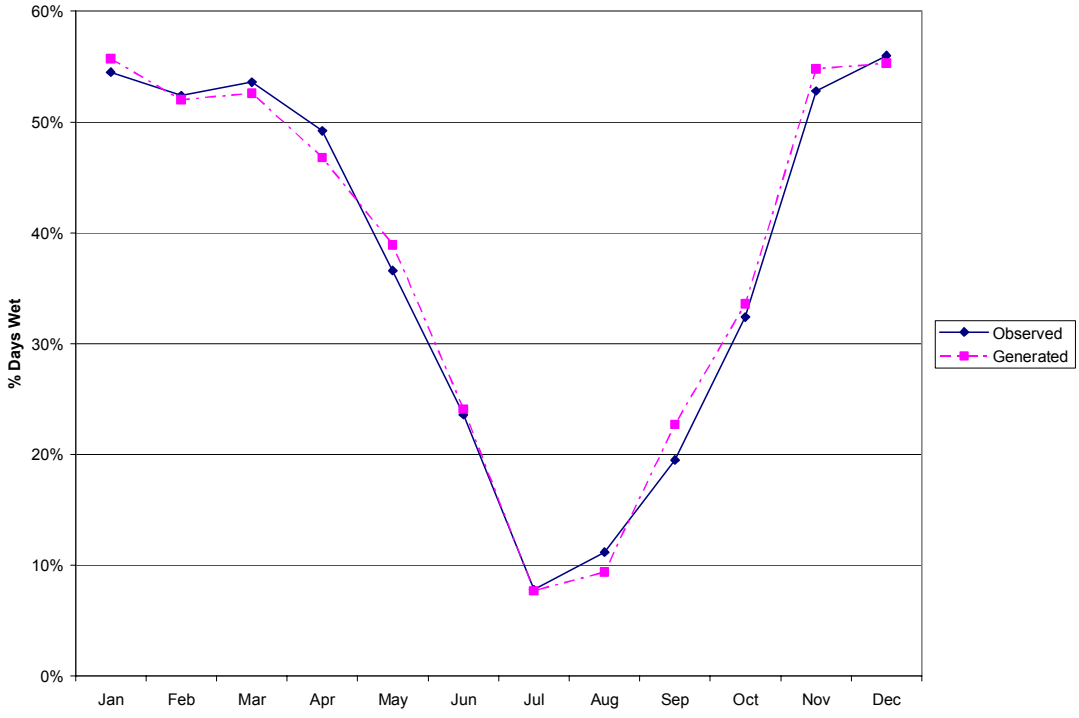

Figure 4.4-23. Comparison of observed and generated percentage of wet days by month.

4.5 Conclusions, observations, and future work

A stochastic model was developed to simulate the daily meteorological data for Waldo Lake required as input to the CE-QUAL-W2 model. The simulation approach was tested and shown to reproduce monthly and annual statistics of the selected variables. The parameter values were estimated using available data for the site which is limited at present to less than two years of hourly observations. The lack of available data also meant that the model was tested against the same data that it was based upon, and therefore the similarity of generated values to observed ones is somewhat exaggerated. Nevertheless, the methodology is sound, and as more data become available, the model can be validated and the parameter estimates can be refined for more accurate long term simulations.

This model will need to be refined for direct application with CE-QUAL-W2 model. Daily data are likely not of sufficient resolution for the model and techniques will need to be developed for disaggregating the simulated daily values into hourly values. Statistical disaggregation models have been used for similar purposes, are well understood and can be applied in this case. A further refinement that may better preserve the inter-annual and longer time scale behavior of the model is to assess how the parameters of the stochastic model are related to large scale patterns in the climate – in particular the El Niño/Southern Oscillation (ENSO) and the Pacific Decadal Oscillation (PDO). These two indices have been shown to be related to the local climate and streamflow in the vicinity of Waldo Lake. This type of variation is not explicitly reflected in the stochastic model presented here. In particular, the decadal scale patterns of persistent period of above or below average variation are unlikely to be present in the data generated from the model over a time scale of several decades. If long term simulations of Waldo Lake are to be undertaken, then this refinement will be important.

5 Water Quality Modeling CE-QUAL-W2

5.1 Introduction

The application of a hydrodynamic and water quality model to the Waldo Lake ecosystem summarizes and synthesizes the physical, chemical, and biological characteristics of the lake into a tool which can be used to look at management strategies to improve water quality. The model represents the Waldo Lake ecosystem and responds to both meteorological and hydrological forcing processes (Figure 5.1-1). Temperature monitoring, water quality sample collection, phytoplankton photosynthetic efficiency and hydrologic analyses are necessary work tasks for the construction of a water quality model of Waldo Lake. This chapter reviews the work completed to construct and calibrate a lake model for water temperature.

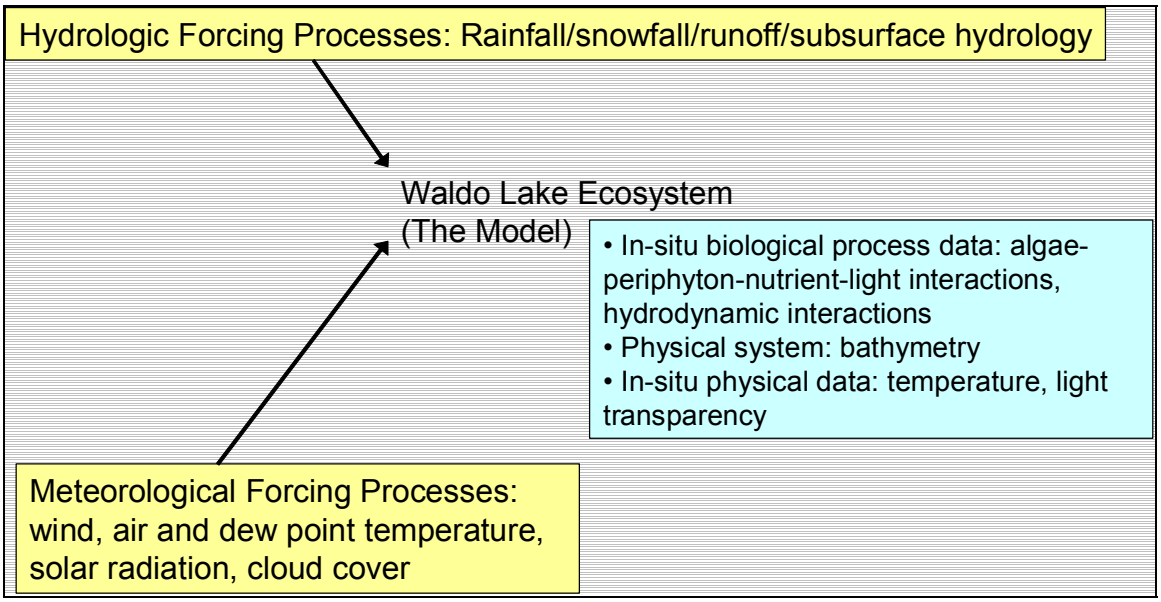

Figure 5.1-1. The response of the Waldo Lake ecosystem, the model, to external forcing processes.

Waldo Lake is located approximately 93 km southeast of Eugene, Oregon near McCredie Springs and Oakridge, Oregon. Waldo Lake lies in a glaciated basin with lateral and end moraines at an elevation of 1650 m (NGVD29) in the central Oregon Cascade Mountains, Figure 5.1-2. The model development and calibration period was January 1 to December 31, 2004.

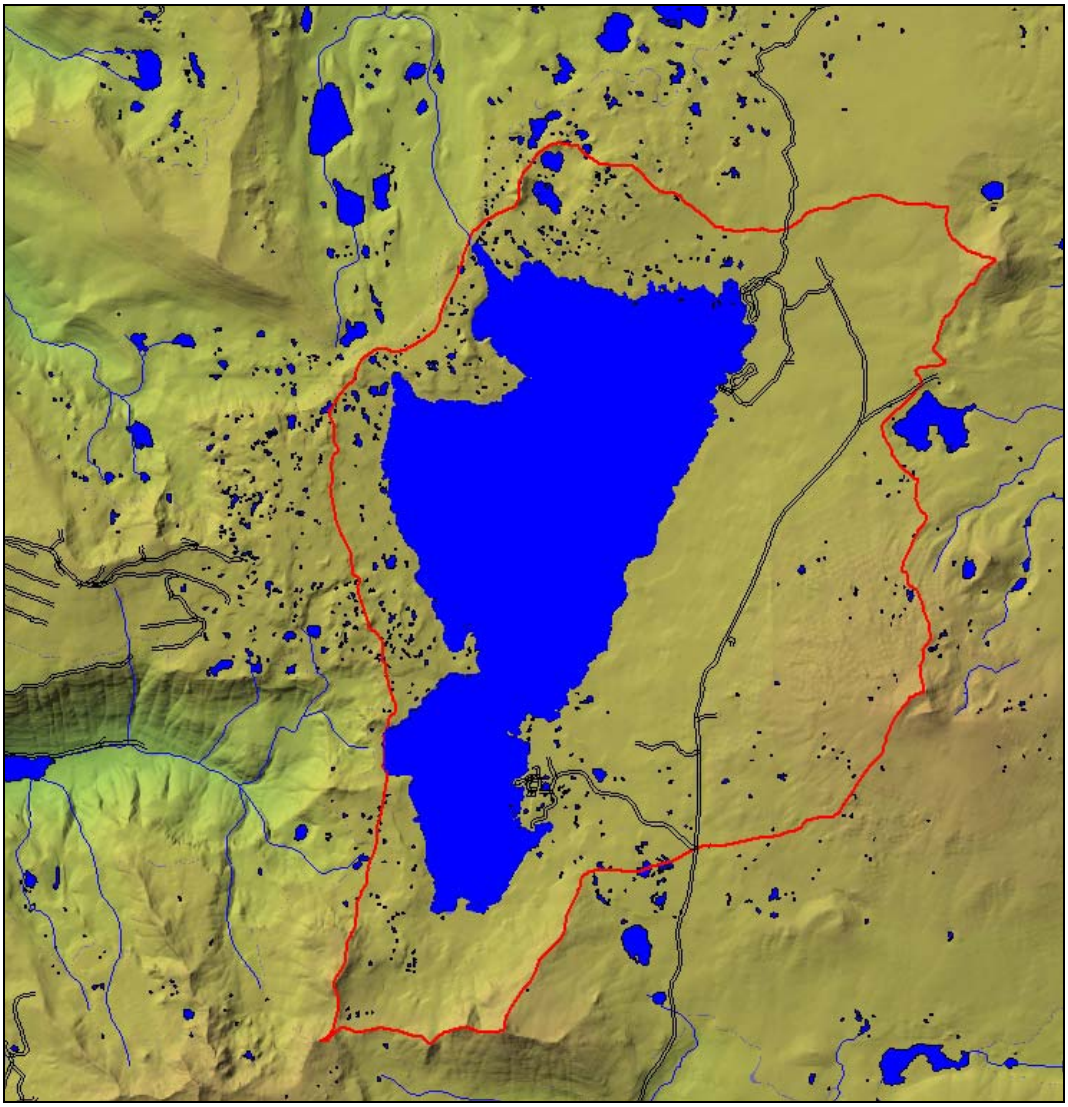

Figure 5.1-2. Waldo Lake watershed.

There are three general data requirements for developing a CE-QUAL-W2 model application of a lake system: The bathymetry of the lake, the meteorological conditions, and the boundary conditions for the lake such as inflows and outflows.

5.2 Model Development

Bathymetry

The bathymetry of Waldo Lake was measured through several bathymetric surveys conducted by the Center for Lakes and Reservoirs (CLR) at Portland State University (Sytsma et al. 2004). Figure 5.2-1 shows the bathymetry for Waldo Lake including the topography surrounding the lake full pool water line. The outer line surrounding the lake in the figure represents the extent of the topographic elevation data and the inner line represents the separation between the bathymetry data and the topographic data.

The topographic elevation data was obtained from the digital elevation model (DEM) data from the U.S. Geological Survey (USGS). The figure also includes an estimate of a general centerline of the lake which was used to develop the model grid.

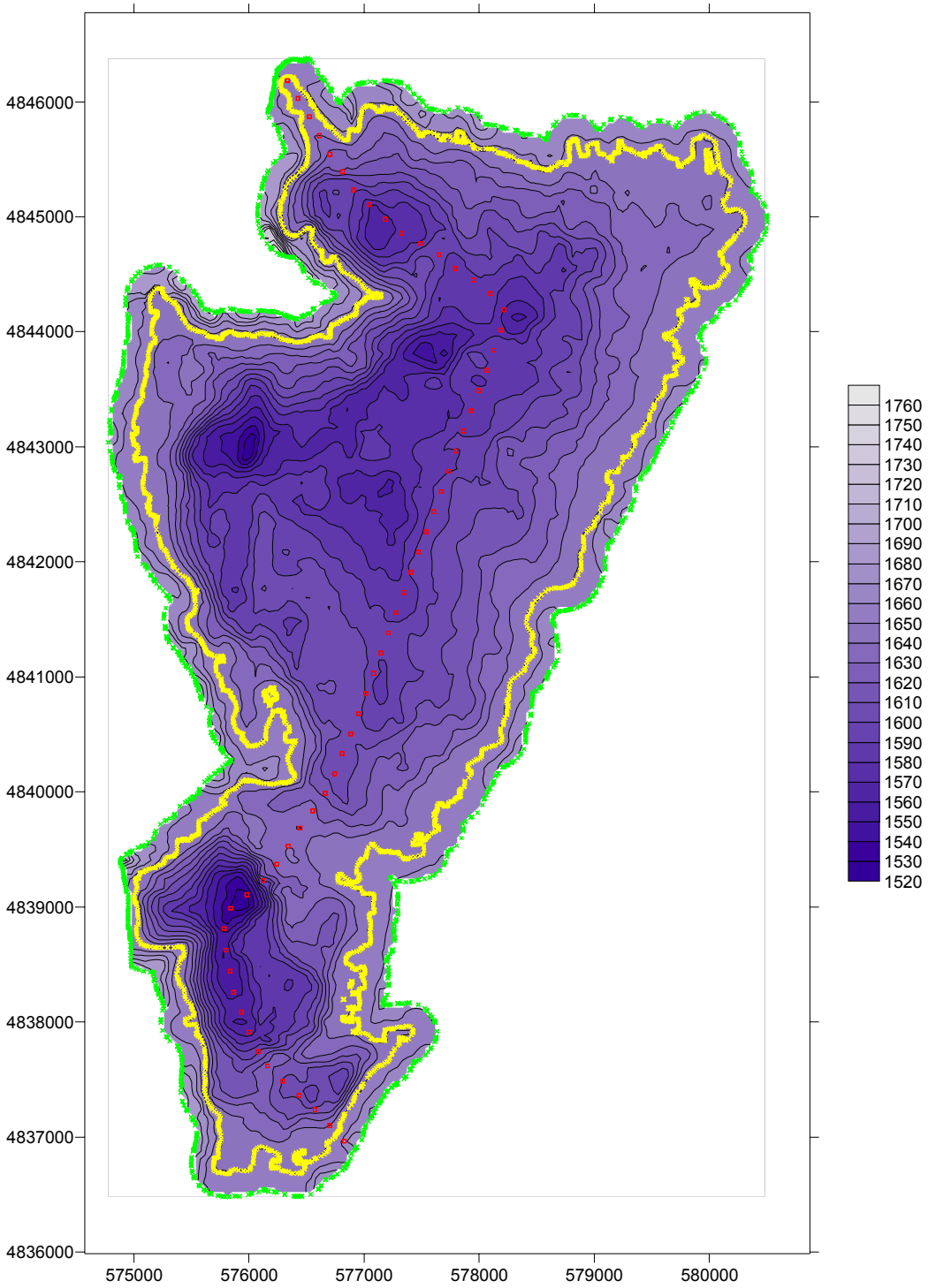

Figure 5.2-1. Waldo Lake bathymetry.

The lake bathymetry was used to create a volume-elevation curve that was compared to historical data. Figure 5.2-2 shows a volume-elevation curve for the bathymetric survey results (Sytsma et al.

2004) and historical volume-elevation data from the USGS. Although the historical volume-elevation data are limited, the figure shows there is good agreement between the recent bathymetric survey volume-elevation results and the historical data.

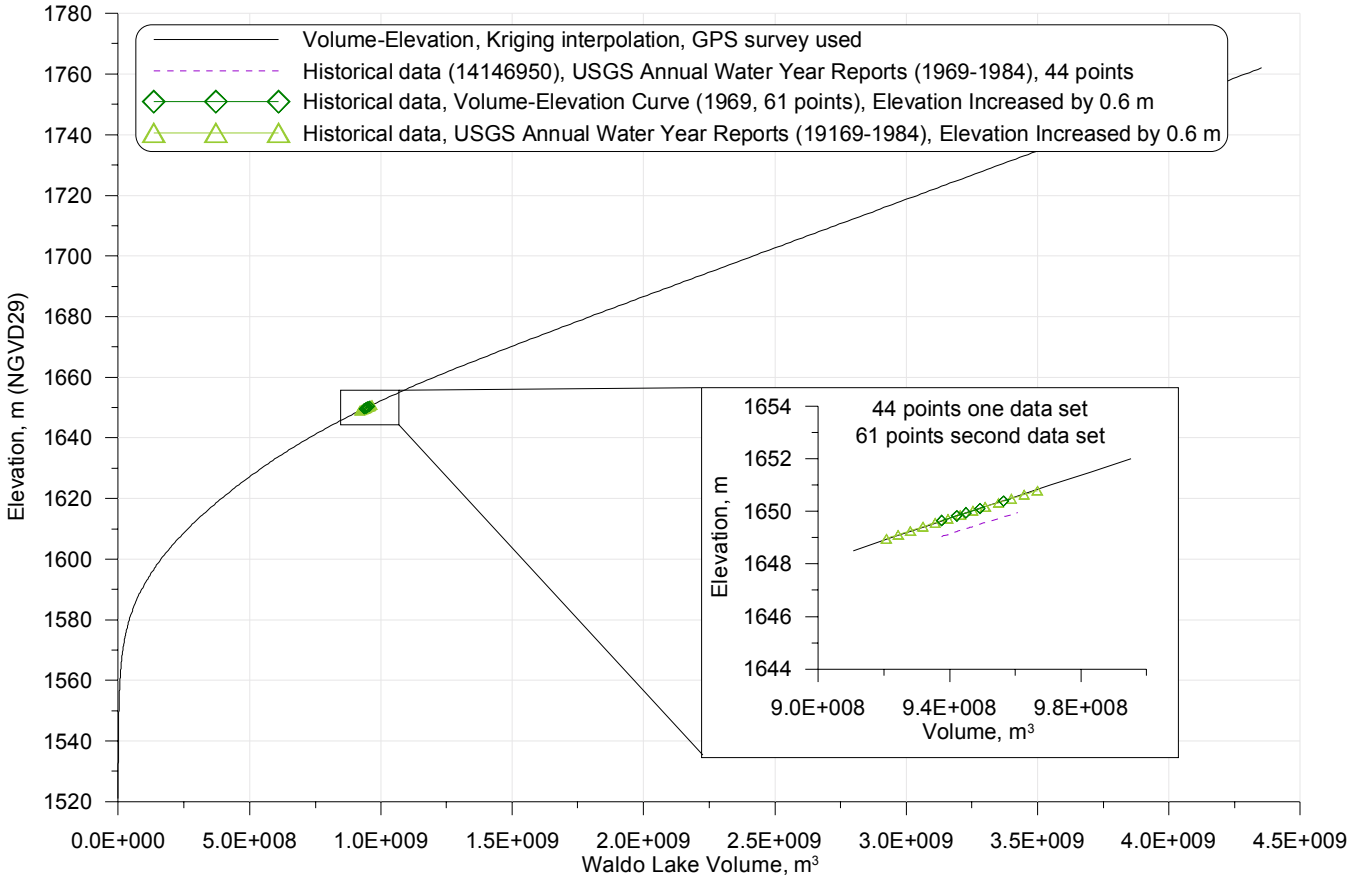

Figure 5.2-2. Volume-Elevation curve for Waldo Lake including recent survey results and historical data.

Model Grid

The bathymetric and topographic elevation data were then used to construct a computational grid for the lake model. The centerline shown in Figure 5.2-1 was used to slice the contour plot in equal length segments and use the volume-elevation relationship for each slice to obtain average model widths for the CE-QUAL-W2 model. Table 5.2-1 lists the model grid specifications, and Figure 5.2-3 shows a plan view of the model grid layout. Model grid layer heights were set to 1 m to ensure that the thermocline was captured in the model results and that volume was correctly represented over the depth of the lake. Figure 5.2-4 shows a side view of the model grid and Figure 5.2-5 shows an end view of model segments 3 and 36.

Table 5.2-1. Waldo Lake model grid characteristics.

Water body	Branch	Start Segment	End Segment	Segment length, m	Layer Height, m
1	1	2	61	187.6	1

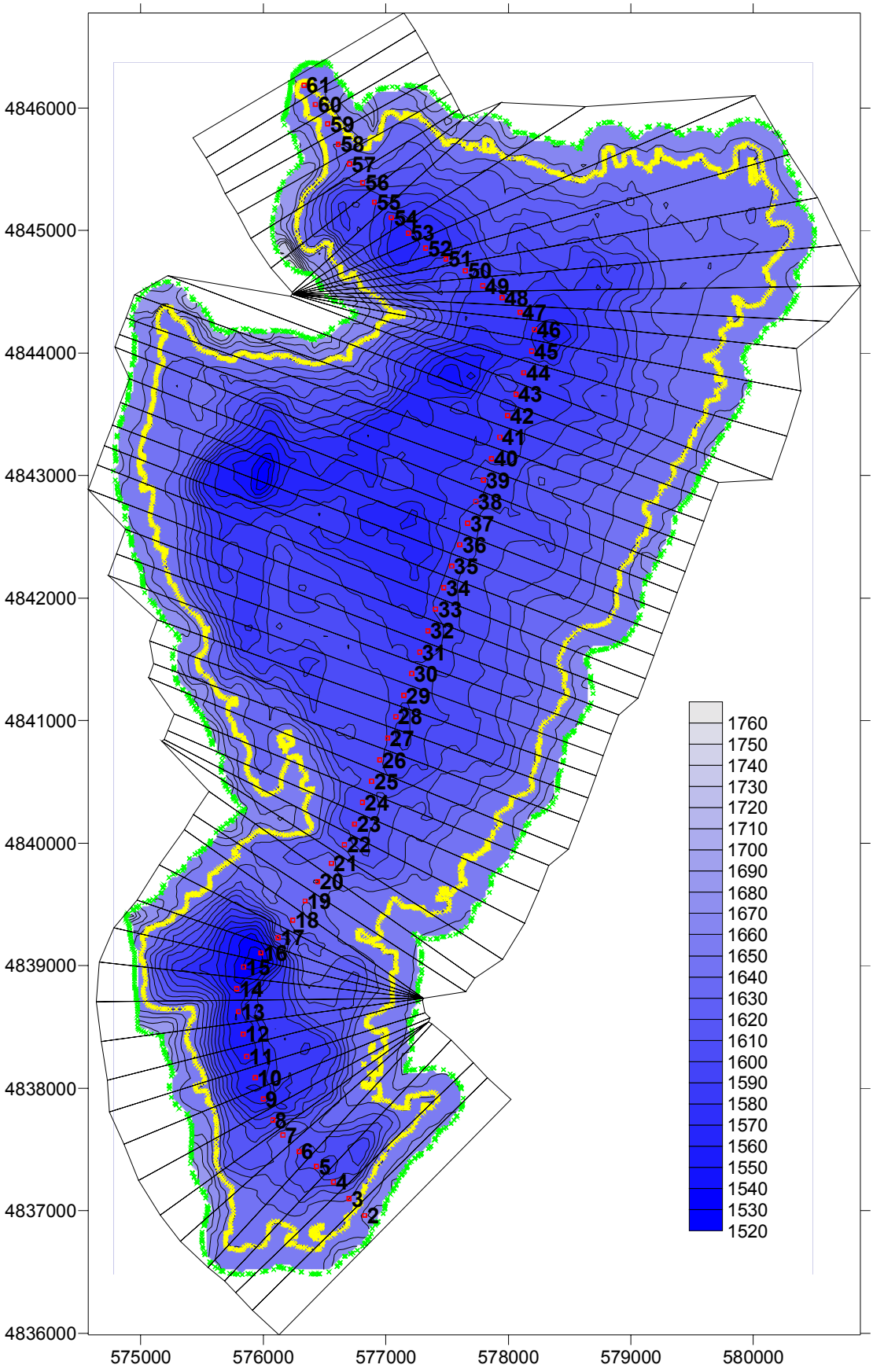

Figure 5.2-3. Waldo Lake model grid layout, plan view.

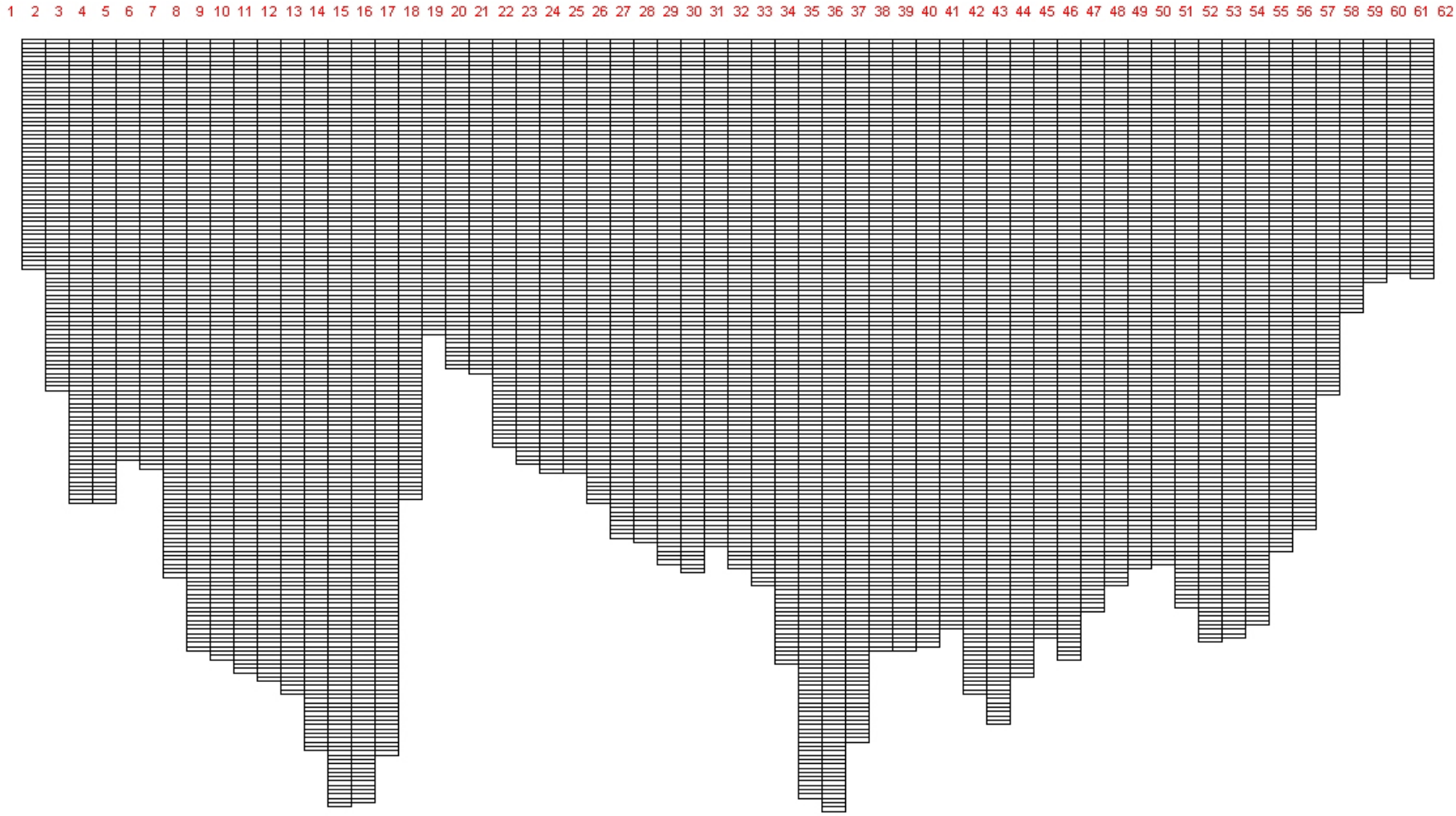

Figure 5.2-4. Waldo Lake model grid layout, side view.

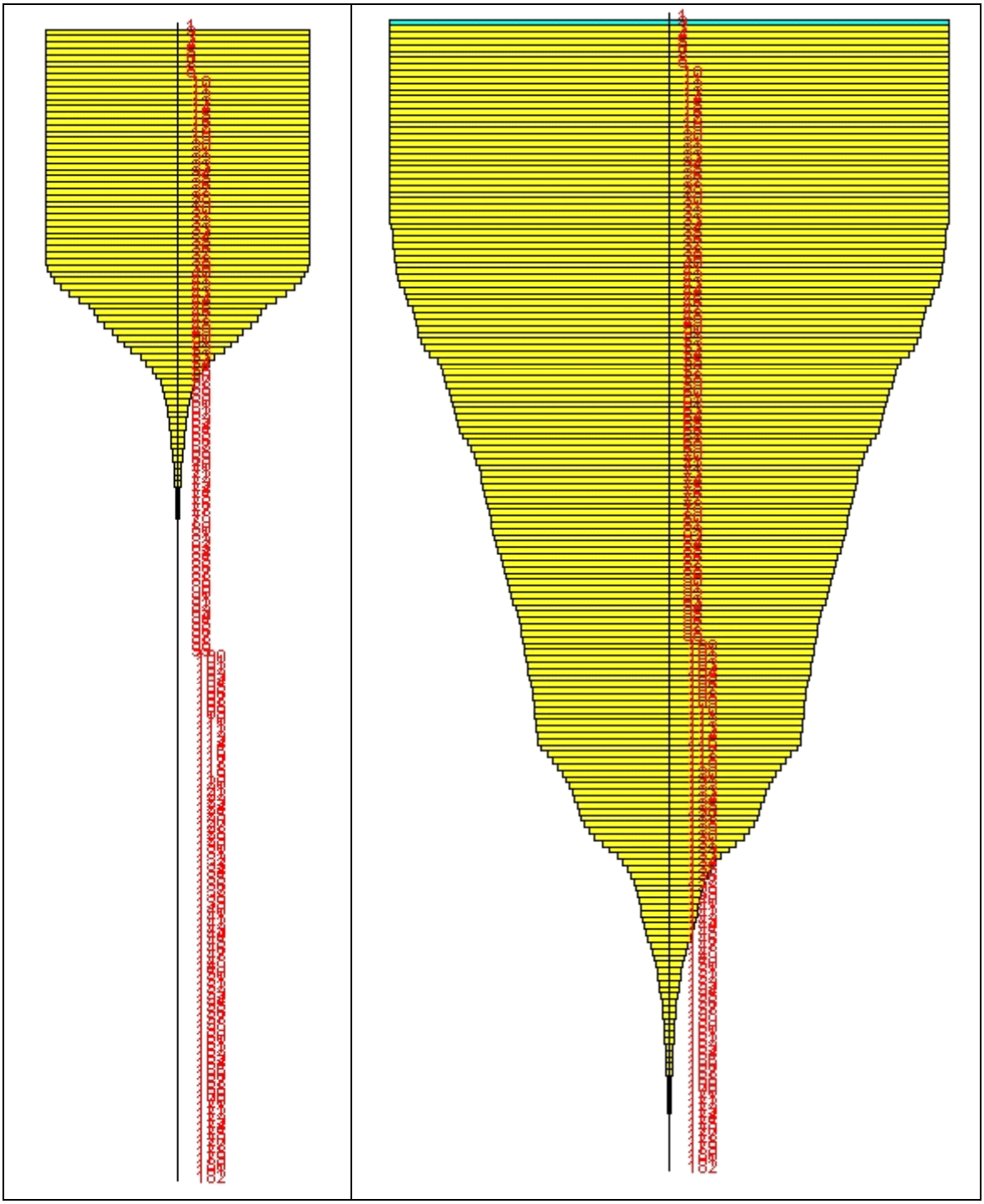

Figure 5.2-5. Waldo Lake Grid layout end view of Segment 3 (left) and segment 36 (right).

The volume-elevation relationship for the model grid was compared to the volume-elevation curve from the bathymetric survey (Sytsma et al. 2004). Figure 5.2-6 compares the model grid and bathymetric data volume-elevation curves and shows the model is accurately representing the lake volume over the depth of the lake.

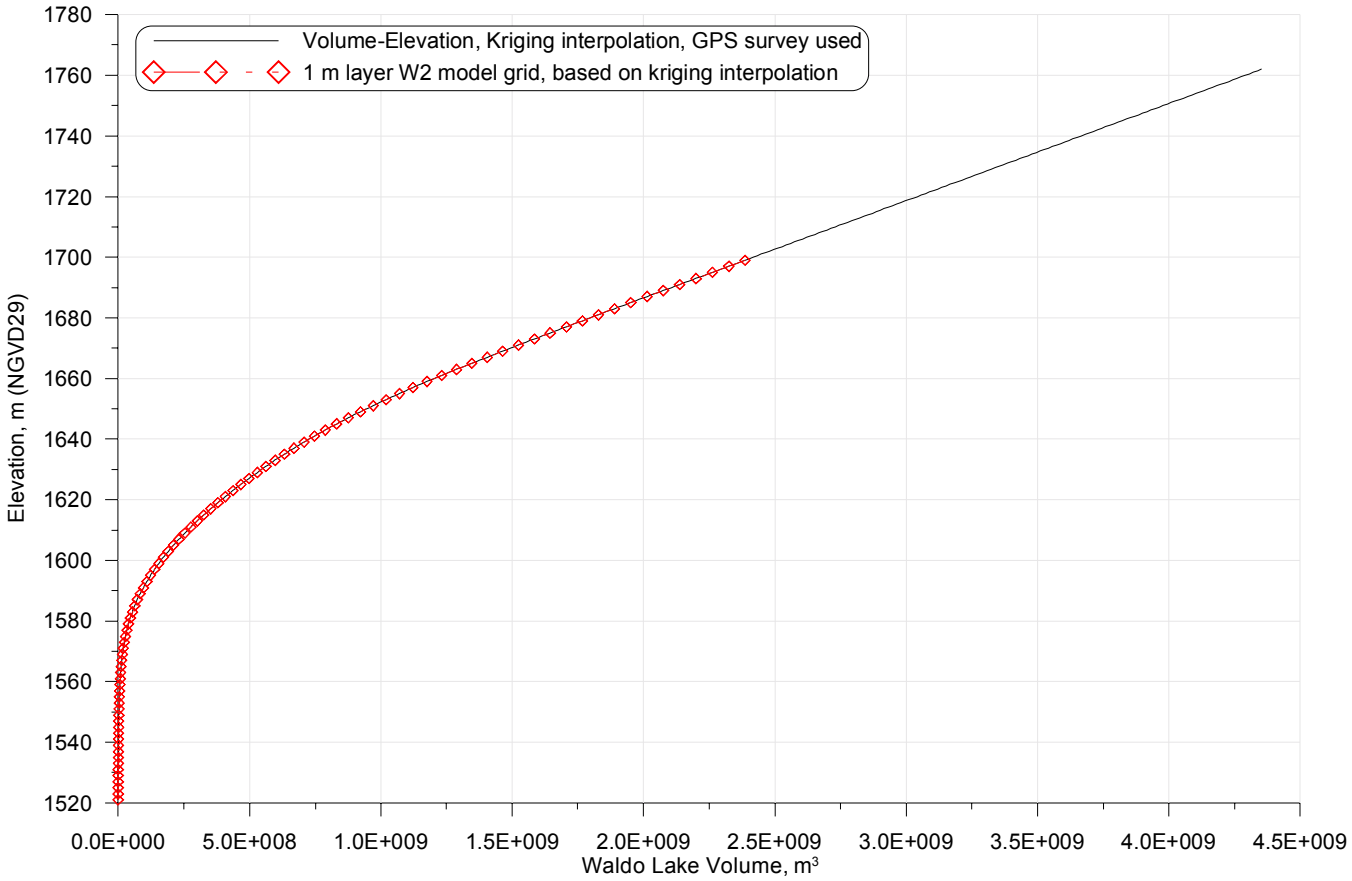

Figure 5.2-6. Waldo Lake volume elevation, bathymetric survey and CE-QUAL-W2 model grid.

Meteorology

Meteorological data were collected at Waldo Lake from 2003 through 2005 at a monitoring site located at the Islet Campground (Figure 5.2-7). The monitoring site is maintained by the U.S. Forest Service (USFS) and records barometric pressure, air temperature, relative humidity, wind speed and direction, precipitation and solar radiation on an hourly basis.

The CE-QUAL-W2 lake model uses air temperature, dew point temperature, wind speed and direction and either cloud cover or solar radiation. If cloud cover data are used the model calculates the theoretical clear sky solar radiation and attenuates it based on the cloud cover data. The Waldo Lake model used the solar radiation data directly as model input. Since Waldo Lake has a large surface area, precipitation data were included in the model.

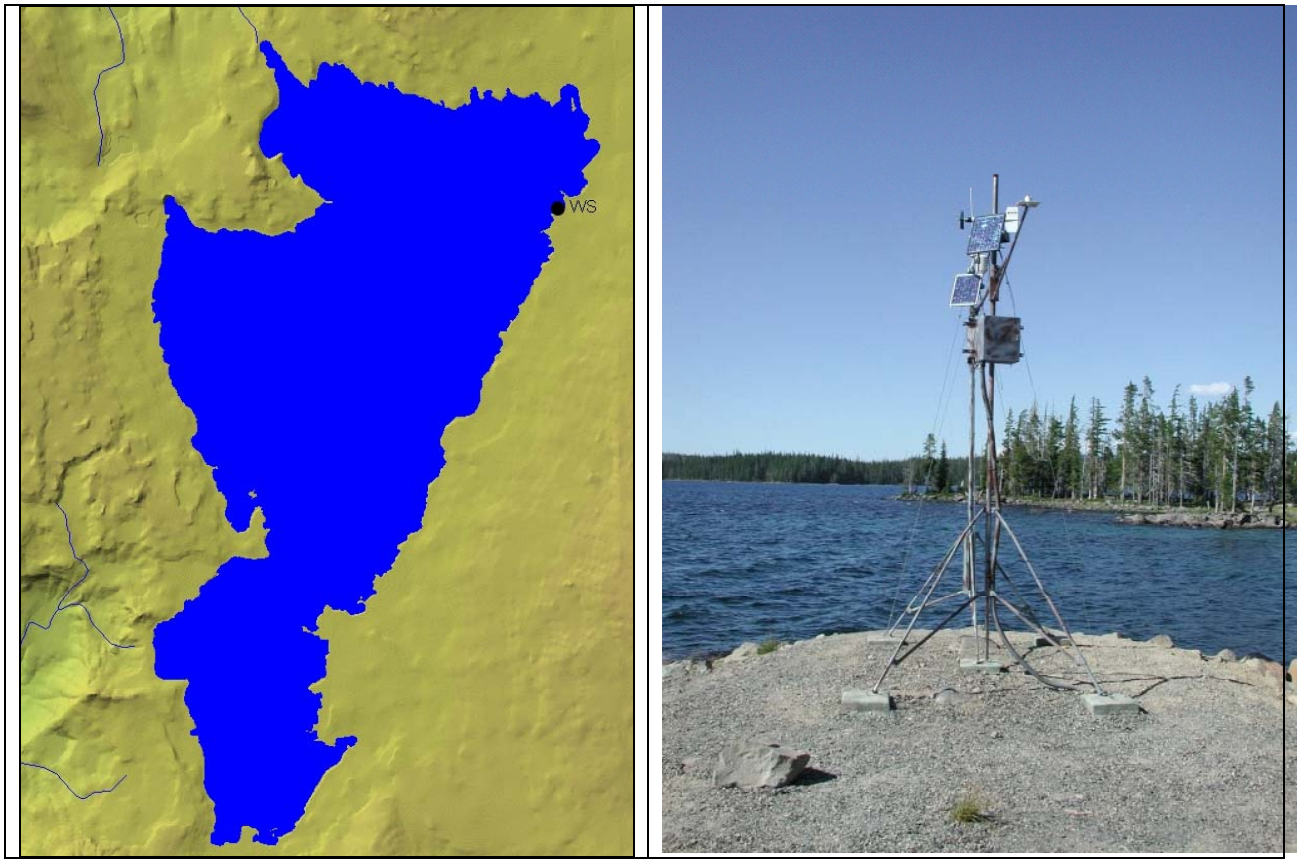

Figure 5.2-7. Waldo Lake meteorological monitoring site.

The air temperature data recorded at the Waldo Lake meteorological monitoring site (WS) and used in the model are shown in Figure 5.2-8. The figure shows seasonal trends and diurnal fluctuations in temperature. Dew point temperature data were not recorded at the lake so it was calculated using the air temperature and relative humidity with an equation from Singh (1992):

$$RH = \left[\frac{112 - 0.1T_a + T_d}{112 + 0.9T_a} \right]^8$$

where T_a and is the air temperature, RH is the relative humidity and T_d is the dew point temperature.

Figure 5.2-9 shows the time series of the calculated dew point temperatures used in the model. Figure 5.2-10 shows the wind speed recorded at the lake and indicates there is a decrease in wind at the lake in summer between June and August. In addition to the wind speed, the wind direction was recorded hourly. Figure 5.2-11 shows the wind direction data which indicates the predominant wind direction is from either east or west with the exception of a large wind frequency in the southwest (220 to 225 degrees). The wind direction data was corrected by 87 degrees to align North with zero degrees

azimuth (A. Johnson, pers. comm.). Solar radiation data recorded at the lake are shown in Figure 5.2-12 and indicate the typical seasonal pattern in radiation. The figure also includes several outlier radiation measurements which may indicate spurious readings. Although the readings may not be accurate they were included in the model because there were a limited number of instances and there was not enough information to justify eliminating them.

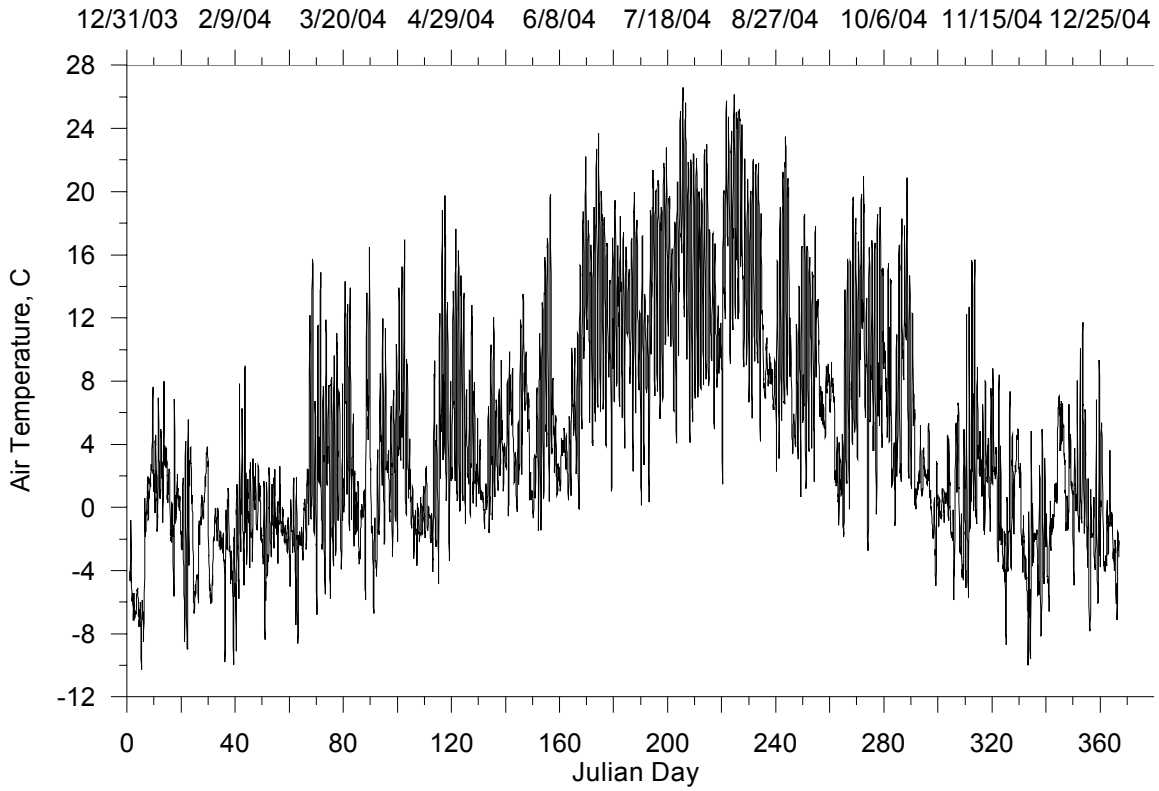

Figure 5.2-8. Air temperature at Waldo Lake.

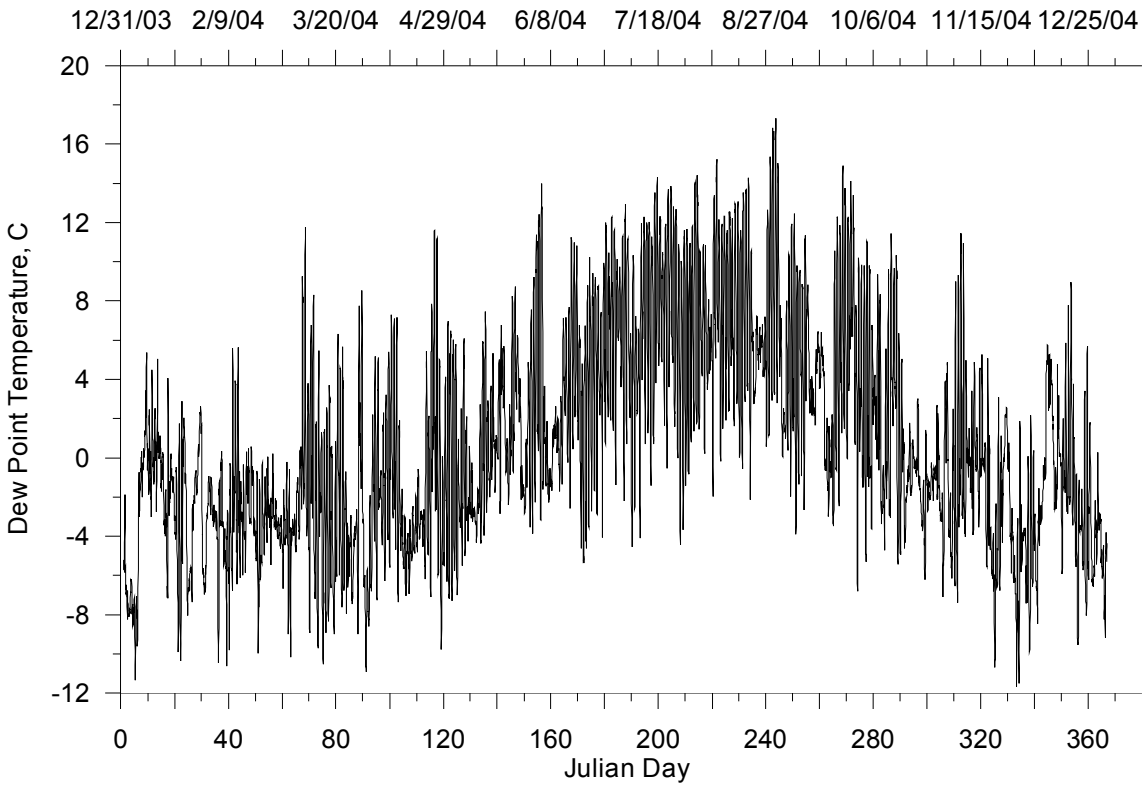

Figure 5.2-9. Dew point temperature at Waldo Lake.

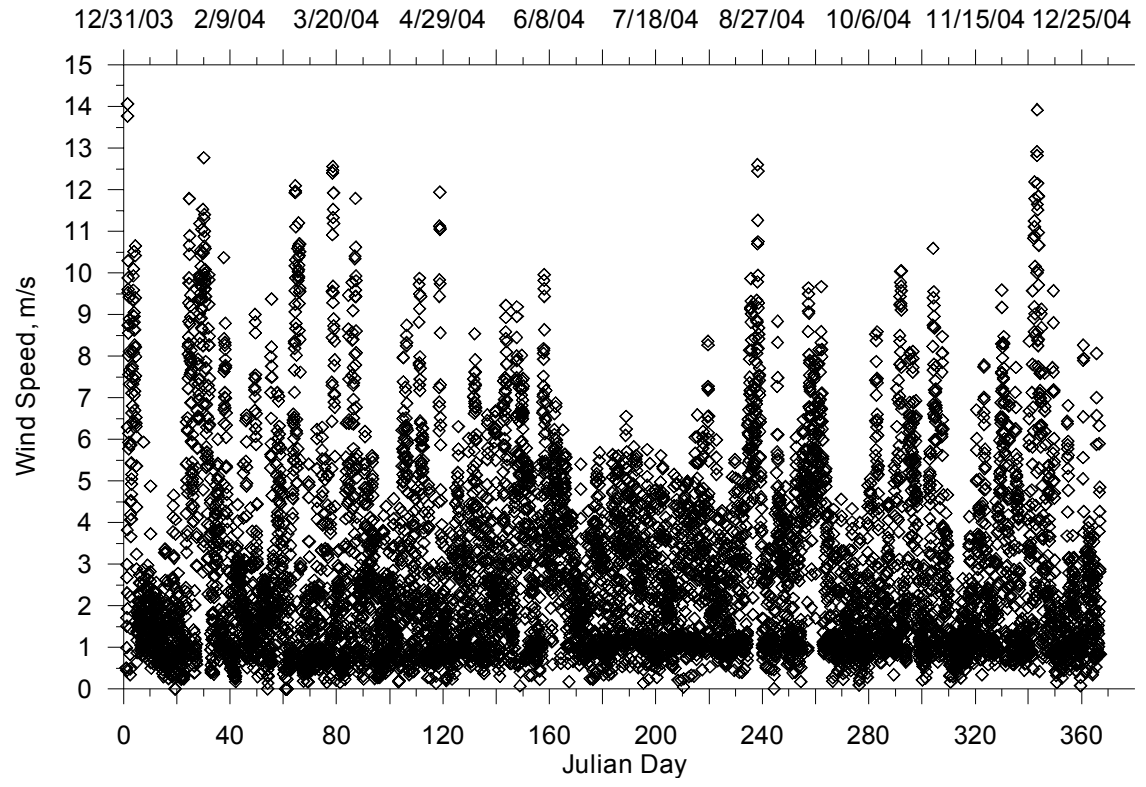

Figure 5.2-10. Wind speed at Waldo Lake.

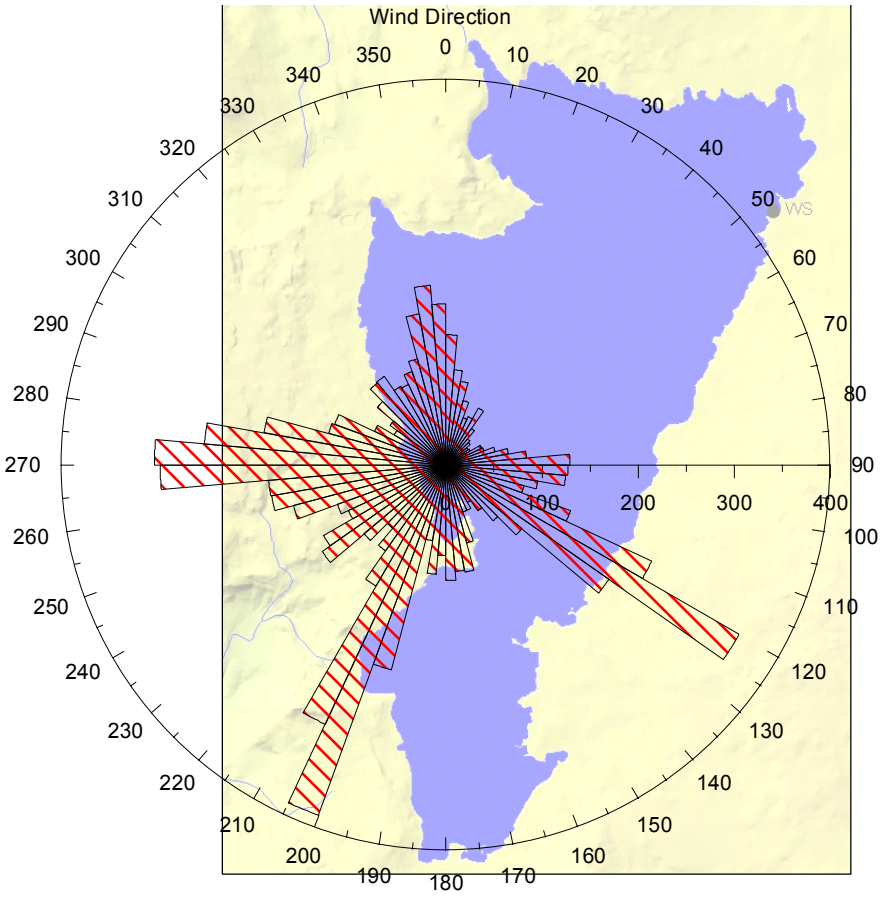

Figure 5.2-11. Wind direction at Waldo Lake.

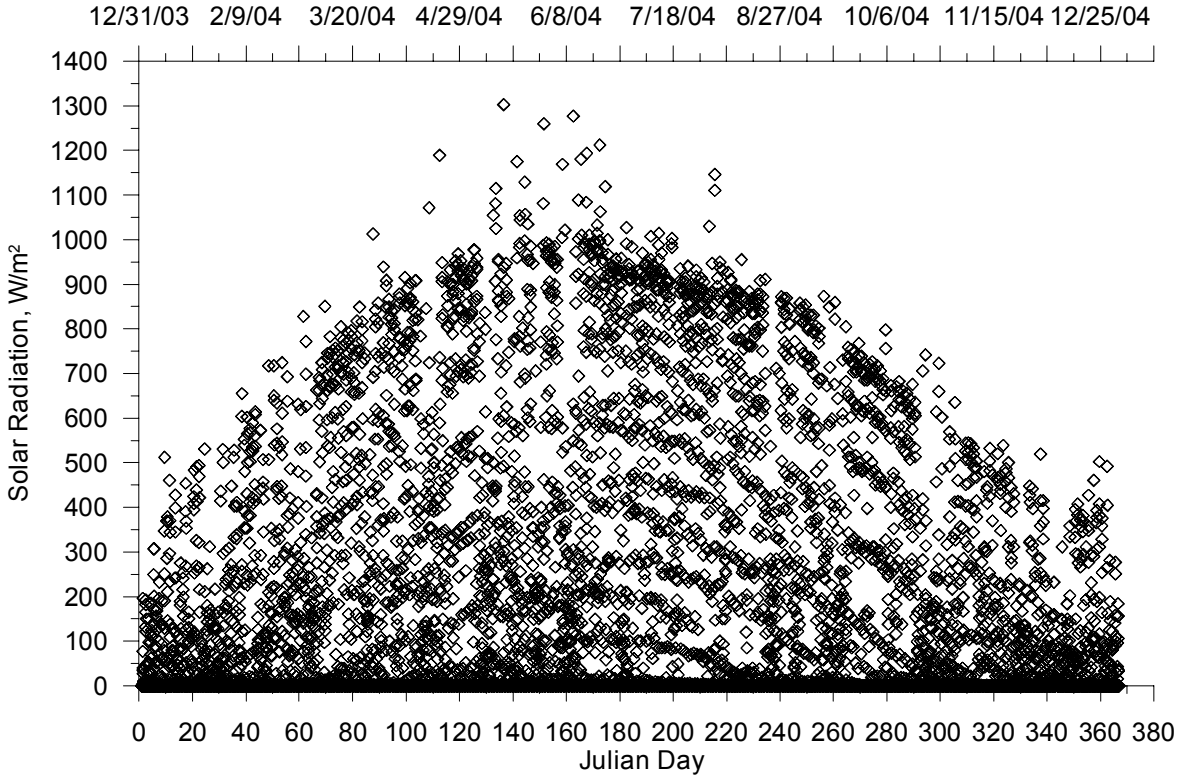

Figure 5.2-12. Solar radiation recorded at Waldo Lake.

Precipitation measurements were included in the meteorological monitoring at Waldo Lake. However, the instrumentation was found not to be working properly, therefore no direct precipitation data were available. As a result several sites were compared in the vicinity of Waldo Lake to determine if there was another data set which could be used in the model. Table 5.2-2 lists the precipitation sites examined and Figure 5.2-13 shows a map of the Waldo Lake watershed area where the precipitation sites are located with the exception of the Eugene/Mahlon Sweet airport.

Table 5.2-2. Precipitation monitoring sites reviewed.

Site ID	Site Name	Monitoring Program/Agency
350049	Rail Road Overpass	SNOTEL/NRCS
350031	Irish Taylor	SNOTEL/NRCS
350011	Cascade Summit	SNOTEL/NRCS
350054	Salt Creek Falls	SNOTEL/NRCS
Fields	Fields, near McCredie Springs, OR	RAWS/USFS
Eugene	Eugene WSO airport Mahlon Sweet	METAR/NWS

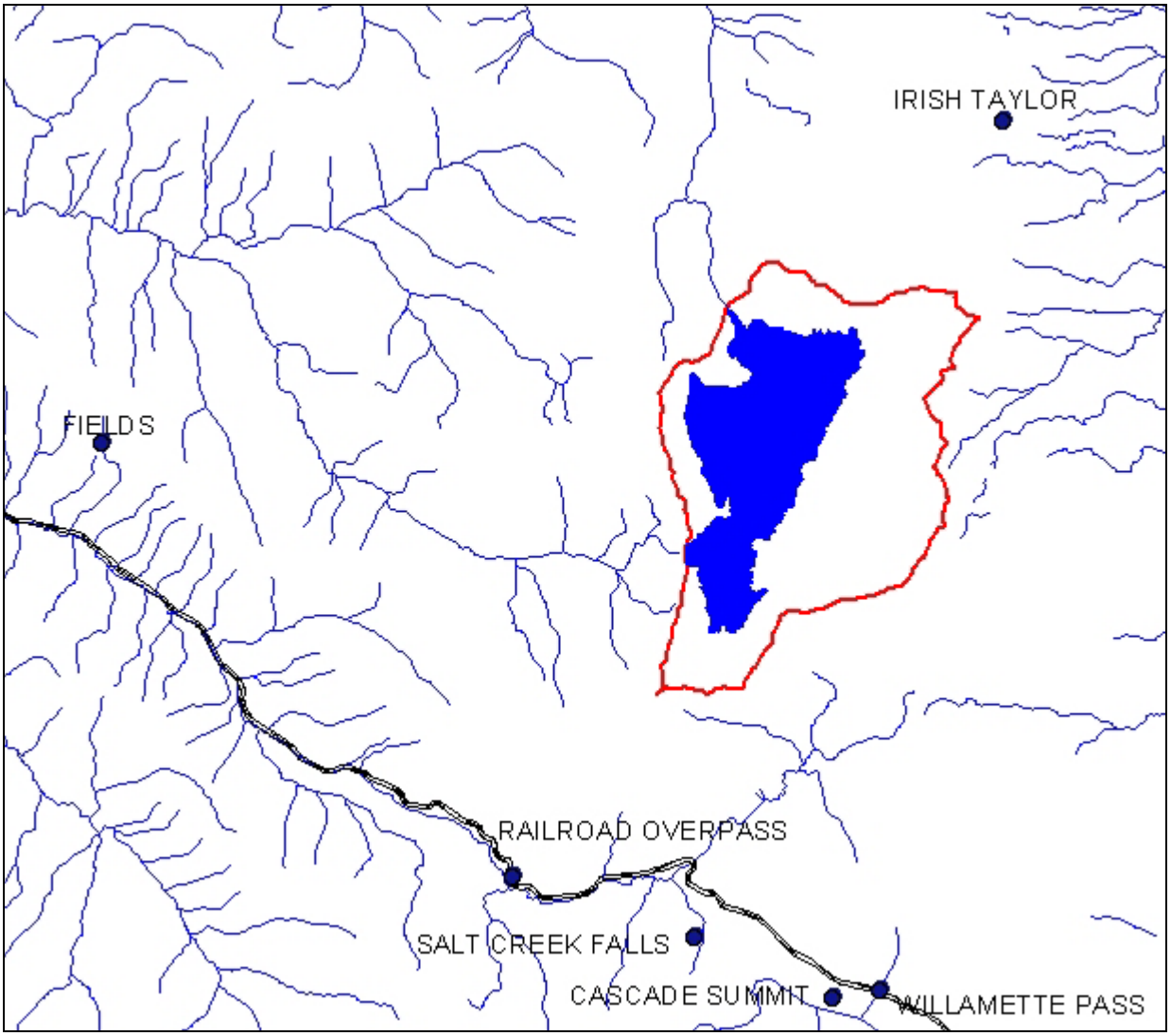

Figure 5.2-13. Precipitation monitoring sites near Waldo Lake.

Figure 5.2-14 and Figure 5.2-15 show time series of the precipitation data at each of the monitoring sites. The data were recorded on an hourly basis and were presented as incremental precipitation in inches/hr. The figures show the Fields and Eugene sites had less precipitation than the SNOTEL monitoring sites. The two figures also show the SNOTEL sites record a lot of small values, 0.01 in/hr, which correspond to the minimum detection limit for the instrumentation. The data from theses SNOTEL sites appear to have a lot of minimum detects when no rain is detected at the nearby Fields site. These minimum detection values may be over counting the precipitation received in the area. There are many uncertainties related to precipitation measurements that include: areal variability, altitude variability, and instrumentation error. The model therefore used the precipitation data recorded the Eugene airport which had a more reliable data record and was similar to the Fields site near Waldo Lake. Uncertainties related to the precipitation data will be accounted for in the hydrodynamics calibration.

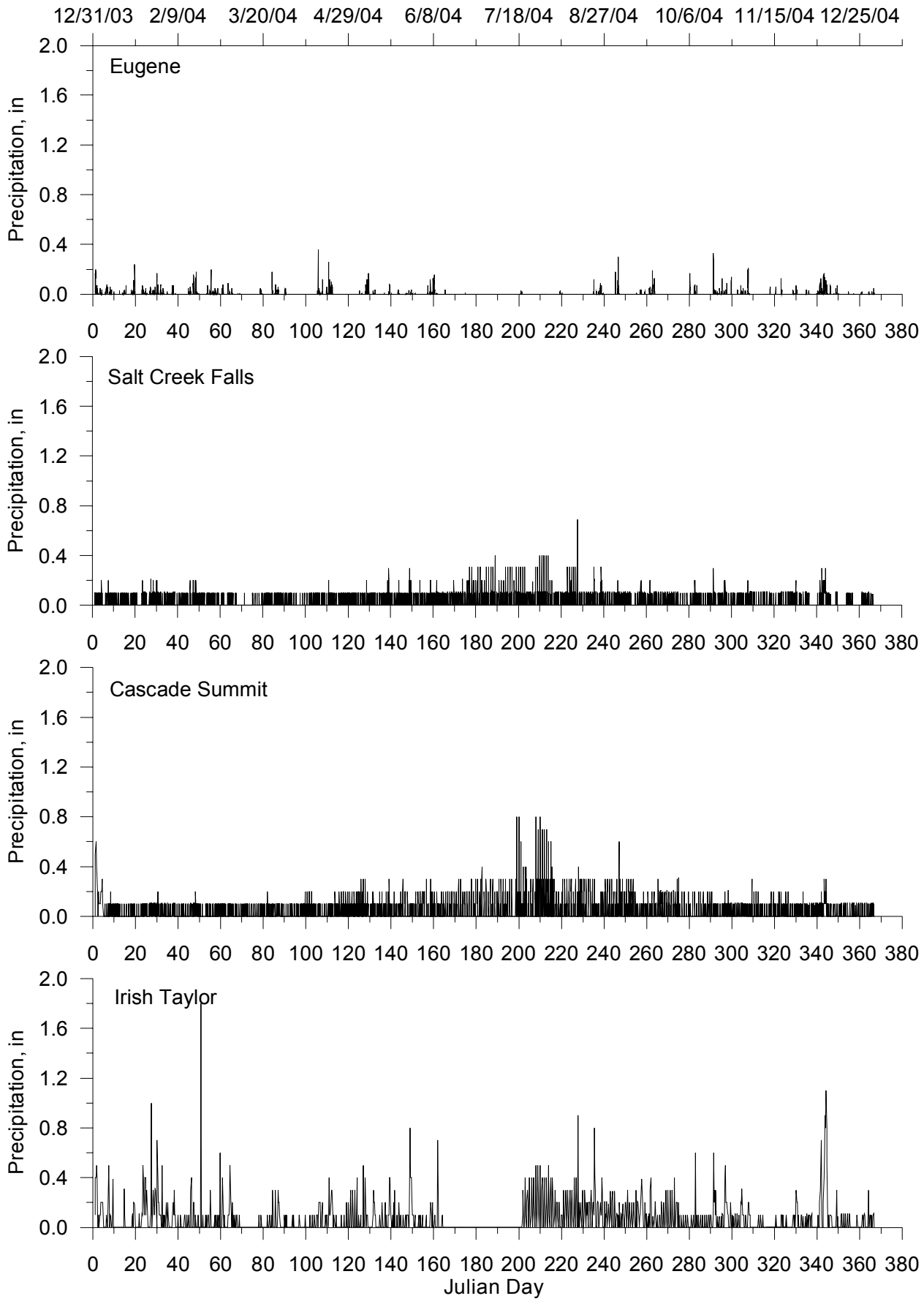

Figure 5.2-14. Precipitation recorded at several sites near Waldo Lake and in the Willamette valley.

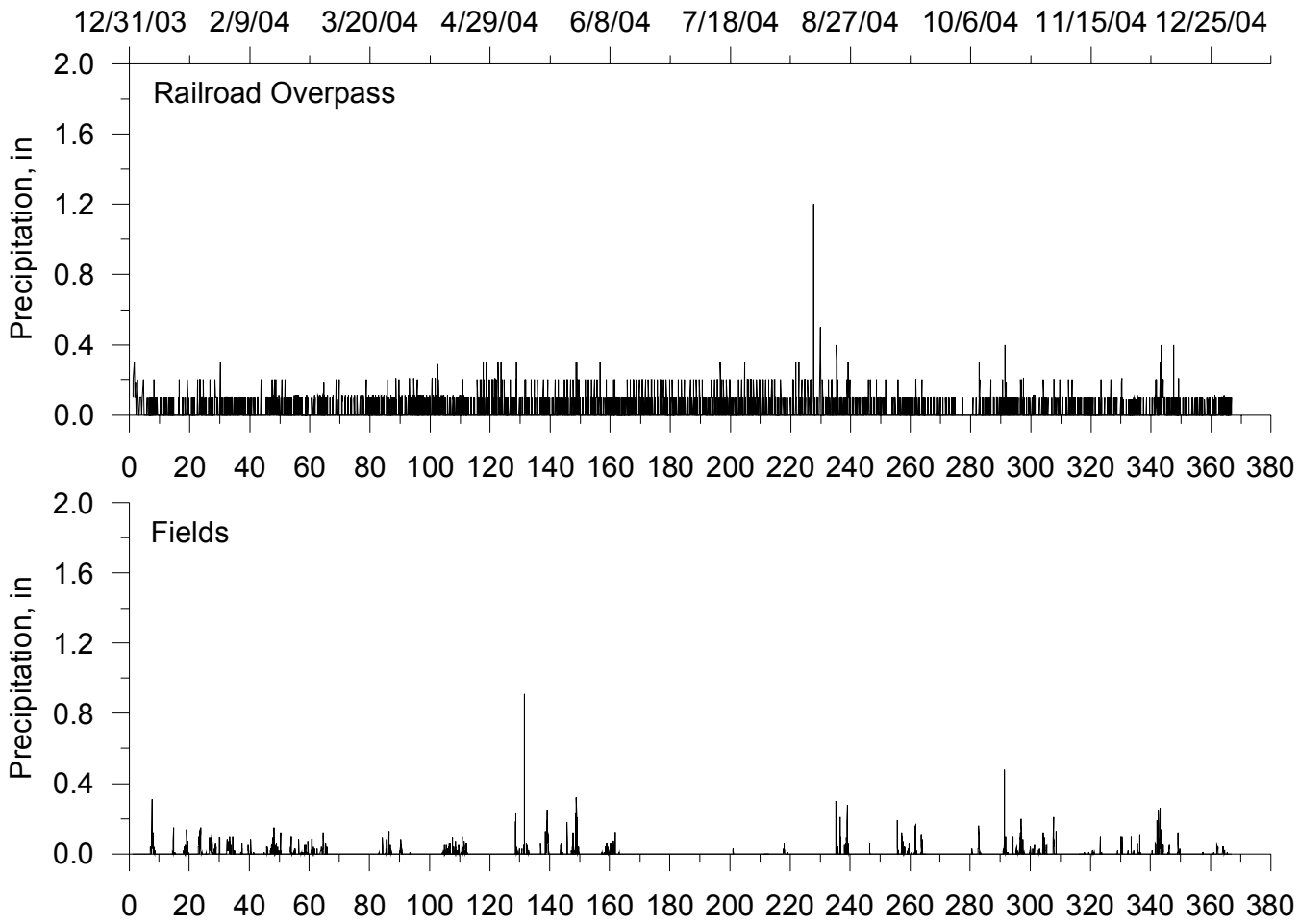

Figure 5.2-15. Precipitation recorded at Railroad Overpass and Fields monitoring sites near Waldo Lake.

The precipitation data from Eugene which was used in the Waldo Lake model are plotted in Figure 5.2-16. In addition to providing the precipitation inflow to the lake, precipitation temperatures needed to be specified. The temperature for the precipitation was assumed to be similar to the air temperature at Waldo Lake so the air temperature at Waldo Lake was used with the exception of temperatures below 0.10 ^{o}C, which were set to 0.10 ^{o}C. Figure 5.2-17 shows the time series of the modified temperature data used to characterize the precipitation inflow temperature to the model.

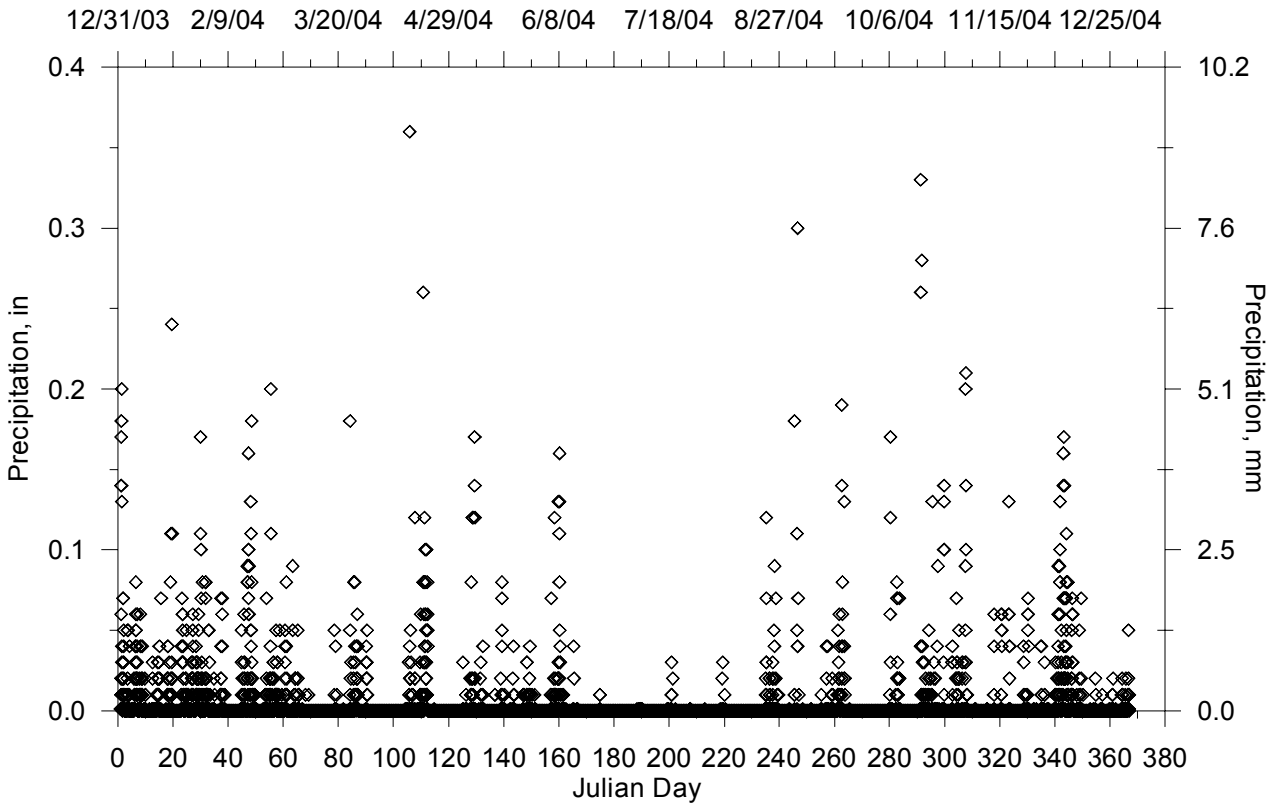

Figure 5.2-16. Precipitation data from Eugene, Oregon.

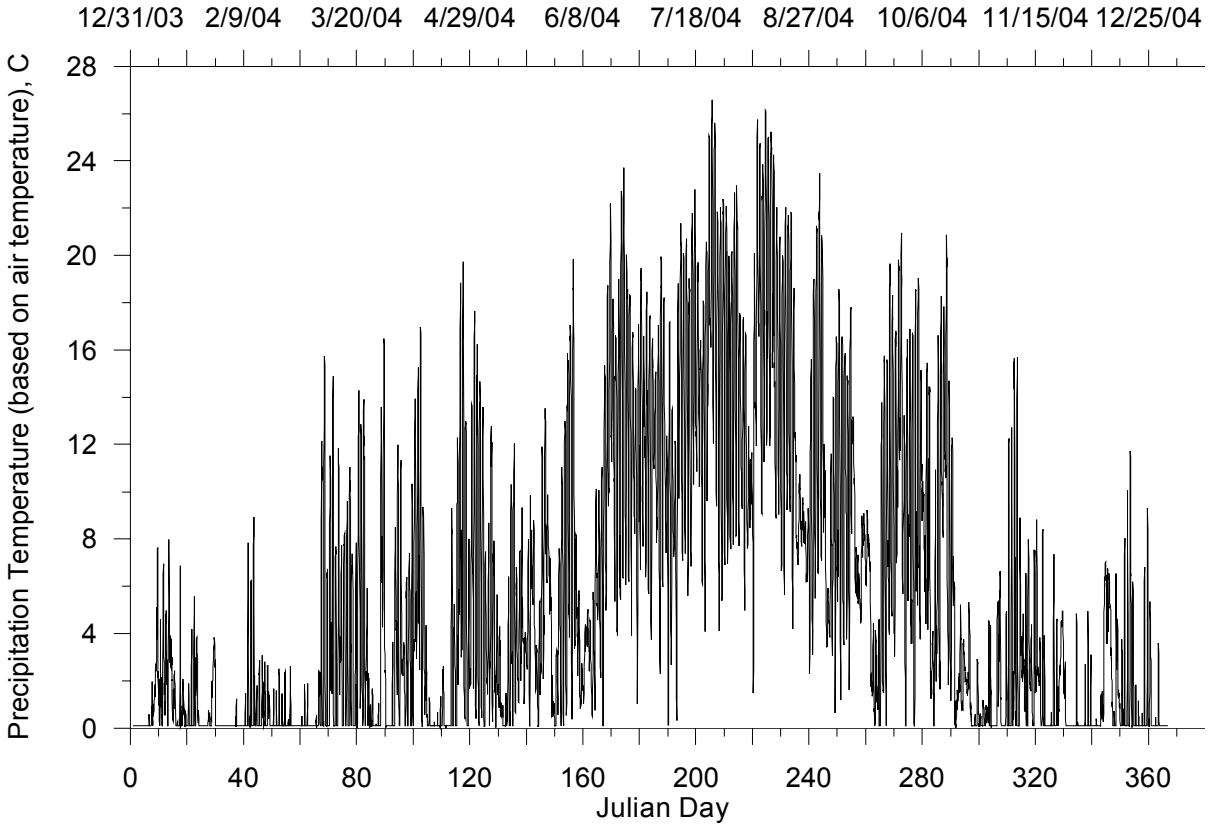

Figure 5.2-17. Precipitation temperature, C (based on air temperature at Waldo Lake).

Boundary Conditions

There are no inflows to Waldo Lake and there is one known outflow from the lake which forms the headwaters of the North Fork of the Middle Fork of the Willamette River. As a result the boundary conditions for the model are characterizing the lake outflow and the lake water level for use in model calibration.

Water Level

The water level monitoring gage station was historically located near the lake outlet and maintained by the USGS. More recently the USFS installed a water level monitoring gage at the Islet Campground. In addition to the water level gage which takes measurements every 30 minutes, there is a staff gage at this location. Both gages and the bathymetric survey were all tied to the same datum elevation at the lake. The datum elevation was measured by Donn Rowe (USFS) using a global position system (GPS) unit as 1650.88 m (5416.26 ft) with an accuracy of +/- 0.58 m (1.9 feet).

Figure 5.2-18 shows lake water level measurements from 2000 to early 2005 based on the "grab" measurements from the staff gage and the continuous monitoring gage. The figure also indicates two time periods when (Al Johnson, pers. comm.) the data were erroneous based on large decreases in water level over a short periods of time. The erroneous data were removed and the data gaps were filled in by linearly interpolating the water level. Figure 5.2-19 shows the water level stage data converted to water level elevation with the data gaps filled. The water level elevation in the lake was assumed to be constant before April 1. Figure 5.2-20 shows the water level elevation for Waldo Lake in 2004 which was used for comparing with model results.

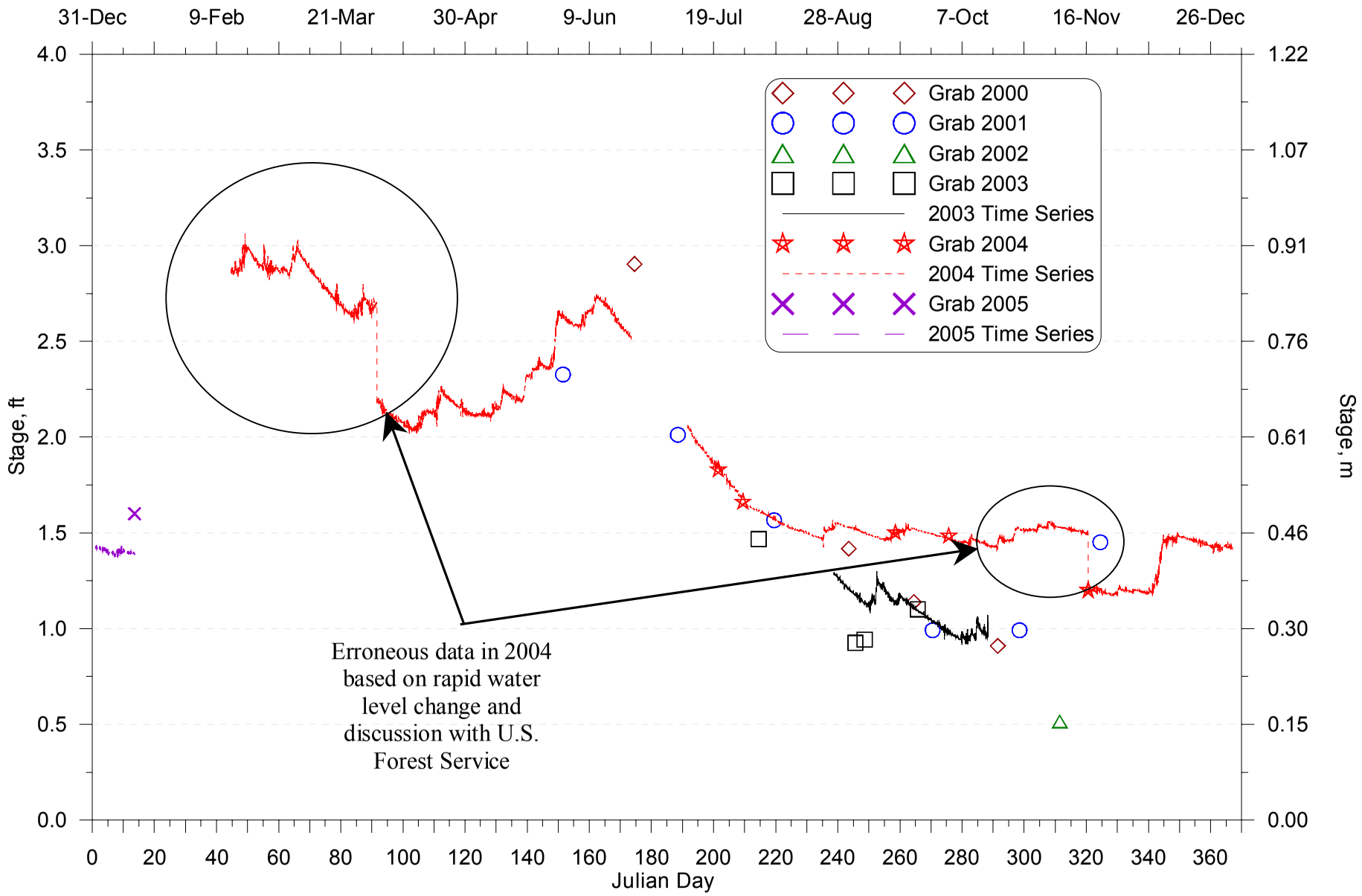

Figure 5.2-18. Recent water level measurements recorded at Waldo Lake with some erroneous data identified in 2004.

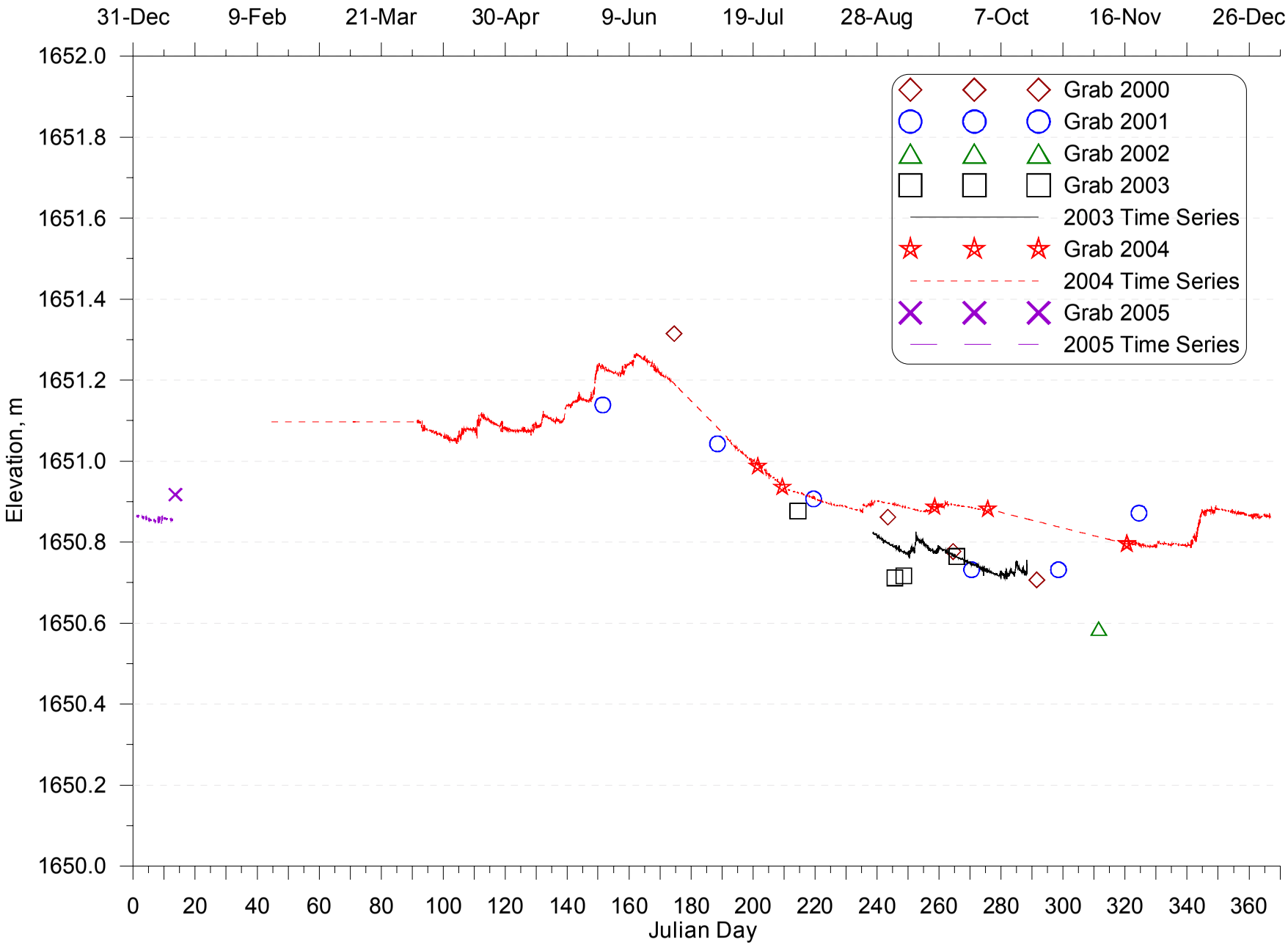

Figure 5.2-19. Recent water level measurements recorded at Waldo Lake with erroneous data removed in 2004 and interpolated.

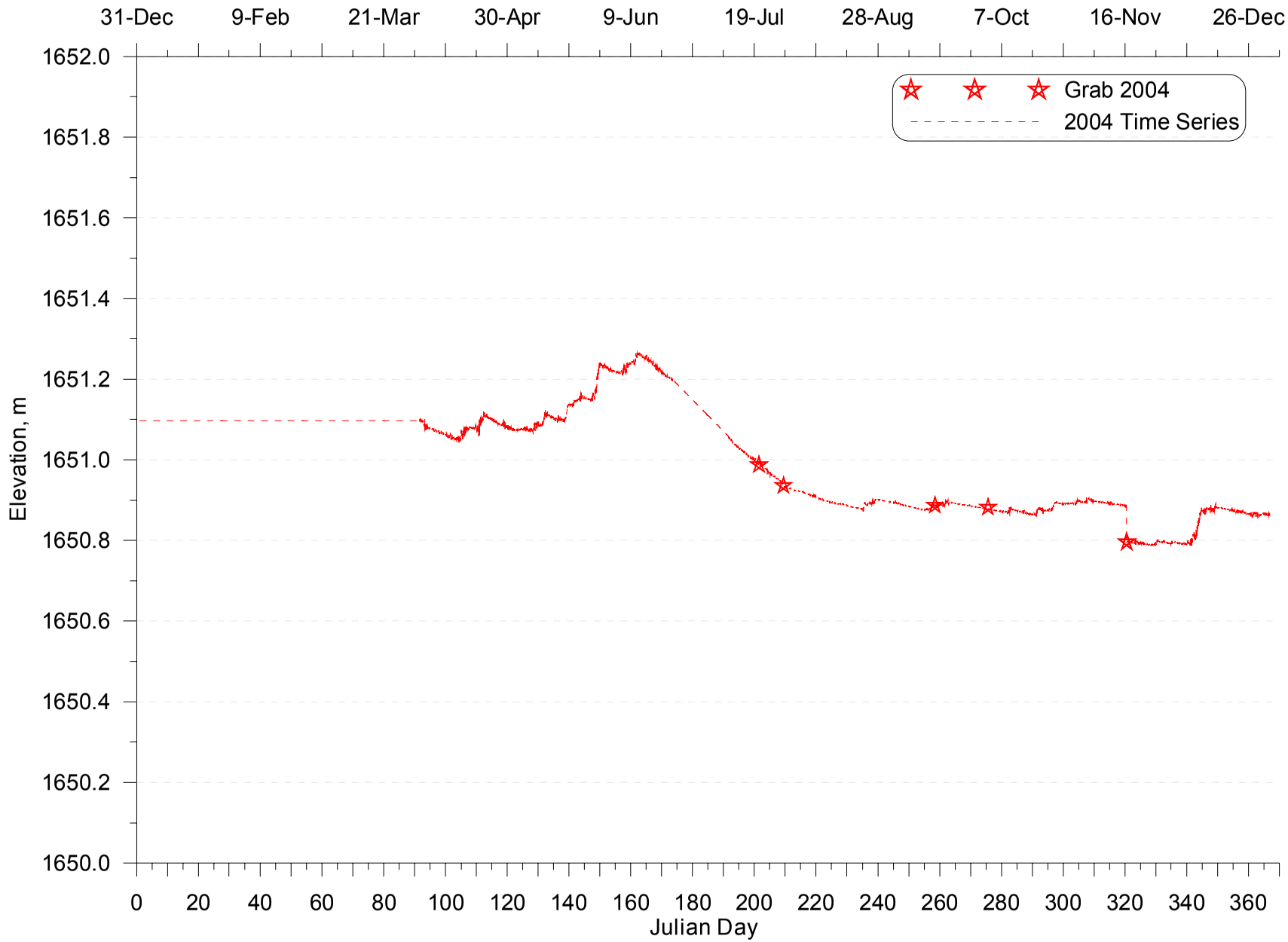

Figure 5.2-20. Waldo Lake water level in 2004 with data gaps interpolated.

Waldo Lake Outflow

The USGS had a stage and outflow gage station at the outlet of Waldo Lake from 1969 to 1984. The outlet structure modifications are still in place so the USFS installed equipment to monitor the stage and outflow from the lake using the historical stage-flow rating curve developed by the USGS. The instrumentation was in place for 2004 but there were problems with the equipment and no reliable outflow data were obtained.

Figure 5.2-21 shows map of the area near Waldo Lake with several USGS gage stations downstream of the lake. These gage stations were reviewed to determine if they could be used to correlate the historical daily outflows from Waldo Lake with gage station flows with more complete flow records, including 2004. The gage stations downstream of the Waldo Lake with the most complete flow records were found to be influenced by dam operation on the Middle Fork of the Willamette River. The other gage stations were found to have flow data up to 1994 only.

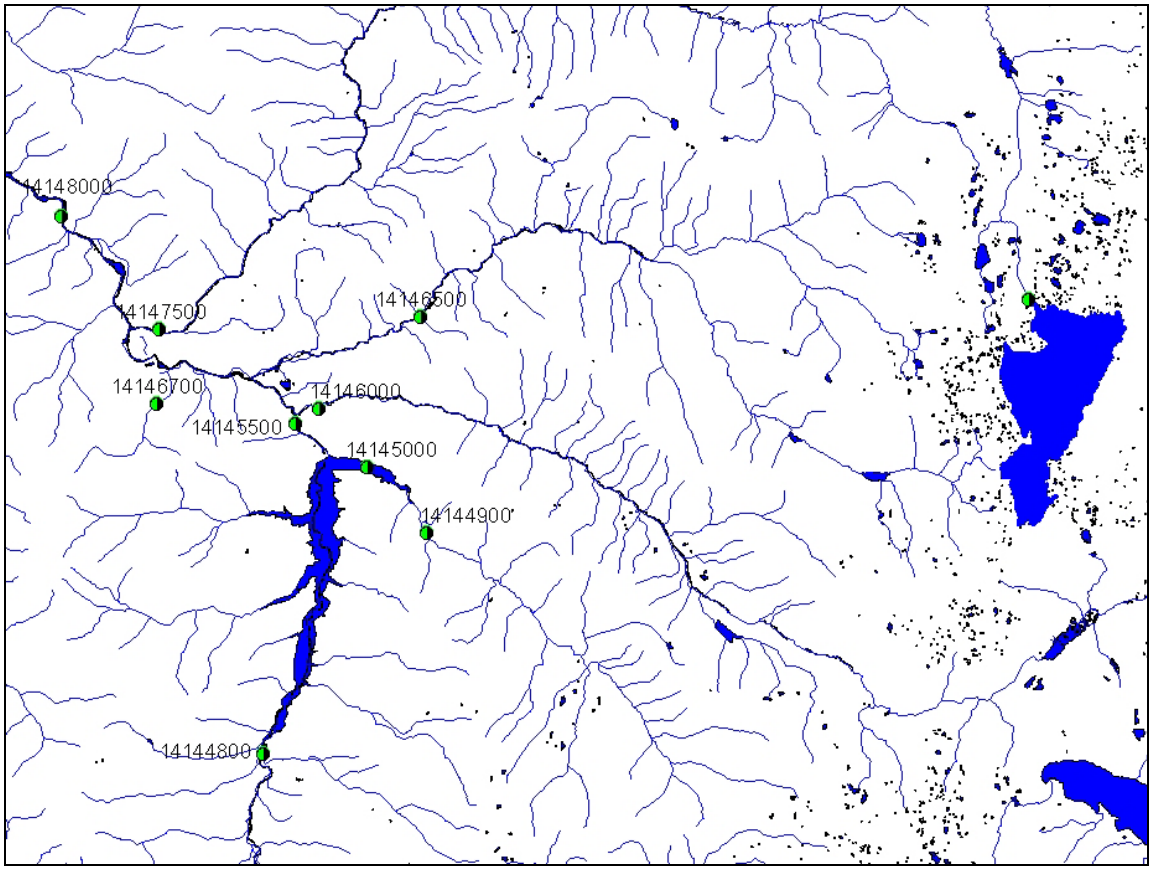

Figure 5.2-21. USGS gage station in the vicinity of Waldo Lake.

In order to characterize the outflow from the lake, an attempt was made to try to relate the historical outflow stage-flow rating curve from the USGS to the lake water level monitored by the US Forest

Service. There were several sets of data which were used to estimate the lake outflow: the lake bathymetry developed by the CLR (Sytsma et al. 2004) adjusted using the GPS survey of the elevation datum at the Islet Campground, the historical lake stage and elevation data from the USGS annual Water Resources Data reports, and the lake volume-elevation and stage-outflow rating curves from the USGS.

Figure 5.2-22 compares the volume-elevation curves from two historical data sets at the USGS gage 14146950 and the bathymetry data (Sytsma et al. 2004). The historical USGS gage used to measure the lake level was on the side of the lake by the outlet and had a gage datum elevation of 5410 ft (1648.97 m) +/- 20 ft (6.1 m), which was taken from a topography map. By increasing the water surface elevations of the historical data set by 0.6 m the volume-elevation curve matches the more recent bathymetric survey results.

The adjusted water surface elevations in the historical data set were then compared with data collected more recently at the Islet Campground. Figure 5.2-23 shows continuous and grab sample water surface elevations for 2000 to 2005 and the historical data from 1969 to 1984. Based on this figure, the historical water surface elevations were further adjusted to more closely match the recent data. The average of the water surface elevations in 2003 and 2004 after August 18th of each year were calculated and compared to the average water surface elevation of the historical data after August 18th. The time period after August 18th was used for comparison since it represents a period when inflows and outflows would be minimized and the water level should be more constant. Figure 5.2-24 shows the same water surface elevation data from Figure 5.2-23 and includes the summer averages for the two data sets. The figure indicates there is a difference of 0.94 m between the historical data set and the data from 2003 and 2004. The historical data have a relative amount of "noise" so an estimated adjustment of 0.94 m was made.

The USGS provided 2 stage-flow rating curves, dated from 1969 and 1988, at the lake outlet gage station (14147000). The outlet gage station used the datum elevation of 5410 ft, based on a topography map. Figure 5.2-25 shows both rating curves, which are the same, and a fitted curve based on a power function. Using the adjustments made for the volume-elevation curve and the historical stage data, the datum for the outlet gage was adjusted from 1648.97 m (5410 ft) to 1650.51 m (1650.51 = 1648.97 + 0.94 + 0.6 m). The datum elevation was then associated with a stage reading of 0.0 m at the lake outlet and used to calculate lake outflows for 2004 using the power function from Figure 5.2-25.

Historical Waldo Lake daily averaged outflow data were obtained from the USGS (gage: 14147000) from 1936 to 1984. Figure 5.2-26 shows a time series plot of the daily flows for all years with data.

The figure indicates some variability between years but all of the flows were within the range of 0.0 to 4.0 m^3/s. The average, minimum, and maximum flows for each day of the year, across all years were taken and compared with the flow estimates for 2004.

Figure 5.2-27 shows a plot of the flow estimates for 2004 (diamonds with solid line) and includes the average, minimum and maximum of the daily average flows across all year of the historical data. The figure indicates the calculated 2004 flows are higher than the historical daily maximum values. By increasing the gage station datum by 0.1 m, the flow estimates were recalculated and presented in Figure 5.2-27 (triangles with solid line). The new calculated 2004 flows fall more within the maximum and minimum flows from the historical data.

Due to all the uncertainties in using the stage-flow rating curve and water level data from 2004 the calculated flows were not used in the model. Instead the daily flows averaged over all of years of historical data were used. Figure 5.2-28 shows the daily flows averaged over all of the historical data.

The use of the averaged outflows is considered a starting point for modeling Waldo Lake. Future model development and calibration work will be refined based on improved data sets characterizing the lake level and outflows. Both data sets will critical in getting a better understanding of the hydrologic water balance for the watershed and improve the model calibration.

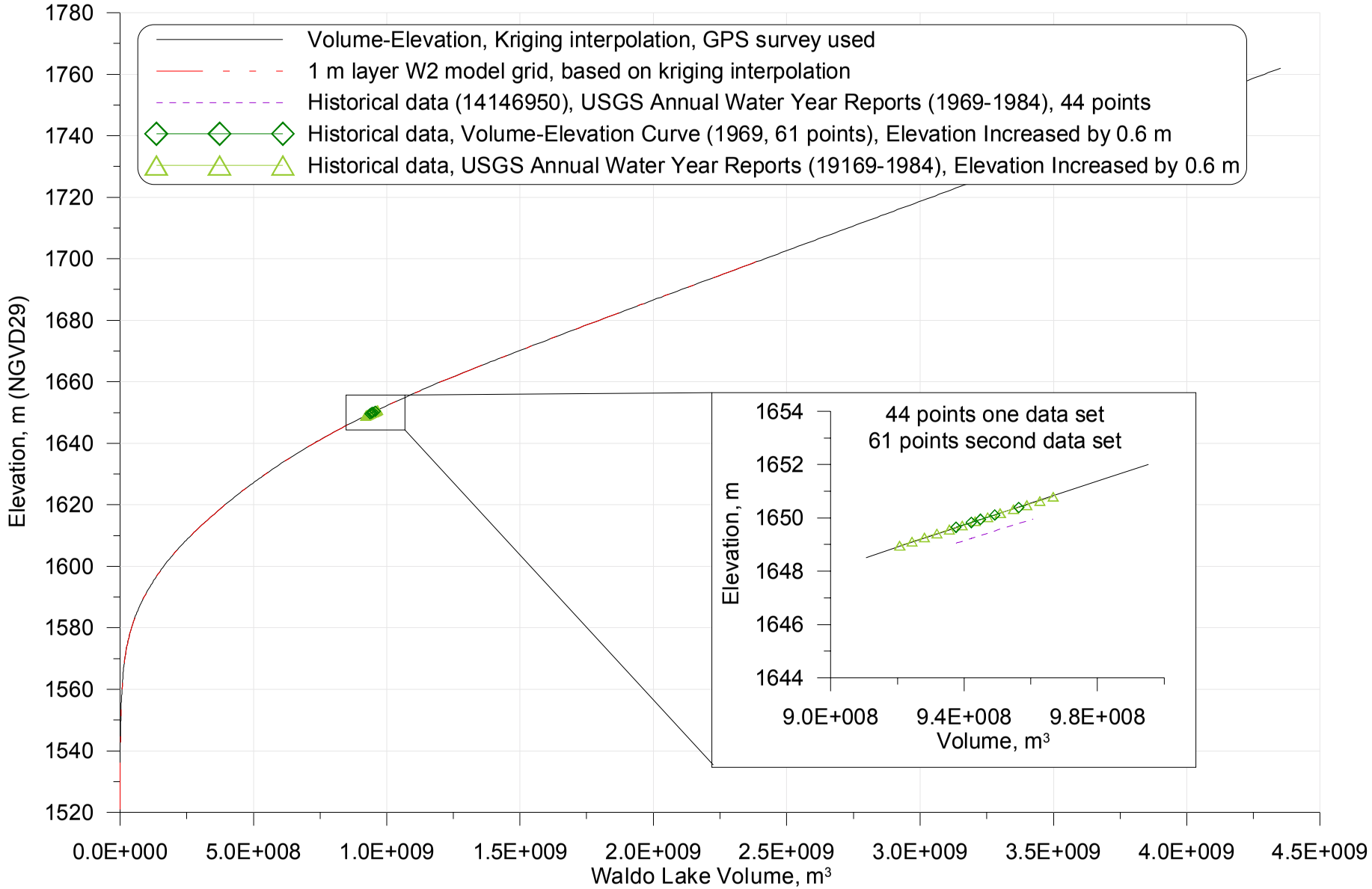

Figure 5.2-22. Recent and historical (USGS) volume - elevation rating curves for Waldo Lake.

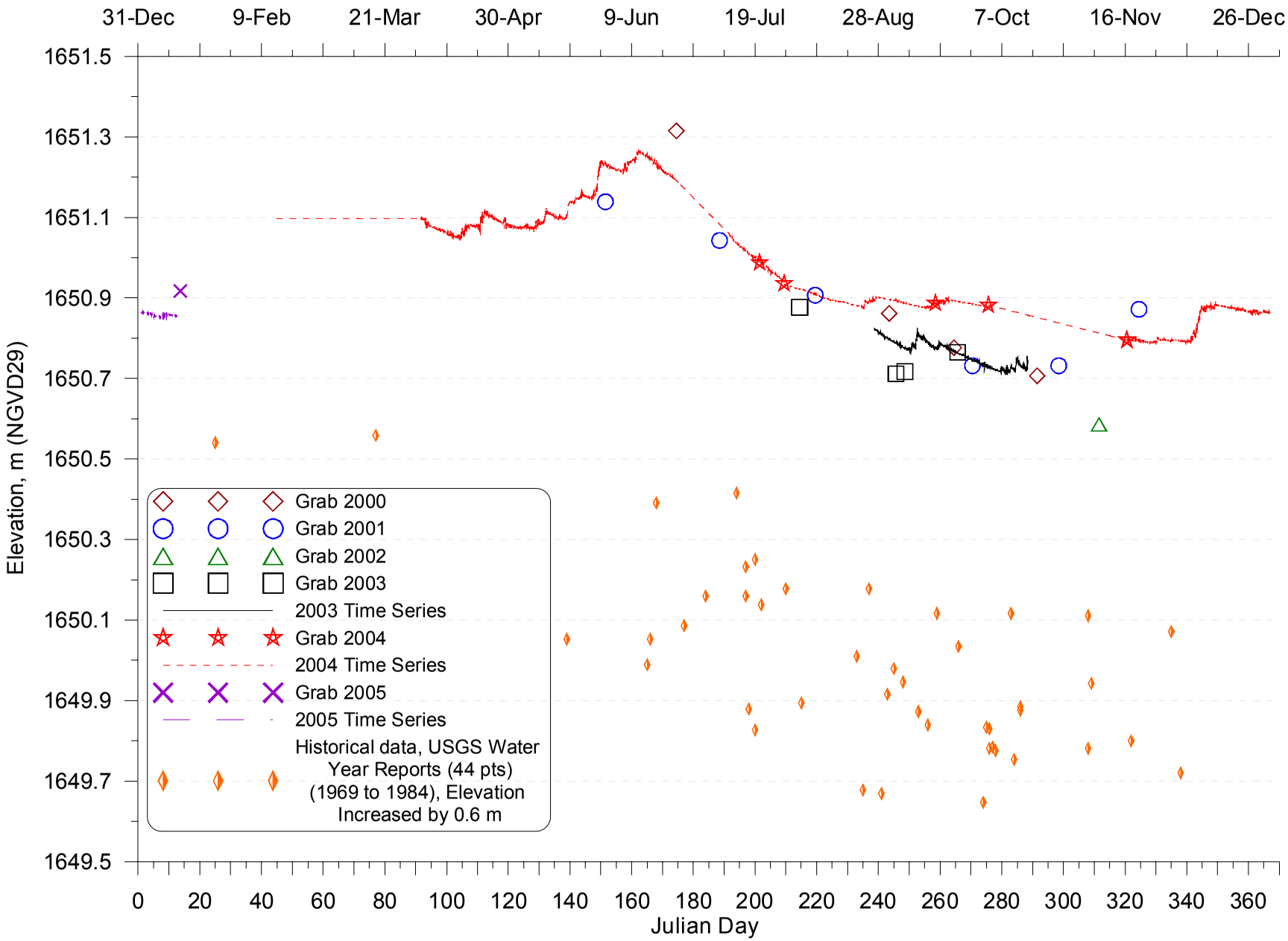

Figure 5.2-23. Recent and historical (USGS) water level elevation data at Waldo Lake.

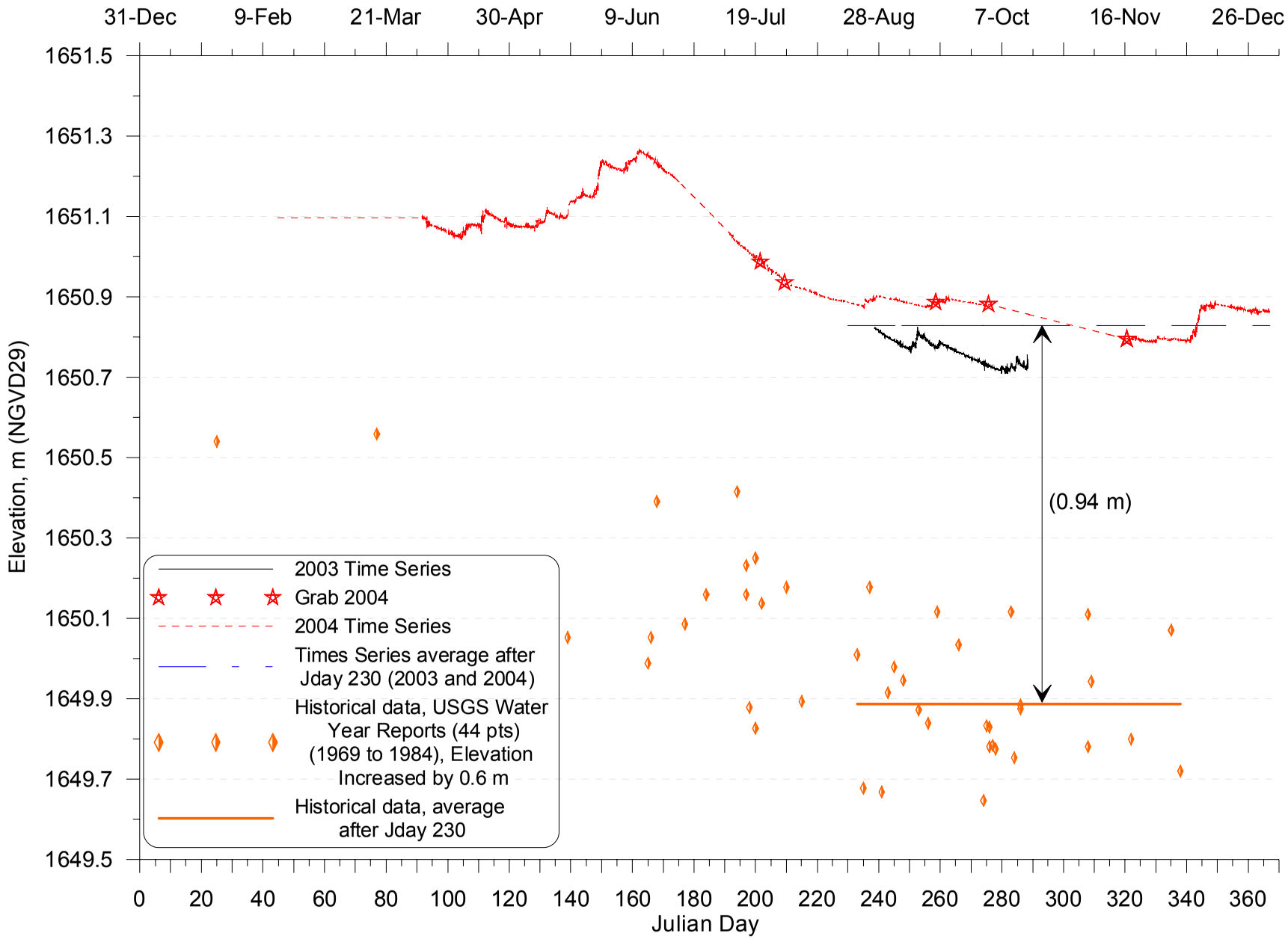

Figure 5.2-24. Difference between recent and historical (USGS) water level elevation data at Waldo Lake.

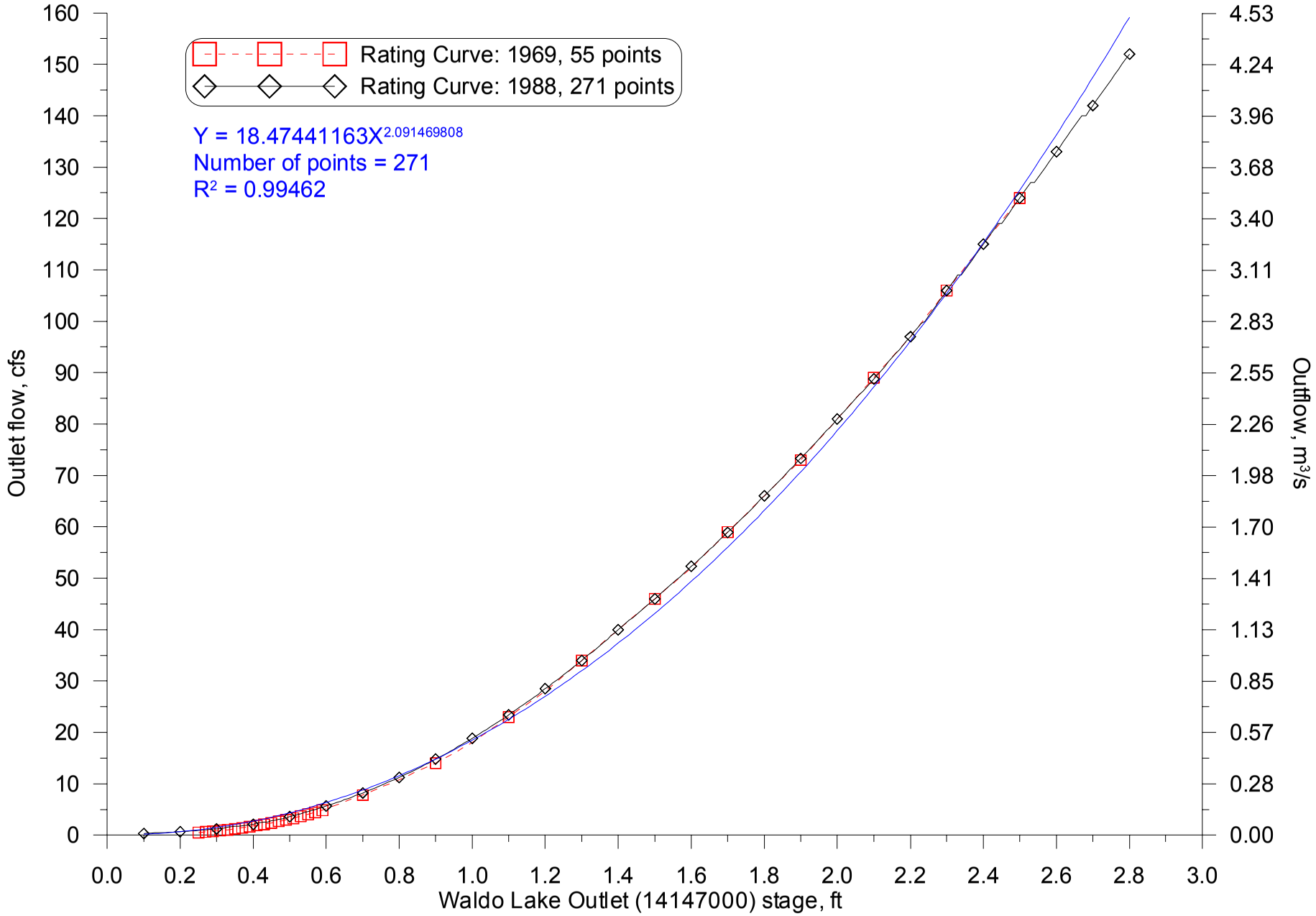

Figure 5.2-25. Waldo Lake outflow stage-flow rating curve.

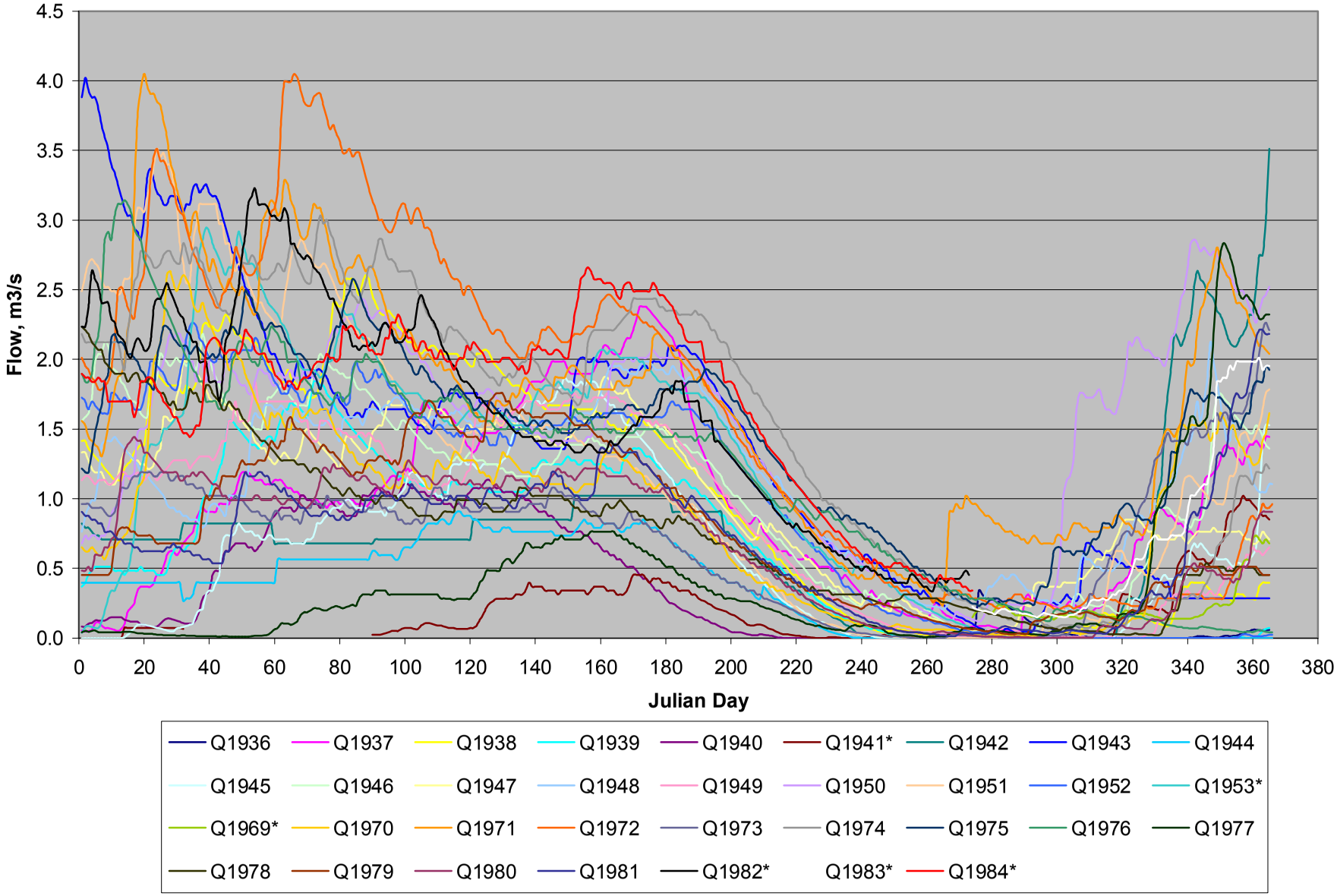

Figure 5.2-26. Historical daily average flow data (Asterisk next to year indicates incomplete data record for the year).

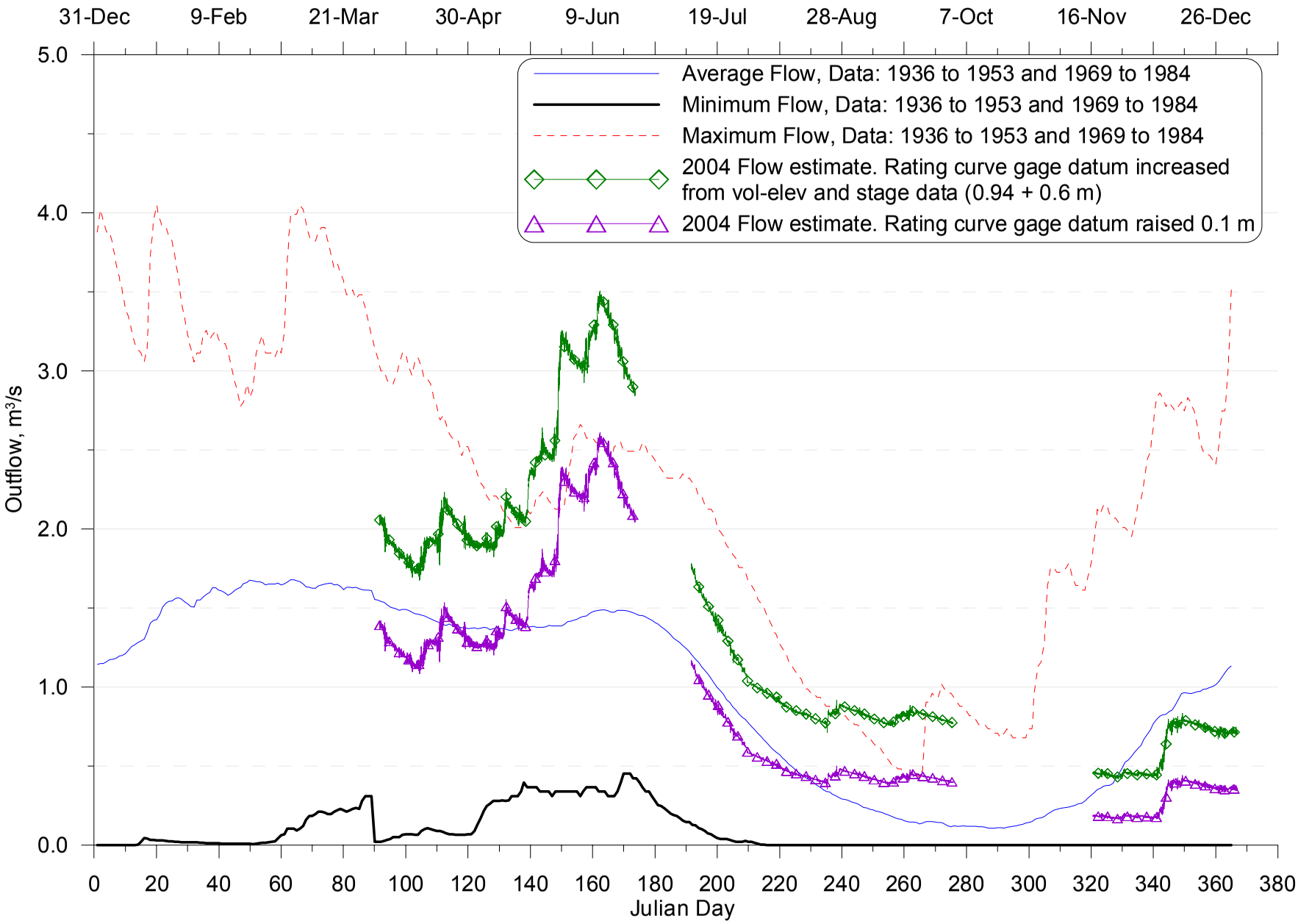

Figure 5.2-27. Corrected stage-flow rating curve results compared with historical flow statistics.

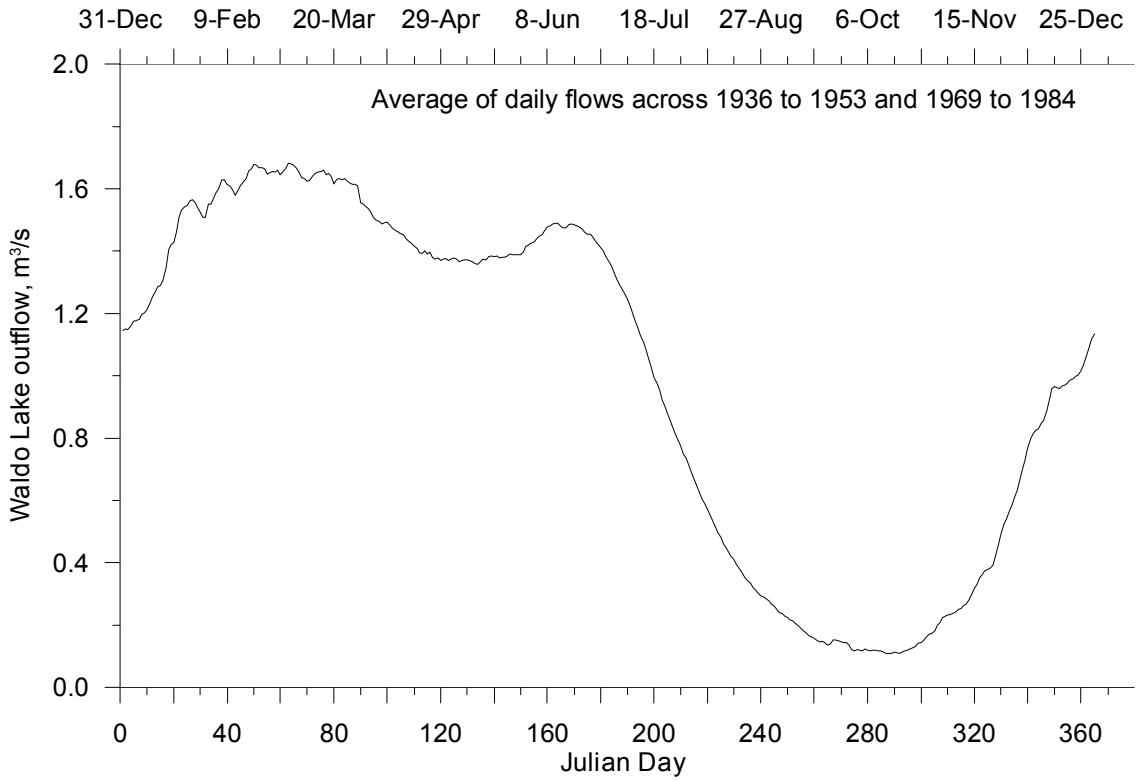

Figure 5.2-28. Waldo Lake estimated outflows for 2004, based on historical data.

5.3 Model Calibration

The model calibration process consisted of first calibrating the model for the hydrodynamics and then calibrating the model for water temperature.

Hydrodynamics

The hydrodynamics calibration consisted of running the model and comparing the water level elevation data measured at the Islet Campground with the water level predictions at segment 48 which correspond to the gage station location. The difference between the data and model results were then used with a utility program to conduct a water balance and generate a time series of inflows and outflows to improve the model-data water level comparisons. The process was repeated iteratively until the model results match the data. Table 5.3-1 shows the water level elevation model-data error statistics and Figure 5.3-1 shows a time series plot comparing the model and data water level elevations in 2004.

Table 5.3-1. Water level monitoring site for calibrating the lake model hydrodynamics.

Gage Name	Model Segment	Sample size, N	Mean Error, m	Absolute ME, m	RMS Error, m
Islet Campground	48	17468	0	0.003	0.005

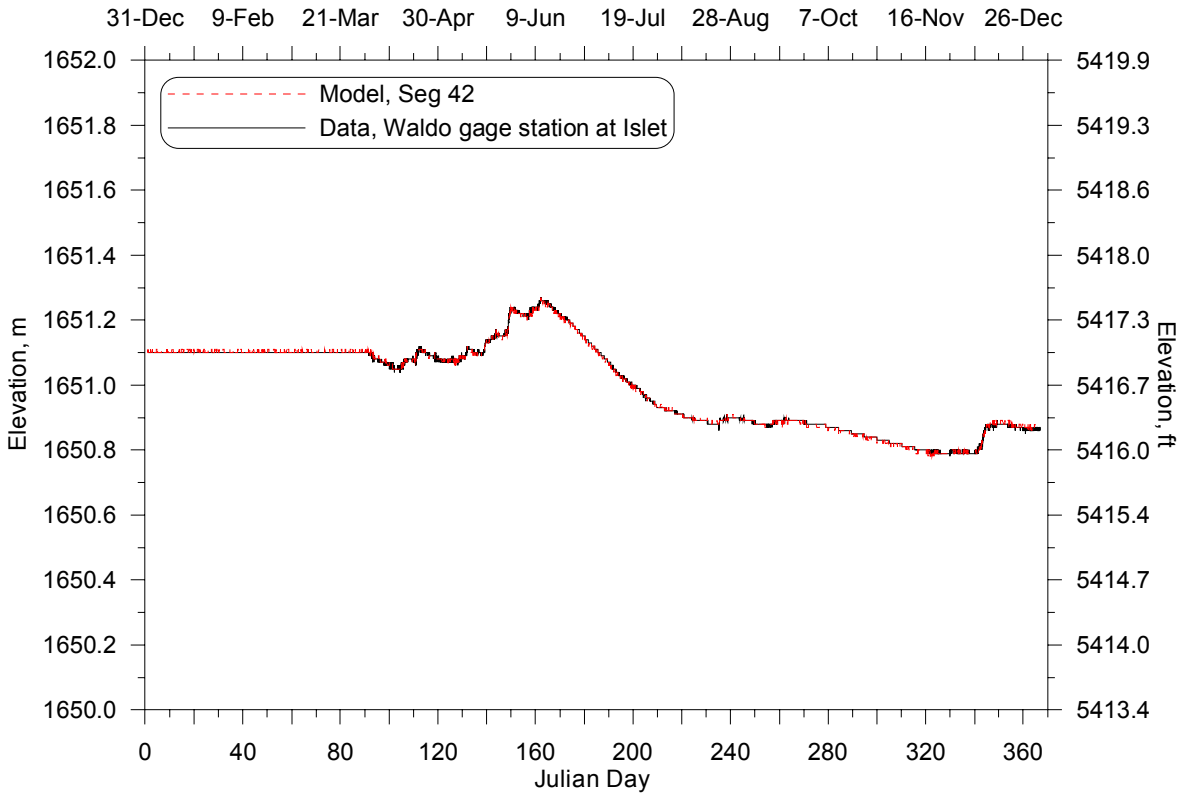

Figure 5.3-1. Model-data water level comparison for Waldo Lake, 2004 (data reflects data gaps filled by linear interpolation).

The average water balance flows used to correct the model water level predictions was -0.0001 m^3/s over the simulation period from January 1 to December 31, 2004. These water balance flows represent all of the uncertainties in the inflows and outflows to the lake such as the daily outflows averaged from the historical data, the precipitation data from outside the basin, the groundwater gains and losses and the water level data record. The model included evaporation in the water budget and volume predictions. Figure 5.3-2 shows the half-hourly water balance flows over the simulation, with some large positive and negative flows, but they are over very short periods. Water balance flows are usually distributed included in a model as a distributed tributary which distributes the water balance flows over all of the model segments in the surface layer. In order to reduce the impact of these flows on lake temperatures the water balance flows

were distributed over a depth of 45 m in one segment (Elevation range of 1520 to 1570 m at model segment 36, layers 132 to 177) at the bottom of the lake for temperature are more constant.

Since the water balance flows represent flows in and out of the lake a temperature file had to be associated with the flows and included in the model. In order to further minimize the impact of these flows on lake temperature the water balance flows temperatures were set based on the temperature data recorded at the Mid Lake site at a depth of 60 m, which corresponded to the restricted 45 m depth interval where the distributed flows were input to the model. Figure 5.3-3 shows a time series plot of the water temperature data used for the water balance flows. Data were collected until September 22, 2004. This is the date when the thermistors were deployed in the lake so temperature data after September 22, 2004 are not available until the thermistors will be retrieved during the summer of 2005. To fill in the data gap from September 22 to December 31, 2004, the temperature at December 31, 2004 was set to the water temperature on January 1, 2004 and the model linearly interpolated between the two dates.

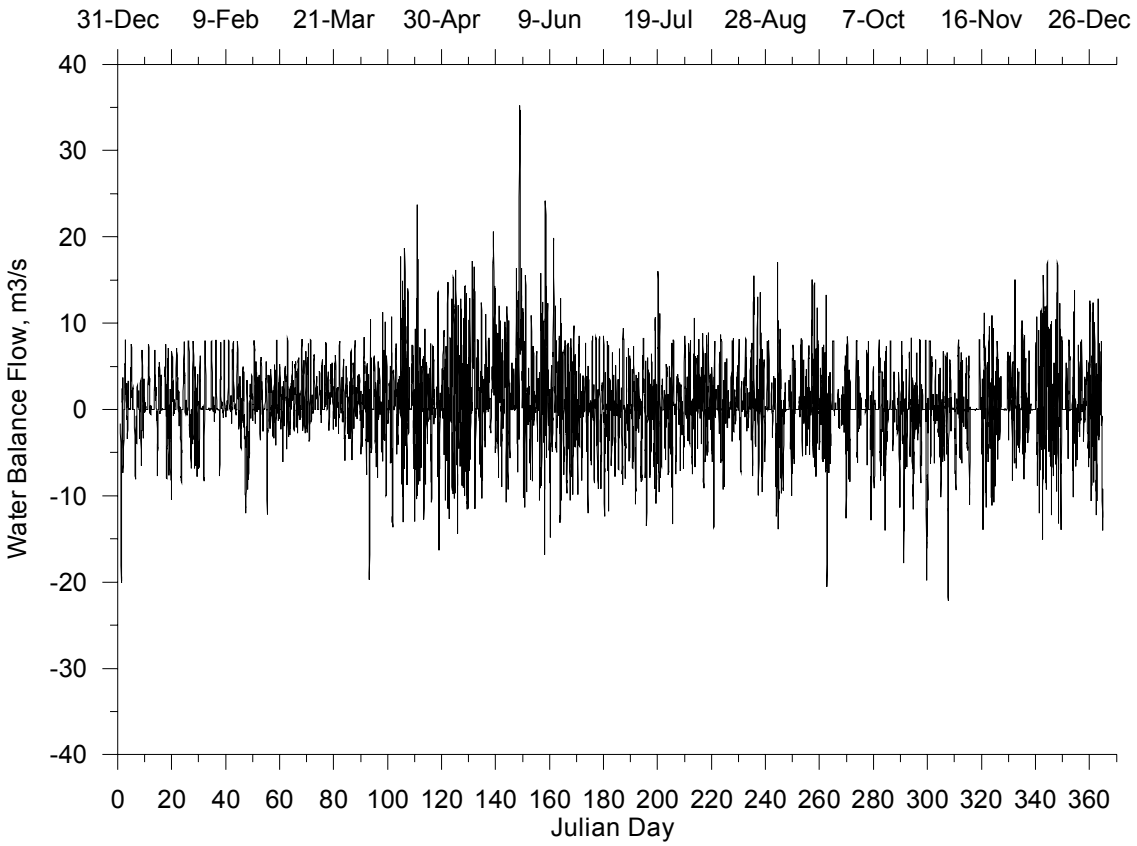

Figure 5.3-2. Waldo lake water balance flows, 2004.

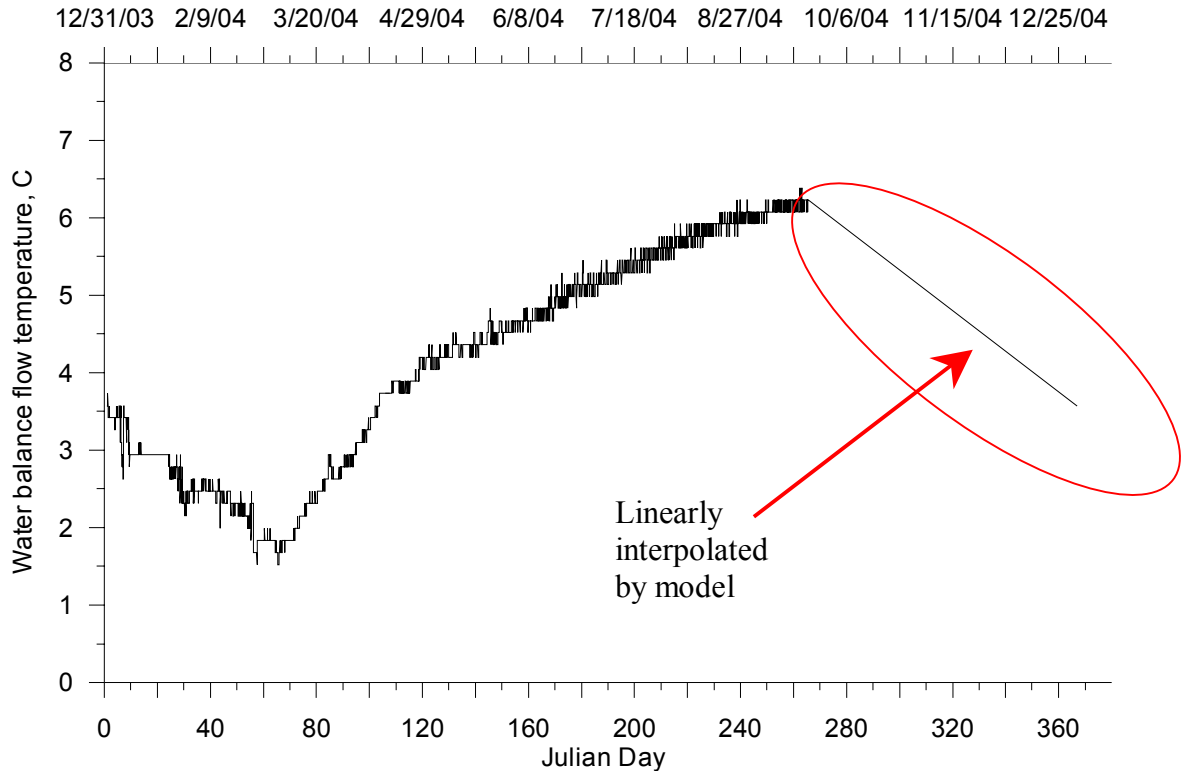

Figure 5.3-3. Waldo lake water balance flow temperature, 2004.

Water Temperature

Once the hydrodynamic calibration was done the water temperature calibration was conducted. The temperature calibration was conducted by adjusting the wind sheltering coefficient, the light extinction coefficient and the fraction of radiation lost in the water surface layer. CE-QUAL-W2 models light extinction using Bear's Law:

$$I_z = (1-\beta) I_o e^{-\eta z}$$

where I_z is the short wave radiation at depth z, I_o is incident short wave radiation on the lake surface, β is the fraction of radiation absorbed in the water surface and η is the light extinction coefficient. Light extinction and Secchi disk depth were recorded in Waldo Lake by the CLR at Portland State University in the summer of 2004 and historical data from the lake were also assessed and analyzed to identify initial calibration values for β and η.

CLR collected light extinction data using a light photometer with measurements every 5 m in depth. The measurements at a depth of 5 m were used to estimate β and the remaining data were used to calculate extinction coefficients. An average β value of 0.65 was calculated for five dates in 2004 when light measurements were taken. The historical record of Secchi disk depths at the Long Term Monitoring site were used with two different methodologies to calculate the light extinction coefficient. CLR also collected light extinction data using a spectroradiometer measuring light in 2 nm wavelength bands from 302 to 712 nm wavelengths. The data set in the wavelength range of 400 to 650 nm were used to calculate light extinction coefficients since this corresponds to PAR wavelength range. The light extinction coefficients from each of the data sources and methodologies are summarized in Figure 5.3-4. The average light extinction coefficient for the values presented in Figure 5.3-4 is 0.10 m^{-1}.

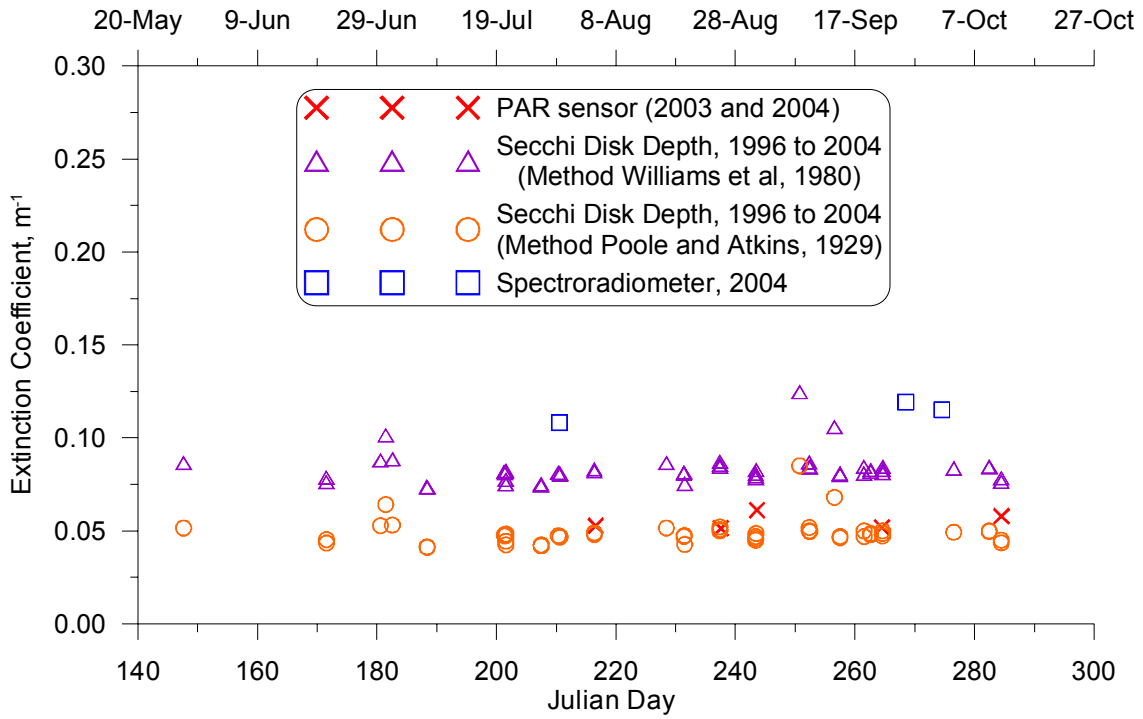

Figure 5.3-4. Light extinction coefficients at Waldo Lake.

The estimated values of the light extinction coefficient and the fraction of light lost at the surface were used as a starting point in the temperature calibration and were adjusted to improve model-data agreement. The temperature of the lake sediments was also set in the model, initially based on the annual air temperature of 4.83 ^{o}C but later changed to the annual average of the water temperature measured at the long-term monitoring site at a depth of 60 m. The difference had negligible impact on the model results but latter was more justifiable.

The wind sheltering coefficient adjusts the wind speed data input to the model to represent the effective wind on the water surface of the lake. The wind sheltering coefficient can be adjusted over time and individually for each model segment. During some time periods the wind sheltering coefficient was reduced from 1.00 to a range of 0.75 to 0.90 to reduce the amount of wind on the water surface and increase surface warming. The final calibration values for each of the four variables adjusted are summarized in Table 5.3-2. The table shows the light extinction coefficient and fraction of light at the surface were adjusted slightly from the values based on data, but both fall within the range of data collected at Waldo Lake.

Table 5.3-2. Final model calibration values for the Waldo Lake model, 2004.

Model Coefficient	Description	Calibration values
β	fraction of radiation absorbed in the water surface	0.48
η	light extinction coefficient	0.08
WSC	Wind sheltering coefficient	0.75 to 0.90
TSED	Lake sediment temperature	5.05 ^{o}C

Water temperature data were collected at several sites across Waldo Lake. Data included synoptic vertical profiles using a Hydrolab instrument and vertical arrays of thermistors recording temperatures at multiple depths on an hourly basis. Figure 5.3-5 includes a map of Waldo Lake with the temperature monitoring sites and Table 5.3-3 lists the monitoring sites for 2004 and 2005 and each corresponding model segment. Some of these monitoring sites do not have data yet because the instruments will be retrieved during the summer of 2005.

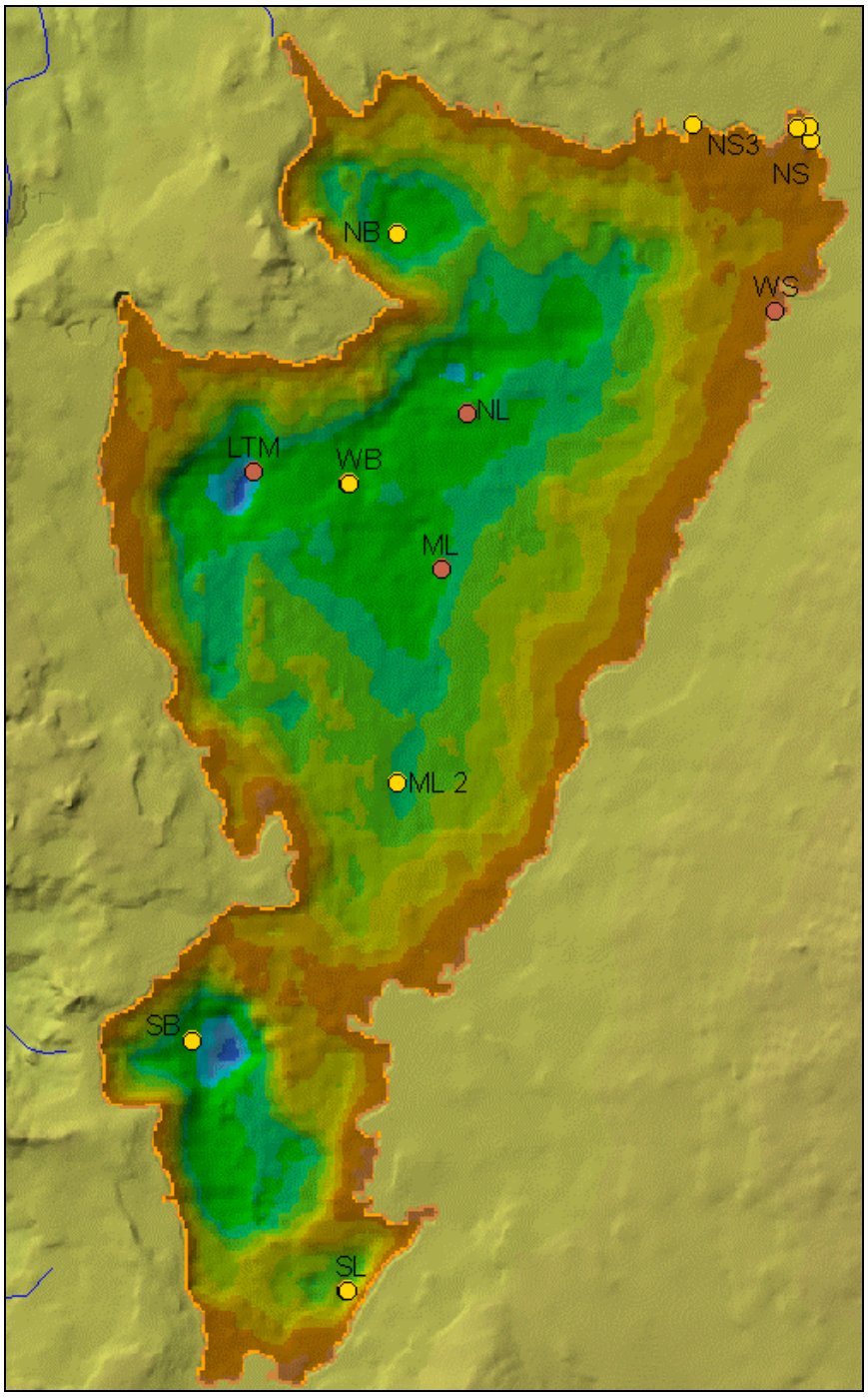

Figure 5.3-5. Waldo Lake temperature monitoring sites.

Table 5.3-3. Waldo Lake temperature monitoring site locations.

Site ID	Site Name	Latitude	Longitude	Model Segment
SL	South Lake	43.687	-122.0486	4
SB	South Bay	43.703	-122.0618	15
ML 2	Mid Lake 2	43.7192	-122.0436	28
ML	Mid Lake	43.7328	-122.0396	36
LTM	Long-Term Monitoring Site (LTR)	43.7391	-122.0559	37
WB	West Bay	43.7383	-122.0475	38
NL	North Lake	43.7426	-122.0371	42
WS	Weather Station	43.7489	-122.01	48
NB	North Bay	43.7541	-122.043	52
NS	North Waldo Boat Ramp	43.7597	-122.0068	52
NS1	North Shore 1	43.7606	-122.0069	53
NS2	North Shore 2	43.7605	-122.008	53
NS3	North Shore 3	43.7608	-122.0171	53

Time Series Data

The time series water temperature data recorded on the vertical arrays at each monitoring site were compared with model output for their corresponding model segment location and depth. Table 5.3-4 lists the model-data comparison sites and depths, the number of comparisons for each depth and the model-data error statistics. Water

temperature data at South Lake at a depth of 15 m was not compared to model results because the data was determined to be erroneous

A common problem in the calibration of the time series data was the precise elevation of the temperature probe. The temperature probes vertical location in the water column was probably know to within +/- 1.5 m. This could account for issues with model-data comparisons shown below.

Figure 5.3-6 shows time series model-data comparisons for multiple depths at the South Lake monitoring site. This site was the more difficult to calibrate because there were warmer temperatures deeper in the water column compared to other monitoring sites.

Figure 5.3-7 shows time series model-data comparisons for multiple depths at the South Bay monitoring site. This site was also difficult to calibrate compared to the other sites in Waldo Lake

Figure 5.3-8 shows model-data comparisons for the Mid Lake monitoring site for various depths and Figure 5.3-9 shows time series comparisons of model results and data at the West Bay monitoring site. The North Lake monitoring site data is compared to model output in Figure 5.3-10.

Overall the model results show the model is closely matching data at all of the sites with some better than others. A few sites show the model slightly cooler than data at the deepest locations. The model-data error statistics show a range of 0.3 to 1.4 ^{o}C with the worst model-data error statistics at the South Lake site and most model-data errors under 1.0 ^{o}C.

Table 5.3-4. Model-data time series water temperature comparison error statistics.

Monitoring Site	Model Segment	Depth, m	Number of Comparisons	ME, ^{o}C	AME, ^{o}C	RMS, ^{o}C
South Lake	4	5	7884	-0.24	0.62	0.8
	4	10	7884	-0.15	0.68	0.85
	4	20	7884	0.93	0.97	1.29
	4	25	7884	0.28	0.36	0.5
	4	30	4860	0.11	0.3	0.38
	4	35	7884	-0.68	0.86	1.12
	4	40	7884	-0.85	1.03	1.36
South Bay	15	5	7925	-0.41	0.71	0.82
	15	10	7926	0.16	0.6	0.74
	15	15	7925	0.38	0.52	0.63
	15	20	7925	0.95	0.97	1.24
	15	25	7925	0.43	0.46	0.63
	15	35	7925	-0.07	0.46	0.53
	15	45	7925	0.05	0.26	0.33
	15	60	7925	0.1	0.24	0.31
Mid Lake	36	5	7858	-0.49	0.68	0.85
	36	10	7858	0.21	0.52	0.66
	36	15	7859	0.38	0.56	0.71
	36	20	7858	0.44	0.5	0.66
	36	25	7858	-0.03	0.29	0.36
	36	35	7858	-0.14	0.41	0.48
	36	45	7858	-0.3	0.53	0.66
	36	60	7858	-0.23	0.42	0.5
West Bay	38	5	3028	-0.86	0.86	0.95
	38	10	3028	-0.33	0.71	0.79
	38	15	7883	0.22	0.45	0.58
	38	35	7883	-0.12	0.39	0.45
	38	45	7883	-0.29	0.55	0.67
	38	60	3029	-0.76	0.76	0.76
North Lake	42	5	7863	-0.19	0.5	0.6
	42	10	7863	0.34	0.62	0.79
	42	15	7863	0.3	0.49	0.61
	42	20	7863	0.54	0.56	0.73
	42	25	7863	0.25	0.3	0.36
	42	35	7863	-0.17	0.4	0.48
	42	45	7863	-0.37	0.54	0.68
	42	60	7863	-0.3	0.43	0.52

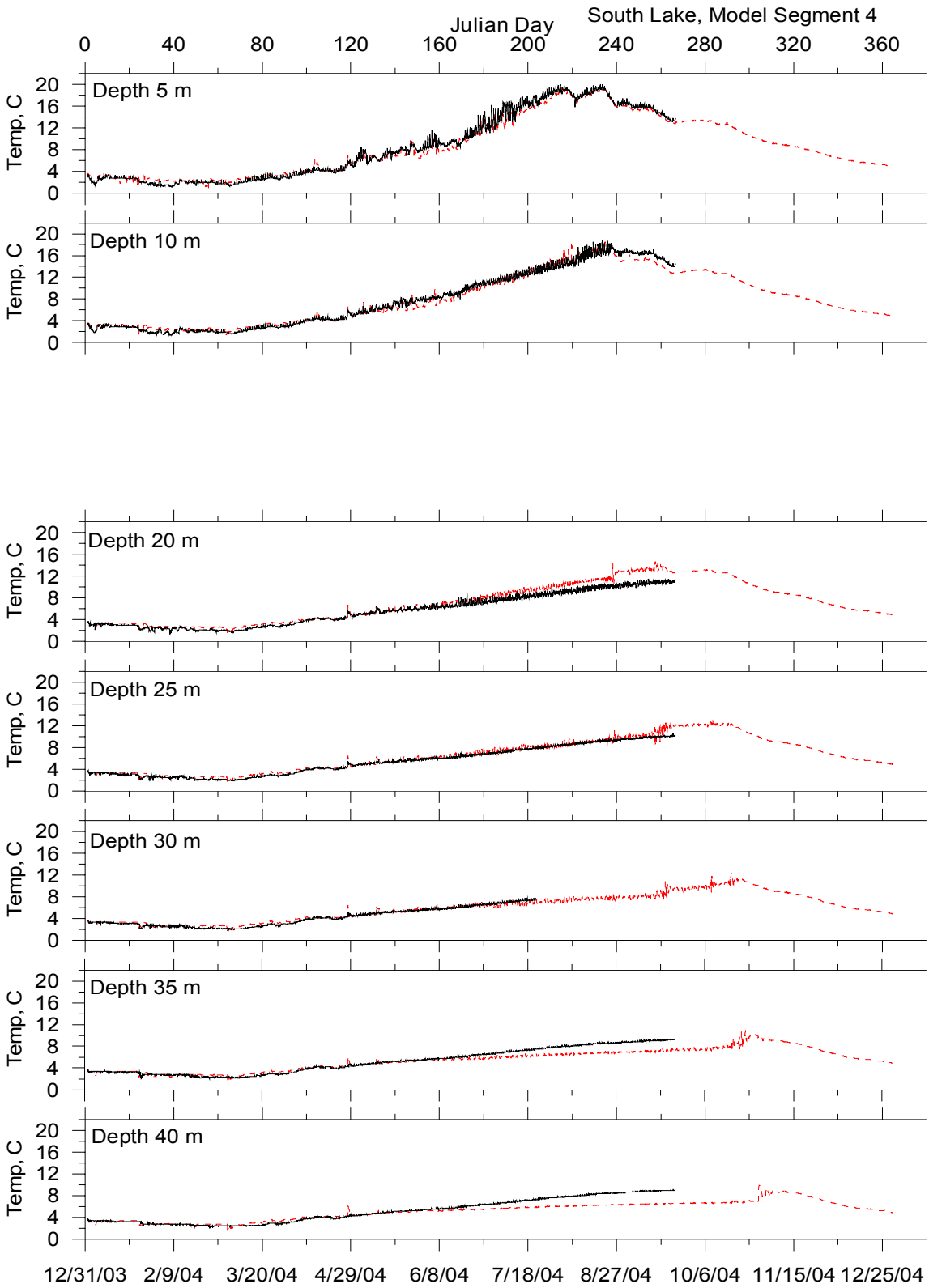

Figure 5.3-6. South Lake model-data water temperature comparisons for multiple depths.

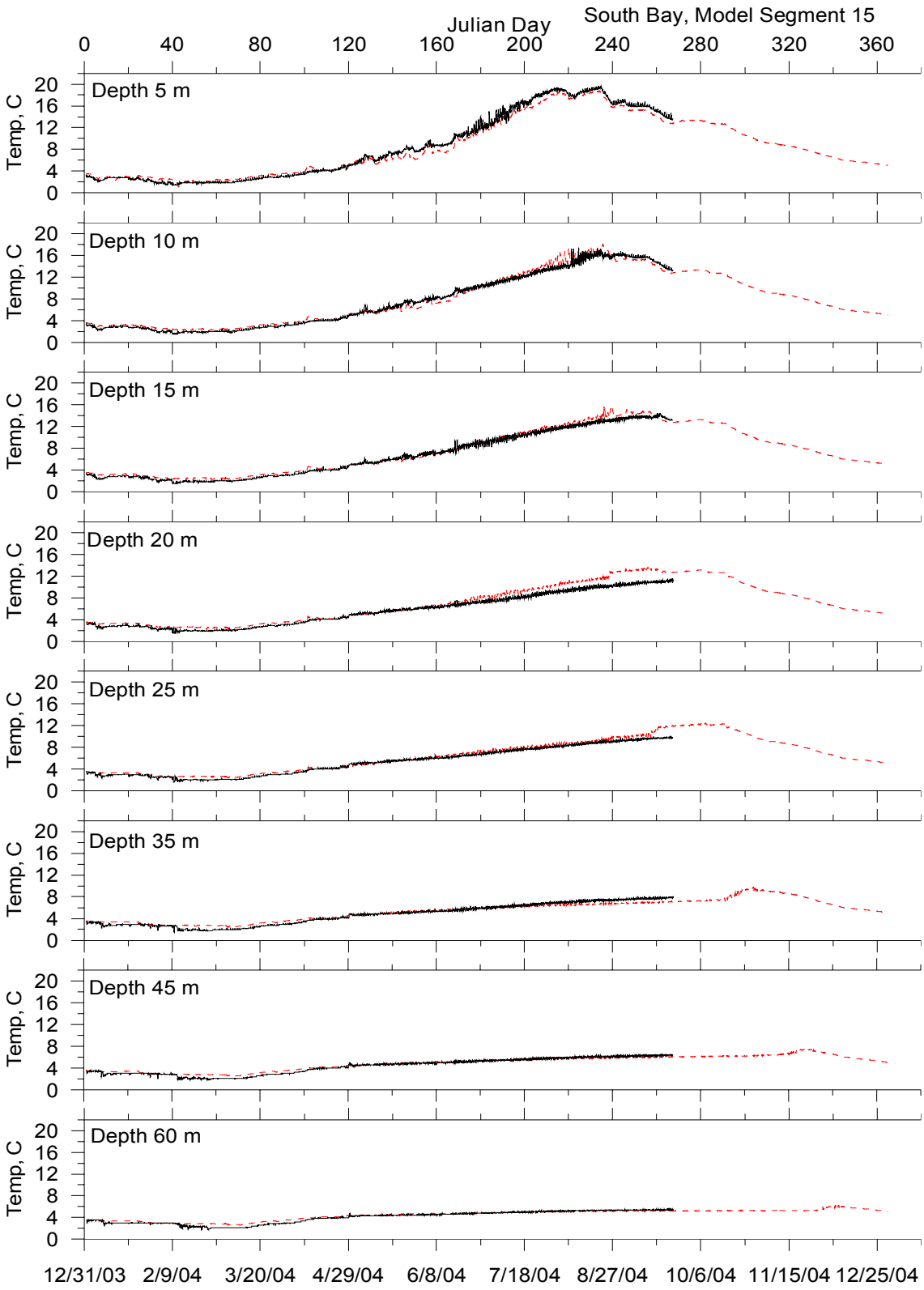

Figure 5.3-7. South Bay model-data water temperature comparisons for multiple depths.

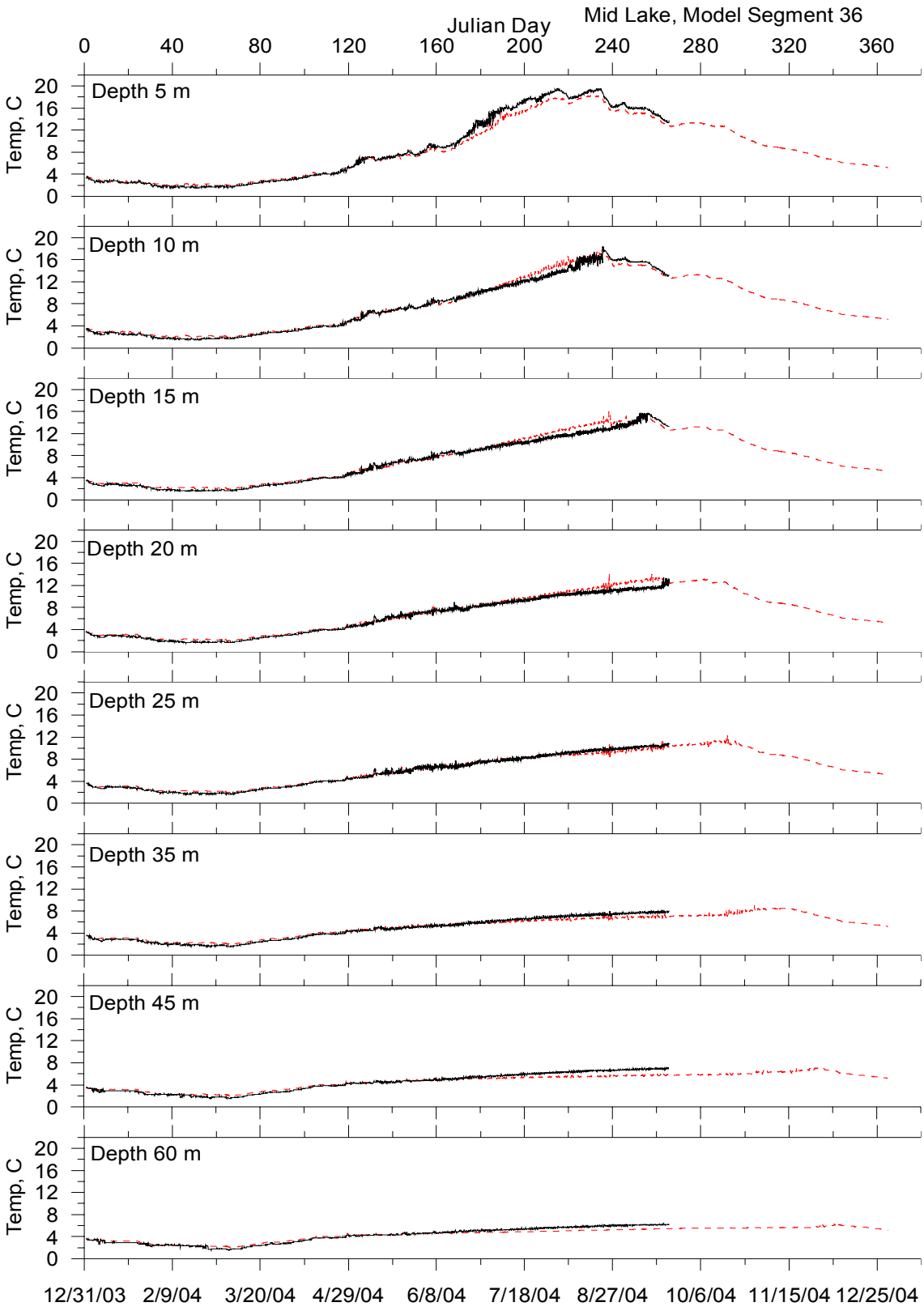

Figure 5.3-8. Mid Lake model-data water temperature comparisons for multiple depths.

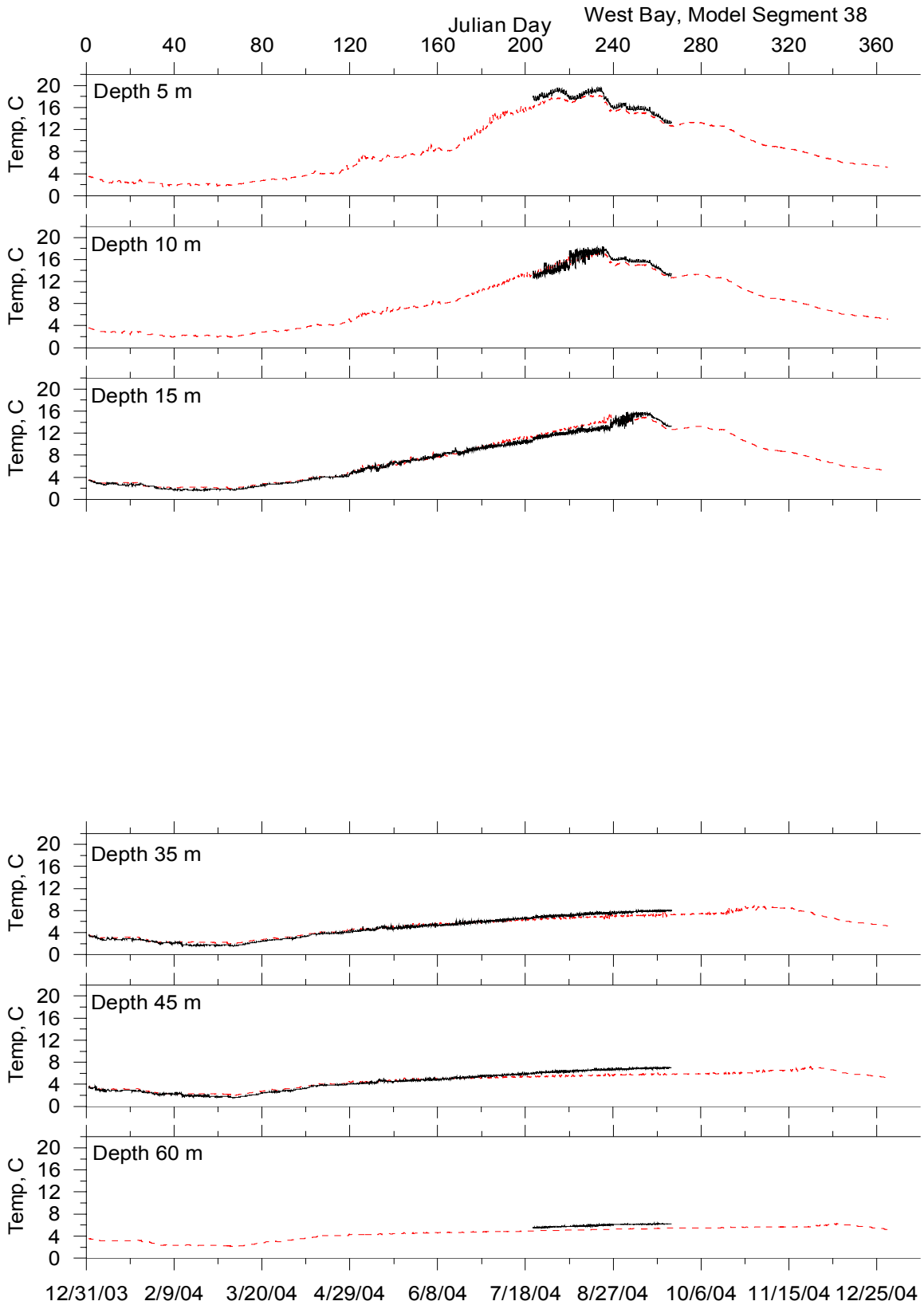

Figure 5.3-9. West Bay model-data water temperature comparisons for multiple depths.

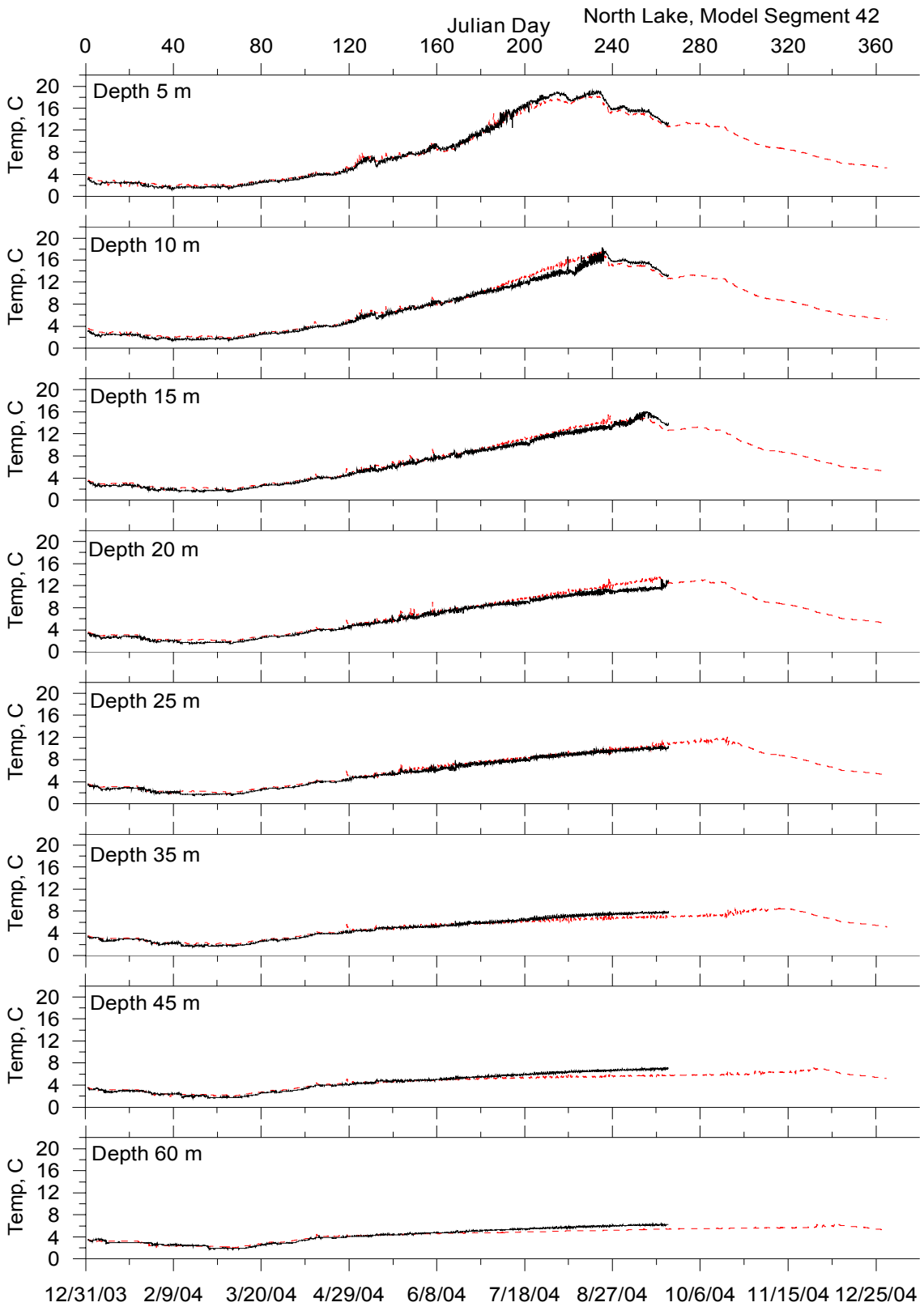

Figure 5.3-10. North Lake model-data water temperature comparisons for multiple depths.

Vertical Profile Data

In addition to the times series water temperature data collected at the monitoring sites several vertical profiles of water temperature were taken during 2004 by CLR and John Salinas. The water temperature vertical profiles were compared to model output for the sites listed in Table 5.3-5. The table also lists the number of profiles compared and the model-data error statistics for all the data points in the vertical profiles.

Table 5.3-5. Model-data vertical profile water temperature comparison error statistics.

Site ID	SL	SB	ML2	ML	LTM	WB	NL	NB
Model Segment	4	15	28	36	37	38	42	52
Number of Profiles	2	2	1	1	6	2	1	1
ME, ^{o}C	-0.28	0.17	-0.46	-0.11	-0.1	-0.25	-0.14	-0.45
AME, ^{o}C	1.05	0.43	0.65	0.47	0.69	0.52	0.55	0.65
RMS, ^{o}C	1.24	0.73	0.74	0.54	0.79	0.6	0.62	0.77

The water temperature model-data vertical profile comparisons are separated by monitoring sites. Each vertical profile consists of model output as a continuous blue line with diamonds filled in and each data set is a series of red open diamonds. Several of the vertical profiles were taken after the time series data set ended (until it is downloaded this summer) and as result the vertical profiles were the only way to evaluate the model calibration in late summer.

South Lake

Figure 5.3-11 shows a comparison between the data collected at the South Lake monitoring site with the model output from segment 4. The two profiles show similar results to the times series output and data shown Figure 5.3-6. The model is under predicting temperatures at lower depths and in the case of the September 22, 2004 profile, the model is missing the depth of the thermocline.

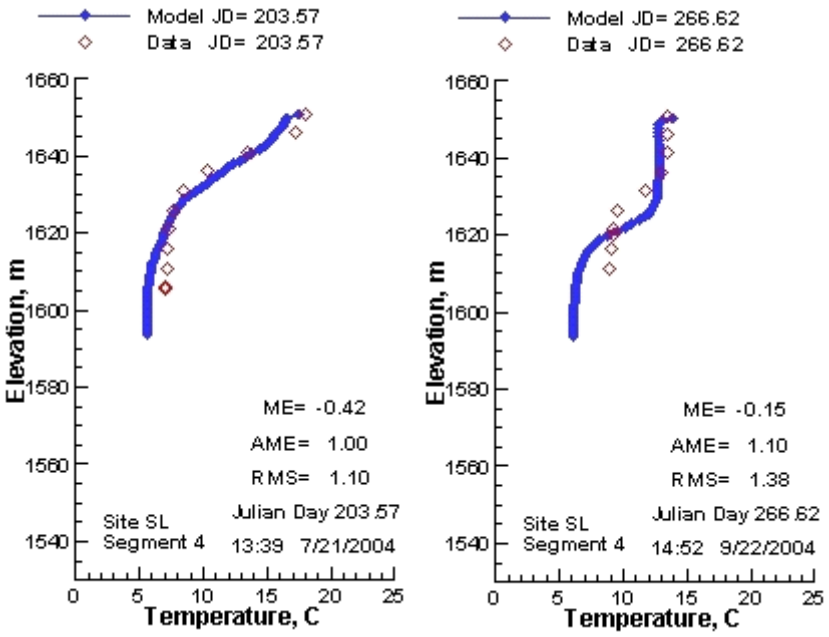

Figure 5.3-11. South Lake model-data vertical profile water temperature comparisons.

South Bay

Figure 5.3-12 shows a comparison between the data collected at the South Bay monitoring site and the model output from segment 15. The profiles show the model is doing well simulating the temperatures at lower depths but is missing the thermocline in late summer.

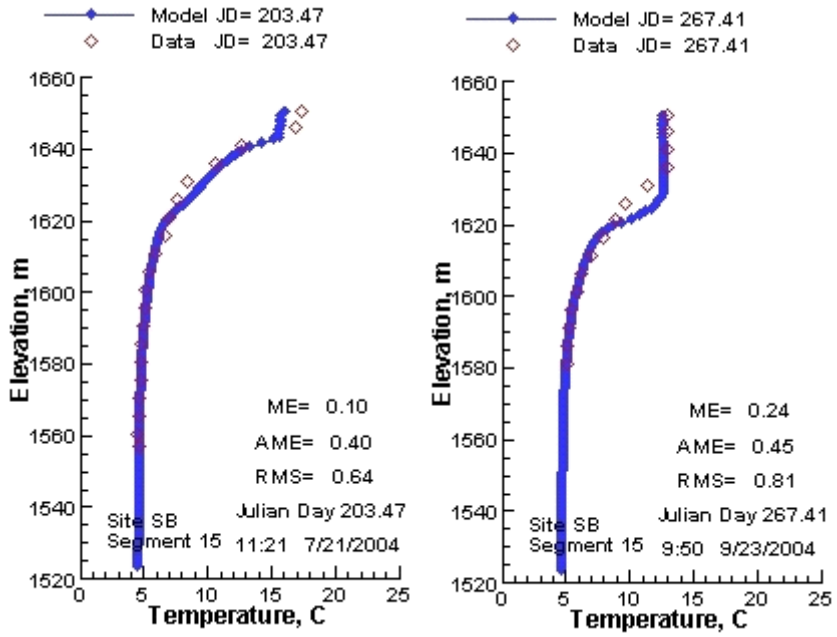

Figure 5.3-12. South Bay model-data vertical profile water temperature comparisons.

Mid Lake 2

The Mid Lake 2 site was a new site for deploying a vertical array of thermistors from the summer of 2004 through the summer of 2005 so there is only one vertical profile taken at this site. Figure 5.3-13 shows the vertical profile data compared with model output from segment 28. The figure shows the model is doing well compared to data with the results slightly cooler than data at the deepest locations.

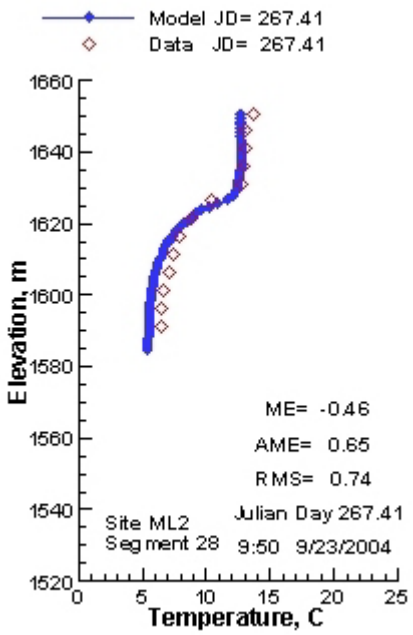

Figure 5.3-13. Mid Lake 2 model-data vertical profile water temperature comparisons.

Mid Lake

Figure 5.3-14 shows a comparison between the data collected at the Mid Lake site with the model results from segment 36 on July 20, 2004. The model is doing very well simulating the thermocline and matching temperatures at the surface and at depth.

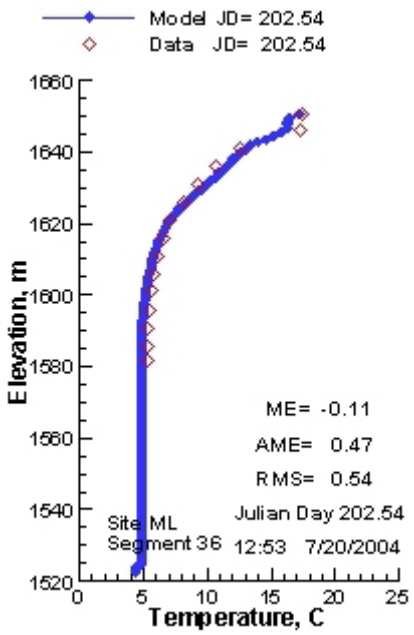

Figure 5.3-14. Mid Lake model-data vertical profile water temperature comparisons.

Long-Term Monitoring site

The long-term monitoring site had the largest number of vertical profiles in 2004 because it was monitored by both John Salinas and CLR at Portland State University. Model results from segment 37 were compared to data from this site as shown in Figure 5.3-15. The model does well simulating the thermocline but is a little too cool at depth in the late summer.

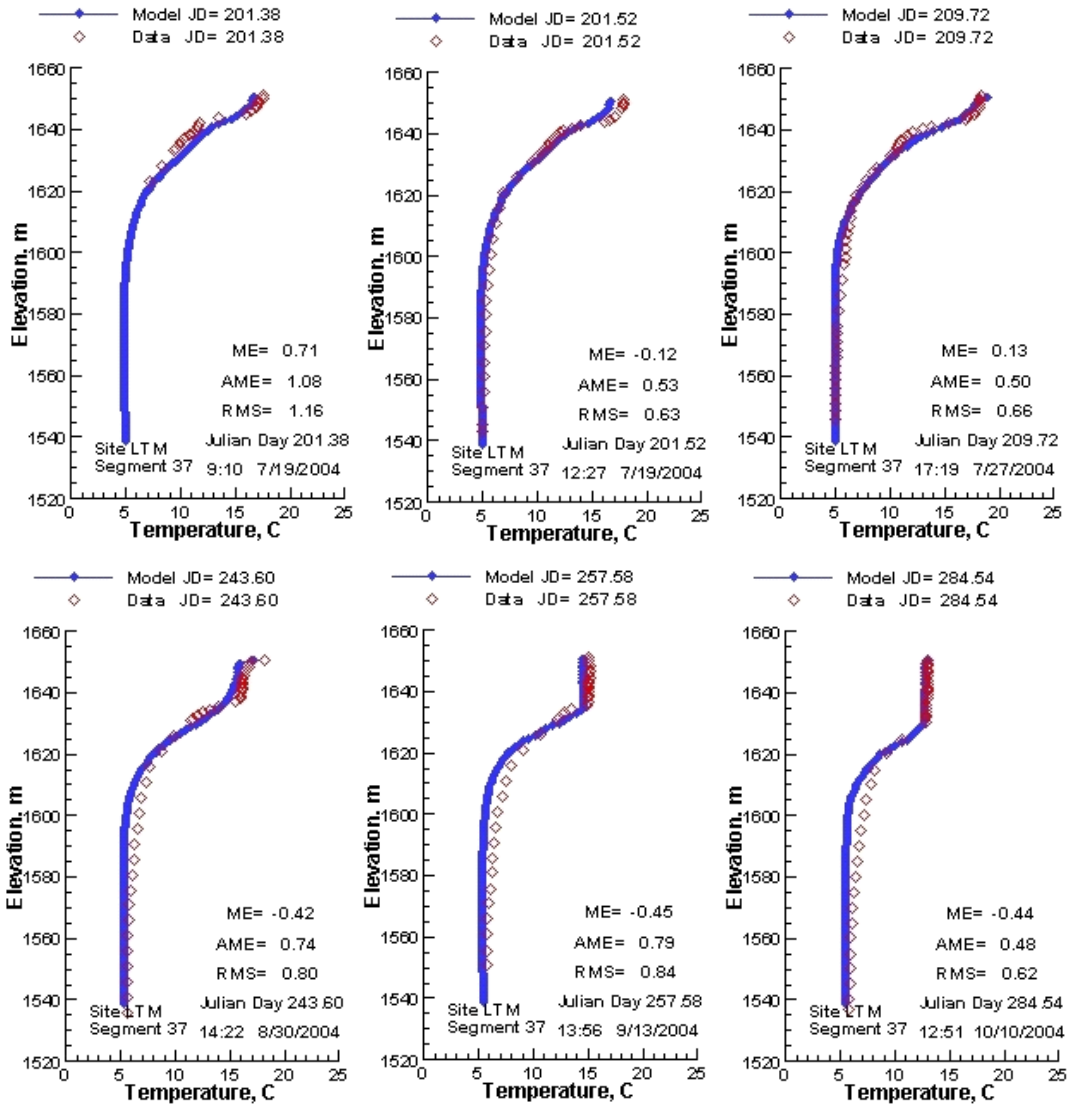

Figure 5.3-15. Long-term monitoring site model-data vertical profile water temperature comparisons.

West Bay

Figure 5.3-16 shows a comparison between model results from segment 38 and the vertical profile temperature data recorded at the West Bay monitoring site. The model does well in both the middle and late summer in matching the thermocline but in late summer the model is a little too cool at deeper locations. The model results are similar to those shown for the long-term monitoring site in late summer.

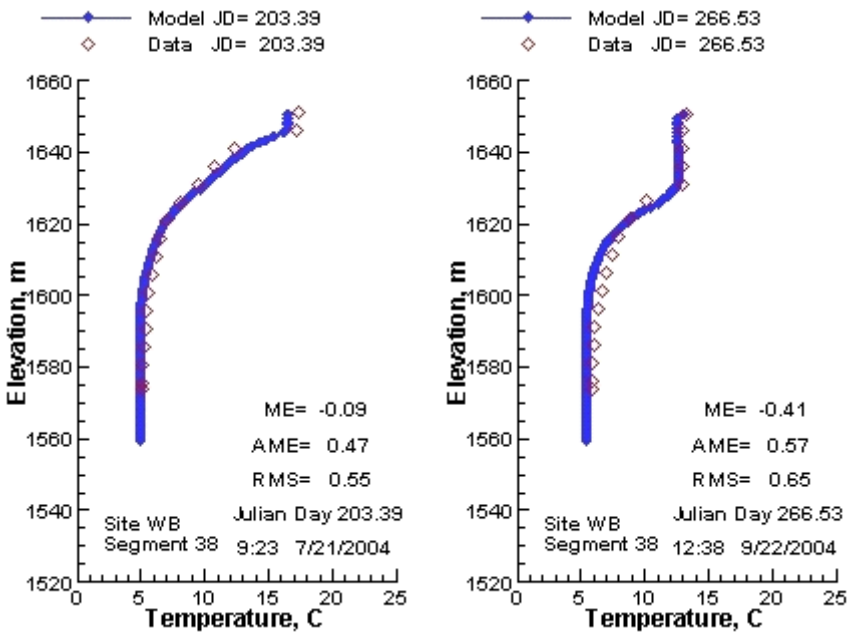

Figure 5.3-16. West Bay model-data vertical profile water temperature comparisons.

North Lake

Figure 5.3-17 shows a comparison between the model results from segment 42 and the vertical profile data collected at the North Lake monitoring site on July 20, 2004. The figure shows there is good model-data agreement throughout the profile.

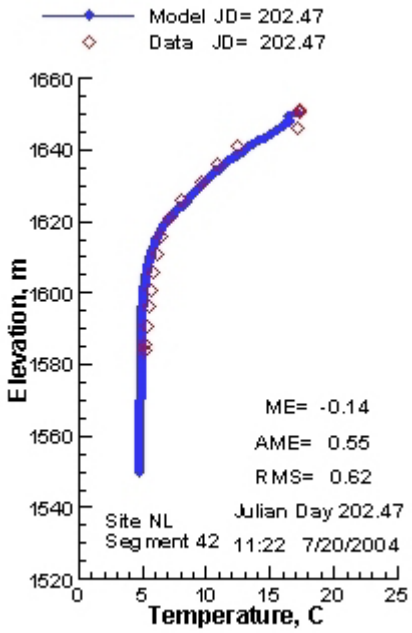

Figure 5.3-17. North Lake model-data vertical profile water temperature comparisons.

North Bay

Figure 5.3-18 shows a comparison between the vertical profile data collected at the North Bay monitoring site and the model results from segment 52. The figure shows the model is doing well capturing the thermocline but is a little too cool at lower elevations in the lake.

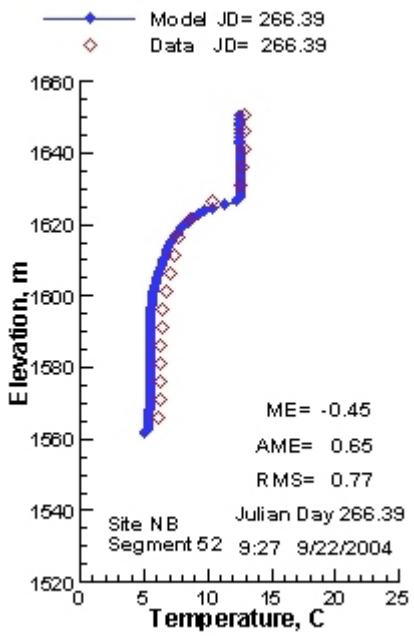

Figure 5.3-18. North Bay model-data vertical profile water temperature comparisons.

5.4 Summary

Development of the Waldo Lake water quality model was undertaken and initial hydrodynamic and temperature calibrations were conducted for 2004. The hydrodynamic calibration showed good model-data agreement with matching the water surface elevation. The temperature calibration shows good model data-agreement with both the time series data and the vertical profile data. Water temperature model-data error statistics ranged from 0.3 to 1.4 ^{o}C.

Future work will include expanding the model calibration period and improving the calibration results by including more accurate lake water level and outflow data from the lake. Both of these data sets will be critical to refining the water temperature calibration

and getting a better understanding of the hydrologic budget. Future work will also include:

1) Expanding the model to include water quality
2) Modeling algae assemblages
3) Adding a zooplankton model compartment and
4) Refining the phytoplankton and periphyton models as more data becomes available

References

Abbott, M. R., P. J. Richerson, and T. M. Powell. 1982. In situ response of phytoplankton fluorescence to rapid variations in light. Limnology and Oceanography 27:218-225.

Alverson, A., K. Manoylov, and R. Stevenson. 2003. Laboratory sources of error for algal community attributes during sample preparation and counting. Journal of Applied Phycology 15:357-369.

Arar, E. J., and G. B. Collins. 1997. *In Vitro* determination of Chlorophyll *a* and Pheophytin *a* in Marine and Freshwater Algae by Fluorescence. National Exposure Research Laboratory, Office of Research and Development, U.S. Environmental Protection Agency, Cincinnati, Ohio.

American Public Health Association, American Water Works Association, and Water Pollution Control Federation. 1998. Standard methods for the examination of water and wastewater. 20th edition. APHA, Washington, D.C.

Bergstrom, A., M. Hansson, S. Drakare, and P. Blomqvist. 2003. Occurrence of mixotrophic flagellates in relation to bacterioplankton production, light regime and availability of inorganic nutrients in unproductive lakes with differing humic contents. Freshwater Biology 48:868-877.

Biosonics, Inc. 2000. DT/DE Series Users Manual Version 4.02. Seattle, WA.

Biosonics, Inc. 2004. Visual Analyzer™ 4 User Guide. Seattle, WA.

Boeing, W. J., D. M. Leech, C. E. Williamson, S. Cooke, and L. Torres. 2004. Damaging UV radiation and invertebrate predation: conflicting selective pressures for zooplankton vertical distribution in the water column of low DOC lakes. Oecologia 138(4): 603-612.

Boraas, M., K. Estep, P. Johnson, and J. Sieburth. 1988. Phagotrophic phototrophs: The ecological significance of mixotrophy. Journal of Protozoology 35:249-252.

Caron, D., J. Goldman, and M. Dennett. 1988. Experimental demonstration of the roles of bacteria and bacterivorous protozoa in plankton nutrient cycles. Hydrobiologia 159:27-40.

Carty, S. 2003. Dinoflagellates. *in* J. D. Wehr and R. G. Sheath, editors. Freshwater Algae of North America: Ecology and Classification. Elsevier Science, San Diego.

Clark, K. R., and R. N. Gorley. 2001. Primer v5 User Manual/Tuitorial. Primer-E Ltd., Plymouth, UK.

Clesceri, L., A. Greenberg, and A. Eaton. 1998. Standard Methods for the Examination of Water and Wastewater, 20th edition. United Book Press Inc., Baltimore.

Cole, P. C., C. Leucke, W. A. Wursbaugh, and G. Burkart. 2002. Growth and survival of *Daphnia* in epilimnetic and metalimnetic water from oligotrophic lakes: the effects of food and temperature. Freshwater Biology 47: 2113-2122.

Currie, D., and J. Kalff. 1984. A comparison of the abilities of freshwater algae and bacteria to acquire and retain phosphorus. Limnology and Oceanography 29:298-310.

DeMott, W. R. and W. C. Kerfoot. 1982. Competition among cladocerans: nature of the interaction between *Bosmina* and *Daphnia*. Ecology 63:1949-1966.

Dodson, A. N. and W. H. Thomas. 1964. Concentrating plankton in gentle fashion. Limnology and Oceanography 9:455.

Fahnenstiel, G. L., C. Beckmann, S. E. Lohrenz, D. F. Millie, O. M. E. Schofield, and M. J. McCormick. 2002. Standard Niskin and Van Dorn bottles inhibit phytoplankton photosynthesis in Lake Michigan. Verhandlungen der Internationalen Vereinigung für Theoretische und Angewandte Limnologie 28:376-380.

Fee, E. J. 1976. The vertical and seasonal distribution of chlorophyll in lakes of the Experimental Lakes Area, northwestern Ontario: Implications for primary production estimates. Limnology and Oceanography 21:767-783.

Flynn, K. J. 1988. The concept of "primary production" in aquatic ecology. Limnology and Oceanography 33:1215-1216.

Geiger, N. S. 2000. Epiphytic algae on deep-dwelling bryophytes in Waldo Lake, Oregon. Lake and Reservoir Management 16:100-107

Goldman, J. C., and E. J. Carpenter. 1974. A kinetic approach to the effect of temperature on algal growth. Limnology and Oceanography 19:756-766.

Harris, G. P., S. I. Heaney, and J. F. Talling. 1979. Physiological and environmental constraints in the ecology of the planktonic dinoflagellate *Ceratium hirundinella*. Freshwater Biology 9:413-428.

Hein, M. 1997. Inorganic carbon limitation of photosynthesis in lake phytoplankton. Freshwater Biology 37:545-552.

Helsel, D. R., and R. M. Hirsch. 1993. Statistical Methods in Water Resources. Elsevier, Amsterdam.

Isaksson, A. 1998. Phagotrophic phytoflagellates in lakes-a literature review. Archives of Hydrobiologia Special Issue Advances in Limnology 51:63-90.

Jansson, M., P. Blomqvist, A. Jonsson, and A. Bergstrom. 1996. Nutrient limitation of bacterioplankton, autotrophic and mixotrophic phytoplankton, and heterotrophic nanoflagellates in Lake Ortasket. Limnology and Oceanography 41:1552-1559.

Johnson, A. C., and R. W. Castenholtz. 2000. Preliminary observations of the benthic cyanobacteria of Waldo Lake and their potential contribution to lake productivity. Lake and Reservoir Management 16:85-90.

Johnson, G. L, C. L. Hanson, S. P. Hardegree, and E. B. Ballard. 1996. Stochastic weather simulation: Overview and analysis of two commonly used models. Journal of Applied Meteorology 35(10):1878-1896.

Johnson, L. D. 2003. Waldo Lake long-term monitoring field sampling quality assurance and quality control project plan. Prepared for the USDA Forest Service. Center for Lakes and Reservoirs, Portland State University.

Johnson, L. D. *in prep*. Diurnal vertical migration of phytoplankton in Waldo Lake, Oregon. M.S. Portland State University, Portland, Oregon.

Jones, R. 2000. Mixotrophy in planktonic protests: an overview. Freshwater Biology 45:219-226.

Jones, R. A. 2000. Use of a remote operated vehicle and sonar to characterize and estimate the distribution of benthic vegetation in Waldo Lake, Oregon. Lake and Reservoir Management 16:108-113.

Kalff, J. 2002. Limnology Inland Water Ecosystems, 1st edition. Prentice Hall, Upper Saddle River, New Jersey.

Kirk, J. T. 1994. Light and photosynthesis in aquatic ecosystems, 2nd edition. University Press, Cambridge.

Koch, R.W. 1992. Stochastic simulation of climate input for water supply forecasting, Proceedings: Water Forum 1992, American Society of Civil Engineers. Baltimore, MD.

Larson, D. W. 1970. On reconciling lake classification with the evolution of four oligotrophic lakes in Oregon. Ph.D. Thesis, Department of Fisheries and Wildlife. Oregon State University, Corvallis, Oregon.

Larson, D. W., and J. T. Salinas. 1995. Waldo Lake, Willamette Nation Forest, Oregon Limnological Investigations: 1986-1995. CAS-9505, USDA Forest Service, Oakridge, Oregon.

Li, A., D. Stoecker, and D. W. Coats. 2000. Mixotrophy in *Gyrodinium galatheanum* (Dinophyceae): Grazing responses to light intensity and inorganic nutrients. Journal of Phycology 36:33-45.

LI-COR Inc. 1984. LI-1800UW Underwater Spectroradiometer Instruction Manual. Lincoln, NE.

Malueg, K. W., J. R. Tilstra, D. W. Schults, and C. F. Powers. 1972. Limnological observations on an ultra-oligotrophic lake in Oregon, USA. Verhandlungen der Internationalen Vereinigung für Theoretische und Angewandte Limnologie 18:292-302.

Marcogliese, D. J., and G. W. Esch (1992).Alterations of Vertical Distribution and Migration of Zooplankton in Relation to Temperature. American Midland Naturalist 128(1): 139-155.

Medina-Sanchez, J. W., and M. Villar-Argaiz. 2002. The interaction of phytoplankton and bacteria in a high mountain lake: Importance of the spectral composition of solar radiation. Limnology and Oceanography 47:1294-1306.

Medina-Sanchez, J. W., and M. Villar-Argaiz. 2004. Neither with nor without you: A complex algal control on bacterioplankton in a high mountain lake. Limnology and Oceanography 49:1722-1733.

Merritt, R. W., and K. W. Cummins. 1978. An introduction to the aquatic insects of North America. Kendall-Hunt Publishing, Dubuque, Iowa.

Morris, D. P., H. Zagarese, C. E. Williamson, E. G. Balseiro, B. R. Hargreaves, B. Modenutti, R. Moeller, and C. Queimalinos. 1995. The attenuation of solar UV radiation in lakes and the role of dissolved organic carbon. Limnology and Oceanography 40:1381-1391.

Orcutt, J. D., and K. G. Porter. 1983. Diel vertical migration by zooplankton: Constant and fluctuating temperature effects on life history parameters of *Daphnia*. Limnology and Oceanography 28:720-230.

Orion Research Inc. 1991. Laboratory Research Group Portable pH/ISE Meter Instruction Manual. Boston, MA.

Page, K. A., S. A. Connon, and S. J. Giovanonni. 2004. Photosynthetic reaction center genes found in oligotrophic bacterial isolates from Crater Lake, Oregon. *in* 10th International Symposium on Microbial Ecology, Cancun, Mexico.

Peterson, B. 1980. Aquatic primary productivity and the ^{14}C-CO_2 method: a history of the productivity problem. Annual Review of Ecology and Systematics 11:359-385.

Prepas, E. E., and F. H. Rigler. 1982. Improvements in quantifying the phosphorus concentration in lake water. Canadian Journal of Fisheries and Aquatic Sciences 39: 822-829.

Raven, J. A. 1997. Phagotrophy in phototrophs. Limnology and Oceanography 42:198-205.

Raven, J. A., and K. Richardson. 1984. Dinophyte flagella: A cost-benefit analysis. New Phytologist. 98:259-276.

Reddy, A. R., and A. Gnanam. 2000. Photosynthetic productivity prospects under CO2-enriched atmosphere of the 21st century. Pages 342-363 *in* U. P. Mohammad Yunus and P. Mohanty, editors. Probing Photosynthesis: Mechanisms, regulation and adaptation. Taylor and Francis, London.

Reynolds, C. S. 1984. The Ecology of Freshwater Phytoplankton. University Press, Cambridge.

Reynolds, C. S. 1997. Vegetation Processes in the Pelagic. ECI, Oldendorf.

Rhode, S. C., M. Pawlowski, and R. Tollrian. 2001. The impact of ultraviolet radiation on the vertical distribution of zooplankton of the genus *Daphnia*. Nature 412:69-72.

Richardson, C. W. 1981. Stochastic simulation of daily precipitation, temperature and solar radiation. Water Resources Research 17(1):182-190.

Salas, J. D., J. W. Delleur, V. Yevjevich, and W. Lane. 1980. Applied Modeling of Hydrologic Time Series, Water Resources Publications, Littleton, Colorado, 484 p.

Salinas, J. 2000. Thermal and chemical properties of Waldo Lake, Oregon. Lake and Reservoir Management 16:40-51.

Salinas, J., and D. W. Larson. 2000. Phytoplankton primary production and light in Waldo Lake, Oregon. Lake and Reservoir Management 16:71-84.

Scheffer, M., S. Carpenter, J. Foley, C. Folke, and B. Walker. 2001. Catastrophic shifts in ecosystems. Nature 413: 591-596.

Schreiber, U. 1997. Chlorophyll fluorescence and photosynthetic energy conversion: Simple introductory experiments with the TEACHING-PAM Chlorophyll Fluorometer.

Singh, V. 1992. Elementary Hydrology. Prentice Hall, New York.

Stanton, T. K., D. Chu, P. H. Wiebe, L. V. Martin, and R. L. Eastwood. 1998. Sound scattering by several zooplankton groups. I. Experimental determination of dominant sound scattering mechanisms. Journal of the Acoustical Society of America 103:225-235.

Stich, H. B., and W. Lampert. 1981. Predator evasion as an explanation of diurnal vertical migration by zooplankton. Nature 293: 396-398.

Stockner, J. G., and K. G. Porter. 1988. Microbial Food Webs in Freshwater Planktonic Ecosystems. *in* S. R. Carpenter, editor. Complex Interactions in Lake Communities. Springer-Verlag, New York.

Swanson, N. L., W. J. Liss, J. S. Ziller, M. G. Wade, and R. E. Gresswell. 2000. Growth and diet of fish in Waldo Lake, Oregon. Lake and Reservoir Management 16:133-143.

Sweet, J. 2000. Phytoplankton composition and distributions in Waldo Lake, Oregon. Lake and Reservoir Management 16:63-70.

Sytsma, M., J. Rueter, R. Petersen, R. Koch, S. Wells, R. Miller, L. Johnson, and R. Annear. 2004. Waldo Lake Research in 2003: Report to the USDA Forest Service, Willamette National Forest. Center for Lakes and Reservoirs, Portland State University.

Taylor, J. R. 1982. An introduction to error analysis: The study of uncertainties in physical measurement. University Science Books, Sausalito.

Tittel, J., V. Bissinger, B. Zippel, U. Gaedke, E. Bell, A. Lorke, and N. Kamjunke. 2003. Mixotrophs combine resource use to outcompete specialists: Implications for aquatic food webs. PNAS 100:12776-12781.

Turner Designs. 2002. Self-contained Underwater Fluorescence Apparatus Users Manual. Sunnyvale, CA.

Vinebrooke, R., and P. Leavitt. 1999. Differential responses of littoral communities to ultraviolet radiation in an alpine lake. Ecology 80:223-237.

Vogel, A. H., and J. Li. 2000. Recent changes in the zooplankton assemblage of Waldo Lake, Oregon. Lake and Reservoir Management 16:114-123.

Wagner, D. H., J. A. Christy, and D. W. Larson. 2000. Deep-water bryophytes from Waldo Lake, Oregon. Lake and Reservoir Management 16:91-99

Wetzel, R. G. 2001. Limnology: Lake and River Ecosystems, 3rd edition. Academic Press, San Diego, California.

Wetzel, R. G., and G. E. Likens. 2000. Limnological Analyses. Springer-Verlag, New York.

Williamson, C. E. 1995. What role does UV-B radiation play in freshwater ecosystems? Limnology and Oceanography 40:386-392.

Williamson, C. E., R. W. Sanders, R. E. Moeller, and P. L. Stutzman. 1996. Utilization of subsurface food resources for zooplankton reproduction: Implications for diel vertical migration theory. Limnology and Oceanography 41:224-233.

Williamson, C. E., and J. W. Reid. 2001.Copepoda. *In* Ecology and Classification of North American Freshwater Invertebrates, Second Edition, J. H. Thorp and A. P. Covich eds. Academic Press, New York, NY.

Zar, J. H. 1996. Biostatistical Analysis, 3rd edition. Prentice Hall, Upper Saddle River, New Jersey.

Appendix A

Temperature Monitoring, Waldo Lake, Oregon Quality Assurance/ Quality Control Plan

Prepared by Laura Johnson
Center for Lakes and Reservoirs,
Department of Environmental Sciences and Resources
Portland State University
March 2005

Detailed temperature monitoring of Waldo Lake by the Center for Lakes and Reservoirs has provided information for development of a water quality model of the ecosystem (Sytsma et al. 2004 and 2005). This document describes the quality assurance and quality control procedures followed by CLR during the detailed temperature monitoring study completed from July 2003 through October 2004.

Project Management

1. Problem Identification and Background

Temperature mixing dynamics influence both the distribution of phytoplankton in the water column and light attenuation with depth. The thermocline depth and seasonal mixing events are important parameters for characterizing lakes.

No continuous water temperature data had been collected at Waldo Lake previous to this work. Data collection described here will help determine if similar data are needed in the future and to what extent temperature should be monitored as part of the long-term

monitoring program. Information collected regarding changes in water column temperature will be used to make decisions regarding timing and frequency of future long-term monitoring sampling activities and will be used for lake modeling purposes.

2. Project Description and Task Summary

Forty temperature loggers were deployed at eight depths in five locations around the lake. These temperature loggers will record continuously from July 2003 through October 2004. Water temperature data were analyzed in conjunction with wind and air temperature data to draw conclusions regarding changes in thermal stability of the lake throughout the duration of the study period.

Table B-1: Timeline of Events

Date	Event
July 2003	Installation of temperature loggers
October 2003	Downloading of logger data
July 2004	Downloading of logger data
October 2004	Retrieval and downloading of temperature loggers

3. Personnel Contact Information

Mark Sytsma	(503) 725-3833	sytsmam@pdx.edu
Richard Petersen	(503) 725-4241	petersenr@pdx.edu
Laura Johnson	(503) 725-3834	ljohnso@pdx.edu

4. Data Quality Objectives

Data quality goals for this section of the project are similar to those in the Waldo Lake Long-Term Monitoring Field Sampling Quality Assurance and Quality Control Project Plan. Data quality objectives for the multi-parameter probe and the weather station are available in the Waldo Lake Long-Term Monitoring Field Sampling Quality Assurance and Quality Control Project Plan. Table 2 shows data quality objectives for equipment used for temperature monitoring.

Accuracy

Table B-2: Data quality objectives for equipment.

Parameter	General Method	Expected Range	Accuracy
Water Temperature	Onset® Temperature Loggers	0 to 30°C	± 0.5° C (a)
Wind Speed	Maximum DIC 3 handheld Anemometer	0-30 m.p.h.	

Based on manufacturer's specifications

Completeness

For temperature logger data collection, a 90 % goal for completeness has been set.

5. Documentation and Records

Data collected from temperature logger downloads will be stored in a MS ACCESS database. All of the data collected will be summarized graphically and statistically.

6. Uses and Distribution of Data and Reports

Data collected from temperature logger downloads will be used by other research staff at Portland State University, specifically by for use in modeling.

Data Measurement and Data management

7. Sampling Process Design

Temperature logging thermistors are located at five locations around the lake, in order to capture horizontal variation in lake temperature. 4 out of 5 locations are in deeper waters, the fifth location, South Lake, is much shallower. The South Bay location is the most sheltered from the wind and is also the deepest. Figure 1 shows their locations and Table 3 lists their depths and GPS coordinates from the July 2003 deployment. Temperature loggers will collect continuous data from July 2003 through September 2004.

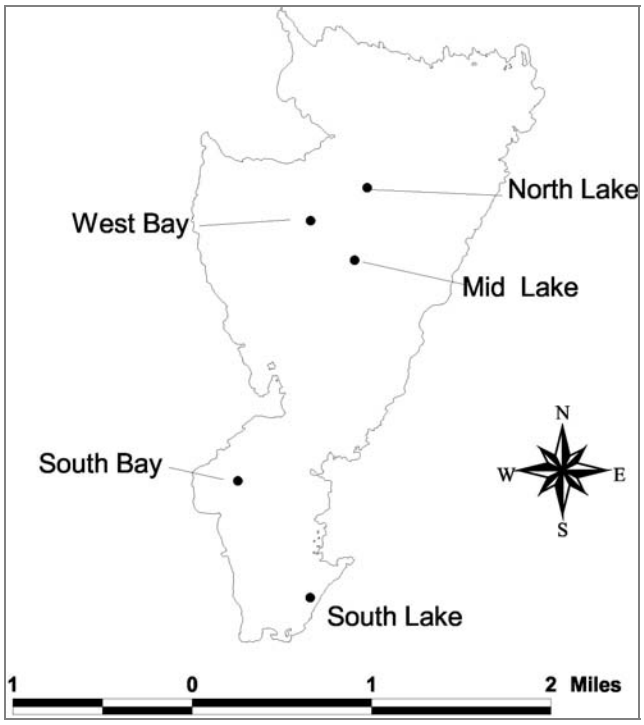

Figure B-1: Thermistor Locations

Table B-3: Thermistor locations

Location	GPS Coordinates Latitude	Longitude	Depth of Lake at the Station	Approximate depth of Thermistors
West Bay	43.73819 N	122.04773 W	77 m	5,10,15,20,25,35,45,60 m
South Bay	43.70297 N	122.06183 W	94 m	5,10,15,20,25,35,45,60 m
North Lake	43.74262 N	122.03710 W	65 m	5,10,15,20,25,35,45,60 m
Mid Lake	43.73277 N	122.03960 W	74 m	5,10,15,20,25,35,45,60 m
South Lake	43.68695 N	122.04864 W	47 m	5,10,15,20,25,30,35,40 m

8. Sampling Methods and Requirements

Temperature loggers

Loggers record temperature at 30-minute intervals during the summer season, between July and October, and at 1-hour intervals over the winter, between October and July. Temperature loggers will be downloaded twice a season, at the opening of the roads and before road closure. Temperature loggers will be calibrated pre- and post-deployment using standardized procedures of the U.S. Forest Service. Replacement loggers will be readily available and calibrated at the times of downloading in case a logger is damaged or missing. Preparedness will reduce the loss of data.

Multi-parameter probe measurement

In order to perform a field audit of temperature logger performance, the same protocol will be used as in the long-term monitoring field protocol, but at 5-meter increments descending the water column and at specific depths where temperature loggers are located ascending the water column, as a quality control check. This will be done at the time of downloading.

9. Quality Control Requirements

Quality control requirements for reporting of data are defined in the long-term monitoring field protocol. Table 4 summarizes quality control methods that specifically apply to the temperature monitoring study. Temperature logger accuracy will be graded based on the scale from the Waldo Lake Long-Term Monitoring Field Sampling Quality Assurance and Quality Control Project Plan.

Table B-4: Summary of quality control methods and requirements

Parameter	Completion Goal	QA Method	Calibration Check	Required Resampling	Required Assessment of data collection protocol
Temperature loggers	90%	Frequent Downloading Prepared replacements for lost loggers	Pre and Post Deployment calibration	N/A	Grading of loggers after field audits using a calibrated multi-parameter probe Grading of loggers after post deployment calibration audit based on instrumental drift during deployment

10. Instrument/Equipment Inspections and Maintenance

Instrument and equipment inspections and maintenance will follow protocol written in Waldo Lake Long-Term Monitoring Field Sampling Quality Assurance and Quality Control Project Plan.

11. Instrument Equipment Calibration and Frequency

Calibration of the multi-parameter probe used as a quality control check will follow protocol written in Waldo Lake Long-Term Monitoring Field Sampling Quality Assurance and Quality Control Project Plan. Calibration of the temperature loggers will

follow the protocol of the U.S. Forest Service. Temperature logger calibration will occur at the beginning of the study period and at the end of the study period.

Appendix B

Evaluation of changes in the Waldo Lake plankton community using multivariate statistical techniques.

Table A-1: "Major" species of zooplankton

Species Name	Species Code	Group
Alona costada	ALCO	Cladocera
Bosmina longristris	BOLO	Cladocera
Copepod nauplii	CONP	Copepod
Difflugia sp.	DIFX	Other
Diaptomus kenai x shoshone	DPKS	Copepod
Diaptomus signicauda	DPSG	Copepod
Small Diaptomus copepodite	SMDC	Copepod
Large Diaptomus copepodite	LGDC	Copepod
Diaptomus copepodite	DPCO	Copepod
Harpacticoid copepodite	HPCO	Copepod
Keratella cochlearis	KTCH	Rotifer
Collotheca pelagica	CLPG	Rotifer
Collotheca sp.	CLXX	Rotifer

Table A-2: "Major" species of phytoplankton

Species Name	Species Code	Class
Achnanthes lanceolata	ACLC	Bacillariophyceae
Achnanthes linearis	ACLN	Bacillariophyceae
Achnanthes minutissima	ACMN	Bacillariophyceae
Asterionella formosa	ASFO	Bacillariophyceae
Cocconeis placentula	COPC	Bacillariophyceae
Cymbella minuta	CMMN	Bacillariophyceae
Diatoma hiemale mesodon	DTHM	Bacillariophyceae
Eunotia elegans	EUEL	Bacillariophyceae
Eunotia incisa	EUIN	Bacillariophyceae
Eunotia pectinalis	EUPC	Bacillariophyceae
Fragilaria vaucheria	FRVA	Bacillariophyceae
Gomphonema angustatum	GFAN	Bacillariophyceae
Gomphonema subclavatum	GFSB	Bacillariophyceae
Gomphonema tenellum	GFTN	Bacillariophyceae
Navicula cryptocephala veneta	NVCV	Bacillariophyceae
Navicula seminulum	NVSM	Bacillariophyceae
Navicula sp.	NVXX	Bacillariophyceae
Nitzschia acicularis	NZAC	Bacillariophyceae
Nitzschia dissipata	NZDS	Bacillariophyceae
Nitzschia frustulum	NZFR	Bacillariophyceae
Nitzschia paleacea	NZPC	Bacillariophyceae
Peronia sp.	PXXX	Bacillariophyceae
Synedra radians	SNRD	Bacillariophyceae
Synedra rumpens	SNRM	Bacillariophyceae
Ankistrodesmus falcatus	AKFL	Chlorophyceae
Chlamydomonas sp.	CHXX	Chlorophyceae
Crucigenia sp.	CGXX	Chlorophyceae
Golenkinia radiata	GKRD	Chlorophyceae
Oocystis lacustris	OCLA	Chlorophyceae
Oocystis pusilla	OCPU	Chlorophyceae
Selenastrum minutum	SLMN	Chlorophyceae
Sphaerocystis schroeteri	SCSC	Chlorophyceae
Tetraedron minimum	TEMN	Chlorophyceae
Tetraedron regulare	TERG	Chlorophyceae
Tetraedron sp.	TEXX	Chlorophyceae
Rhodomonas minuta	RDMN	Chryptophyceae
Chromulina sp.	KMXX	Chrysophyceae
Chrysochromulina sp.	KKXX	Chrysophyceae
Dinobryon sertularia	DBST	Chrysophyceae
Wolosynzskia neglectum	GDNG	Dinophyceae
Gymnodinium sp.	GNXX	Dinophyceae
Hemidinium sp.	HDXX	Dinophyceae
Unidentified flagellate	MXFG	Unknown

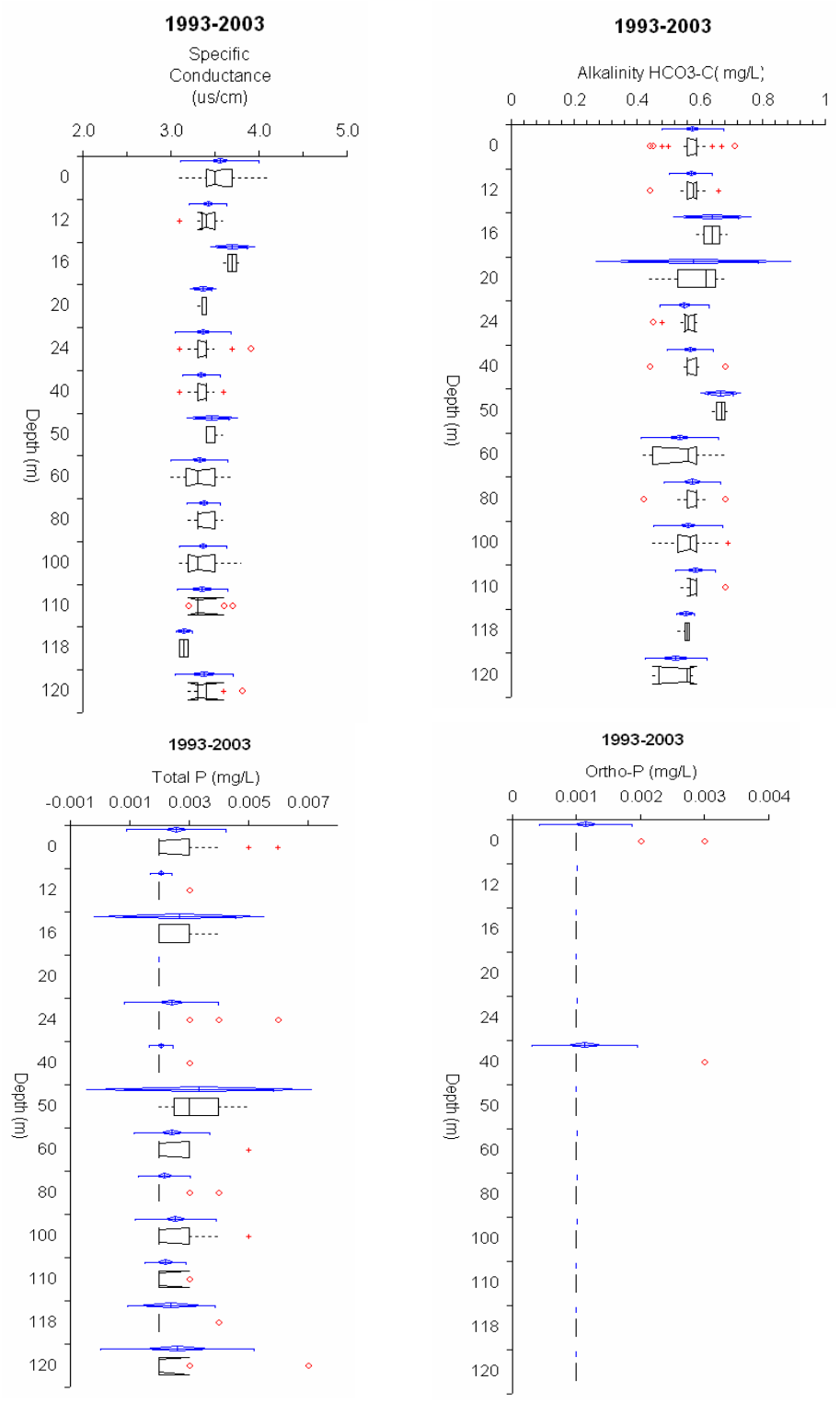

Figure A-1: Chemistry variables: spatial variation

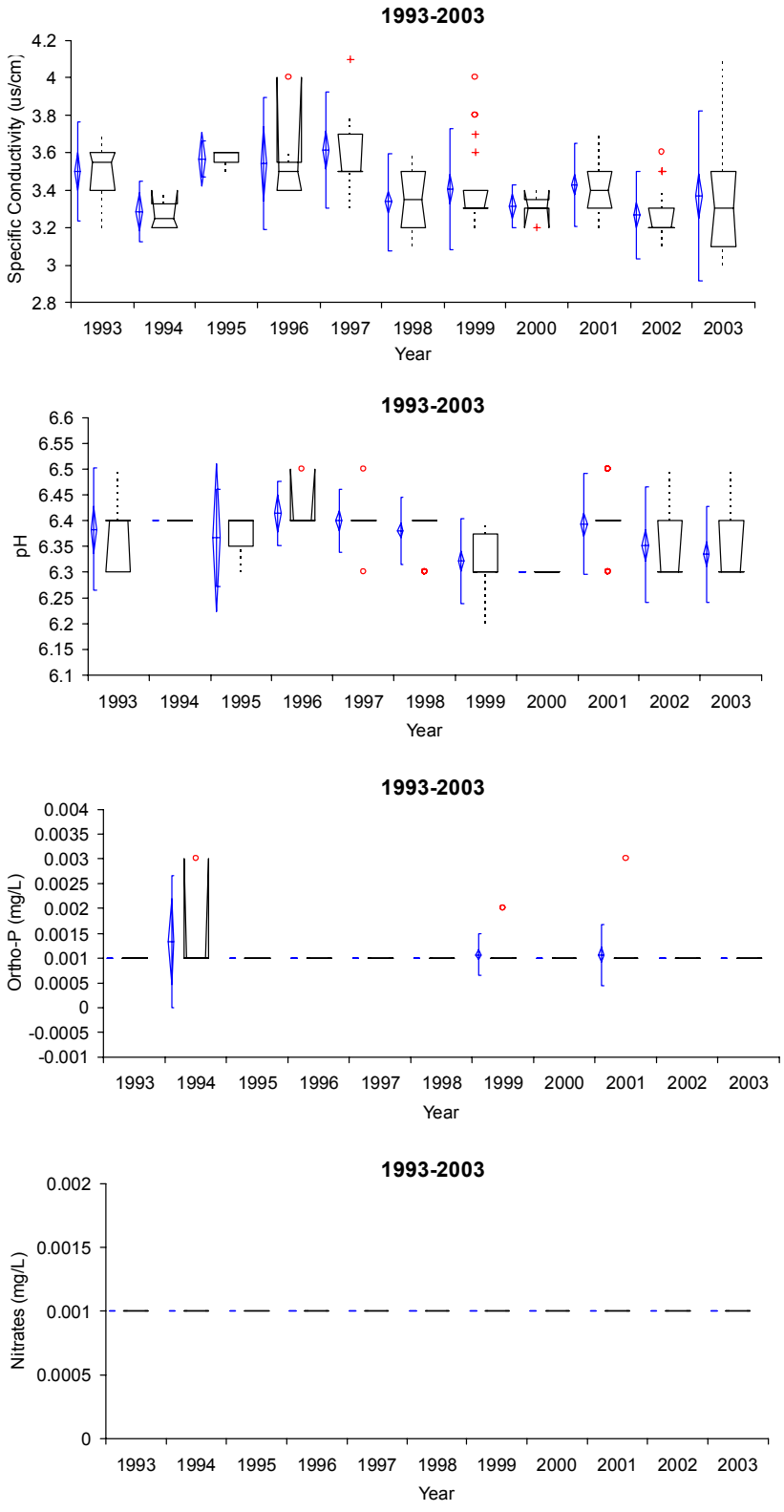

Figure A-2: Chemistry variables: yearly variation

1993-2003

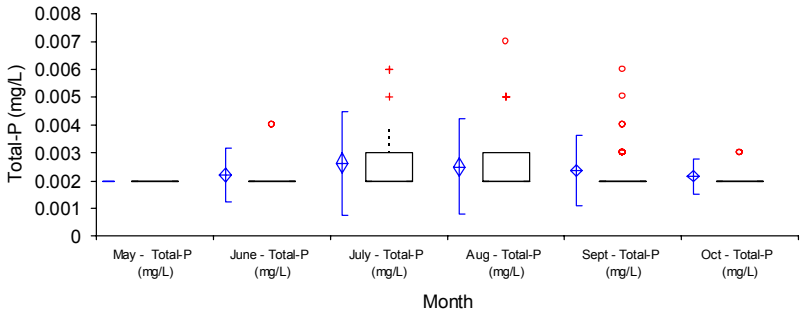

1993-2003

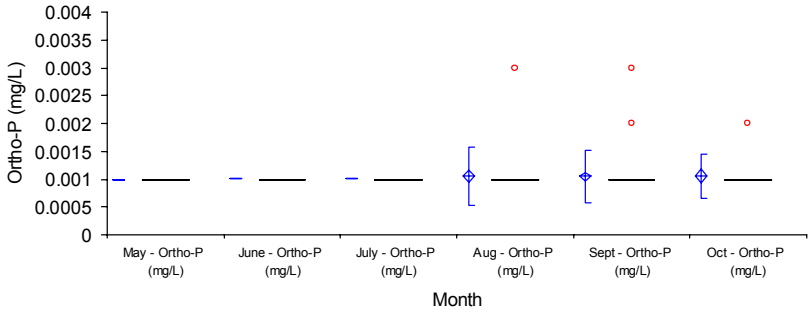

1993-2003

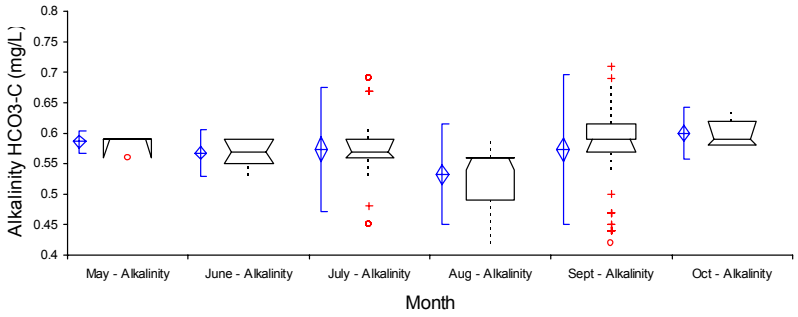

1993-2003

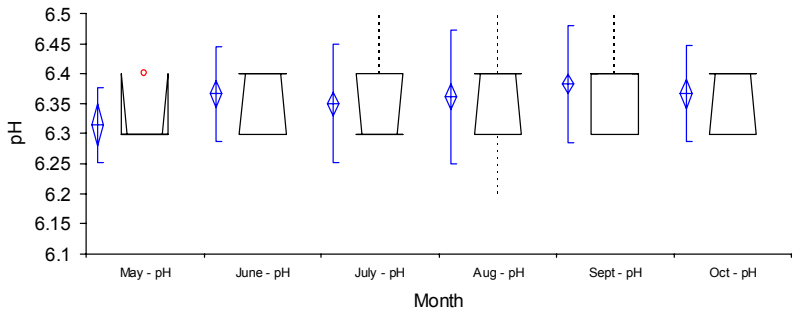

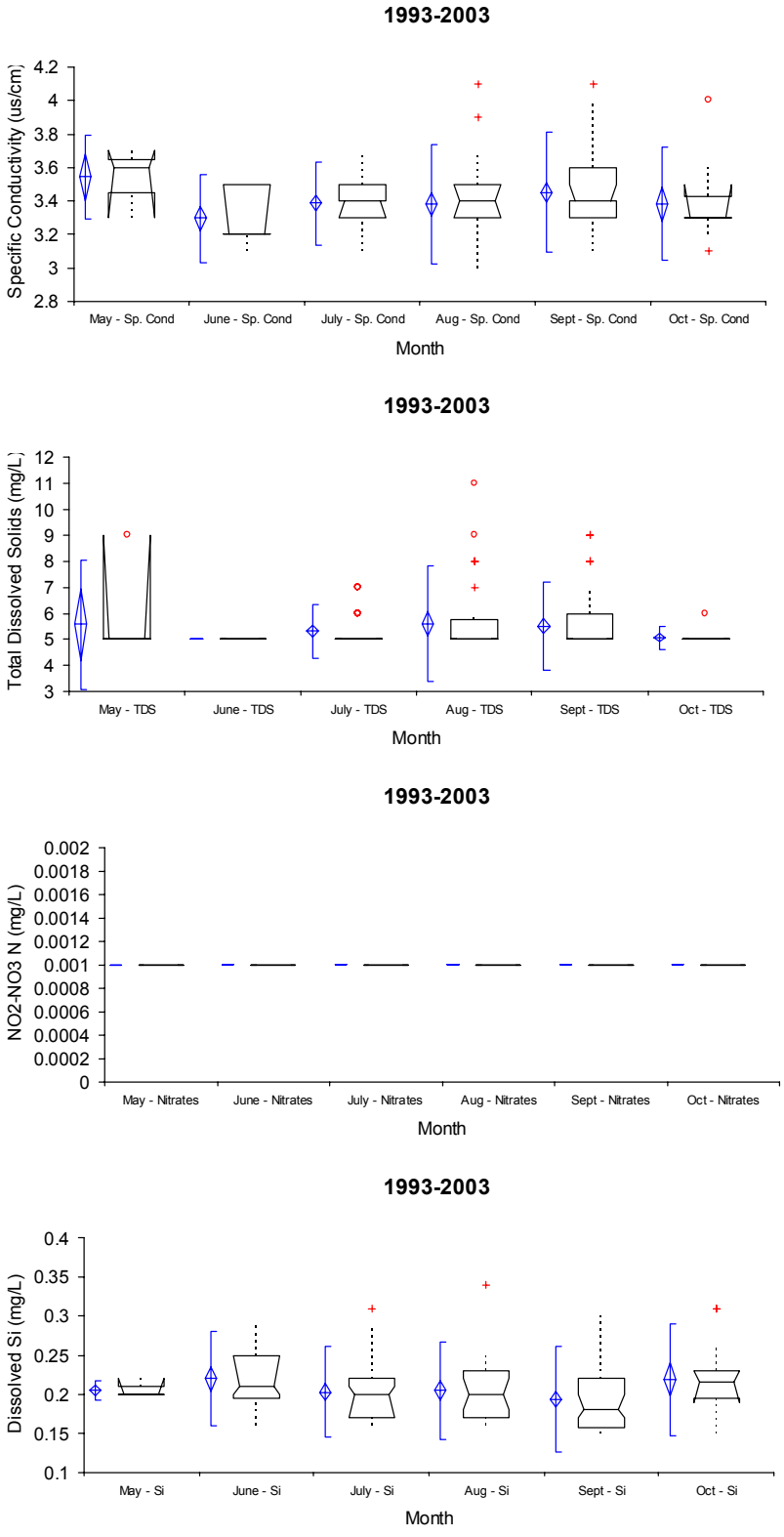

Figure A-3: Chemistry variables: monthly variation

Cladocera-Copepoda

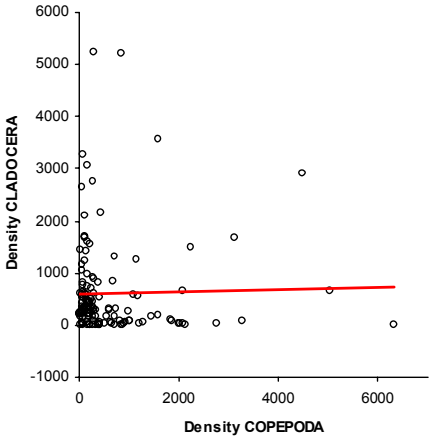

n	134
Spearman correlation coefficient	-0.21
95% CI	-0.37 to 0.04
2-tailed p	0.0153

Others-Cladocera

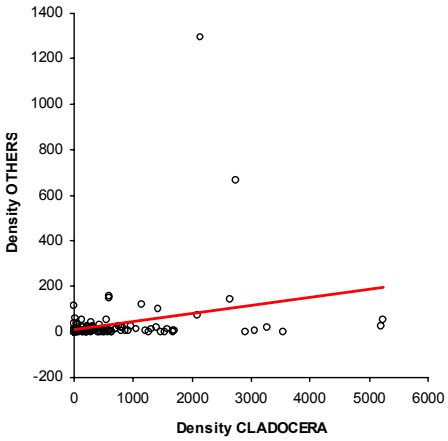

n	134
Spearman correlation coefficient	0.26
95% CI	0.10 to 0.42
2-tailed p	0.002

Figure A-4: Spearman rank-based correlation based on density for groups of zooplankton at Waldo Lake, between 1996 and 2003.

PCA omitting 9/6/1996 and 10/9/1999 (reported values)

Eigen values

PC	Eigen values	% Variation	Cumulative % Variation
1	1.39	34.6	34.6
2	1.02	25.5	60.1
3	0.92	22.9	83
4	0.68	17	100

Eigen vectors

Variable	PC1	PC2	PC3	PC4
TP (mg/l)	0.548	0.239	0.613	-0.516
Alkalinity	-0.594	0.432	-0.187	-0.653
Si (mg/l)	-0.504	0.253	0.709	0.423
TDS (mg/l)	0.304	0.832	-0.294	0.358

PCA including 9/6/1996 and 10/9/1999

Eigen values

PC	Eigen values	% Variation	Cumulative % Variation
1	1.41	35.1	35.1
2	1.02	25.4	60.6
3	.91	22.7	83.3
4	.67	16.7	100.0

Eigen vectors

Variable	PC1	PC2	PC3	PC4
TP (mg/l)	0.547	0.196	0.639	-5.04
Alkalinity	-0.603	0.411	-0.139	-0.670
Si (mg/l)	-0.515	0.183	0.721	0.426
TDS (mg/l)	0.269	0.872	-0.229	0.340

Figure A-5: Assessment of the importance of omitted dates, comparison of PCA results for chemistry.